

**COMPRESSIONAL DEFORMATION AND EXHUMATION IN  
SEDIMENTARY BASINS AT ‘PASSIVE’ CONTINENTAL  
MARGINS, WITH IMPLICATIONS FOR HYDROCARBON  
EXPLORATION AND DEVELOPMENT**

*by*

**David Ronald Tassone**

The Australian School of Petroleum



**THE UNIVERSITY**  

---

*of* **ADELAIDE**

This thesis is submitted in fulfilment of the requirements for the degree of

Doctor of Philosophy

in the Faculty of Science, The University of Adelaide

September 2014



*“Throughout the coast of Brazil, and certainly for a considerable space inland, from the Rio Plata to Cape St. Roque, lat. 5°S, a distance of more than 2,000 geographical miles, wherever solid rocks occurs, it belongs to a granitic formation. The circumstance of this enormous area being thus constituted of materials, which almost every geologist believes to have been crystallized by the action of heat under pressure, gives rise to many curious reflections. Was this effect produced beneath the depth of a profound ocean? Or did a covering of strata formerly extend over it, which has since been removed? Can we believe that any power, acting for a time short of infinity, could have denuded the granite over so many thousand square leagues?”*

—Charles Darwin, Bahia or San Salvador, Brazil,

29 February 1832 (Darwin, 1839, p. 12)

## Abstract

There is growing recognition that extensive phases of compressional deformation and exhumation have interrupted the post-rift subsidence histories of some economically important ‘passive’ continental margins. Understanding the distribution, magnitude, chronology and causes of exhumation and compressional deformation at these margins can reduce exploration uncertainty. The Otway and Faroe-Shetland basins along the southern Australian margin and northwest European Atlantic ‘passive’ margins, respectively, provide ideal natural laboratories to further understand syn and post-rift compressional deformation, inversion and exhumation.

Post-Albian exhumation in the Otway Basin was quantified to be ~400-3600 m across the eastern and northern parts of basin using a new sonic transit time-depth trend, which represents normal compaction of volcanoclastic shales deposited within a fluvio-lacustrine environment – unlike any other such trends previously published. These estimates are consistent with those from complementary thermal, palynological and seismic datasets. Whilst the impacts of exhumation are well known for *conventional hydrocarbon systems*, this study is amongst the first to highlight the implications of exhumation on *unconventional hydrocarbon systems*, in particular related to petrographical and geomechanical rock properties.

Exhumation in the Otway Basin is mainly related to mid-Cretaceous and Neogene neotectonic compressional deformation and inversion episodes, with the latter strongly governed by the contemporary stress state. Using complementary geophysical datasets and considering lithological heterogeneity, basement fabrics and variations in structural style with depth – factors generally neglected in previous geomechanical-focused studies in this region – it is possible to better understand the relationship between neotectonic deformation and stress.

Comparisons between bulk crustal strain rates based on Neogene shortening estimates, and present-day strain rates based on earthquake data and geological observations demonstrates that strain rates in the Otway Basin have declined since the onset of Neogene compressional deformation and exhumation. Neogene bulk crustal strain rates determined independently from shortening estimates and exhumation magnitudes yield similar results, suggesting that Neogene exhumation in the eastern Otway Basin can be accounted for solely by crustal shortening within a mildly compressional intraplate stress field, with ~30% of the total present-day strain rate accounted for by aseismic deformation.

In the central parts of the offshore Otway Basin, where there is very thick preserved Upper Cretaceous sequence and few indications of major post-Albian tectonic activity, significant and

previously unreported overpressures are examined. Pore pressure gradients exceed  $\sim 16$  MPa/km within the fine-grained Upper Cretaceous Belfast and Flaxman formations, and are most likely due to a disequilibrium compaction associated with Pliocene burial by a proto-Murray River discharge.

Estimating exhumation in the Otway Basin using sonic log data provided consistent values with thermal-based techniques, indicating that heating can be related (in part) to deeper burial. However, this may not hold true in all basins. More than  $\sim 400$ m of post-Danian exhumation was quantified using sonic data along the Rona High in the Faroe-Shetland region where thermal history data indicates anomalous heating due to transient hot fluid flow and is problematic for exhumation analyses. This exhumation likely occurred during the Oligocene to Mid-Miocene in response to a major reorganisation of the northern North Atlantic spreading system.

# Table of Contents

Declaration .....	v
Statement of Author's Contribution .....	vi
Acknowledgements .....	vii
1 Contextual Statement .....	1
2 Literature Reviews .....	8
2.1 LITERATURE REVIEW I: Methods for Quantifying Exhumation of Sedimentary Basins .....	9
2.2 LITERATURE REVIEW II: Tectonic Setting and Hydrocarbon Systems of the Otway Basin .....	37
References .....	77
3 Thesis Conclusions .....	95
4 First Author Journal Publications .....	98
PAPER 1: Quantifying Cretaceous-Cenozoic exhumation in the Otway Basin using sonic transit time data: implications for conventional and unconventional hydrocarbon prospectivity .....	99
4.1 PAPER 2: Overpressures in the central Otway Basin: the result of rapid Pliocene–Recent sedimentation? .....	153
4.2 PAPER 3: Contemporary stress and neotectonics in the Otway Basin, southeastern Australia .....	176
4.3 PAPER 4: Quantifying Neogene plate-boundary controlled uplift and deformation of the southern Australian margin .....	261
4.4 PAPER 5: Constraining Cenozoic exhumation in the Faroe-Shetland region using sonic transit time data .....	284
5 Contributions to Additional Journal Publications .....	323
5.1 PAPER A: Cenozoic Post-breakup Compressional Deformation and Exhumation of the Southern Australian Margin .....	324

5.2	PAPER B: Continental margin compression: A comparison between compression in the Otway Basin of the southern Australian margin and the Rockall-Faroe area in the northeast Atlantic margin.....	351
5.3	PAPER C: Paleothermal and seismic constraints on late Miocene–Pliocene uplift and deformation in the Torquay sub-basin, southern Australian margin .....	370
5.4	PAPER D: Reassessing the in-situ stress regimes of Australia’s petroleum basins .....	392
5.5	PAPER E: Cenozoic deformation in the Otway Basin, southern Australian margin: implications for the origin and nature of post-breakup compression at rifted margins	404
6	Conference Attendances and Presentations .....	433
6.1	CONFERENCE 1: 21 <sup>st</sup> International Geophysical Conference & Exhibition / Australian Society of Exploration Geophysicists and Petroleum Exploration Society of Australia – 22-26 August 2010, Sydney, Australia .....	434
6.2	CONFERENCE 2: The E.M. Anderson Meeting – 6-8 September 2010, Glasgow, Scotland.....	4400
6.3	CONFERENCE 3: 51 <sup>st</sup> Australian Petroleum Production and Exploration Association Conference & Exhibition – 10-13 April 2011, Perth, Australia .....	4444
6.4	CONFERENCE 4: 73 <sup>rd</sup> European Association of Geoscientists and Engineers Conference & Exhibition – 23-26 May 2011, Vienna, Australia .....	4477
6.5	CONFERENCE 5: American Association of Petroleum Geologists Annual Conference & Exhibition – 22-25 April 2012, Long Beach, United States of America .....	455

## Declaration

I certify that this work contains no material which has been accepted for the award of any other degree or diploma in any university or other tertiary institution and, to the best of my knowledge and belief, contains no material previously published or written by another person, except where due reference has been made in the text. In addition, I certify that no part of this work will, in the future, be used in a submission for any other degree or diploma in any university or other tertiary institution without the prior approval of the University of Adelaide and where applicable, any partner institution responsible for the joint-award of this degree.

I give consent to this copy of my thesis when deposited in the University Library, being made available for loan and photocopying, subject to the provisions of the Copyright Act 1968.

The author acknowledges that copyright of published works contained within this thesis resides with the copyright holder(s) of those works.

I also give permission for the digital version of my thesis to be made available on the web, via the University's digital research repository, the Library catalogue and also through web search engines, unless permission has been granted by the University to restrict access for a period of time.

---

David Ronald Tassone

---

Date



## **Statement of Author's Contribution**

The research summarised in the papers that constitute this thesis was undertaken within the Seismic, Structure & Stress (S<sup>3</sup>) Research Group at the Australian School of Petroleum (*Dr. Simon P. Holford, Dr. Rosalind King, Dr. Mark Tingay and Dr. Adrian K. Tuitt*) and with external collaborators at Geotrack International Pty. Ltd. (*Dr. Paul F. Green and Dr Ian R. Duddy*), the British Geological Survey (*Dr. Martyn S. Stoker and Dr. Howard Johnson*), The University of Edinburgh (*Prof. John R. Underhill*) and the Deep Exploration Technologies CRC (*Prof. Richard R. Hillis*). Hence all the papers presented herein are co-authored by either members of this research group and/or external collaborators, and detailed statements of their relative contribution are summarised below and endorsed by the co-authors.

## Acknowledgements

This Thesis documents my research into '*Compressional deformation and exhumation in sedimentary basins at 'passive' continental margin, with implications for hydrocarbon exploration and development*'. It also documents the collaborative research I have fortunately been involved in with respect to this subject over the duration of my postgraduate studies at the Australian School of Petroleum, The University of Adelaide, as well as some of the opportunities to present my work I have been to privileged to experience. This research work would not have been possible without the continual support and encouragement of a number of people.

- ***My Principal supervisor Dr. Simon P. Holford*** – Words cannot fully describe how thankful I was to have you as my Principal supervisor. Your ongoing support, enthusiasm, time, effort, encouragement and punctuality are just a few words and it has been truly appreciated. You have given me so many fantastic opportunities throughout the duration of my PhD, whether it has been through travel, demonstrating, collaboration, presenting and publishing my work, all of which has broaden my geological knowledge and provided me with a strong foundation to the remainder of my career as a geologist in the energy industry. Thank you Simon.
- ***My Co-supervisor Dr. Rosalind King*** – Thank you Ros for your help, technical discussions and support, especially towards the end of the PhD.
- ***My external supervisors Prof. Richard R. Hillis, Dr. F. Paul Green, Dr. Ian R. Duddy and Dr. Martyn S. Stoker*** – Although your presence was brief, thank you Richard for your professionalism and guidance at the start of my PhD that provided me with a determination and willingness to achieve my goals. Thank you Martyn for not only helping me understand the geological evolution of the Northeast Atlantic margin, but providing me the opportunity to visit and work in beautiful Edinburgh and the British Geological Survey; a memory that I will treasure forever. I also thank the Executive Director of the British Geological Survey (Natural Environment Research Council) to allow the permission of Dr. Stoker (and Mr. Johnson) to co-author publications of PAPER 2 and PAPER 3. Thank you Paul and Ian. Firstly, for providing me with your datasets for my research and your invaluable discussions in regards to basin analysis using thermal history data as well as the geology of the Otway Basin and southern Australian margin. I'd always look forward to your insights and passionate discussions. Secondly, your contributions to my papers and providing an opportunity to conduct contract research.

- **Collaborative researchers Dr. Mark Tingay, Dr. Adrian K. Tuitt, Dr. Howard Johnson and Prof. John R. Underhill** – Thanks for all your help, support and advice throughout my research and your contribution to the papers we have now published together or in the process of publishing. All your help has been really appreciated.
- **Seismic, Structure & Stress ( $S^3$ ) Research Group** – Thanks to all the members of our research group for all the excellent discussions and support over the four years.
- **Sponsors** – Thanks to Australian Research Council (ARC Discovery Project DP0879612) for supporting and funding Dr. Holford and Prof. Hillis' research to investigate the 'Compressional Deformation and Uplift of Australia's Passive Southern Margin', in which my opportunity to undertake a PhD would not have existed. I would also like to thank the Australian Society of Exploration Geophysics (ASEG) for their funding (ASEG Research Foundation Project RF09P04) that enabled me to collect new data and present my research at national and international conferences. My supervisors and I thank Will Jones, Adam Smith, Iain Brown, and Huw Edwards of PGS for provision of SAMDA, SMT/IHS for provision of KINGDOM software and JRS Petroleum Research (now Ikon Geoscience) for provision of JRS Suite. We also gratefully acknowledge Geoscience Australia, DMITRE, DPI Victoria, the British Geological Survey, and Occam Technologies for access to seismic and well data.
- **JRS Petroleum Research (now Ikon Geoscience)** – Thanks to Dr. Jerry Meyer, Dr. Scott Mildren and Dr. Oliver Bartdorff for giving me the opportunity to gain valuable industry work experience as well as geomechanical-related help and advice throughout my PhD.
- **My Friends** – I would like thank my new friends that I have made throughout the duration of my PhD at the Australian School of Petroleum. In particular, Ali, Abbas, Ernest, Jess, Tess, Julien, Mohammad, Sara and Maqsood for their ongoing support. Last, but not least, I would like to thank Justin for his encouragement and enthusiasm that has been truly inspirational.
- **My Family** – The completion of this PhD could not have been possible without my brothers and sisters, and in particular, my parents Meryl and Sam. Thanks for all your love, support and guidance, not only over the last the 4 years during my PhD, but throughout my whole academic life, and providing me the opportunity to pursue my goals and dreams. I also hope I've done the name 'Ronald' proud, grandpa.

- ***My Friend, My Girlfriend, My Fiancé, and now Wife*** – Flor, your love throughout the duration of my PhD has truly been appreciated. Let this hard work, sacrifice and commitment bounded by these pages be the foundation of a fruitful life together, and a reminder to you of the pursuit of happiness I dream for us. This PhD Thesis is dedicated to you.

## 1 Contextual Statement

'Passive continental margins are so-called due to the commonly held belief that following rifting and subsequent plate separation, the tectonic histories of these fundamental physiographic features that fringe the continents are dominated by thermally controlled subsidence, with little or no extrinsically driven deformation. The past decade has witnessed growing recognition, however, that extensive phases of compressional deformation, fault reactivation and exhumation have punctuated the syn- and post-rift subsidence histories of some economically important passive margin basins. With mounting global demand for hydrocarbon resources, exploration in these geologically complex, high-risk basins, requires sound understanding of the distribution, magnitude, chronology and causes of exhumation and compressional deformation to reduce uncertainty and evaluate prospectivity.

This thesis primarily investigates mid-Cretaceous and Neogene compressional deformation and exhumation episodes in the Otway Basin, located along Australian's southern passive margin, in order to evaluate the implications for the hydrocarbon prospectivity of this region. The Otway Basin is a rift basin with proven conventional gas accumulations both onshore and offshore that is still actively explored, with particular interest in recent years focused on onshore unconventional hydrocarbon plays. This study of the Otway Basin is complemented by a comparative investigation of exhumation in the Faroe-Shetland region, located along the northwest European Atlantic margin. Whilst both regions have experienced complex vertical motions during the Mesozoic and Cenozoic, the Faroe-Shetland region has witnessed extensive break-up magmatism which means that burial history modelling using thermal history data alone is problematic without the aid of complementary datasets, such as compaction, seismic reflection and biostratigraphic data.

### *PAPER 1*

*Net exhumation* is a term that describes the difference between the present-day burial depth of a reference unit and its maximum burial depth prior to exhumation. Net exhumation magnitudes for 110 onshore and offshore petroleum wells located in the Otway Basin, southeastern Australia, were estimated for 'overcompacted' Lower Cretaceous fluvial shales using sonic transit time data. When compared with derived baseline trends representing normal burial of Eumeralla Formation's volcanoclastic shales, sonic transit time data indicates significant post-Albian (i.e., mid-Cretaceous) net exhumation around the Otway Ranges (>1500 m), Merino high (>690 m), Colac trough (>580 m), and Torquay sub-basin (>560 m), and minor to negligible amounts of exhumation (generally

## CONTEXTUAL STATEMENT

<200 m) around the Penola trough, Port Campbell Embayment, and Shipwreck Trough, where most of the gas fields in the Otway Basin are located.

These estimates of net exhumation were further complimented with published thermal history, palynological, and seismic datasets (e.g., Green et al., 1995, 2004; Cooper & Hill, 1997; Duddy et al., 1998; Constantine & Liberman, 2001; Holford et al., 2010, 2011). A very good correlation existed with estimates of net exhumation derived independently from thermal history data for when maximum burial and subsequent exhumation occurred in the mid-Cretaceous, as represented by the regional Cenomanian-age ‘Otway’ unconformity. A similar correlation does not exist for net exhumation estimates associated with maximum burial and subsequent exhumation occurring in the Cenozoic, with one plausible explanation for this being that thermal history analyses incorrectly assumed higher thermal conductivities in the eroded section thereby overestimating the amount of removed section.

The distribution of exhumation in relation to mid-Cretaceous and Neogene compressional structures primarily observed in the eastern Otway Basin from seismic profile data and surface structural mapping indicates that exhumation was dominantly controlled by short-wavelength basin inversion.

The implications of both mid-Cretaceous and Cenozoic exhumation and compression deformation in the Otway Basin towards elements and processes of petroleum systems vital for defining prospectivity were also discussed in detail for both *conventional* and *unconventional* hydrocarbon plays. With respect to conventional hydrocarbon plays, the timing of maximum burial of the Eumeralla Formation (i.e., Austral 2 source rock) was regionally mapped showing correlations with discovered hydrocarbon accumulations (O’Brien et al., 2009) in close proximity to where the Eumeralla Formation is presently at maximum burial. This map also shows the cessation of hydrocarbon generation in the mid-Cretaceous following maximum burial and subsequent exhumation and cooling, as well as examples of partially and fully breached traps likely caused by reactivation of basement faults during Miocene–Holocene basin inversion, resulting in palaeo-hydrocarbon columns (Lyon et al., 2007). Furthermore, water analysis data from conventional reservoir in close proximity to Neogene inversion structures (where aquifers outcrop) show formation water to have very low salinity content, and coupled with biodegraded oils in adjacent hydrocarbon fields, this suggests possible meteoric water flushing.

Whilst the impacts of exhumation are better known with respect to *conventional* hydrocarbon plays (e.g. Doré et al., 2002b; Turner & Williams, 2004), it is believed that this study is amongst

## CONTEXTUAL STATEMENT

the first to directly address the implications of exhumation and compressional deformation to *unconventional* hydrocarbon plays, which are of increasing global importance. Key geological features of the Otway Basin, such as source richness and type, depositional environment and structural style were firstly compared to basins in the United States with prospective unconventional plays (e.g. Barnett and Marcellus Shales). This review highlights the observation that a number of basins (e.g., Piceance Basin (Nuccio and Roberts, 2003; Fall et al., 2012); Appalachian Basin (Blackmer et al., 1994; Reed et al., 2005); FortWorth Basin (Montgomery et al., 2005; Ewing, 2006)) have witnessed significant magnitudes of net exhumation (700-4400 m), which has brought brittle, thermally mature source-seal-reservoir rocks to shallower depths. The impacts of deeper burial and subsequent exhumation to the petrographical and geomechanical properties of the Eumeralla Formation has caused primary porosity to be significantly lower, but the resulting dense and brittle-behaviour has potentially generated greater secondary porosities (i.e., natural fractures) and higher vertical stress gradients.

This is the first time an integrated exhumation analysis using sonic transit time and thermal history data has been undertaken for the southern Australian margin and the results were published in *AAPG Bulletin*.

### **PAPER 2**

A number of wells located within the offshore Voluta Trough displayed anomalous sonic transit time-depth relations indicative of potentially both *overcompaction* and *undercompaction*. Whilst the state of overcompaction was assessed in detail for the Lower Cretaceous Eumeralla Formation shale units in Paper 1 across the entire Otway Basin to constrain burial depth histories, undercompaction is a phenomenon related to formation overpressure.

Drilling and wireline data from several wells in the Voluta Trough indicated that formation overpressures occurred within the Upper Cretaceous Belfast and Flaxman formation shale units. Shales overpressures were also estimated at four offshore well locations using the Eaton (1972) method (exponent of 3), which required calculation of vertical stress gradients and normal sonic transit time-depth baseline trends. These estimates of overpressure were, in most cases, consistent with available overpressure data when ‘apparent’ exhumation magnitudes were considered and indicated that overpressures were likely generated by a disequilibrium compaction mechanism. This is largely supported by the observation at Bridgewater Bay-1 where a very thick Belfast Mudstone sequence was penetrated and ~700 m Pliocene-Holocene marine clastic sediments were

## CONTEXTUAL STATEMENT

rapidly deposited subsequent to any post-Miocene exhumation in submarine channels (Leach & Wallace, 2001), generating pore pressure gradients exceeding ~16 MPa/km. This rapid sediment accumulation rate (~130-190 m/Ma) is perhaps linked to a proto-Murray River (Miranda et al., 2009).

This study was published in the *APPEA Journal* and is the first to investigate the magnitudes, distribution and mechanisms of overpressures in the offshore Otway Basin.

### PAPER 3

A key conclusion of the Paper 1 is that the distribution of net exhumation magnitudes in the eastern Otway Basin is strongly controlled by mid-Cretaceous and Neogene neotectonic compressional structures that developed during several phases of basin inversion.

Orientations of contemporary maximum horizontal stresses determined from new hydrocarbon exploration data were determined to be  $\sim 135 \pm 15$  °N based on wellbore failure analysis, which are generally consistent with findings from previous studies (e.g., Nelson et al., 2006). This orientation is also consistent with stress determinations from basement seismicity (Denham et al., 1981; Nelson et al., 2006) and palaeostress trends inferred from Holocene volcanic features (Lesti et al., 2008). However there is less certainty regarding the nature of stress magnitudes in the Otway Basin. Whereas seismic profile data and surface structural mapping (Cooper & Hill, 1997) points to a reverse fault stress regime (i.e.  $SH_{max} > Sh_{min} > S_V$ ) as evidenced by the neotectonic faulting and folding record, past studies of contemporary stress magnitudes, using hydrocarbon exploration data have mostly indicated normal or strike slip fault stress conditions (i.e.  $SH_{max} > S_V > Sh_{min}$  or  $S_V > SH_{max} > Sh_{min}$ ; Hillis et al., 1995; Nelson et al., 2006).

Lithological heterogeneity, basement fabrics and variations in structural style with depth (i.e., ~1-3 km) was demonstrated to exert important controls on horizontal stress magnitudes within the basin and its relationship to the vertical stress. Leak-off pressures which provide a proxy for the minimum horizontal stress magnitudes, are very high (often greater than lithostatic) in Oligocene-Miocene-age marl and carbonate-dominated formations deposited during post-rift basin subsidence. Neotectonic deformation in these sequences is typically manifested by northeast-southwest trending folds with low amplitudes (~100-500 m) and long wavelengths (10-25 km). In Eocene and older formations that were deposited during syn-rift subsidence and tend to be dominated by siliciclastic rocks, leak-off pressures indicate that the least principle stress is horizontal, with sand-rich formations typically display minimum horizontal stress magnitude



## CONTEXTUAL STATEMENT

gradients that are ~3-4 MPa/km lower than shale-dominated formations. Within the syn-rift sections there is an overall increase in the minimum horizontal stress gradient of ~1-2 MPa/km from west to east across the basin. This increase corresponds to a marked change in structural style across the basin. In the western Otway Basin, the strikes of rift-related faults are near-parallel to the contemporary maximum horizontal stress azimuth and there are comparatively low levels of neotectonic activity. In the eastern Otway Basin rift-related faults strike near-orthogonal to the contemporary maximum horizontal stress azimuth, the level of neotectonic faulting and uplift is much higher. The key observation of strike-slip fault stress regimes within syn-rift sections of the basin may be due to the underestimation of horizontal stress magnitudes interpreted from leak-off pressures. Alternatively, the observed partitioning of both stress regimes and deformation styles with depth, with the shallow, post-rift Oligocene to Miocene sequence characterised by a reverse fault stress state, and the deeper, syn-rift Cretaceous-Paleocene siliciclastic sequence characterised by a strike-slip fault stress state, may reflect varying mechanical properties of the basin fill.

This study is currently in preparation to be submitted for publication in *Tectonophysics* and improves upon previous studies by firstly demonstrating the presence of significant overpressures (as observed in Paper 2) and by considering other basin-wide geological factors that relate neotectonic deformation and stress, which have often been neglected in previous more geomechanical-focused studies.

### **PAPER 4**

The Otway Basin, along with other parts of the Australian continent, exhibit unusually high levels of neotectonic deformation and contemporary seismicity for a so-called stable continental region (Hillis et al., 2008). Late Pliocene to Quaternary bulk crustal strain rate in the eastern onshore Otway Basin was estimated to be  $\sim 1.09 \times 10^{-17} \text{ s}^{-1}$  from neotectonic geological observation (Sandiford et al., 2003a,b). This is greater than a horizontal present-day brittle strain rate of  $\sim 5.07 \times 10^{-18} \text{ s}^{-1}$  estimated from seismic moment release calculations based on seismicity over a 30 year period, indicating that ~30% of the total present-day strain rate can be accounted for by aseismic deformation.

Longer-term, Neogene bulk crustal strain rates determined independently from both shortening (Cooper & Hill, 1997) and exhumation (Holford et al., 2011; Paper 1) estimates yield similar strain rates of  $\sim 2 \times 10^{-16} \text{ s}^{-1}$ . This indicates the estimated magnitudes of Neogene exhumation in the eastern Otway Basin can be accounted for solely by crustal shortening within a mildly

## CONTEXTUAL STATEMENT

compressional intraplate stress field. Given the orthogonal relationship between inverted post-Miocene structures and maximum horizontal stress orientation, this result also validates the notion that plate-boundary forces (Reynolds et al., 2003) are capable of generating mild but appreciable deformation and uplift within continental interiors.

Comparisons between present-day and Neogene strain rates in the eastern Otway Basin demonstrate significant temporal variation in bulk crustal strain rates, with an overall decline since the onset of compressional deformation at ~10 Ma. Normalisation of the horizontal present-day brittle strain rate shows that the eastern Otway Basin lies in between the very seismically active Flinders Ranges (C  lerier et al., 2005) and inactive Murray Basin (Sandiford et al., 2004) and accounts for ~3% of the total Australian seismic strain (C  lerier et al., 2005).

This study was published in a *Geological Society of London Special Publication*, and expands on the studies of Neogene exhumation and neotectonic compressional deformation presented in Papers 1 and 3, by using a novel approach to quantify Neogene plate-boundary controlled uplift and deformation.

### PAPER 5

In contrast to the Otway Basin, the Faroe-Shetland basins located along the northwest European Atlantic continental margin, have been strongly influenced by large post-breakup enigmatic compressional features, anomalous subsidence patterns and magmatism that have rendered the ability to quantify magnitudes of exhumation using thermal history data (e.g. AFTA, VR) problematic. Since the compaction-based technique is less susceptible to distortions from transient heating events in this region, few studies have successfully quantified the magnitude and timing of exhumation in this region.

A new normal sonic transit time-depth baseline trend was firstly constructed based on reliable thermal history data and used to demonstrate that Danian to Campanian marine shale units of the Shetland Group penetrated by wells in the southwestern parts of the Faroe-Shetland region have been more deeply buried in the past. Post-Danian net exhumation estimates increased from ~200-350 m along the central and northeastern parts of the Rona High to ~400-1000 m for wells located in the West Shetland Basin, North Rona Basin and southwestern parts of the Rona High. In contrast, Danian to Campanian marine shale units in the M  re and Magnus basins in the northeast of the Faroe-Shetland region as well as in the deeper-water Faroe-Shetland Basin (i.e. Flett and Foula sub-basins) indicate maximum, or near (i.e. within  $\leq 100$  m net exhumation) maximum burial

## CONTEXTUAL STATEMENT

at the present-day. The new marine shale baseline trend is consistent with other marine shale baseline trends of different ages from nearby basins.

The precise timing of post-Danian exhumation was difficult to constrain due to the complex syn- to post-rift tectonostratigraphic history of vertical movements within the Faroe-Shetland region. Our estimates of missing section, together with available thermal history constraints and seismic-stratigraphic evidence, nevertheless, implies that maximum burial and subsequent exhumation most likely occurred during an Oligocene to Mid-Miocene tectonic phase. This was probably in response to major post-breakup tectonic reshaping of this segment of the NE Atlantic Margin linked to a coeval and significant reorganisation of the northern North Atlantic spreading system. This indicates that fluctuations in intraplate stress magnitude and orientation governed by the dynamics of plate-boundaries forces exerts a major control on the spatial and temporal variations in differential movements along complexly structured continental margin.

This study was published in a thematic issue of *Basin Research* focussed on 'Deep-Water Continental Margins', and uses the compaction-based approach developed in Paper 1 to provide new constraints on Cenozoic burial and exhumation magnitudes in the UK sector of the Faroe-Shetland region.

## 2 Literature Reviews

The thesis covers a broad range of petroleum geology concepts and disciplines related to the topics of '*Compressional deformation and exhumation in sedimentary basins at 'passive' continental margin, with implications for hydrocarbon exploration and development*'. Given the breadth of concepts covered and multiple regions investigated, only two literature reviews have been written, with the first addressing the *methods used to quantify exhumation within sedimentary basins* and the second covering the *tectonic setting and hydrocarbon systems of the Otway Basin*.

## ***2.1 LITERATURE REVIEW I: Methods for Quantifying Exhumation of Sedimentary Basins***

### **INTRODUCTION**

The ever increasing demand for petroleum products in today's society has led petroleum companies to recognise the increasing need to explore in higher risk basins (Doré et al. 2002b). Although no basin is without geological uncertainties, one type of basin that is categorised as high risk is an *exhumed* basin; the earlier this is identified in the exploration process the better, as exploration of such basins calls for different hydrocarbon exploration practices and constraints on resource prediction (Doré et al. 2002b). Causes of sedimentary basin exhumation are various with mechanisms including post-orogenic unroofing, rift-shoulder uplift, hotspot activity, compressive tectonics, eustatic sea-level change, glaciation and isostatic readjustment, with the effects of several of these processes often superimposed (Doré et al. 2002a; Ware & Turner 2002). Typical characteristics of an exhumed basin, according to Doré et al. (2002b), include large basin-centred gas fields; smaller, peripheral, remigrated oil accumulations; two-phase accumulations; residual oil columns; biodegraded oils; and under-filled traps.

Nyland et al. (1992) and Doré & Jensen (1996) were among the first to highlight the impact of exhumation on petroleum systems, both negative and positive, when exploring for hydrocarbons along the NW European Atlantic margin. A critical factor that most researchers agree is of key economic importance when assessing standard parameters used to calculate resource prospectivity and preservation (e.g. porosity, water saturation, net-to-gross/recovery factors), is the *quantification of the magnitude and timing of exhumation* events (Doré et al. 2002a,b; Corcoran & Doré 2005).

Estimates of the timing and magnitude of exhumation events in petroliferous sedimentary basins have been applied to a number of extensional basins within intra-plate and passive margin setting, most notably in the North Sea, offshore UK and Norway (e.g., Hillis 1995a,b; Japsen 1998, 2000; Japsen et al. 2002, 2007; Green et al. 2002; Holford et al. 2005a,b;). The implications of exhumation for petroleum systems, in particular the relationships between magnitude of exhumation, and the timing of oil generation and migration with respect to trap formation, have been recognised in many studies (e.g. Bray et al. 1992; Hillis 1995a; Doré et al. 2002a; Turner & Williams 2004; Corcoran & Doré 2005) and can have both positive and negative effects. A

## LITERATURE REVIEWS

summary of positive and negative implications that exhumation has on petroleum systems are listed in Table 1.

The aim of this literature review is to review some of the main techniques used to quantify exhumation in sedimentary basins, and to assess the uncertainties associated with each those methods. Methods that utilize one-dimensional measurements such as compaction and thermal history data are discussed in most detail but a brief overview of other less common thermal techniques is also presented. For more information, the reader is referred to Corcoran & Doré (2005), who provide a comprehensive review of the techniques used for estimating the magnitude and timing of exhumation in sedimentary basins, although, more specifically to offshore basins.

**Table 1: Positive and negative implications of exhumation on petroleum systems (adapted from Doré et al. 2002b; Corcoran & Doré 2005).**

Positive	Negative
Local re-deposition of erosional products which may give rise to an isolated working hydrocarbon kitchen.	A limited hydrocarbon budget is available to charge traps as a result of the 'switch-off' of source rock maturation during exhumation.
Development of fracture permeability in tight reservoirs as a result of a changing stress regime during exhumation.	A reduced probability of effective top-seal exists in exhumed basins, except where highly ductile seals are present.
Introduction of a light oil budget due to retrograde condensate drop-out caused by pressure reduction during uplift and re-migration of hydrocarbons to shallower reservoirs.	Generally, higher levels of reservoir diagenesis (with respect to present day burial) prevail and this can impact the net-to-gross ratio, porosity, water saturation and recovery factor for exhumed reservoirs
Ex-solution of methane from formation waters, due to decreasing solubility as temperature and pressure reduces during uplift, offers an alternative mechanism for charging gas accumulations	A predominance of gas over oil is observed due to the liberation of methane from oil, formation water and coal induced by pressure release during exhumation causing gas flushing and the spillage of oil accumulations.
	Faults are often reactivated, causing them to become conduits for hydrocarbon leakage to the surface.
	Potentially attractive reservoirs may, likewise, be overcompacted and downgraded.
	Regional tilting during uplift results in changes to trap configurations and fluid migration directions.

### KEY DEFINITIONS

Exhumation is one term amongst a lexicon of terms (e.g. uplift, crustal uplift, surface uplift) that has been used interchangeably in the past for this field of study to describe and measure the vertical displacement of a rock column from a specified reference datum (England & Molnar 1990; Hillis 1995a). This has often resulted in confusion with different research groups and disciplines, thus, reinforcing the need of formal definitions. Table 2 presents a series definitions associated with exhumation that have been reviewed by Corcoran & Doré (2005). The parameter of most interest to petroleum explorers is *net exhumation* (see Table 2) because it affects the maturation, compaction and diagenetic state of source, reservoir and seal rocks. However, *gross exhumation* is commonly quoted in literature to describe the amount of erosion or rock removed from the column (Table 2).

*LITERATURE REVIEWS*

**Table 2: Definitions of terms in previous studies that have been used to describe exhumation and uplift (Corcoran & Doré 2005).**

<b>Term</b>	<b>Summary definition</b>	<b>Frame of reference</b>
Uplift	Non specific term referring to displacements “opposite to the gravity vector” (England & Molnar 1990)	Object displaced and/or reference frame not specified
Surface uplift	Displacement of Earth’s surface averaged over area $> 10^3$ - $10^4$ km <sup>2</sup> (England & Molnar 1990); upward movement of the Earth’s surface (the land or sea bottom) with respect to a specific datum (Doré et al. 2002a).	Geoid or mean sea level
Crustal uplift	Also ‘uplift of rocks’ – vertical displacement of rock column (England & Molnar 1990); upward movement of the rock column with respect to a similar datum (Doré et al. 2002a).	Geoid or mean sea level
Net uplift	Present elevation of a marker bed above its maximum burial depth (Doré & Jensen 1996; Riis & Jensen 1992).	Ground level or seabed
Epeirogeny	Broad regional uplift of continental interiors driven by thermal, isostatic or intra-plate stress fields (Turner & Williams 2004); Large scale uplift of the Earth’s surface without significant folding or fracture (Summerfield 1991).	Geoid
Inversion	Compressional reactivation of formally extensional fault systems leading ultimately to extrusion of synrift fills (Cooper & Williams 1989).	Pre-extensional regional elevation
Erosion	Local subareial or submarine removal of material by both mechanical and chemical processes (Riis & Jensen 1992; Riis 1996).	Fixed subsurface coordinates
Denudation	Loss of mass from both surface and subsurface parts of a drainage basin or regional landscape by all types of weathering, physical and chemical (Leeder 1999).	Fixed internal reference axes within bedrock
Exhumation	Descriptive term describing removal of overburden material such that previously buried rocks are exposed (Doré et al. 2002a).	Ground level
Net exhumation	Difference between present-day burial depth of a reference unit and its maximum burial depth prior to exhumation (Corcoran & Doré 2005).	Relative to seabed, ground level or stratigraphic marker
Gross exhumation	Magnitude of erosion which must have occurred at a particular unconformity prior to post-exhumation re-burial (Corcoran & Doré 2005).	Relative to seabed, ground level or stratigraphic marker
Apparent exhumation	Displacement, along the depth axis, of the observed compaction trend from the normal, undisturbed trend (Hillis 1995a,b). Equivalent to <i>net exhumation</i> .	Normal compaction trend, maximum burial depth

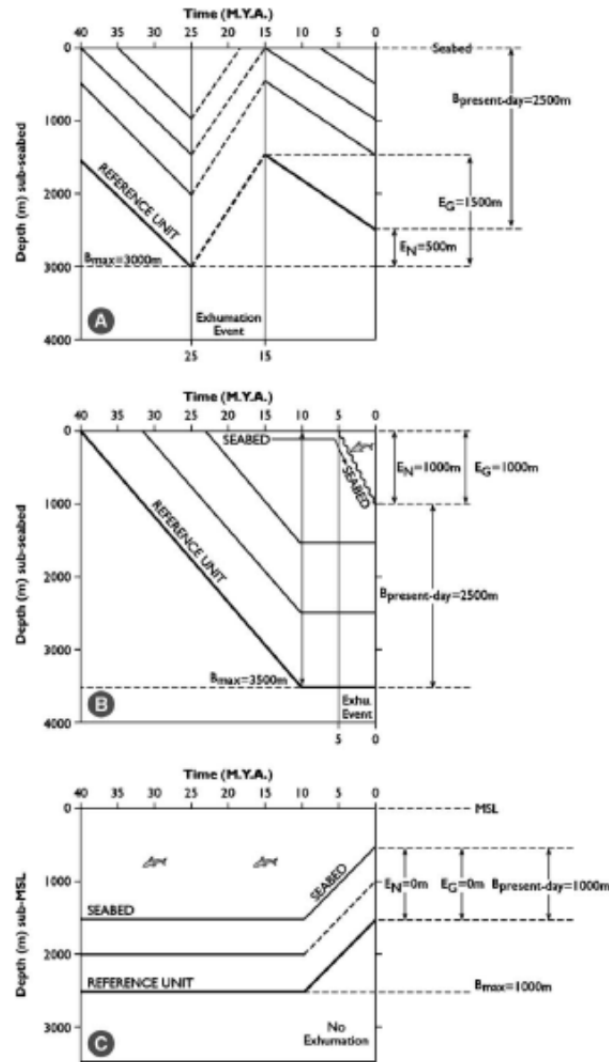


Figure 1: Schematic explanation of the difference between *net* and *gross exhumation* (after Corcoran & Doré 2005).

## METHODS FOR QUANTIFYING THE MAGNITUDE OF SEDIMENTARY BASIN EXHUMATION

Methods for quantifying the magnitude of exhumation are reviewed in depth by Corcoran & Doré (2005). They categorise different methods with respect to four different generic frames of reference, which are compaction-based, thermal, tectonic or stratigraphical approaches. In addition to Corcoran & Doré (2005), Japsen & Chalmers (2000) also highlight a number of the different techniques that have been used to study uplift and erosion. In this section, three common methods corresponding to compaction-based and thermal techniques, respectively, will be discussed in detail: compaction data, Apatite Fission Track Analysis (AFTA) and Vitrinite Reflectance (VR).



Tectonic and stratigraphic techniques to quantify exhumation will not be discussed in this literature review as they are not directly applied in any of the papers that comprise this thesis.

### *Compaction-based Techniques*

Calculating the magnitude of exhumation using compaction-based techniques has been used effectively and with great success in many studies (e.g. Ware & Turner 2002; Hillis 1995a,b; Densley et al. 2000 Japsen et al. 2002; Mavromatidis & Hillis 2005; Holford et al. 2005a, 2009a). It remains a popular and widely used method because it utilises data that is readily available from petroleum exploration wells and therefore, does not require additional laboratory expenses (Skagen 1992; Hillis 1993).

### *Compaction data*

The term compaction refers to the reduction in sediment volume which occurs during burial and is the result of mechanical and thermo-chemical processes (Sclater & Christie 1980; Bulat & Stoker 1987; Corcoran & Doré 2005). It is generally expressed by the reduction in porosity with vertical burial depth, or more correctly expressed by Hubbert & Rubey (1959) as the porosity variation with total effective stress. Giles et al. (1998), however, prefer that compaction be defined as the three-dimensional strain, rather than expressed as the vertical change in sediment thickness because it is also necessary to account for lateral compaction (i.e. bulk shortening) in compressive settings. For this reason, the Giles et al. (1998) definition of compaction takes into consideration increases in solid volume (e.g. by introduction of cement) in addition to volumetric strains and not just simply porosity loss due to burial.

Since no compaction mechanism links porosity with depth simply, directly and universally, many laboratory tests and empirical observations (Luo & Vasseur 1995; Giles et al. 1998) are relied upon to describe this relationship. A critical observation that forms the basis of compaction-based techniques for the assessment of exhumation (Corcoran & Doré 2005) is that porosity loss with increasing depth is largely irreversible (Giles et al. 1998). However, porosity can increase, although generally insignificant and less common, through grain dissolution (Giles et al. 1998) and/or porosity 'rebound' (through the recovery of deformation when effective stress is reduced) during exhumation (Corcoran & Doré 2005). Exhumed basins tend to exhibit anomalously low porosities at a given depth compared to continuously subsiding basins (Giles et al. 1998, Holford et al. 2005a) and so the porosity-depth trend is commonly determined by the maximum paleo-burial

depth rather than the present-day depth of burial. Nevertheless, caution is advised when assessing anomalously low porosities as phenomena such as overpressure of hydrocarbon-filled porosities can inhibit normal compaction (Hillis 1995a).

In terms of modelling the variation of porosity with depth, it has long been thought that the best representation of this relationship follows an exponential trend (Eq. 1; Athy 1930; Hubbert & Rubey 1959), although, simpler, linear trends have been proposed and used (Giles et al. 1998).

$$\phi = \phi_0 e^{-cy} \quad (1)$$

Where:  $\phi$  is the porosity at depth  $y$

$\phi_0$  is the porosity of sediments at the time of deposition

$c$  is a constant lithology-dependent compaction coefficient which determines the shape of the porosity-depth curve

This model and the parameters used by Sclater & Christie (1980) resulting from their study in the North Sea has subsequently become the most commonly used model to define a reference, normally compacted curve in exhumation studies. There are however, a wide range of porosity-depth curves for any given lithology in a given area based on empirical observations (in order to calibrate model parameters to achieve a good fit of the data). For example, the variety of porosity vs. depth trends for sandstones, shales and carbonates can be seen in Fig. 2, taken from Giles et al. (1998), showing that for the same depth, different data sets exhibit differences in porosity of more than 20%. Possible factors that may explain the differences between porosity vs. depth curves for the same lithology, according to Giles et al. (1998), include differences in composition, age, geothermal gradient, overpressure, and initial porosity and packing. Although studies have successfully used sandstones (Bulat & Stoker 1987; Hillis 1995a; Densly et al. 2000; Japsen et al. 2002) and carbonates (Hillis 1995a), in good agreement with estimates from other techniques to calculate the magnitude of exhumation, shales are generally chosen for the analysis of maximum burial depths. Shales are preferred because they exhibit relatively simple normal compaction trends with their porosity decreasing rapidly with depth (Magara 1978), are often more homogeneous in terms of grain size and mineralogy, and they do not act as an aquifer with the consequent porosity variations (Japsen et al. 2002; Ware & Turner 2002). Coarser-grained, argillaceous lithologies such as sandstones or carbonates are susceptible to anomalous compaction behaviour, largely as a result of diagenetic effects (Ware & Turner 2002; Holford et al. 2005a). Nevertheless, Hillis (1995a) and

## LITERATURE REVIEWS

Japsen (2000) suggest that it is advantageous in compaction-based analysis of uplift and maximum burial depth to analyse several stratigraphic units because a single unit may not be present in all wells and may not provide good regional coverage. Furthermore, by averaging the apparent uplift in several units for a particular well, the anomalous influence of sedimentological and/or diagenetic processes (i.e. burial-depth independent factors) within a single unit can be reduced.

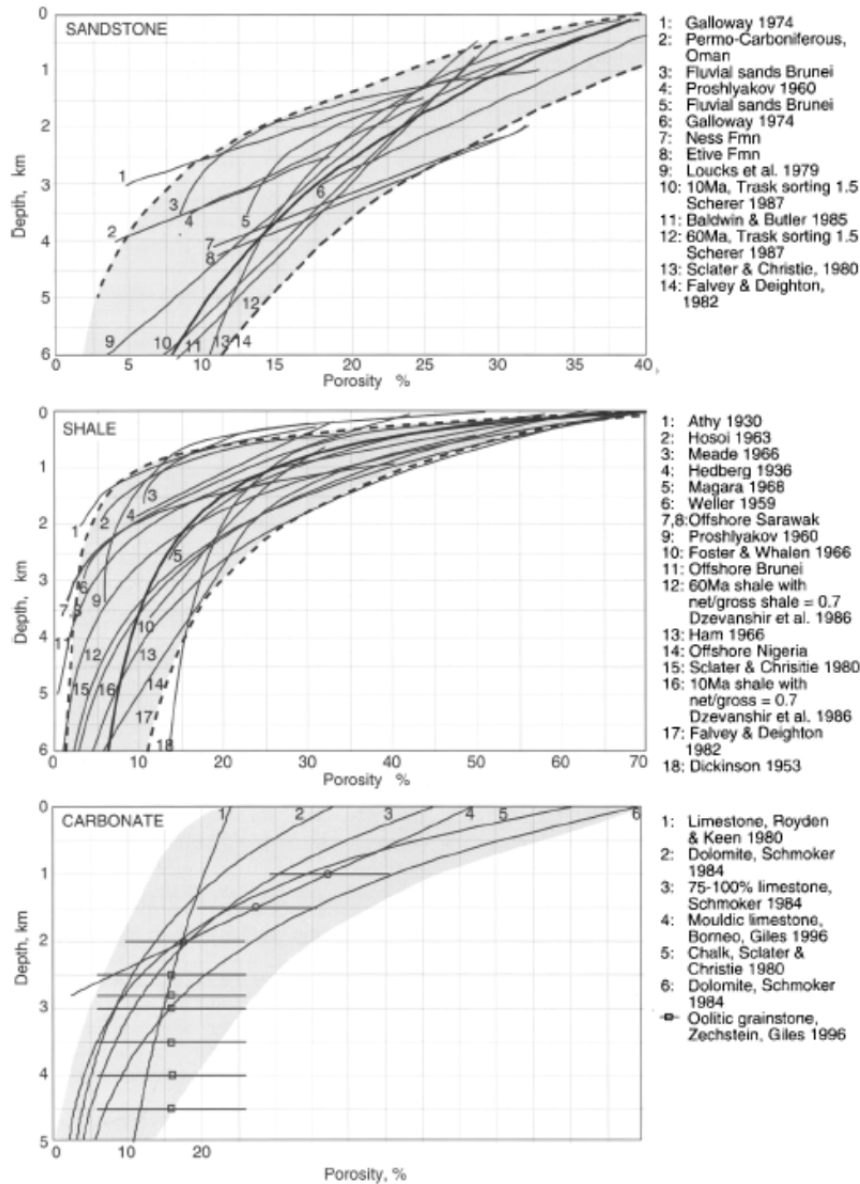


**Figure 2: Empirically derived porosity vs. depth relationships for (a) sandstones, (b) shales and (c) carbonates, taken from Giles et al. (1998). Each graph shows that for a given lithology, there is a wide range of trends which are dependent on factors including initial porosity, sorting, grain size, composition, age, pressure regime and temperature gradient.**

### Magnitude of exhumation calculation

Quantifying the magnitude of exhumation, in an exhumed basin, for any given well location using a compaction-based technique firstly requires a reference porosity-depth curve of a sedimentary succession which is: presently at its maximum burial depth (unexhumed), is hydrostatically pressured and exhibits anomalously low porosities (Japsen et al. 2002; Holford et al. 2005a; Corcoran & Doré 2005). If the entire basin has been exhumed, then a reference trend from a different, unexhumed basin can be used as long as the reference trend has been constructed for a sufficiently similar lithology. Otherwise, it is usually constructed from an area within the basin that has experience no exhumation and is ‘normally buried’ (e.g. Corcoran & Mecklenburgh 2005; Holford et al. 2009b). Methodologies employed by Ware and Turner (2002), Japsen et al. (2002), and Corcoran & Mecklenburgh (2005) offer alternative approaches to define a ‘normal’ compaction trend in areas affected by regional exhumation (Corcoran & Doré 2005).

The displacement of the observed porosity values or compaction trend (or some proxy thereof, e.g. density, sonic), along the depth axis from the ‘normal’ unexhumed or maximum burial depth trend yields an estimate of *net exhumation* ( $E_N$ ) is expressed in a simple relationship between maximum burial depth ( $B_{max}$ ) and the present-day burial depth ( $B_{present-day}$ ) (Eq. 2). In addition, where post-exhumation burial ( $B_E$ ) has occurred, *gross exhumation* ( $E_G$ ) can be calculated (Eq. 3; Menpes & Hillis 1995; Corcoran & Doré 2005).

$$B_{max} = E_N + B_{present-day} \quad (2)$$

$$E_G = E_N + B_E \quad (3)$$

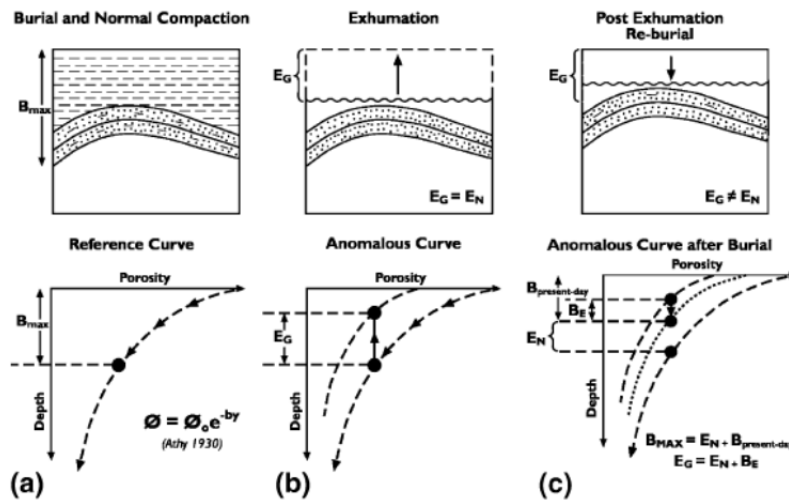


Figure 3: Graphical representation of the evolution of porosity-depth trends in exhumed sedimentary basins; (a) ‘normal compaction (exponential decay of porosity with burial depth, under hydrostatic conditions) in subsiding basin – the reference curve. (b) exhumation leads to anomalous porosity vs. depth trend with vertical

displacement from the reference curve yielding an estimate *gross Exhumation* ( $E_G$ ). (c) *post-exhumation reburial* ( $B_E$ ) reduces the vertical displacement between the anomalous curve and the reference curve to *net exhumation* ( $E_N$ ) at a given well location (after Corcoran & Doré 2005).

Compaction-based techniques may directly employ core-porosity measurements in order to generate porosity-depth trends, however, porosity proxies, such as density and sonic velocity or sonic transit times inferred from wireline log data, can be used to infer porosities and are commonly used (Giles et al. 1998).

### Sonic transit time-depth trends

Although porosity directly describes compaction state, sonic transit times is widely used as an indicator of compaction because it is strongly dependent on porosity (e.g. Wyllie et al. 1956) and is routinely logged in wells (Hillis 1995a), and so can be used for quantifying the magnitude of exhumation (e.g. Japsen 2000; Ware and Turner 2002).

Sonic wireline log data records a formation's interval transit time ( $\Delta_t$ , reciprocal of velocity), which is usually expressed in microseconds per foot or metre. The sonic tool consists of a transmitter that emits a compressional sound wave, and a receiver that records the time required for the sound wave to traverse one foot of formation (Schlumberger 1989; Rider 1996). It is a measure of the formations capacity to transmit soundwaves, which will vary according to lithology and rock texture, notably porosity (Rider 1996). Using (and rearranging) Wyllie et al. (1956)'s time-average equation and if the lithology of a formation is known, porosity ( $\phi$ ) can be calculated (Eq. 4) and applied to porosity-depth trends.

$$\phi = \frac{(\Delta_t - \Delta_{tma})}{(\Delta_t - \Delta_{tf})} \quad (4)$$

Where:  $\phi$  is porosity

$\Delta_t$  is the measured interval transient time

$\Delta_{tma}$  is the interval transient times through the solid matrix

$\Delta_{tf}$  is the interval transient times through pore fluid space

Alternatively, exhumation can be quantified directly from the comparison of measured velocity-depth trends and normal velocity-depth trends without expressing it in terms of porosity.

## LITERATURE REVIEWS

This approach has been used effectively in many studies (Bulat & Stoker 1987; Hillis 1995a), however, Japsen et al. (2002) advises that velocity baselines are not an arbitrary choice of mathematical functions and regression parameters, but should be considered as setting up a physical model for a given lithology. Apparent exhumation,  $E_A$ , (see Table 2) can be estimated graphically from the plots of interval transit time ( $\Delta t_u$ ) against the mid-point depth of the formation being analysed. However, in practice, it is determined numerically using Equation 5 where a normal compaction (reference) trend is assumed to be close to linear (Bulat & Stoker 1987) and is defined by the straight line linking the two wells with the highest interval transit time for their burial depth (Fig. 4; Hillis 1993; 1995a,b). Furthermore,  $d_u$  is the depth of the formation mid-point below sea-bed of the well under consideration, and  $m$  is the slope of the normal compaction line.

$$E_A = \frac{1}{m(\Delta t_u - \Delta t_0) - d_u} \quad (5)$$

Where:  $E_A$  is the apparent exhumation

$\Delta t_u$  is the interval transit time

$\Delta t_0$  is the surface intercept of the normal compaction line (greater than the velocity of seawater  $\sim 1500$  m/s)

$d_u$  is the depth of the formation mid-point below sea-bed of the well under consideration

$m$  is the slope of the normal compaction line

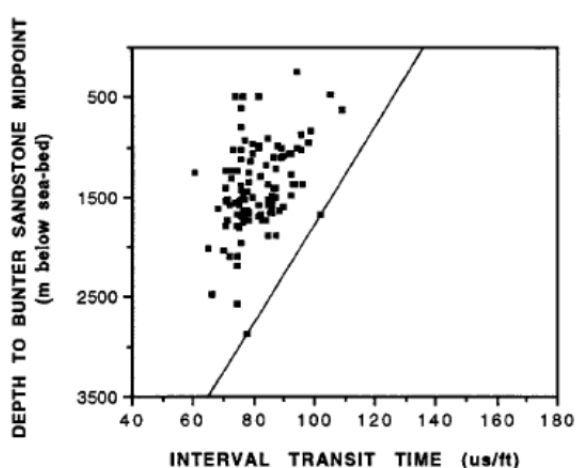


**Figure 4: Mean interval transit time vs. depth to unit mid-point for Bunter Sandstone in the Southern North Sea, United Kingdom. The normal compaction relationship (i.e. reference curve) for the unit is defined by the straight line linking the two wells with the highest interval transit time for their burial depth (after Hillis 1995a).**

### Bulk density-depth trends

Porosities are most commonly derived from sonic velocity data (e.g. Magara 1978), however, some studies (e.g. Holford et al. 2005a, 2009b) opted to use density wireline log data as a porosity proxy because they found velocities anomalously slow within some sedimentary successions, indicative of undercompaction, thereby overestimating porosity calculations.

The density log provides a continuous record of a formation's bulk density which is the overall density of a rock, incorporating the density of the rock's mineral matrix and the volume of free fluid it encloses, i.e. porosity (Rider 1996). The density logging tool emits gamma rays which are scattered and lose energy as a result of collisions with electrons in the formation (Allen & Allen 2005). The number of scattered rays recorded at a detector on the logging tool depends on the electron density of the formation, which is related to the true bulk density of the formation (Schlumberger 1989) and hence provides a relationship between bulk density and porosity. Using (and rearranging) Schlumberger (1989)'s equation and assuming other rock density values, porosity can be calculated (Eq. 6) and applied to porosity-depth trends.

$$\phi = \frac{(\rho_{ma} - \rho_b)}{(\rho_{ma} - \rho_f)} \quad (6)$$

Where:  $\phi$  is porosity

$\rho_b$  is bulk density

$\rho_{ma}$  is the average density of the rock matrix

$\rho_f$  is the average density of the fluid occupying the pore space (a function of temperature, pressure and salinity)

### ***Palaeo-thermal Techniques***

Palaeo-thermal techniques use the general principle that sedimentary rocks are progressively heated during burial and cool at the initiation of exhumation. This provides information, firstly, about the movement of rocks relative to a thermal frame of reference and secondly, quantitative estimates of the temperatures attained by individual rock samples at a palaeo-thermal maximum, prior to the onset of cooling (Green et al. 1995, 2002; Corcoran & Doré 2005; Holford et al.

2005b). In a vertical succession of rocks, peak palaeo-temperature profiles are interpreted from palaeo-thermal indicators, such as AFTA and VR data, which can be used to estimate the magnitude of exhumation.

#### *Apatite Fission-Track Analysis (AFTA)*

AFTA provides a powerful method of thermal history assessment in sedimentary basins that have experienced higher temperatures in the past, because not only does it provide estimates of maximum palaeo-temperatures (from which exhumation magnitudes can be estimated), but it also provides the *time* at which a sedimentary section began cooling from maximum palaeo-temperatures (Bray et al. 1992; Green et al. 2002; Holford et al. 2005a).

#### Fission-track generation

Fission-track analysis is the study of radiation damage zones (fission tracks) which form when charged nuclear particles travel through insulating solids, leaving trails of disrupted atoms (Fig. 5) (Hurford & Green, 1983; Gallagher et al. 1998). Fission tracks are produced continuously through geological time, as a result of the spontaneous fission of  $^{238}\text{U}$  atoms in detrital or accessory minerals, such as apatite [ $\text{Ca}_5(\text{PO}_4)_3(\text{F},\text{OH},\text{Cl})$ ], zircon [ $\text{ZrSiO}_4$ ] and sphene [ $\text{CaTiO}(\text{SiO}_4)$ ], which are generally found in sandstones and other clastic sedimentary rocks or igneous rocks, respectively (Green 2002). To produce detectable amounts of fission tracks, mineral grains must contain sufficient concentrations (~1-1000 ppm) of uranium (Green 2002). More complex distributions of track lengths results in more complex thermal histories where in rare cases, up to three episodes can be defined within a single sample if they sufficiently separated in time and temperature (Green et al. 2001a; Japsen et al. 2009). However, to define the whole thermal history is impossible because that part of the history prior to the onset of cooling is overprinted by the thermal maximum (Green et al. 1989, 2002).

#### Fission track annealing

The length and population density of any fission track depends on ‘annealing’, where annealing is the temperature dependent process whereby the crystal lattice repairs the damage caused by  $^{238}\text{U}$  fission (Fleischer et al. 1965; Green et al. 1986). The final length of each individual track is determined by the maximum temperature which that track has experienced at that time (Green et



al. 1986, 1989, 2002). Studies devoted to fission track annealing were conducted by various groups worldwide in the early-mid 1980's, however, it was not until the detailed kinetic studies of Hurford & Green (1983), Green et al. (1986), Laslett et al. (1987) and Green et al. (1989) that a significant understanding of fission track annealing kinetics came to light. In particular, Green et al. (1986) and Laslett et al. (1987)'s studies on the Durango granite in Mexico in which modern fission track annealing and kinetic models are based upon.

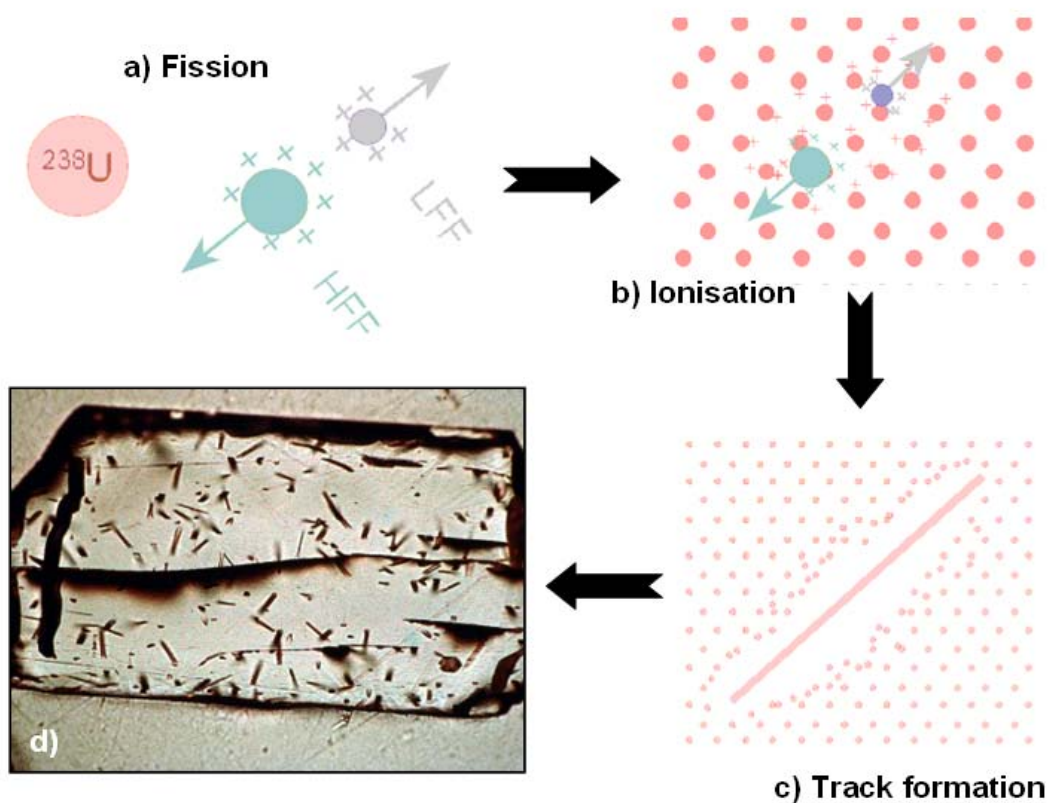


**Figure 5:** The formation of fission tracks in a uranium bearing mineral; (a) spontaneous fission of  $^{238}\text{U}$  produces two highly charged particles of different masses (heavy fission fragments (HFF) and low fission fragments (LFF)), which recoils as a result of Coulomb repulsion and interact with other atoms within the crystal lattice by electron stripping or ionisation (b). This results in further deformation of the lattice as the ionised lattice atoms repel each other. (c) As the fission particles capture electrons they slow down and begin to interact by atomic collision, which further reduces the particles' energy until they come to rest, leaving a radiation damage trail of 'fission-track' (after Gallagher et al. 1998); (d) Apatite from the Cheviot granite, NE England, showing a moderate spontaneous track density (adapted from GEOTRACK - <http://www.geotrack.com.au/afta-why.html>)

AFTA is generally preferred in the petroleum industry over zircon or sphene fission track analyses because apatite fission tracks totally anneal (i.e. the track length is reduced to zero) at temperatures that coincide with hydrocarbon generation (Green et al. 2002). Apatites totally anneal at temperatures (often referred to as the closure temperature) exceeding approximately  $110^{\circ}\text{C}$ ,

## LITERATURE REVIEWS

however, Gleadow & Duddy (1981) demonstrated that significant annealing within apatite occurs over a temperature range of at least 60°C, often referred to as the *partial annealing zone* (Wagner 1979). In contrast, zircon fission tracks are more stable, and the maximum palaeo-temperature must exceed ~350°C for total annealing (Gallagher et al. 1998).

Studies by Gleadow & Duddy (1981) and Green et al. (1985,1986) have also shown that apatites of different composition anneal at different rates. It was recognised by Green et al. (1985, 1989) that the amount of chlorine, in particular, in the apatite lattice exerted a subtle compositional control on the degree of annealing, with apatites poorer in chlorine being more easily annealed than those richer in chlorine (Green et al. 1986; Japsen et al. 2009). Green et al. (1989) and Duddy (1994) showed that annealing in fluorine-rich apatites from the Otway Ranges occurred between ~60-110°C whilst chlorine-rich apatites annealed between ~110-150°C (Fig. 6). The general annealing window for apatite fission tracks is therefore ~20-150°C, although annealing at temperatures less than 60°C requires very long periods of geological time (Cooper 1995). Other studies, for example Barbarand et al. (2003b) and Carlson et al. (1999), have found that other than chlorine, Rare Earth Elements, and Sr and Mn elements, respectively, exerted an appreciable control on annealing rates. This effect produces a variation in the degree of fission-track annealing, and thus, the accuracy of palaeo-temperature determination in different apatite grains within a single sample, which cannot be described using a kinetic model based on a single apatite species such as the Laslett et al. (1987) model (Green et al. 2002). A good model that has been used with considerable success in many studies around the world in a variety of tectonic settings (e.g. Crowhurst et al. 2002; Green et al 2001a,b; Holford et al. 2005a; Japsen et al. 2009) is Green et al. (1986)'s 'multi-compositional' model. This was derived directly from geological data and in combination with laboratory data (Green et al. 2002). This model uses a similar kinetic model to Laslett et al. (1987)'s "fanning Arrhenius Plot" model, but with kinetic constraints which vary systematically with chlorine content. Comparing Laslett et al. (1987) and Green et al. (1986), it is widely accepted that the Laslett et al. (1987) model under predicts the degree of annealing at low temperatures and commonly suggests up to 30°C or more of late Cenozoic cooling and anomalously high amounts of removed section. The Green et al. (1986) model, on the other hand, provides an excellent fit to control data at low temperatures (Green et al. 2002).

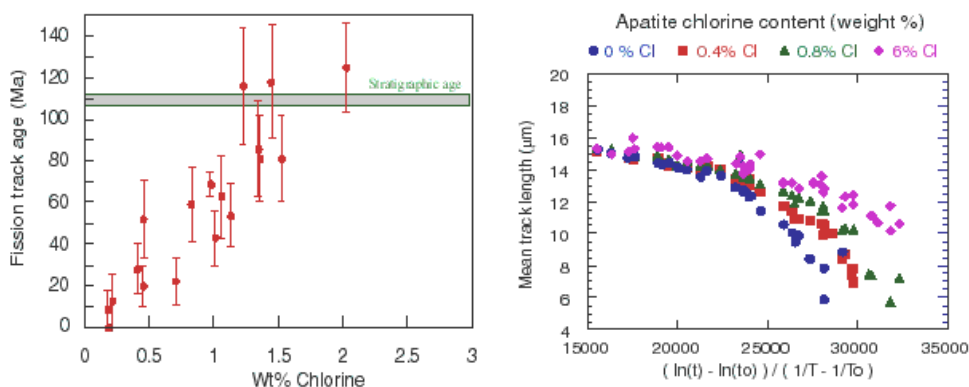


**Figure 6: Variation of fission track age with Chlorine content.** (a) shows single grain ages plotted against wt% Cl from a sample of Early Cretaceous sandstone from present-day temperature of 100°C (~2585m depth) in Flaxmans -1 well in the Otway Basin, South East Australia. Fission track ages in apatites with low Cl contents are close to zero, while values in apatites containing 2 wt% Cl are still close to depositional age, and have undergone very little age reduction. (b) Shows results from laboratory isothermal annealing experiments involving four apatites with different chlorine contents. Mean track length in each apatite is plotted against a combined function of annealing temperature and time, to reduce the data to a common scale. Pure fluorapatite is totally annealed in conditions where the mean track length in apatite containing 0.8 wt% Cl is still around 12 microns (adapted from Green et al. 1986).

In addition to temperature and chlorine content, other controls such as time, pressure, chemical solutions and ionizing radiation may also influence the fission track evolution after initial formation (Gallagher et al. 1998). Recent experimental work on the pressure dependence of apatite fission track annealing by Wendt et al. (2002) suggested that the stability field of fission tracks in apatite increases towards temperatures higher than 110°C depending on the absolute pressures. This would have major implications on current models that consider pressure effects to be negligible over geological timescales (e.g. Fleischer et al. 1965; Naeser & Faul 1969; Laslett et al., 1987; Green et al., 1989); however, these results have been refuted by studies such as Kohn et al., (2003) for a number of reasons. In relation to VR, total annealing of fission tracks in apatite corresponds approximately to a VR value of 0.7% (Green et al. 2004).

### *Vitrinite Reflectance (VR)*

Vitrinite is a type of maceral derived from plant cell walls, cell contents or precipitated gels, and its reflectance increases with the percentage of carbon in mineral-free coal (i.e. coal rank), which in turn, increases with increasing burial time and temperature. (Beardsmore & Cull 2001). For this reason, VR is used as a palaeo-thermal indicator to assess the thermal maturity of organic matter (post-Silurian only) and has been adopted in hydrocarbon exploration as a standard measure for modelling source rock maturation (Burnham & Sweeney 1989; Green et al. 2002; Patersen et

## LITERATURE REVIEWS

al. 2009). Its popularity in petroleum industry is due to the fact that hydrocarbons are by-products of the metamorphism of organic material (kerogen) and the degree at which metamorphism has progressed is measured by VR (Beardsmore & Cull 2001).

Source rock maturity is primarily a function of time and temperature (Burnham & Sweeney, 1989) and a number of kinetic models have been suggested for the evolution of reflectance (e.g. Tissot, 1969; Waples, 1980), however, Burnham & Sweeney (1989) and Sweeney & Burnham (1990)'s chemical kinetic model is undoubtedly the most successful (Green et al. 2002). Barker & Pawliewicz (1986) proposed an empirical relationship between reflectance and temperature which has been employed in some studies (e.g. Corcoran & Clayton 2001), although this model ignores the influence of time (Green et al. 2002). In contrast, the Burnham & Sweeney (1989) and Sweeney & Burnham (1990) model uses Arrhenius rate constants (Eq. 8) and considers separate reactions for the elimination of water, carbon dioxide, methane, and higher hydrocarbons from the maceral, and then calculates vitrinite reflectance from correlations of reflectance with carbon content and with H/C and O/C atomic ratios.

$$K = Ae^{\left(\frac{-E_A}{RT}\right)} \quad (8)$$

where:  $K$  is the reaction constant,

$A$  is a constant sometimes referred to as the frequency factor (it is the maximum value that can be reached by  $K$  when given an infinite temperature)

$E_A$  is the activation energy

$R$  is the Universal Gas constant (8.314472 J/K.mol)

$T$  is absolute temperature (in Kelvins)

VR derived palaeo-temperature estimates using this model have a precision between 5 and 10°C (Crowhurst et al. 2002) and shows good agreement between measured and predicted VR values (at least up to c. 1.0%) in sediments that have undergone progressive burial, and are now at their maximum post-depositional palaeo-temperatures. Thermal history modelling provided by AFTA data confirms the validity of the kinetic model for 0.3% <VR< 4% values in realistic geological conditions (Burnham & Sweeney, 1989; Bray et al. 1992; Green et al. 2002).

## LITERATURE REVIEWS

### *Less common methods to estimate palaeo-temperatures*

Other, less common, techniques used to measure palaeo-temperatures in sedimentary basins are compared by Beardsmore & Cull (2001) and are shown in Table 3. However, Green et al. (2002) advises that apart from AFTA and VR, no other palaeo-thermal indicators are currently understood in sufficient detail to allow quantitative estimation of maximum palaeo-temperatures and additional errors and uncertainties may occur when converting other less common palaeo-thermal indicators to equivalent VR values (e.g. Thermal Alteration Index (TAI), Conodont Alteration Index (CAI) and  $T_{\max}$ , Spore Colour Index (SCI)).

### *Estimating the magnitude of exhumation from palaeo-thermal indicators*

As described above, palaeo-thermal indicators provide qualitative estimates of the temperatures attained by individual rock samples at a palaeo-thermal maximum, prior to the onset of cooling (Green et al. 1995, 2002; Holford et al. 2005a). For this reason, they can be used to reconstruct more complete histories, for example, in places where significant unconformities are present from which sedimentary successions have been removed/eroded, than techniques based purely on the preserved rock record (Green et al. 2002). This is fairly straight forward in sections with only one unconformity where conventional techniques such as back stripping and seismic interpretation can be employed; however, sections with multiple unconformities may be more difficult to estimate the amount of removed section during the unrepresented time intervals (Green et al. 2002; Holford et al. 2005b).

AFTA and VR data are the most commonly used palaeo-thermal indicators and the two different data sets are often integrated in thermal history reconstructions because they provide independent constraints on maximum palaeo-temperatures and give greater confidence in the palaeo-geothermal gradient estimation. Integration of the two data sets is especially useful (and preferred) in studying regional tectonics, in revealing and delineating episodes of basin inversion, regional uplift and erosion and heating due to hot fluid circulation (Bray et al. 1992; Green et al. 2004). A slight difference between the two, however, is that VR data can provide discrete estimates of maximum post-depositional palaeo-temperatures, whilst AFTA can provide either upper or lower limits, or a range of values for the maximum palaeo-temperature (Bray et al. 1992; Green et al. 2002; Holford et al. 2005b). In addition, VR data can be used to extend the temperature and depth range of gradient information beyond that of AFTA and can give

## LITERATURE REVIEWS

information over parts of a well section where AFTA data is not available: where suitable lithologies are not present (Bray et al. 1992).

Analysis of a series of palaeo-temperature estimates, from AFTA and/or VR, over a range of depths from exploration wells (or elevations of onshore outcrop samples in mountainous terrains) show the variation of maximum palaeo-temperature with depth, which in turn, generates a palaeo-temperature profile or palaeo-geothermal gradient. The generation of a palaeo-geothermal gradient is important in exhumation studies because it then allows interpretation on the likely mechanisms of heating and cooling in the rock successions' history in comparison to present-day temperatures (obtained from bottom-hole temperature measurements) (Bray et al. 1992; Holford et al. 2005b). If heating is solely caused by deeper burial then the palaeo-temperature-depth profile should be approximately linear with a similar gradient to the present-day temperature profile. In contrast, heating which was primarily a consequence of elevated basal heat flow (possibly also with a component of deeper burial) should produce a more or less linear palaeo-temperature profile, although it will have a higher gradient than the present temperature profile (Duddy et al. 1994). Green et al. (2002) agrees that a linear approximation is reasonable; nevertheless, the palaeo-temperature profile varies depending on the lithologies' thermal conductivity. However, practical experience shows that in most situations, small-scale variations in lithology serve to blur any local thermal conductivity contrasts.

Having then interpreted the palaeo-temperature profile to be linear and due to deeper burial, the amount of section (which was once more deeply buried) removed as a result of exhumation can be estimated by extrapolating this profile to an assumed palaeo-surface temperature (Fig. 7). In the absence of such palaeo-surface temperature information, either the present day value can be used, or else calculations can be performed for a range of likely values (Green et al., 2002; Holford et al. 2005b).

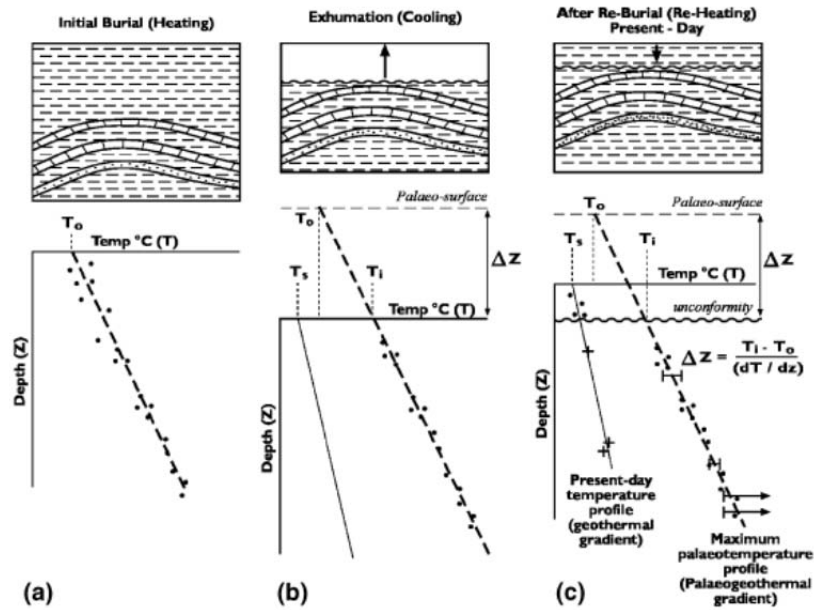


Figure 7: Thermal history based techniques rely on the general principle that rocks are heated as they are buried but cool as they are exhumed. (a) Initial burial and heating recorded and ‘locked-in’ by thermal indicators followed by (b) exhumation and cooling of rocks which facilitates (c) determination of peak palaeo-temperature vs. depth profile from VR and AFT analysis of a vertical sequence of sample data from the wellbore. Present-day temperature profile is established from corrected BHT measurements. By comparing the palaeo-geothermal gradient with the present-day geothermal gradient it can be deduced if the preserved section has been hotter in the past and interpretations can be made with respect to the cause of the high palaeo-temperatures and the subsequent cooling to present-day temperatures. Under certain conditions, the peak palaeo-temperatures (prior to exhumation) can be used to establish a palaeo-geothermal gradient, and by extrapolation to an assumed palaeo-surface temperature can yield an estimate of exhumation ( $\Delta Z$ ) at unconformity.  $T_i$ =palaeo-temperature intercept at unconformity;  $T_o$ =palaeo-surface temperature;  $T_s$ =present-day surface temperature;  $(dT/dZ)$ =palaeo-geothermal gradient. Magnitude of removed section (gross exhumation) is given by  $\Delta Z = (T_i - T_o) / (dT/dZ)$  (adapted from Bray et al., 1992 and Green et al., 2002) [• Palaeo-temperature point derived from VR; P palaeo-temperature range from AFT; + present-day temperature from corrected BHT data]. After Corcoran & Doré (2005).

Depending on the time-scale of heating, in situations, for example, where heat flow is the result of hot fluids flowing in an aquifer, igneous intrusions or large scale contrasts in thermal conductivity, the palaeo-temperature profile is not likely to be linear. Therefore, the amount of section eroded cannot be estimated using the technique just discussed (Fig. 7; Duddy et al. 1994; Green et al. 2002). To be sure of such effects (which can in some cases mimic the effects of deeper burial), regional data coverage is required (Green et al. 2002).

LITERATURE REVIEWS

Table 3: Summary and comparison of various palaeo-temperatures indicators, modified from Beardsmore & Cull (2001)

Palaeo-temperature indicator	Main rock type	Sediment component analysed	Equipment required	Approximate maturity range (VR <sub>eq</sub> )	Palaeo-temperature precision	Maximum measurable palaeo-temperature	Time information	Limitations
<i>Vitrinite Reflectance (VR)</i>	Vitrinite	Siltstone, shale	Reflecting light microscope, photometer	0.3-5.0	± 5°C	>350°C	None	Reflectance suppression in marine deposits
<i>Fluorescence Alteration of Multiple Macerals (FAMM)</i>	Various macerals		Laser fluorescence microprobe	0.4-1.2		175°C		Small number of laboratories set up for technique
<i>Thermal Alteration Index (TIA)</i>	Polymorphs		Transmitting light microscope, non-colour blind operator	0.3-2.4	± 20°C or higher	260°C		Subjective, poor temperature resolution
<i>Conodont Alteration Index (CAI)</i>	Conodonts	Carbonates		0.3-5.0+	± 20-50°C	>600°C		Subjective, Cambrian-Triassic only, poor resolution
<i>Illite crystallinity</i>	Illite	Shale	X-ray diffraction instrument	0.4-5.5	± 10°C	300°C		Clay composition changes due to fluids
<i>Pyrolysis</i>	Organic matter	All sediments	Gas-chromatography mass spectrometer with pyrolysis inlet, or RockEval tool	0.6-1.4	± 5°C	200°C		Must use standard heating rate, results vary from sediment type
<i>Fluid inclusions</i>	Fluid inclusions in calcite, quartz, feldspar grains	Sandstone, limestone	Microscope, heating stage	n/a	± 2°C	>1000°C	Relative timing of different inclusions	Only gives temperature at times of fluid migration
<i>Molecular Biomarkers</i>	Extracts and pyrloysates	All sediments	Gas-chromatography mass spectrometer	0.3-2.0	± 15°C	240°C	None	Most indices are poorly calibrated to VR
<i>Apatite Fission Track Analysis (AFTA)</i>	Apatite	Sandstone	Microscope, thermal-nuclear reactor, mass spectrometer	0.3-1.0	± 5-10°C	130°C	Absolute age of last cooling event	Composition of apatite must be determined
<i>(U-Th)/He</i>	Apatite	Sandstone	Mass spectrometer	~0.3-0.7	± 7°C*	80°C	Absolute age of last cooling event	Composition of apatite must be determined

\* From Wolf et al. (1996).



## METHODS FOR QUANTIFYING THE TIMING OF SEDIMENTARY BASIN EXHUMATION

The best techniques to quantify the timing of sedimentary basin exhumation utilize low temperature thermochronological methods such as AFTA and (U-Th)/He dating of apatite. AFTA is by far the most commonly used method to estimate thermal histories and has been used with considerable success (e.g. Green et al 2002; Holford et al 2005a), however, the novel technique of (U-Th)/He dating of apatite is emerging as an important low-temperature thermochronometer that can be applied to many geological settings (Crowhurst et al. 2002). As discussed in Section 3.2.1, AFTA generally provides maximum palaeo-temperatures estimates at approximately  $<110^{\circ}\text{C}$ , and several workers have indicated that at lower temperatures ( $<60^{\circ}\text{C}$ ), fission-track data are unreliable and can produce spurious results for geologically recent exhumation (Doré et al. 2002a). (U-Th)/He dating of apatite, on the other hand, has maximum palaeo-temperature sensitivities ranging between  $50\text{-}80^{\circ}\text{C}$  which can potentially define the timing of more recent cooling episodes with greater precision (Green et al. 2004). Integration of these two techniques can provide improved thermal history constraints in sedimentary basins, particularly on cooling rates and/or resolution of multiple thermal events (Green et al. 2004; Crowhurst et al. 2002). However, this may not be true in all studies (e.g. Japsen et al. 2009) and this method will not be discussed in detail in this literature review.

### *Apatite Fission-track dating*

In addition to being a tool to estimate the magnitude of exhumation, AFTA is a powerful and extremely useful technique in petroleum industry because it provides an independent and objective estimate of the time at which a rock sample began to cool from its maximum palaeo-temperature (Green et al. 1995). Therefore, if cooling can be attributed to exhumation, AFTA can define the timing of the onset of that exhumation (Green et al. 2002). Constraining the timing of exhumation may provide insight into the underlying causes of exhumation (Holford et al. 2005b) as well as assessing the regional hydrocarbon prospectivity and reducing exploration risk by focussing on regions where hydrocarbon generation post-dates structuring (Green et al. 2004).

Unlike other isotopic dating methods, AFTA dates radiation damage rather than another isotope (e.g.  $\text{U} \rightarrow \text{Pb}$ ). For this reason, depositional (or crystallisation) age should not be confused with fission-track age, where depositional age is the time at which the mineral formed whilst fission-track age is the time at which the mineral cooled from its maximum palaeo-temperature. It

may be difficult to discriminate fission-track age from pre-depositional ages if cooling began early or late in its history, which may result in larger or minimal uncertainties, respectively, in dating precision (Green et al. 2002).

The apatite fission track age is given by the proportion of uranium atoms per unit area (Barbarand et al. 2003a). Thus, the areal density of the tracks present in a polished surface of an apatite grain depends on the uranium content of the grain, the time over which tracks have accumulated and the length of the tracks (Green 2002). Apatite fission track analysis, therefore, requires an estimate of the relative abundance of the parent and daughter product, the number of  $^{238}\text{U}$  atoms, and the number of spontaneous fission-track (Gallagher et al. 1998). The Uranium content is determined from an external source (e.g. electron microprobe; Hasebe et al. 2004) and then the zeta ( $\zeta$ ) calibration developed by (Hurford & Green 1983) is used to determine the fission-track age (Eq. 9). Details of the Hurford & Green (1983)'s method to determine fission track age can be seen in Fig. 8.

$$T = \frac{1}{\lambda_D} \ln \left( 1 + \lambda_D \zeta \frac{\rho_S}{\rho_i} \rho_d \right) \quad (9)$$

Where:  $K$  is the reaction constant,

$T$  is the fission track age

$\lambda_D$  is the total decay constant ( $^{238}\text{U} = 1.55125 \times 10^{10}$  per year)

$\rho_S$  is the spontaneous track density

$\rho_i$  is the induced track density

$\rho_d$  is the track density in mica standard

$\zeta$  is the zeta function

## LITERATURE REVIEWS

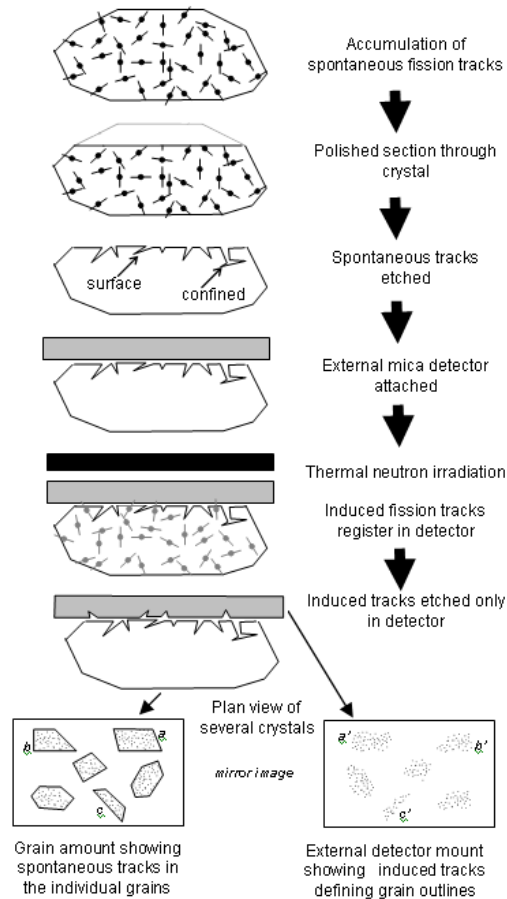


**Figure 8: Diagram representing the sequence of Hurford & Green (1983)'s method in order to determine the fission track age of a mineral. Firstly, the mineral's surface is polished and etched using dilute HNO<sub>3</sub> in order to reveal surface and confined spontaneous fission tracks. A Uranium-free detector (usually muscovite mica) is attached to the etched surface and then the sample is sent to a nuclear reactor where it is irradiated with low energy neutrons which induce fission in <sup>235</sup>U. During fission, some heavy particles cross the interface between the mineral and the mica. The mica is then also etched to reveal the induced tracks. By counting the number of induced tracks in the mica we estimate the uranium, or parent, concentration of the mineral grain, whereas by counting the number of spontaneous tracks in the mineral we estimate the concentration of the daughter product. After Gallagher et al. (1998).**

AFTA involves many analyses that generate a statistical spread of results due to origins of the different grains. For this reason, fission track ages are normally quoted as either a *pooled age* or *central age*. The difference between the two ages is that the pool age is a combined estimate of the age of the population where all grains are consistent with a single population, whereas the central age is an estimate of the model age in a sample containing a distribution of age populations (Galbraith 1990). In order to discriminate which fission track age to use, the  $\chi^2$  statistical test is used (Galbraith 1981) where values of  $\chi^2 > 5\%$  the pooled age is used and values of  $\chi^2 < 5\%$  the central age is used.

The rock column's thermal history is thus determined by modelling AFTA parameters (i.e. fission track age and track length distribution), which are based on a detailed knowledge of the kinetics of the annealing process (incorporating Cl content; see Section 3.2.1.1), through a variety

## LITERATURE REVIEWS

of possible thermal history scenarios (Fig. 9; Green et al. 1989). The magnitude of the maximum palaeo-temperature and the timing of cooling are then varied in order to define the range of values of each parameter which give predictions consistent with the measured data within 95% confidence limits or an absolute uncertainty of between  $\pm 5$ - $10^\circ\text{C}$  (Green 2002; Green et al. 2002). However, Japsen et al. (2009) explain that in some cases, due to the high degree of redundancy in AFTA data, it is not possible to extract explicit thermal history solutions directly because many histories result in the same measured age and length parameters. Green et al. (2002), however, suggest that the accuracy of timing estimates from AFTA mainly depends on the use of an appropriate kinetic model, but precision often depends on critically on the magnitude of the palaeo-thermal effects.

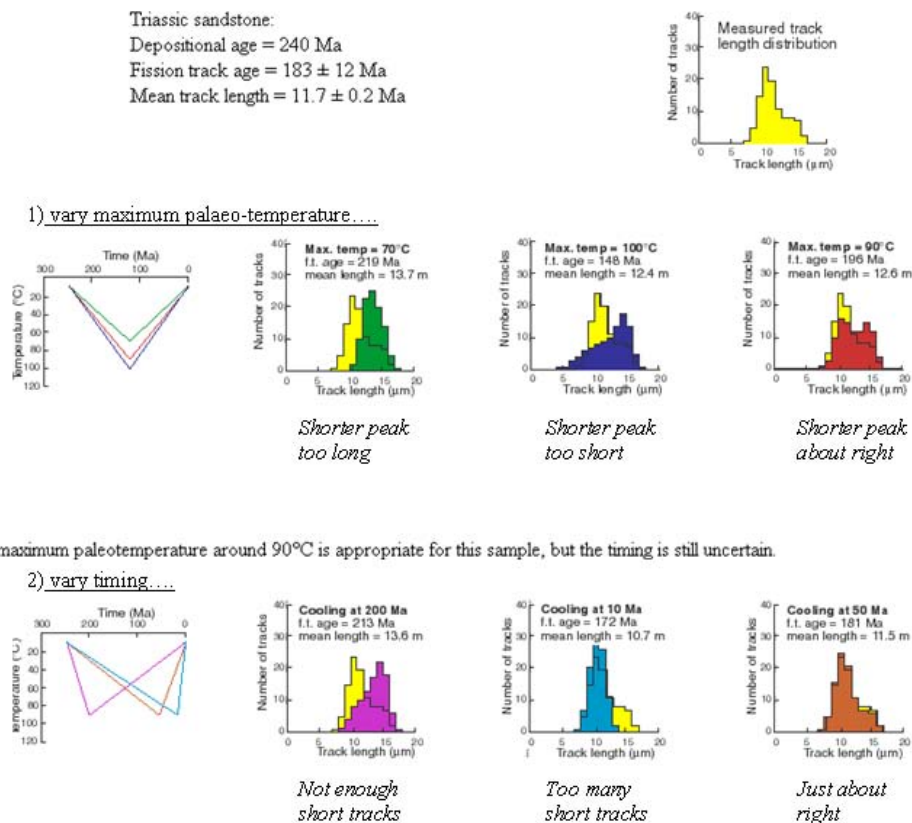


**Figure 9: Extracting thermal history solutions from AFTA data involves modelling AFTA parameters (Green et al. 1989) through various thermal history scenarios, using formal statistical procedures to define the range of maximum palaeo-temperatures and timing of cooling for which predictions are consistent with the measured data. This process requires a detailed knowledge of the kinetics of the annealing process. This synthetic example, based on a notional mono-compositional example, for simplicity, illustrates the basic principles involved. Cooling from a maximum palaeo-temperature of  $90^\circ\text{C}$  beginning at 50 Ma gives the best fit to the data. After Green et al. (2002).**

## UNCERTAINTIES AND LIMITATIONS OF QUANTIFYING EXHUMATION MAGNITUDES USING THERMAL AND COMPACTION-BASED TECHNIQUES

In the preceding sections, methods used to quantify the magnitude and timing of exhumation in sedimentary basin has been discussed. These methods have been used effectively and successfully in many studies (e.g. Corcoran & Mecklenburgh 2005; Holford et al. 2005b, Holford et al. 2009b; Japsen et al. 2007, 2012); often in combination with each other to better constrain a model that incorporates each of these independent data sets. For example, Holford et al. (2005a) used porosity data from shales in conjunction with thermal based proxies because in contrast to AFTA and VR, sedimentary porosities are largely unaffected by transient heating episodes, which in the absences of an interdependent measure of former burial depths, can often be misinterpreted in terms of deeper burial.

In Corcoran & Doré (2005)'s review on exhumation quantification methods, they, like Holford et al. (2005a), believe that cross-referencing estimates of timing and magnitude between different methods is an essential step in reducing uncertainty in the exhumation estimate. Furthermore, they add that the addition of stratigraphic and seismic evidence with these proxies is a critical factor in validating and better constraining this estimate (Japsen et al. 2009). However, although uncertainties may be reduced by integrating different methods together and incorporating stratigraphic and geophysical constraints, each method is not without their limitations that may cause uncertainty to arise. Corcoran & Doré (2005) provide an excellent discussion of the limitations associated with the four different approaches (i.e. compaction-based, thermal, tectonic and stratigraphical) in which the timing and magnitude of exhumation is quantified. Again, only the techniques discussed thus far have their limitations included.

### ***Limitations Associated with Palaeo-thermal Techniques***

Limitations associated generally with palaeo-thermal techniques include:

- Non-linear palaeo-temperature profiles cannot be used to estimate the magnitude of exhumation at a given well location (Duddy et al. 1998).
- Palaeo-thermal indicators such as VR and AFTA are dominated by maximum palaeo-temperatures and do not preserve information on thermal events that occurred prior to peak palaeo-temperatures (Corcoran & Doré 2005).
- An underlying assumption of thermal history techniques is that the measured palaeo-thermal profiles represent the distribution of temperature with depth immediately prior to exhumation. In highly stretched basins and for old (especially syn-rift) stratigraphy, the palaeo-thermal

## LITERATURE REVIEWS

indicators may represent maximum palaeo-temperatures attained early in basin history (e.g. due to heat-flow pulse from rifting) and are not subsequently exceeded (Allen et al. 1998).

- Assumes that the palaeo-temperature-depth profile is linear through the preserved section and that the palaeo-geothermal gradient can be linearly extrapolated through the removed section to the assumed palaeo-surface temperature. This assumption is valid only in cases where the thermal conductivity of the removed and preserved sections is identical (Corcoran & Doré 2005).
- Estimation of palaeo-surface temperature (Bray et al. 1992).
- Effects of early heating are overprinted by later heating when the magnitude of the more recent event exceeds that of the earlier episode (Green et al. 2002).

Limitations specifically associated with AFTA include:

- Cannot provide very precise constraints on the duration of episodes of cooling or rates of cooling, although broad limits on the magnitude and duration of cooling phases may be possible (Green et al. 2002).
- Complete annealing of fission-tracks in apatite generally occurs in the 110–120°C range so AFTA cannot store information on exhumation (cooling) events that occurred prior to the most recent episode of ‘complete annealing’ of tracks (Corcoran & Doré 2005).
- Variability of result cause confidence limits that are so wide that the thermal history solutions provide no useful constraints (Green et al. 2002).

Limitations specifically associated with VR include:

- Translation of VR values into absolute palaeo-temperatures can introduce systematic errors in the estimation of palaeo-geothermal gradients and consequently, the magnitude of exhumation (Green et al. 2002). Although Sweeney and Burnham (1990)’s kinetic model is widely accepted as the most accurate model to convert VR to palaeo-temperatures, other empirically based conversion models are also used over wider maturity ranges (e.g. Barker and Pawliewicz 1986) which produce higher palaeo-geothermal gradients and lower estimates of exhumation relative to the Sweeney and Burnham model

## LITERATURE REVIEWS

- Offsets in VR (palaeo-temperature) profiles have many causes. Some of these can be attributed to geological factors such as faulting, lithological (thermal conductivity) variations or changes in organic provenance. Some result from the limitations of the VR sampling and analytical techniques, such as the deficiencies of cuttings samples and maceral misidentification, which can result in low reproducibility of identical datasets (Corcoran & Doré 2005).
- It is widely accepted that retardation of vitrinite reflectance commonly arises in overpressured sedimentary sequences (Hao & Chen, 1992). The general effect of VR retardation is to decrease the calculated palaeo-geothermal gradient (Corcoran & Doré 2005).
- Suppression of vitrinite reflectance can result from the presence of hydrogen-rich vitrinites, leading to perhydrous compositions particularly in alginite-rich shales. Consequently, variations in the chemical composition of vitrinite between well locations may lead to variation in palaeo-geothermal gradient and associated exhumation estimates. Reliable thermal maturity gradients, however, may be established using a combination of conventional VR measurements and ‘equivalent VR’ values derived from the fluorescence alteration of multiple macerals (FAMM) technique (Petersen et al. 2009).
- A possibly more common problem, which may be more difficult to recognize, concerns the incorrect assignment of the *in situ* Vitrinite population throughout an entire well section due to the subjective nature from which the VR is measured. This can result in systematically low estimates of palaeo-temperature (and therefore palaeo-burial) and maturity levels (Skagen 1992; Green et al. 2002).

### ***Limitations Associated with Compaction-based Techniques***

Limitations associated with compaction data include:

- Using Wyllie’s time average equation for sonic velocity as a proxy for porosity is often invalid because porosity depends critically on lithology (Mavko et al. 1998).
- Stratigraphic units must exhibit a consistent relationship between depth and compaction if they are to be of use in exhumation analysis otherwise the compaction trend is obscured by the ‘data noise’ of lithological variation, diagenetic imprint and other factors (Corcoran & Doré 2005).
- Unreliability in establishing the baseline compaction trend (reference curve) for a basin or rock unit is a key limitation, particularly in basins where pervasive regional exhumation has occurred. Existing methodologies which utilize statistical manipulation to establish a reference

## LITERATURE REVIEWS

curve lack support from physical models and in some cases assume that a heterolithic sedimentary sequence can be described by a single average compaction coefficient (Corcoran & Doré 2005).

- Exhumation may be underestimated if the compaction process is partially reversed due to poroelastic 'rebound' (pore dilation and micro fracturing) caused by the removal of the overburden (Corcoran & Doré 2005).
- Caution must be exercised when interpreting compaction-derived exhumation estimates in basins containing mobile salt layers (Archard et al. 1998). Sonic velocity trends established in the carapace to a mobile salt-layer may contain a component of halokinetically induced exhumation, which is not relevant to the pre-salt stratigraphic units (Corcoran & Doré 2005).
- In hydrostatically pressured extensional basins both effective stress and temperature increase with burial depth, so it is generally uncertain when compaction or thermal processes are responsible for observed decrease in transit time. The sonic velocity method assumes that mechanical compaction is the dominant control on porosity loss through burial which may not always be true (Corcoran & Doré 2005).
- Even in basins where extensive well control is available, the selection of the reference succession is problematic. Ideally, it should represent a relatively homogeneous formation (in terms of mineralogy, cementation and acoustic properties) over an extensive depth range (single wells usually have a limited depth range for a given formation) and represent a hydrostatically pressured 'normal compaction' trend for that stratigraphic unit (Japsen 1998).



## ***2.2 LITERATURE REVIEW II: Tectonic Setting and Hydrocarbon Systems of the Otway Basin***

### **INTRODUCTION**

The Otway Basin is a large, broadly northwest trending basin encompassing onshore and offshore parts of South Australia and Victoria, and Tasmanian waters (Fig. 1; Krassay et al. 2004). It covers an approximate area of 60,000 km<sup>2</sup> and extends approximately 500 km from Mornington Peninsula in Victorian in the east to Cape Jaffa in South Australia in the west (Gallagher & Holdgate 2000; Aburas & Boulton 2001). Furthermore, it is continuous with the Sorrell Basin to the southeast (Moore et al. 2000), and is bounded to the north, northeast and east by Palaeozoic and Proterozoic basement (Krassay et al. 2004).

The Otway Basin is one of several basins (e.g. Gippsland, Bass, Bight, Sorrell, Bremer & Duntroon basins) that developed along the southern margin of Australia as a result of rifting (Southern Rift System (Willcox & Staggs 1990)) and eventual continental separation between Australia and Antarctica during the break-up of Gondwana. Break-up commenced in the Late Jurassic-Early Cretaceous (Norvick & Smith 2001; Lyon et al. 2007) and the now passive margin Otway Basin has since then experienced multiple rift-sag and inversion phases (Krassay et al. 2004), which has created stratigraphic and structural complexities that researchers and explorers sought to understand to better explore for hydrocarbon accumulations.

The Otway Basin is one of the best known and most actively explored basins along the Australian southern margin with more than 200 wells drilled and >35,000 km of 2D seismic lines covered off and onshore in South Australia, Victoria and Tasmanian (Geoscience Australia). A number of hydrocarbon discoveries, both commercial and non-commercial, have been made with workers acknowledging good source rock potential (e.g. Boreham et al. 2004; Edwards et al. 1999), however, almost all are composed of fairly dry gas and no commercial oil discoveries have yet to be identified. Presented in Table 1 are commercial gas discoveries in the Otway Basin (Geoscience Australia), which amount cumulatively to nearly 2 trillion cubic feet (TCF) of gas (O'Brien et al. 2009).

**Table 1: Summary of commercial gas discoveries (after Geoscience Australia; [www.ga.gov/energy/province-sedimentary-basin-geology/petroleum/offshore-southern-Australia/otway.html](http://www.ga.gov/energy/province-sedimentary-basin-geology/petroleum/offshore-southern-Australia/otway.html))**

First Commercial Discoveries	<ul style="list-style-type: none"> <li>• Victoria: 1979, North Paaratte-1</li> <li>• South Australia: 1987, Katnook-1</li> <li>• 1986, first Otway Basin gas supplied to Warnambool</li> </ul>
Onshore	North Parratte, Wallaby Creek, Katnook, Ladbroke Grove, Iona, Grumby, Boggy Creek, (CO <sub>2</sub> ), Caroline (CO <sub>2</sub> ) etc; 17 gas fields in Victoria and 5 in production: Wallaby Creek (19.8 BCF GIP <sup>1</sup> ), Skull Creek (2.2 BCF GIP), North Paaratte (18.2 BCF GIP) and Mylor (11.8 BCF GIP) and Fenton Creek (4.8 BCF GIP) (Mehin & Kamel 2002)
Offshore	La Bella-1 (217), Minerva-1 (558) in 1993, Geographe-1 (500) and Thylacine-1 (600) in 2001, Casino-3
Shows	<p><b>Sub commercial oil show:</b> Windermre-1, in Heathfield Sandstone Member</p> <p><b>Oil shows:</b> Killanoola-1, Redman-1, Sawpit-1 from basement and Crayfish Group.</p> <p><b>Minor oil shows:</b> Windermre-1 and Woolsthorpe-1 – Windermere Member; Port Campbell-4 and Flaxmans-1 – Eumeralla Formation; Breaksea Reef-1, Cape Sorell-1, Lindon-1 – Pebble Point Formation; Wilson-1 – Dilwyn Formation</p> <p><b>Gas shows:</b> Many wells including Pecton-1A, Troas-1, Voluta-1, Triton-1 and Casino-1 and 2 offshore. Recent exploration drilling in the offshore Otway Basin includes Hill-1 in 2003, Martha-1, Amrit-1 and Callister-1 in 2004 and Halladale-1 and Henry-1 in 2005. Gas shows or gas-bearing intervals have been reported for Martha-1, Callister-1, Halladale-1 and Henry-1.</p>

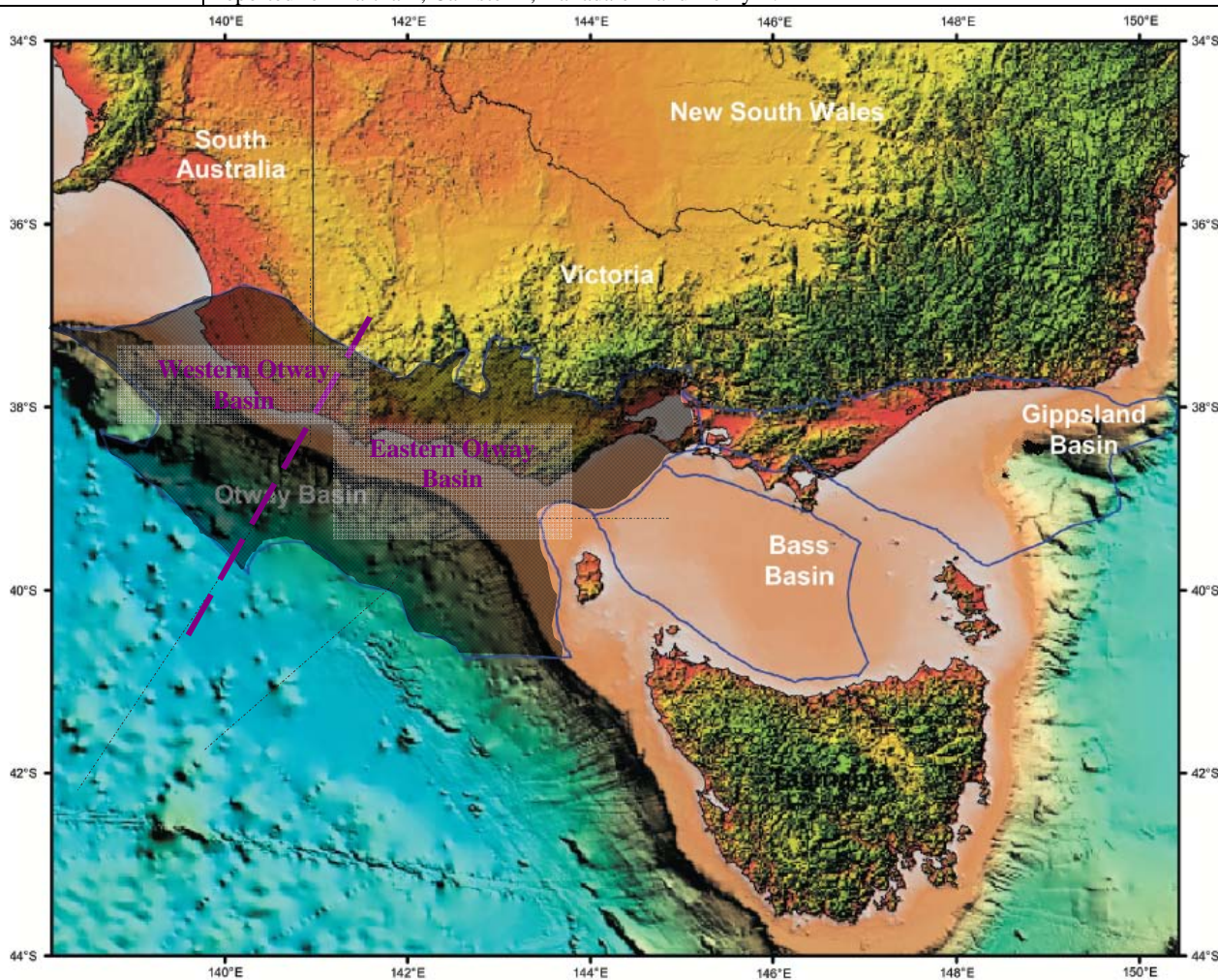


**Figure 1: Location of the Otway Basin in relation to other south-eastern Australian basins, the Bass and Gippsland basins (modified from Nelson et al. 2006). Often workers refer to the western and eastern parts of**

**the basin and this boundary is defined by Moore et al. (2000), which roughly follows the Discovery Bay High (Palmowski et al. 2004).**

The aim of this literature review is to present to the reader an objective overview to some of the studies that have been undertaken over the last couple of decades and to provide some of the conclusions of these studies that have shaped our current understanding of the Otway Basin. This review will first discuss the tectonic history and geological setting of the area near and around the Otway Basin followed by brief insights into the stratigraphy and structure of Otway Basin. A section on uplift is discussed and finally, this review will discuss the different petroleum systems that exist which cause this to be prospective petroliferous basin.

## **GEOLOGICAL SETTING**

### ***Basin Evolution and Tectonic Setting***

The Otway Basin is one of several basins (e.g., Bight, Gippsland, Bass and Sorell) along the southern margin of Australia that developed as a result of rifting and eventual continental separation between Australia and Antarctica (Norvick & Smith 2001; Krassay et al. 2004; Lyon et al. 2007).

As already mentioned, the Otway Basin forms part of the Southern Rift System (Willcox & Stagg 1990). Initial rifting began during the Callovian (Mid-Late Jurassic) at the western edge of the Bight Basin and propagated eastwards to the Otway Basin in the Tithonian (Late Jurassic-Early Cretaceous) (Norvick & Smith 2001; Lyon et al. 2007). The Otway Basin is the site of a triple junction where eastward propagation eventually jumped south along the Tasman Fracture Zone. This caused Tasmania to remain attached to the Australian Craton to form the Sorell Basin to the south, and the intra-cratonic, failed rift Gippsland and Bass Basins and Torquay Sub-basin to the east of the Sorell Fault (Fig. 2; Hill et al. 1994; Palmowski et al. 2004). Figure 3 shows a simplistic overview of the sedimentary sequences that are lithologically equivalent as a result of this west to east propagation of the southern Australian margin (Blevin & Cathro 2008).

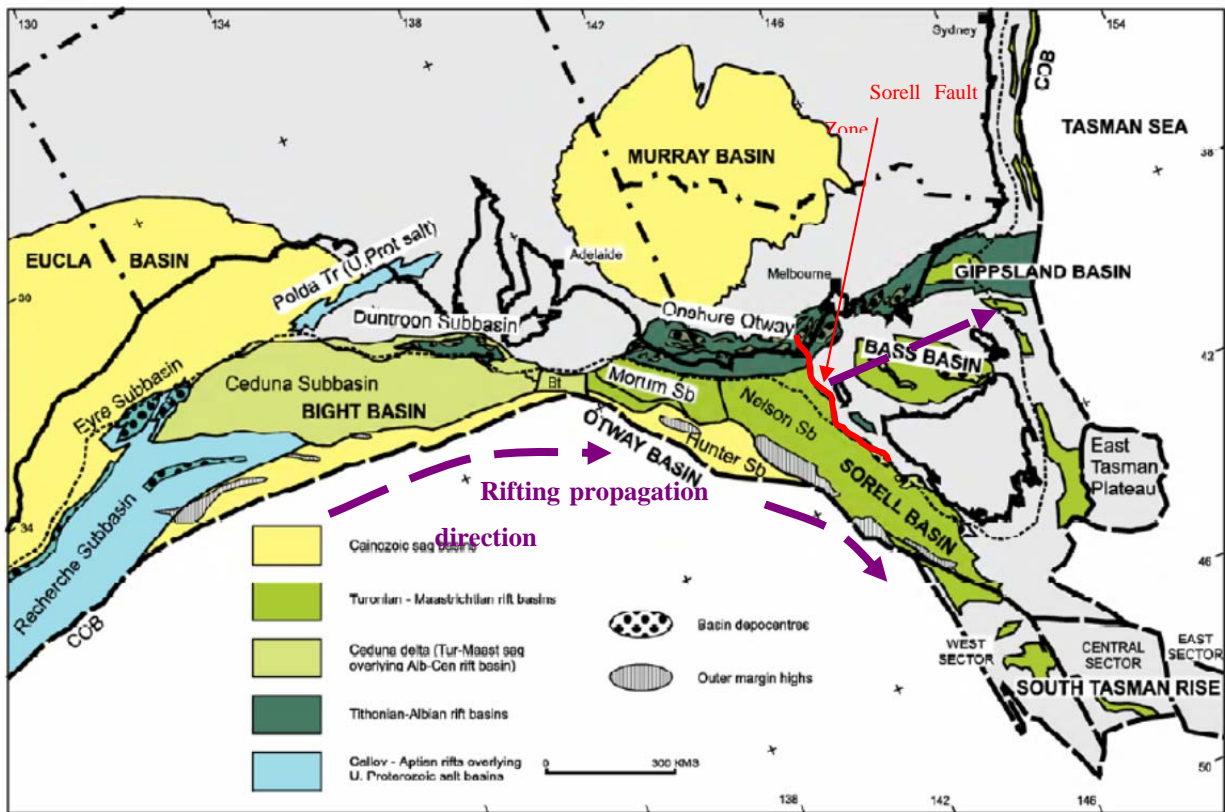


Figure 2: Structural elements map of southeast Australia (adapted from Moore et al. 2000) showing the Southern Margin basins as rifting propagated from west to east and the Otway Basin as the triple junction between the Sorell Basin to the south, Bass and Gippsland Basins to the east and the Bight Basin to the west.

LITERATURE REVIEWS

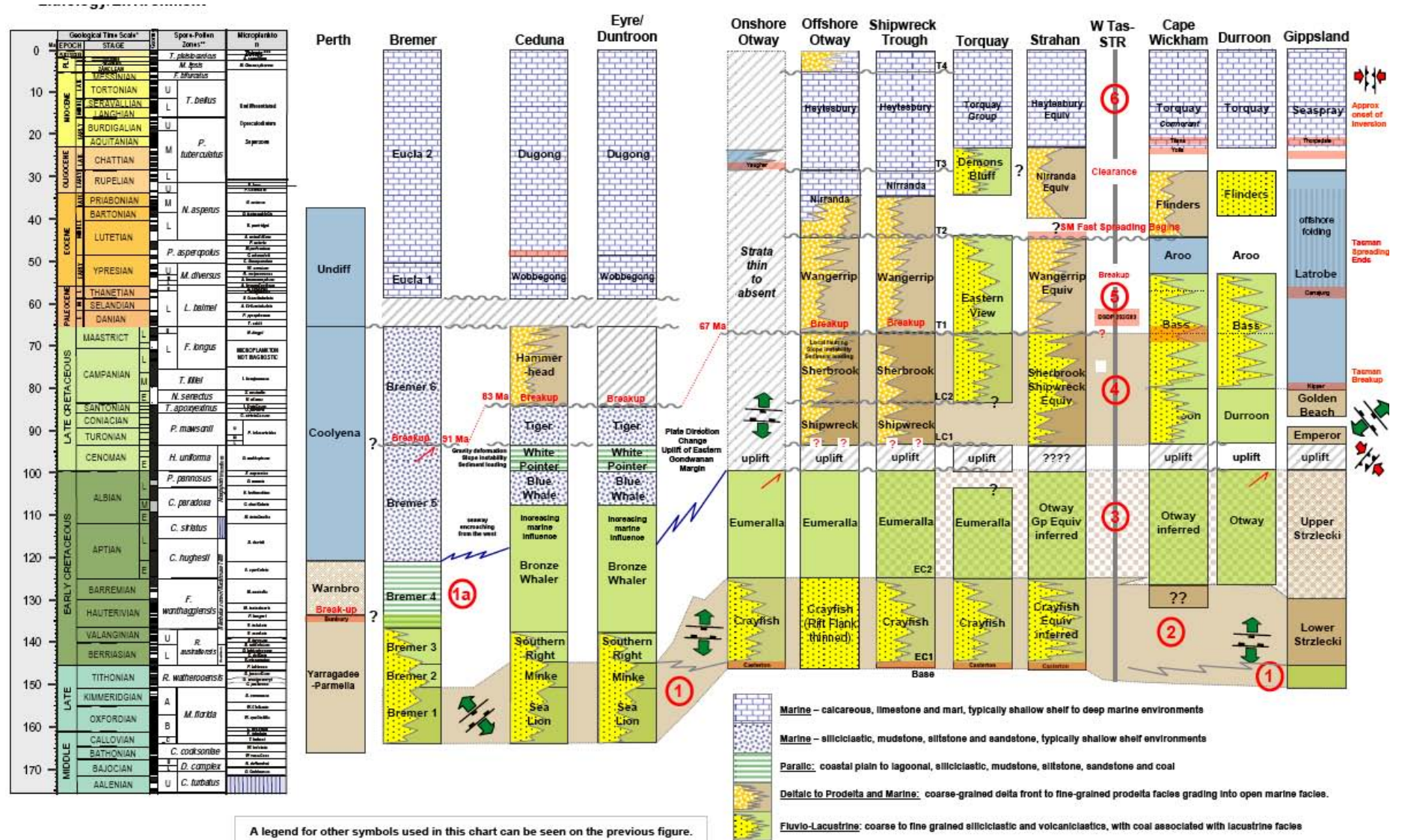


Figure 3: A recent chart correlating the progressive equivalent sedimentary sequences of the southern Australian margin basins from west to east (Blevin & Cathro 2008).

## LITERATURE REVIEWS

Studies by Norvick & Smith (2001), Moore et al. (2000) and Teasdale et al. (2003) are recommended to the reader for a more comprehensive plate tectonic reconstruction, structural framework and basin evolution overview, respectively, for the Southern Australian Margin. However, the complex evolution of the Otway Basin can be briefly described and characterised into five main events:

- Early Cretaceous rifting

Half-grabens developed along the entire Otway coast under the modern shelf with majority of the inner Otway Basin half graben faults dipping towards the north (Palmowski et al. 2001). The first-stage rifts had limited lateral extent (Krassay et al. 2004) and a number of authors have interpreted the extension direction that accommodated these rift structures differently based primarily on fault and depocentre trends. For example, Perincek & Cockshell (1995), Teasdale et al. (2003) suggest a NE-SW extensional direction whilst other earlier workers (Willcox & Stagg 1990; O'Brien et al. 1994; Williams et al. 1990) have proposed a NW-SE extensional regime, and differently again, Hill et al. (1994), Finlayson et al. (1998) and Lyon et al. (2007) have suggested a broadly N-S extensional direction. Initial rifting ceased at the end of the Hauterivian in the western Otway Basin with major faulting activity shifting south of the Tartwaup Fault Zone in the offshore parts of the basin, hence leaving onshore depocentre structures as failed initial rift structures similar to the current East-African graben system (Palmowski et al. 2001, 2004; Lyon et al. 2007). Fault activity slowed down in the Berremian to Albian and was replaced by regional, post-rift thermal subsidence (Palmowski et al. 2001; Lyon et al. 2007). Cooper & Hill (1997) performed seismic section restoration in the eastern Otway Basin and calculated 26% of Early Cretaceous extension

- Mid-Cretaceous inversion

Following initial rifting, the Otway Basin experienced regional NW-SE directed compression in the Cenomanian (c. 92-97.5 Ma) associated with local inversion which coincided with regional uplift and denudation of eastern Australia, erosion of Early Cretaceous sediments, stress reorganisation and divergence of basin development (Noll & Hall 2003; Hill et al. 1995; Palmowski et al. 2004; Norvick & Smith 2001). During this time, the Otway Ranges uplifted due to approximately 8-10% shortening (Hill & Cooper 1996; Cooper & Hill 1997) and effectively isolated the Torquay Sub-basin from the

remainder of the Otway Basin (Krassay et al. 2004). Finally, an earlier study (Smith 1988) proposed Mid Cretaceous uplift in the eastern Otway as a consequence of both thermal uplift associated with breakup, as well as NW-SE compression, based partially on reflection seismic data immediately southwest of the Otway Ranges (Hill et al. 1994).

- *Late Cretaceous rifting*

A hinge zone south of the first Early Cretaceous rift system developed basinward of the Late Cretaceous Tartwaup and Mussel fault zones, and produced NW–SE trending depocentres and widespread, pervasive, mainly south-dipping faults (Palmowski et al. 2001; Noll & Hall 2003) beneath the outer shelf and slope. The extension direction was broadly N-S (similar to the earlier rift phase; Miller et al. 2002), although some workers postulate more oblique extension (e.g. Schneider et al. 2004). This extension has been postulated by Palmowski et al. (2001) to have been developed by a low-angle, north-dipping detachment zone between Australia and Antarctica from which Antarctica was “pulled out” from underneath. This rifting phase largely passed south of Tasmania, thus leaving the Torquay Sub-basin and Bass Strait as a failed rift and, hence, resulting in dextral, oblique extension in the eastern Otway Basin along the Tasman Fracture Zone, the Sorell Fault and its extension into an onshore lineament between Antarctica and the King Island High/western Tasmania (Hill et al. 1995). It eventually led to continental break up in the Great Australian Bight (Santonian, Palmowski et al. 2001; Maastrichtian, Noll & Hall 2003; Krassay et al. 2004, and Mid-Eocene; Norvick & Smith 2001), which propagated east into the Otway Basin by the Eocene (Müller et al. 2000; Palmowski et al. 2004) to form a passive margin (Hill et al. 1995). Oceanic crust was formed in the Early Campanian (Norvick & Smith 2001) south of the Bight Basin (Fig. 4), however, no oceanic crust older than the Middle Eocene has been identified adjacent to the deep-water Otway Basin (Krassay et al. 2004; Royer & Rollet 1997; Moore et al. 2000). This highlights the slow nature of seafloor spreading during this time (Veevers et al. 1991; Royer and Rollet 1997; Müller et al. 1997; Norvick & Smith 2001).

- *Mid Eocene fast spreading*

A change to fast continental drift in the Middle Eocene (~44 Ma) resulted in the final separation of Australia and Antarctica and the first presence of ocean crust dated in the Otway Basin (Royer & Rollet 1997; Norvick & Smith 2001). This fast seafloor spreading

(Fig. 4) eventually led to rapid thermal subsidence, collapse of continental margins and widespread marine transgression (Norvick & Smith 2001) and resulted in hundreds to thousands of kilometres of sinistral slip along the Sorell Fault Zone and the Tasman Fracture Zone (Moore et al. 2000; Miller et al. 2002; Palmowski et al. 2004).

- Miocene to Recent compression

A major change to a NW-SE oriented compressional regime occurred at this time in the Otway Basin that resulted in fault reactivation, right-lateral wrenching, folding, uplift and local basin inversion, which is most pronounced in the Otway and Strzlecki Ranges (Perincek & Cockshell 1995; Krassay et al. 2004; Palmowski et al. 2001; Hill et al. 1995). Borehole breakout data in the offshore Otway and Gippsland Basins (Hillis & Reynolds 2000, Nelson et al. 2006) supports the NW-SE oriented contemporary *in-situ* stress regime (i.e. thrust fault mode; Fig. 5). This stress state has been attributed to a change in the relative plate motion between the Pacific and Indo-Australian Plates (Dickinson et al. 2002; Sandiford 2003a). That is, due to arc collision of Australia with SE Asia to the north coupled with ridge push to the south and compressional forces along the New Zealand and south of New Zealand plate boundaries (Hill et al. 1995; Sandiford 2003a; Nelson et al. 2006). Further evidence suggesting fault-related uplift in the Late Pliocene–Quaternary is, firstly, the active seismicity of reverse-fault and strike-slip earthquake mechanisms across southeast Australia (Sandiford 2003a) and secondly, uplift increases away from the axis of Late Pliocene–Quaternary volcanism centred on a low-lying region to the north of the western highlands. This, therefore, supports fault-related uplift, rather than volcanic doming or underplating of mantle material as the possible cause of uplift in the Otway Basin (Lister et al. 1991; Sandiford 2003b). In contrast to fault related uplift, Wallace et al. (2005) suggested that latest Pliocene Quaternary uplift and/or eustatic changes may be caused by Quaternary glacial episodes which resulted in an unconformable relationship between the Pliocene and Quaternary strandline systems across Victoria. Cooper & Hill (1997) estimated ~ 5% shortening during the Mio-Pliocene inversion, however, Hall & Keetley (2009) have suggested that folds related to inversion of many Early Cretaceous faults in the mid Miocene-early Pliocene, were caused by regional NW-SE directed shortening of up to 12% which lead to the uplift of the Otway Ranges. A major implication of this Neogene compression is that it is responsible for most of the structures that host hydrocarbon accumulations (Dickinson et al. 2001).



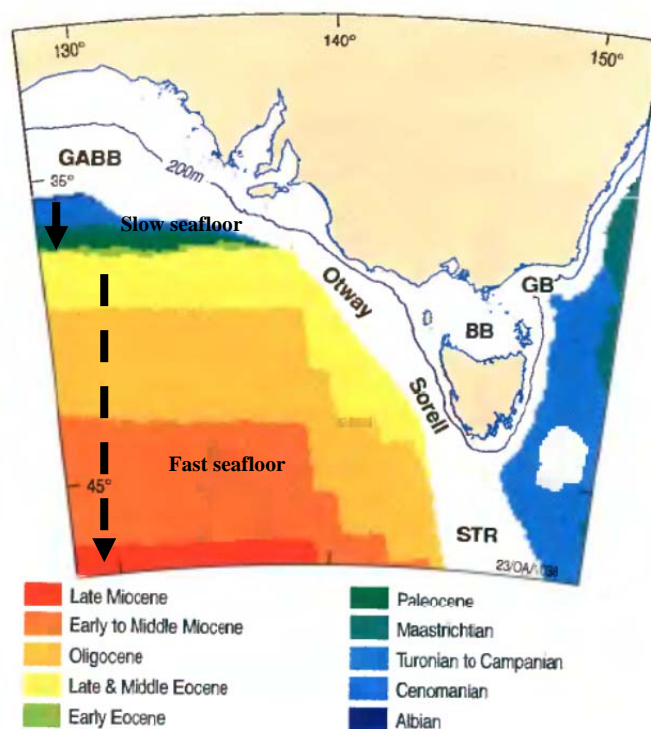


Figure 1: Ages of seafloor adjacent to the Southern Australian Margin adapted from Moore et al. (2000) which was modified from Müller et al. (1997). It shows the extent of oceanic crust throughout the Mesozoic and Cenozoic indicating speeds of seafloor spreading. There is little oceanic crust formed from the Albian to Early Eocene but increases in the Late-Middle Eocene.

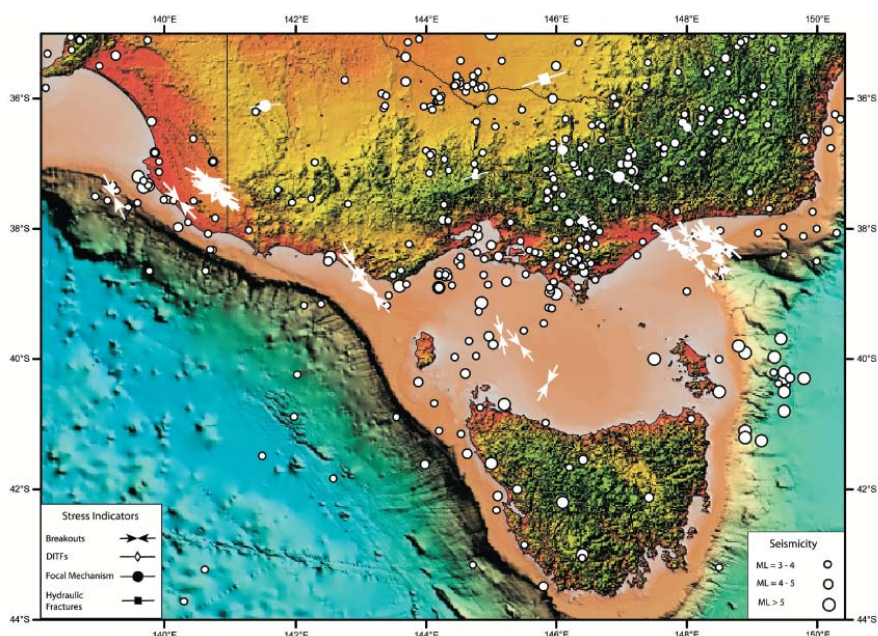


Figure 5: NW-SE oriented present-day stress regime of the Otway, Bass and Gippsland Basins (Nelson et al. 2006)

### *Stratigraphic Record of the Otway Basin*

## LITERATURE REVIEWS

The Otway Basin has been subject to number of stratigraphic studies over the last few decades with early published works (e.g. McQueen 1962; Leslie 1966; White 1968,1995; Reynolds et al. 1966) based predominately on palynologic, palaeontologic and petrographic data from onshore wells, outcrop and a limited number of wells in the offshore parts of the basin (Moore et al 2000). However, much confusion has existed during this time with over 200 formation names defined (Thompson & Walker 1985) and in at least one case the type section for a unit has been changed as many as seven times (Fig. 5; Boulton et al. 2002). Glenie (1971) first described this confusion where he noted that different stratigraphers were correlating units based on palaeontology rather than lithology. Since Glenie (1971), other problems have arisen to cause further confusion which has been addressed in detail by Boulton et al. (2002). More recent publications that give a good, comprehensive description of the Otway Basin's lithostratigraphy nomenclature include Morton et al. (1994, 1995), Lovibond et al. (1995), Geary & Reid (1998), Partridge (2001), Boulton et al. (2002) and Krassay et al. (2004).

Krassay et al. (2004)'s regional seismic mapping and well correlation study has provided a particularly good redefinition of the stratigraphic succession of the Otway Basin tectonostratigraphic units, which has been referenced in many recent government reports and journals. Their study recognised the deposition of eight supersequence-scaled (2<sup>nd</sup> order) stratigraphies (*sensu* Mitchum & Van Wagoner 1991; Vail et al. 1991) during seven tectonic phases (see Fig. 6). In addition to Krassay et al. (2004)'s study, another commonly referenced stratigraphic succession, in particularly in South Australian studies, is Boulton & Hibbert (2002)'s stratigraphic column (Fig. 7). A couple differences between the two stratigraphic columns (Figures 5 & 6), however, is that in South Australia, the largely marine, Tertiary cover (i.e. Gambier Limestone) is thought as belonging to a separate basin: the Gambier Basin and not to the Otway Basin in which Krassay et al. (2004) defines it. Although, it does form a local Victorian equivalent in the Miocene Port Campbell Limestone (Duddy et al. 2003). Furthermore, it is recognised in South Australia that the Copa Formation is the basal unit to the Sherbrook Group (see Fig. 7), which is distinct from the Waarre Formation recognised more widely in Victoria (see Fig. 6; Duddy et al. 2003).

As previously discussed, the Otway Basin formed as a result of rifting in the Late Jurassic to Early Cretaceous (Noll & Hall 2003) which lead to the initial deposition of the Casterton Formation and Otway Supergroup over deformed Cambrian-Ordovician basement (Krassay et al. 2004). In addition to Figures 5 & 6, which inherently gives a brief indication of the units' deposition environment, tectonic stage and structural event, Table 2 provides a summary of the

## *LITERATURE REVIEWS*

Otway Basin's lithology for each unit in more detail. For good, detailed descriptions of system tracks and formations' chronological distribution with respect to one another over different parts of the basin for the eight supersequences, the reader is recommended to look at Krassay et al. (2004). There is still room for improvement of the Otway stratigraphic column according to Hall & Keetley (2009), especially the "grab-bag" lithostratigraphic name "Belfast Mudstone" which merely represents anything that cannot be distinguished' in the Sherbrook Group, although, Partridge (2001) does give a fairly good revised stratigraphy of the Sherbrook Group. However, Hall & Keetley (2009) suggest that instead of further piecemeal studies, work would be enhanced by working to definitively revise the entire chronostratigraphy. The complexity of the Sherbrook Group stratigraphy can be overwhelming since temporal equivalent units have different names across the basin, thus shows Partridge (2001)'s revised Sherbrook Group Stratigraphy.

LITERATURE REVIEWS

	BOCK AND GLENIE, 1965	REYNOLDS et al., 1966	WOPFNER et al., 1971	GRAVESTOCK et al., 1986	SPRIGG, 1986	WILLIAMSON et al., 1987	KOPSEN AND SCHOLEFIELD, 1990	MORTON, 1990	TICKELL et al., 1995	LOVIBOND et al., 1995	PARTRIDGE 2001	GALLAGER ET AL 2002	THIS VOLUME		
Paaratte Formation	Timboon Sandstone Member	Curdies Formation	Curdies Beds	Timboon Sand	Timboon Sand Member	Curdies Formation Timboon Sand	Paaratte Formation	Timboon Sandstone	Paaratte Formation	Timboon Sandstone	Massacre Shale	Massacre Shale	Timboon Sandstone		
	Nullawarre Greensand	Paaratte Formation	Paaratte Formation	Paaratte Formation	Skull Creek Mudstone Member Nullawarre Greensand Member	Nullawarre Greensand		Paaratte Formation		Paaratte Formation	Skull Creek Member Nullawarre Greensand	Paaratte Formation		Timboon Sandstone	Timboon Sandstone
													Voluta shale	Paaratte Formation	Paaratte Formation
	Belfast Mudstone	Belfast Mudstone	Belfast Mudstone	Belfast Mudstone	Belfast Mudstone Member	Belfast Mudstone		Belfast Mudstone		Belfast Mudstone	Belfast Mudstone	Belfast Mudstone	Argonaut Mbr	Argonaut Mbr	Argonaut Mbr
Flaxman Formation	Flaxmans Formation	Flaxmans Formation	Flaxman Formation	Flaxman Formation	Flaxman Formation	Belfast Mudstone	Flaxman Formation	Flaxman Formation	Flaxman Formation	Flaxman Formation	Flaxman Formation	Flaxman Formation	Flaxman Formation	Flaxman Formation	
Waarre Sandstone	Waarre Formation	Waarre Sandstone		Waarre Formation	Waarre Sandstone		Waarre Sandstone	Waarre Sandstone	Waarre Formation	Waarre Sandstone	Waarre Sandstone	Waarre Sandstone	Waarre Sandstone	Waarre Sandstone	Waarre Sandstone
KORUMBURRA GROUP	Geltwood Beach Formation	Eumeralla Formation	Eumeralla Formation	Eumeralla Formation	Eumeralla Formation	Eumeralla Formation	Eumeralla Formation	Eumeralla Formation	Eumeralla Formation	Eumeralla Formation	Waarre Formation	unnamed member	unnamed member	Waarre Sandstone	
							Windermere Member	Windermere Sandstone Member		Windermere Sandstone Member					
	Pretty Hill Sandstone	Pretty Hill Sandstone	Pretty Hill Sandstone	Pretty Hill Sandstone	Pretty Hill Sandstone	Pretty Hill Sandstone	Pretty Hill Sandstone	D	Katnook Sandstone	Pretty Hill Formation	Katnook Sandstone	Copa Member	Copa Member	Copa Member	Copa Formation
								C	Laira Formation		Laira Formation				
								B	Pretty Hill Sandstone		Pretty Hill Sandstone				
	A	Pretty Hill Sandstone	Pretty Hill Sandstone	Pretty Hill Sandstone	Pretty Hill Sandstone	Pretty Hill Sandstone	Pretty Hill Sandstone	Pretty Hill Sandstone		Pretty Hill Sandstone	Pretty Hill Sandstone	Pretty Hill Sandstone	Pretty Hill Sandstone	Pretty Hill Sandstone	
Unit T	Casterton Beds	Casterton Beds	Casterton Formation	Casterton Beds	Casterton Beds	CASTERTON GROUP	Casterton beds	Casterton Formation	Casterton Formation	Casterton Formation	Casterton Formation	Casterton Formation	Casterton Formation		

Figure 6: The evolution of the Otway Basin stratigraphic column nomenclature from 1965 to 2002 (after Boulton et al. 2002).

LITERATURE REVIEWS

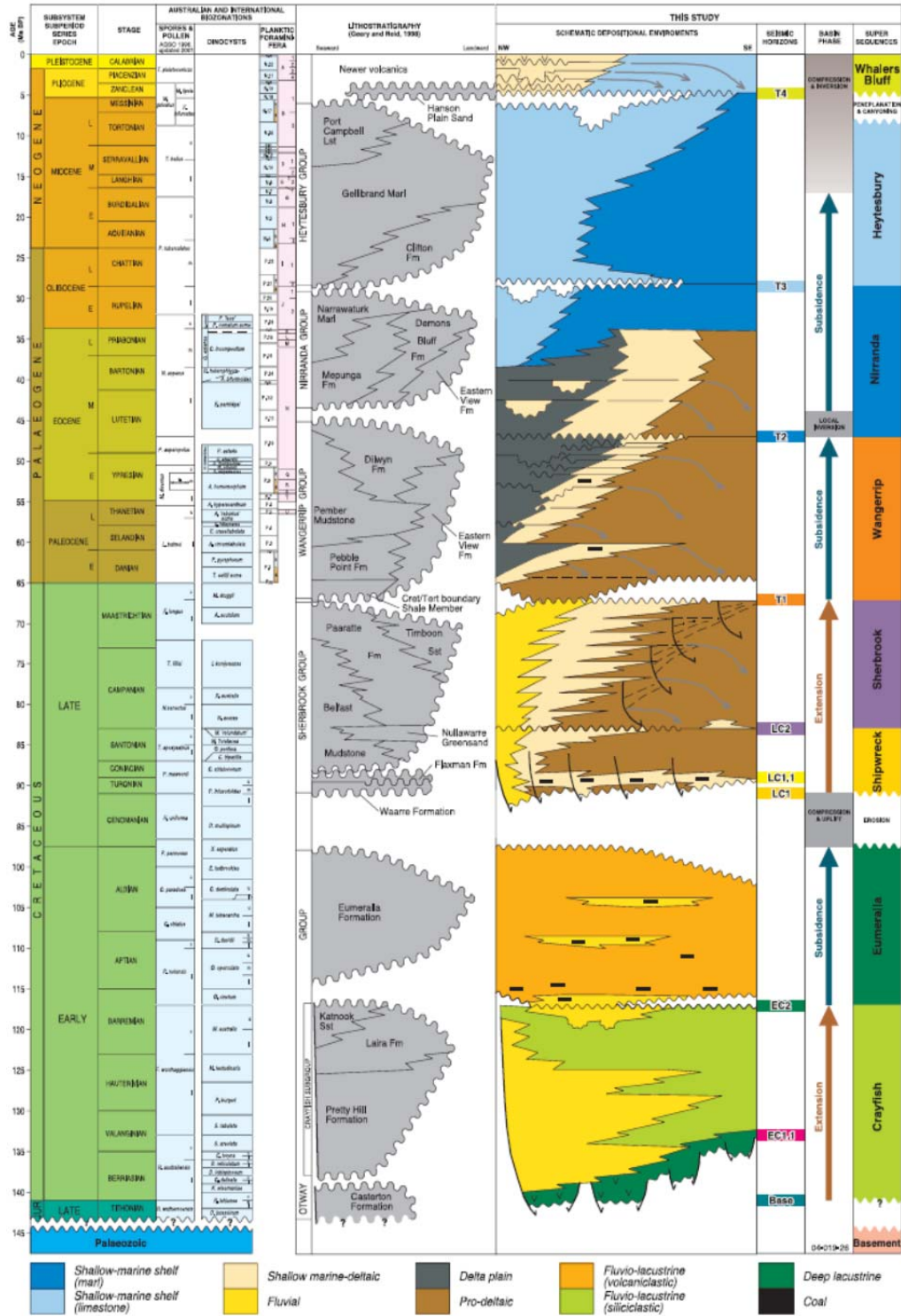


Figure 2: A litho-stratigraphic column for the Otway Basin published by Krassay et al. (2004), but modified from Geary & Reid (1998).

LITERATURE REVIEWS

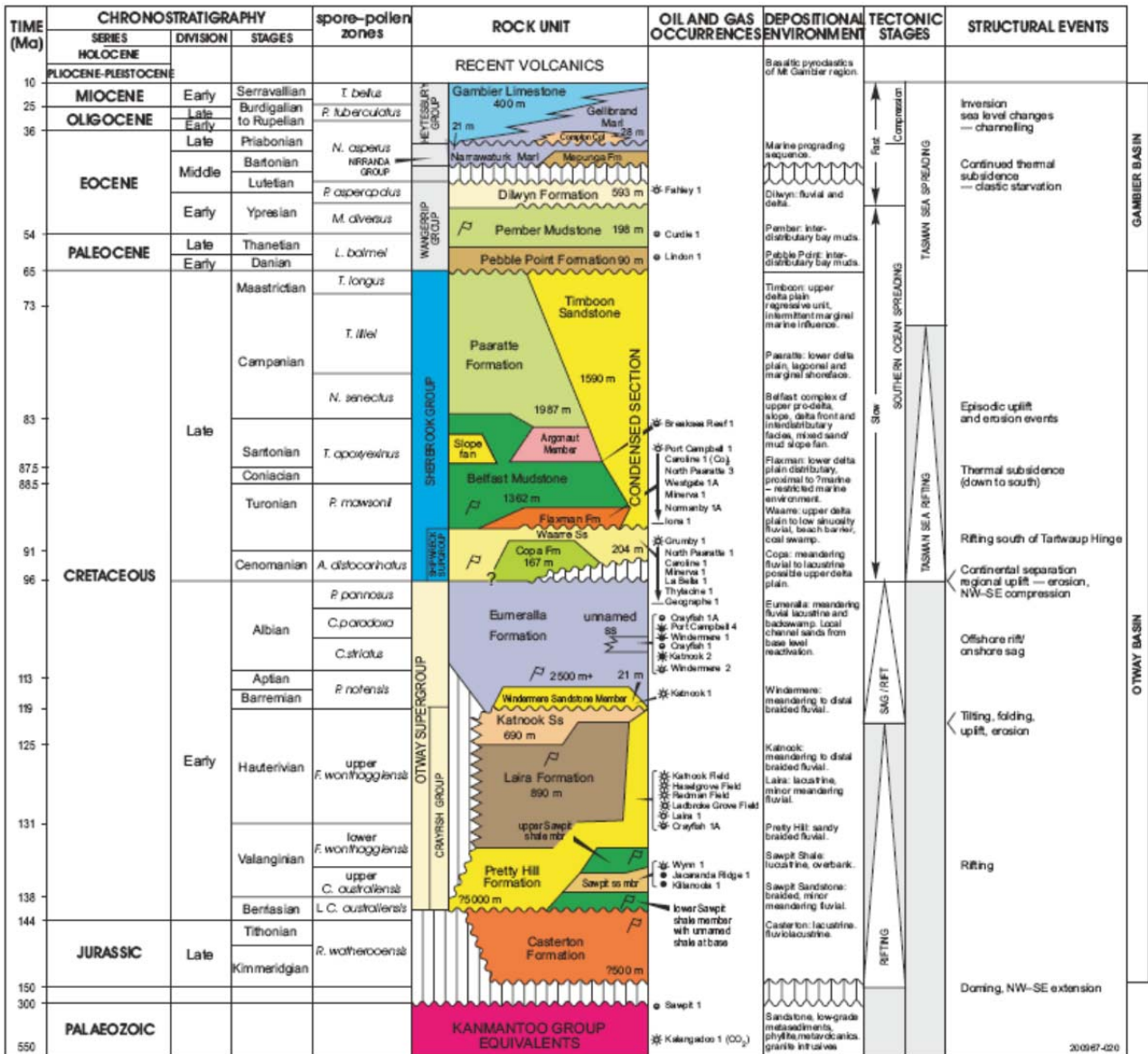


Figure 8: A litho-stratigraphic column for the Otway Basin published by Boulton & Hibbert (2002).

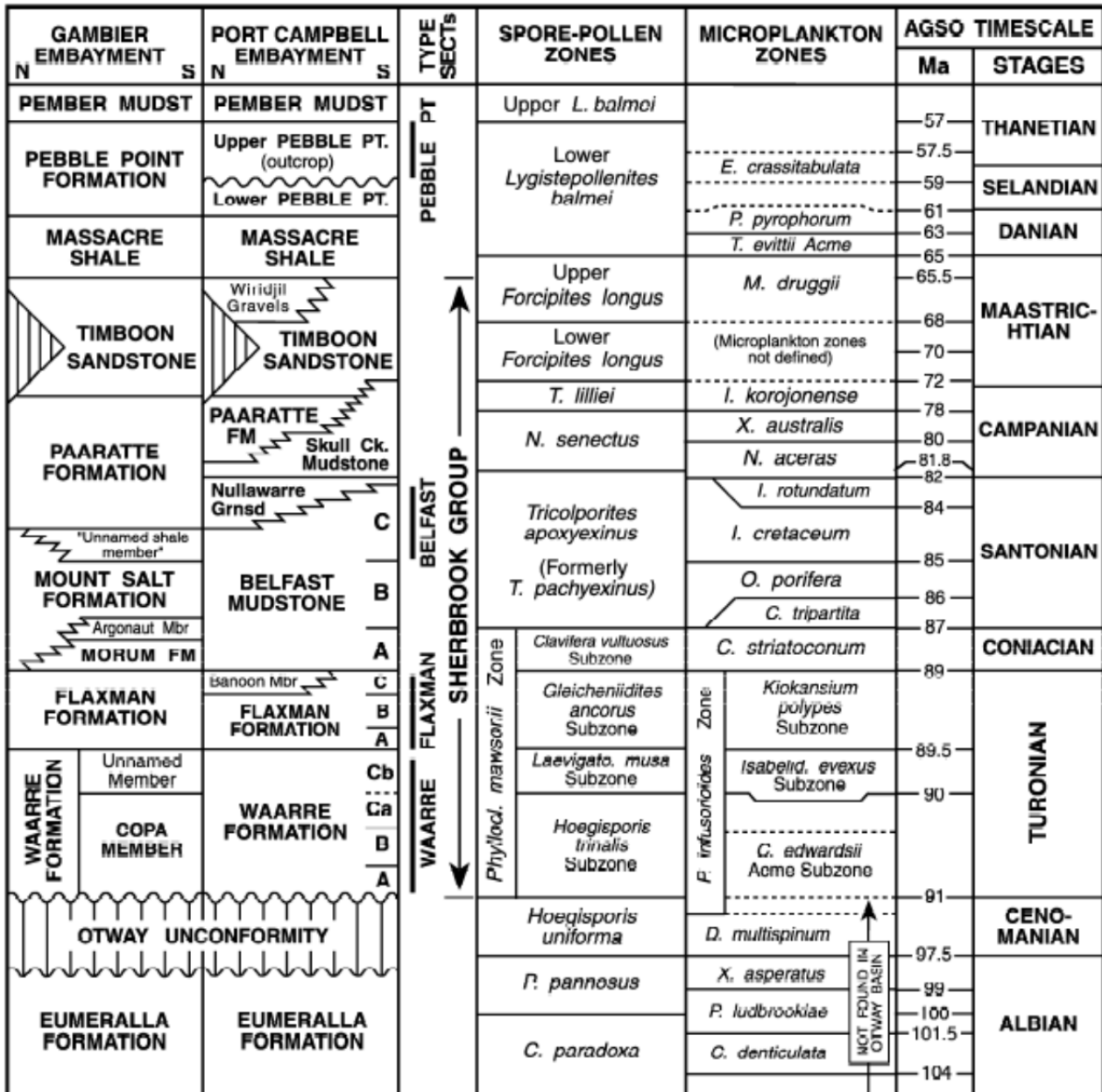


Figure 3: Revised Upper Cretaceous Sherbrook Group stratigraphic section by Partridge (2001).

A number of studies have focussed on regional unconformities to highlight their role in basin evolution in the Otway Basin and surrounding basins (e.g. Dickinson et al. 2002) and finally, the stratigraphic succession in the Torquay Sub-basin is different from the Late Cretaceous onwards (see Fig. 3) and, therefore, will not be discussed further.

LITERATURE REVIEWS

Table 2: A summary of the lithology and deposition environment characteristics of Otway Basin chrono-stratigraphic column.

Groups	Formation	Age	Lithology	Depositional Environment	Comments			
<b>BASEMENT</b>		<i>Palaeozoic</i>	Highly deformed metasediments of the Kanmantoo and Lachlan Fold Belts that were deformed during the Cambro-Ordovician Delamarian and Lachlan Orogenies respectively and igneous intrusives (Lyon et al. 2007; Perincek & Cockshell 1995).	Turbidic(?)				
<b>Unconformity</b>								
<b>Casterton Formation</b>		<i>Tithonian – Berriassian</i>	Interbedded silty carbonaceous mudstone, vesicular olivine basalt and minor feldspathic sandstone and siltstone with coaly laminations	Lacustrine, fluviolacustrine. Volcanogenics postulated from Tasman arc (Norvick & Smith 2001).	Initial elongate half grabens			
<b>Unconformity</b>								
<b>OTWAY SUPERGROUP</b>	<b>Crayfish Group</b>	Pretty Hill Formation	<i>Valanginian-Albian</i>	Mineralogically complex, grey-green litharenite to feldspathic litharenite (Alexander, 1992) with varying proportions of siltstone to shale interbeds.	Sandy braided fluvial; floodplain to lacustrine Fluvio-lacustrine and lacustrine (Obrien et al. 2009)	Deposited in rifted half-grabens (Obrien et al. 2009) on the northern onshore part of the basin in the proto-Robe, Penola, Tantanoola, Ardonachie, Koroit and Colac troughs and the Torquay Sub-basin. Formed large growth wedges.		
		Laira Formation	<i>Valanginian-Hauterivian</i>	Medium to light grey to green siltstone and claystone, with minor fine grained quartzose and feldspathic sandstone interbeds.	Lacustrine, minor meandering fluvial			
		Katnook Sandstone	<i>Valanginian-Hauterivian</i>	Light grey, fine to medium-grained, cross-bedded (arenites and carbonaceous silts) sandstone, interbedded with dark grey micaceous siltstone.	Meandering to distal braided			
	<b>Unconformity</b>							
	<b>OTWAY SUPERGROUP</b>	<b>OTWAY SUPERGROUP</b>	Windermere Sandstone	<i>Barremian</i>	Fine to coarse-grained sandstone and conglomerate with minor siltstone interbeds.		Meandering, low sinuosity and braided fluvial; amalgamated fluvial channel sandstone	Post-initial rift thermal sag phase - relatively structurally-quiet
			Eumeralla Formation	<i>Early Aptian/Barremian-Albian</i>	Laminated greenish grey, chloritic, micaceous, carbonaceous silty claystone with minor, very fine-grained feldspathic sandstone interbeds. Containing up to 53% volcanogenic fragments (Morton et al. 1995).		Meandering fluvial to lacustrine, floodplain, sheet flood, shallow lacustrine and backswamp. Local interbedded channel sands and coal beds from base level reactivation. Tasman Arc volcanism was active at this time from the east (Palaeocurrent observations) (Cooper & Hill 1997)	
<b>Unconformity</b>		<b>Cenomanian</b>	<b>NW-SE directed compression</b>		<b>Local basin inversion</b>			
<b>SHERBROOK GROUP</b>	<b>Shipwreck Subgroup<sup>2</sup></b>	Copa Formation	<i>Cenomanian</i>	Medium grey-brown claystone and dark grey to green carbonaceous siltstone, with minor fine to medium-grained sandstone. Decreasing lithic content and rare coal interbeds.	Meandering fluvial to lacustrine possible upper delta plain	Thick LST non-marine, siliclastic, paralic deltaic sediments, equivalent to the Copa and Waarre formations, infilling initial accommodation created by rifting. Delta systems that progressively prograded from the northern margin of the basin to out beyond the current shelf break.		
		Waarre Sandstone	<i>Cenomanian</i>	Pale grey, fine to very coarse-grained sandstone, with subordinate carbonaceous siltstone and mudstone interbeds. Decreasing lithic content and rare coal interbeds.	Upper delta plain to low sinuosity fluvial, beach barrier, coal swamp			
		Flaxman	<i>Turonian</i>	Intensely bioturbated fine to coarse-grained	Lower delta plain distributary, proximal to		Flooding/2nd-order	



LITERATURE REVIEWS

	Formation		sandstone interbedded with carbonaceous and micaceous muddy siltstone. Sands grade upward into multiple regressive cycles of silts and sands with increasing shale content up-section	?marine-restricted marine environment	transgressive surface
	Belfast Mudstone	<i>Turonian to Santonian</i>	Pale grey to black, pyritic mudstone with fine-grained sandstone and siltstone interbeds.	Complex of upper pro-delta, slope, delta front and interdistributary facies, mixed sand/mud slope fan.	
	Mt Salt Formation	See Partridge (2001a)			
	Argonaut Member	<i>Late Santonian</i>		Aggradational to progradational, deltaic to pro-deltaic HST	change from deeper marine to shelf marine conditions
	Nullawaare Greensand <sup>1</sup>	<i>Turonian to Santonian</i>	Pale grey-green, fine to coarse-grained sandstone with glauconite faecal pellets.		
	Paaratte Formation	<i>Santonian-Maastrichtian</i>	Laminated, black, carbonaceous and pyritic shale interbedded with bioturbated, cross-bedded, fine to coarse-grained sandstone.	Lower delta plain, lagoonal and marginal marine influence. Major deltaic deposition major deltaic deposition.	Thickest basinward of the major Tartwaup and Mussel fault zones. Faulted deltaic environment (Norvick & Smith 2001)
	Timboon Sandstone	<i>Santonian-Maastrichtian</i>	Medium to coarse grained quartz sandstone, interbedded with minor black to brown, very micaceous, bioturbated silty mudstone.	Upper delta plain regressive unit, intermittent marginal marine influence. Major deltaic deposition major deltaic deposition.	
Skull Creek Mudstone	<i>Santonian-Maastrichtian</i>		Major deltaic deposition major deltaic deposition		

Unconformity

WANGERRIP GROUP	Pebble Point Formation	<i>Dandian-Thanetian</i>	Dark green and brown oolitic grit with rounded, fine-grained to granule-sized quartz and carbonaceous material.	Interdistributary bay muds; marginal marine.	Post-Cretaceous thermal subsidence basin phase and were deposited in a range of deltaic and shallow marine environments (Krassay et al. 2004).
	Pember Mudstone	<i>Thanetian-Ypresian</i>	Interbedded brown mudstone, sandy mudstone and muddy sandstone, and includes bioclasts, carbonaceous material, quartz, glauconite, mica, pyrite, chert, ferruginised pellets, ferruginised clasts and rock fragments.	Interdistributary bay muds; Inner shelf, marginal marine, deltaic and fluvial.	
	Dilwyn Formation	<i>Ypresian - Lutetian</i>	Predominantly clean sandstone, with some muddy intervals (Penola Trough) or predominantly muddy, or contains about equal amounts of sandstone and mudstone (South & offshore).	Fluvial and delta; marginal marine (including deltaic) to inner shelf in the more southern and offshore wells.	

Unconformity

NIRRANDA GROUP	Mepunga Formation	<i>Mid Eocene – Late Oligocene</i>	Brown to red-brown, limonitic quartz grit, sand and silty sand, with pyrite and shark teeth, and rare naticid gastropods, non-age diagnostic foraminifera and carbonaceous material. Siliciclastic-dominated LST/TST. Interbedded clays and coarse sand (Cooper Thesis).	Marine prograding sequence deposited in beach, near-shore to mid-shelf environments. Deposited during a major marine transgression when there was an initial fall in relative sea level and during subsidence-driven flooding of the margin (Krassay et al. 2004). Beach or barrier system (Cooper Thesis)	Cool water carbonates with reducing upwards siliclastic content (Gallagher & Holdgate 2000). Generally less than 100 m thick and this thickness variation is strongly controlled by changes in sediment supply
	Narrawaturk	<i>Mid Eocene –</i>	Green and green-brown marls with bioclasts,	Middle shelf or deeper water conditions. Deposited	

LITERATURE REVIEWS

	Marl	<i>Late Oligocene</i>	quartz, glauconite, 'goethite' and ferruginised pellets. HST. Pale-dark marl, calcareous mudstones and minor calcarenites. Contains abundant fossilised bryozans, brachiopods and foraminifers (Cooper Thesis).	during a major marine transgression in which there was continued subsidence of the margin. Open marine environment (Cooper Thesis)	and carbonate growth.
--	------	-----------------------	---	--	-----------------------

**Unconformity**

HEYTESBURY GROUP	Compton Conglomerate	<i>Early Oligocene</i>		Marine shelf channel fill. Open marine in a high energy beach environment	high-amplitude, parallel shelfal topsets, sigmoidal to oblique clinofolds, and transparent slope facies geometries, development of large submarine canyons
	Clifton Formation	<i>Early Oligocene</i>	Cemented bryozoan and shell fragments (Cooper Thesis)	Shallow marine environment (Cooper Thesis)	
	Gellibrand Marl	<i>Early – Mid Miocene</i>	Calcareous clays, silt and is rich in marine fossils	-	
	Gambier Limestone / Port Campbell Limestone	<i>Late Miocene</i>	Fossiliferous calcarenite and bioclastic calcarenite / Weakly cemented bryozoans, echinoids and brachiopods (Cooper Thesis).	Progradational carbonates deposited during regional thermal subsidence deposited on a high-energy, cool-water heterozoan shelf / moderate energy continental-carbonate shelf environment (Cooper Thesis).	

**Unconformity**

WHALERS BLUFF GROUP	Whalers Bluff Formation	<i>Pliocene</i>	Mixed siliciclastic-carbonate succession of fossiliferous calcarenite and calcilutite	NW-SE directed compression cool-water, high-energy carbonate ramp (Boreen & James 1993)	Local basin inversion Progradational succession restricted to an area in the central Otway Basin where accommodation was created between the inverted Copa-Argonaut structures
	Hanson Plain Sands	<i>Pleistocene</i>	Predominantly sands and gravels with some clayey and carbonateous material	Fluviatile environment	
	Bridgewater Formation	<i>Pleistocene</i>	Calcarenite, quartz and shell fragments	Calcareous aeolian sand dunes	
	Newer Volcanics	<i>Pliocene - Recent</i>	Basaltic flow deposit	-	Covers most of the Western District

- <sup>1</sup> Nullawarre Greensand forms a shelf equivalent to the upper Belfast Mudstone. However, the Nullawarre Greensand lithology has not been formerly recognised in South Australia.
- <sup>2</sup> The base of the Shipwreck Supersequence is recognised in many areas as a major unconformity. The Late Cretaceous section is thin or absent on the Crayfish Platform, in the Elignamite Trough area, the Torquay Sub-Basin and along the northern margins of the basin (Krassay et al. 2004).
- Cretaceous section is rarely present in the Torquay Embayment and is absent in the onshore Otway Ranges and Colac Trough (Hill et al. 1995).

### ***Structure Elements of the Otway Basin***

Structural features in the Otway Basin have been well documented in the literature with studies either primarily concerned purely with basin evolution (e.g. Teasdale et al. 2003; Aburas & Boulton 2001) or the implications that faulting has in the development of hydrocarbon systems (e.g. Palmowski et al. 2001; Moore et al. 2000; Lyon et al. 2007). Earlier studies in the Otway Basin include Gloe et al. (1998) and Smith (1988), however, a good study which has been well referenced and has identified (mostly) offshore structural components of the Otway Basin beneath the continental slope and rise is by Moore et al. (2000). Not including the Inner Otway Basin, they used seismic data to divide the basin beneath the continental slope into five provincial depocentres (Fig. 9): the Beachport Sub-basin, Morum Sub-basin, Discovery Bay High, Hunter Sub-basin and the Nelson Sub-basin (which they interpreted to be continuous with the Sorell Basin to the south).

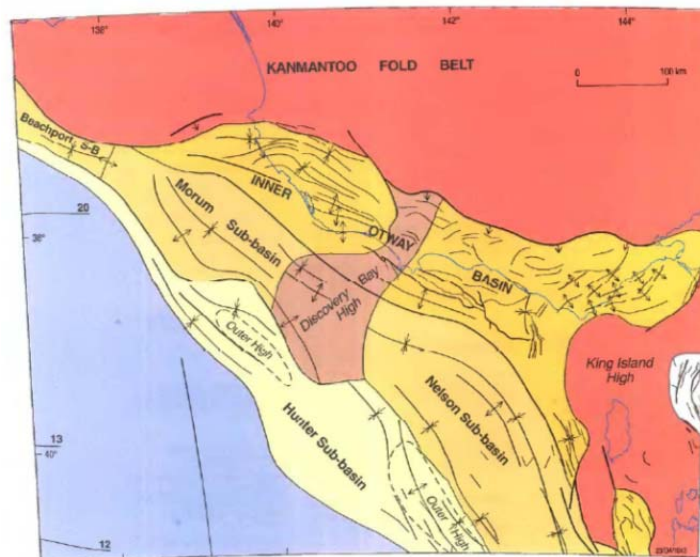


**Figure 10: Tectonic and structural elements by Moore et al. (2000)**

Another useful structural elements map (Fig. 10) was published by Krassay et al. (2004) who used Moore et al. (2000)'s sub-basin terminology and identified several additional structural components/depocentres as described below:

- Penola Trough – a northwest-southeast trending half-graben, bound to the south by a large landward-dipping listric fault zone which has subtle hangingwall doming across several major faults during Miocene compression (Lyon et al. 2007).
- Shipwreck Trough – horst-graben and half-graben formation with tightly folded, north-trending anticlinal structures.
- Torquay Sub-basin – a southwest-northeast trending failed rift basin with NW to NNW dipping, basin bounding faults and steep, relatively planar, en echelon, N and NE-dipping

## LITERATURE REVIEWS

Early Cretaceous extension faults that were subsequently inverted and eroded during the Cenomanian and Mio-Pliocene (Hill et al. 1995; Cooper & Hill 1997).

Other important structural features, from west to east, include the Robe Trough, Crayfish Platform, Tantanoola Trough, Chama Terrace, Portland Trough, Merino High, Ardonachie Trough, Normanby Terrace, Mussel Platform, Koroit Trough, Prawn Platform, Otway Ranges, Colac Trough and Outer-margin High. The Outer-margin High was suggested by Norvick & Smith (2001) to have formed as a core complex over low angle crustal extensional faults in the Turonian.

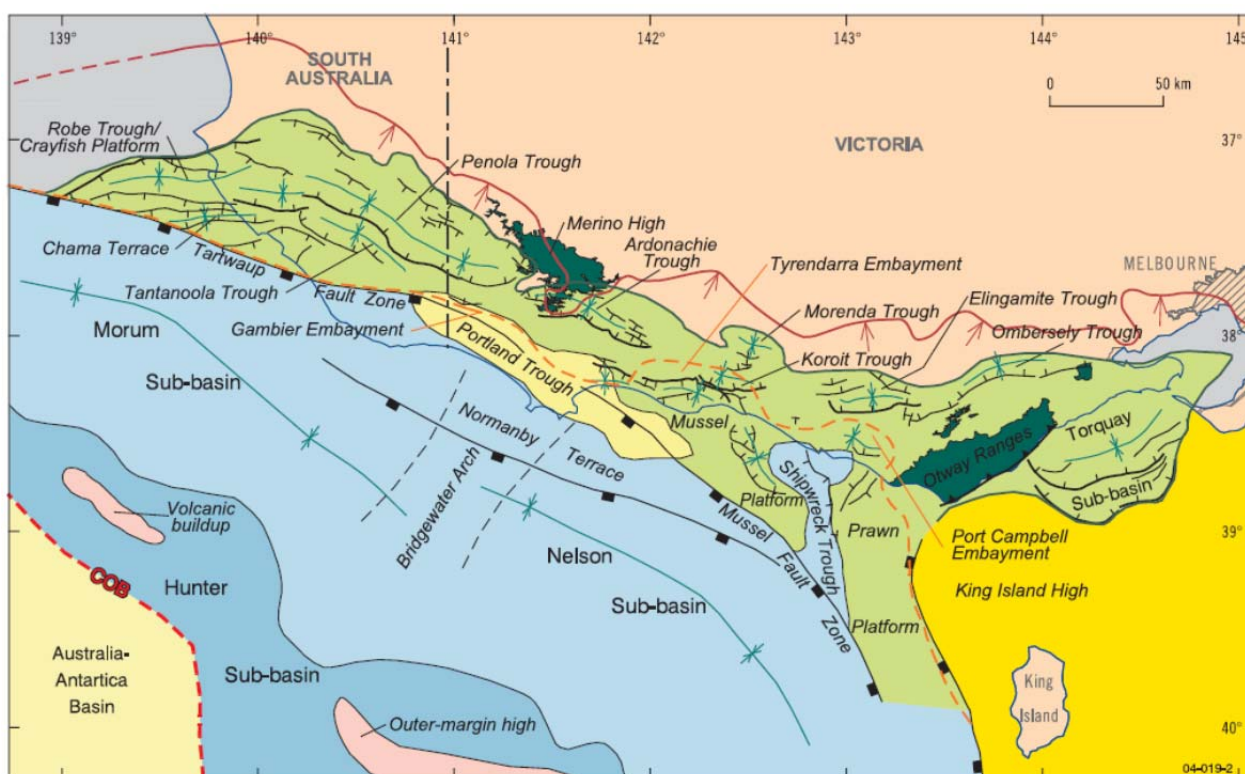


Figure 11: Structural elements map of the Otway Basin by Krassay et al. (2004).

The majority of the work undertaken in the Otway Basin to determine structural features utilise predominately seismic and well data (e.g. Fig. 11; Krassay et al. 2004). Other studies, however, have utilised seismic data in conjunction with other techniques such as thermochronology (Duddy & Erout 2001; Cooper & Hill 1997), gravity and magnetics (Aburas & Boulton 2001; Teasdale et al. 2003) and palynology (Aburas & Boulton 2001; Dickinson et al. 2001). Furthermore, the majority of the work concentrates around regions of known hydrocarbon accumulation such as the Penola (e.g. Boulton et al. 2005) and Shipwreck Troughs (e.g. Cliff et al. 2004; Fig. 10). In these areas, workers have been determined to show the contrasts in the structural styles of the Early Cretaceous half-graben depocentres and intervening basement highs in the west, to the Late Cretaceous

## *LITERATURE REVIEWS*

depocentres further south, and basinward of a major structural hinge zone in the east (e.g. Palmowski et al. 2004; Krassay et al. 2004). As already mentioned, this major hinge zone is known as the Tartwaup-Mussel Fault Zone and it separates the onshore, Inner Otway Basin from the outer sub-basins. A summary and comparison of structural characteristics observed to the north and south of this hinge zone can be seen in Table 3 from Palmowski et al. (2004). In the western Otway Basin, the Tartwaup Hinge-Mussel Fault Zone is an area of closely spaced en echelon WNW-ESE trending Late Cretaceous faults (Duddy et al. 2003) that separates the Crayfish Platform and Chama Terrace to the north from the Morum Sub-basin in the south (Duddy et al. 2003). In addition, it is at this zone where Late Cretaceous fault activity shifted south of the Tartwaup Fault Zone (Fig. 1) into the offshore parts of the Otway Basin, thus leaving the Penola Trough and similar depocentres as failed initial rift structures and later creating oceanic crust (Lyon et al. 2007).

LITERATURE REVIEWS

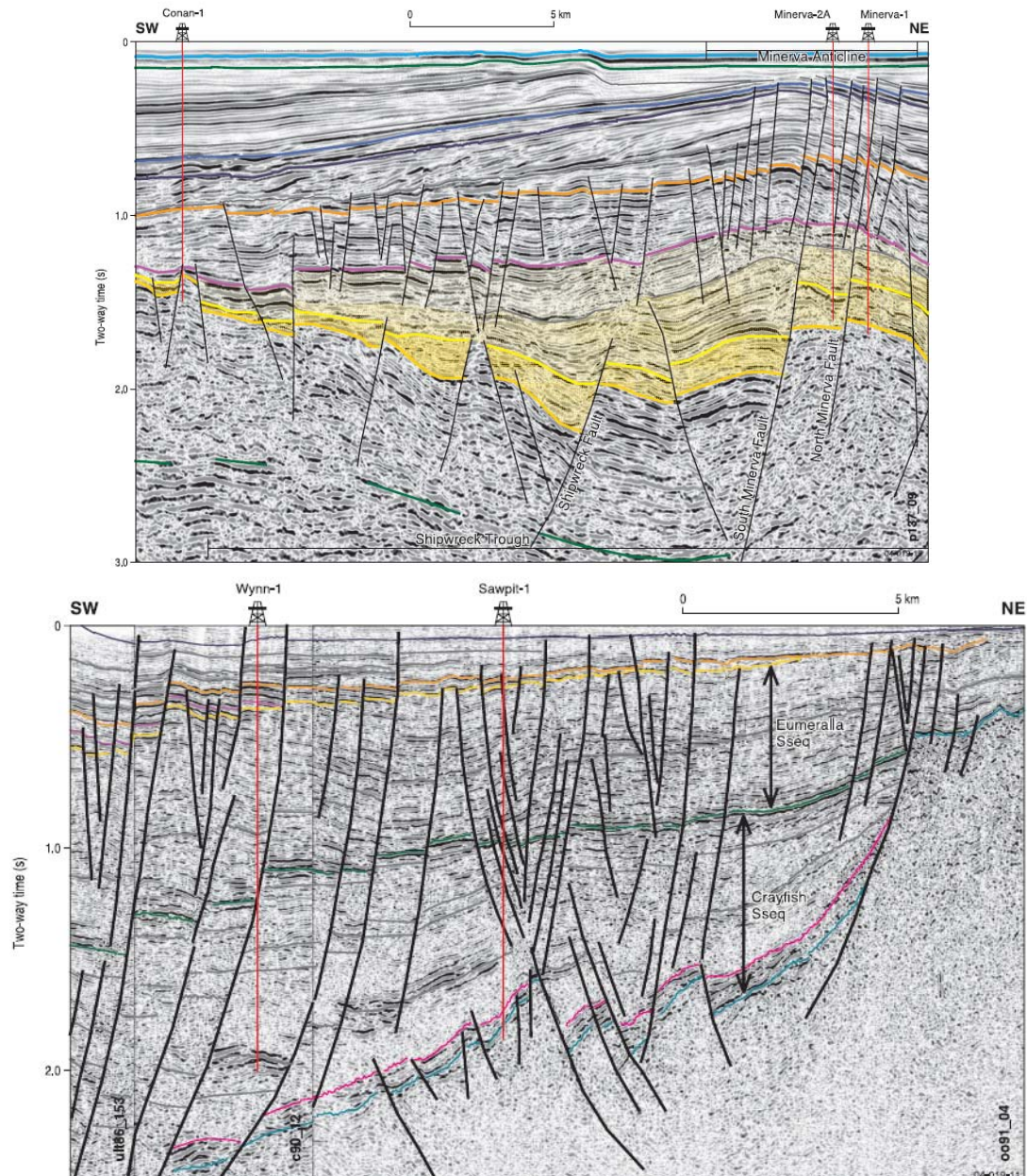


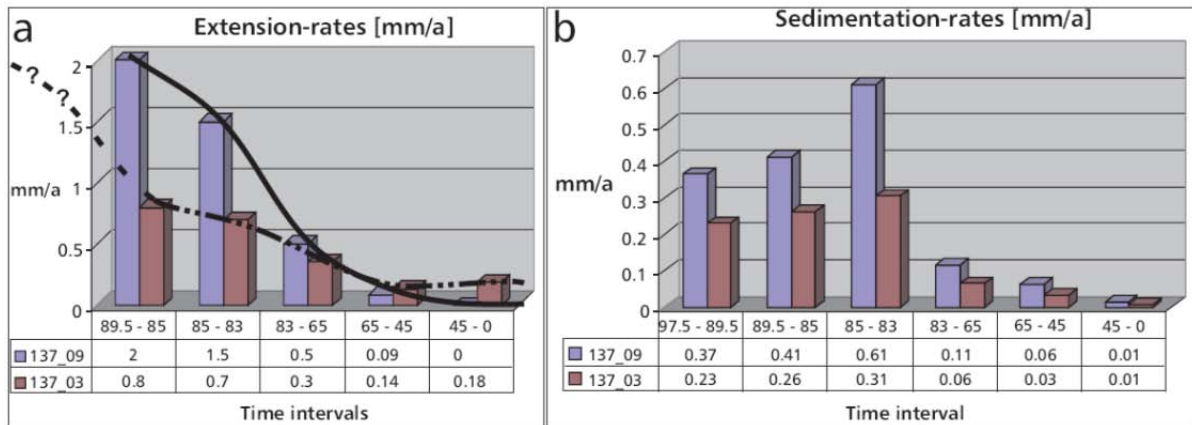
Figure 12: Examples of good seismic interpretation taken from Krassay et al. (2004) showing a) a seismic profile transecting the Shipwreck Trough and, b) a seismic profile transecting the Penola Trough.

Table 3: Summary of the comparison by Palmowski et al. (2004) of the structural characteristics observed to the north and south of the Tartwaup- Mussel fault hinge zones.

North of Hinge Zone	South of Hinge Zone
Early Cretaceous rifts with thick Early Cretaceous sequences, including volcanics	Little evidence for Early Cretaceous rifts and sediments
Thin Late Cretaceous sequences	Thick Late Cretaceous sequences
Mostly oversupplied depocentres	Undersupplied depocentres
Slightly thinned continental crust	Strongly thinned continental crust
Small amount of Late Cretaceous extension	Large amount of Late Cretaceous extension
Limited Late Cretaceous tectonic subsidence	Late Cretaceous tectonic subsidence
Shallow water throughout	Trending to deep water
Continental shelf	Continental slope

2

The structural styles varied spatially across the offshore Otway Basin in which structures propagated from the west to the east, with high angle, NNE-SSW striking sinistral strike-slip faults accommodating differences in extension amounts (Palmowski et al. 2004). In addition, Palmowski et al. (2004) also observed that the high Late Cretaceous sedimentation rates within the Penola and Shipwreck Troughs were reflecting extensional rates (Fig. 13), indicating that most of the subsidence was structurally related and the foci of extension migrated to the east and south. A summary of Palmowski et al. (2004)'s results along with a good summary of the geological history of the Otway Basin including the orientation of faults and structural styles can be seen in Fig. 14. Aburas & Boulton (2001) conducted a palynological study across one of these lateral strike-slip fault zones and concluded there was also up to 1500 m of differential uplift and erosion of the Lower Cretaceous section during inversion.



**Figure 13: After from Palmowski et al. (2004). a) Extension rates for along Penola (137-03) and Shipwreck (137-09) Trough cross-sections and their relationship to b) sedimentation rates calculated from the restoration of the corresponding seismic lines.**

LITERATURE REVIEWS

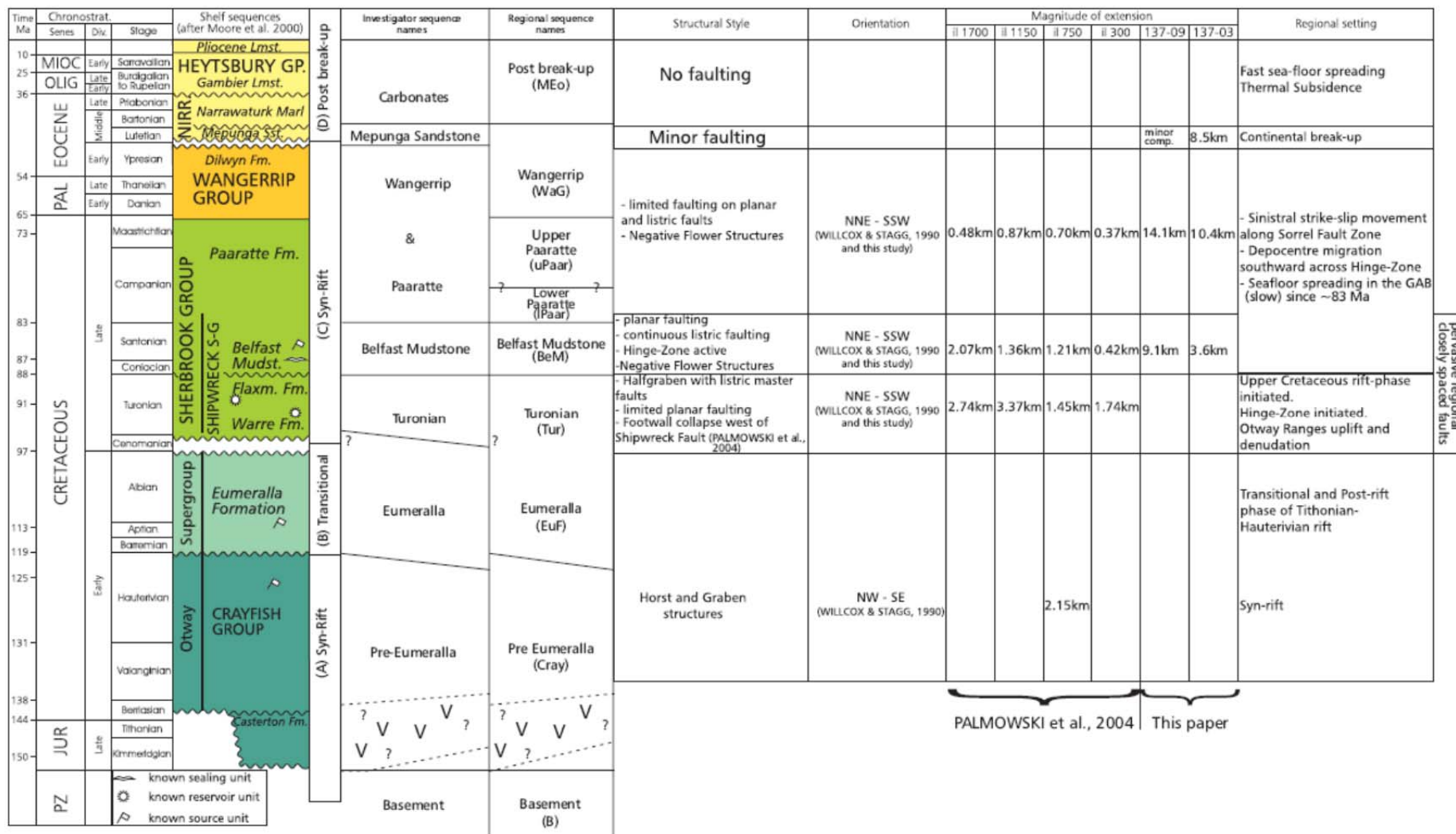


Figure 4: Palmowski et al. (2004)'s Summary of the geological history in the Otway Basin since the Late Jurassic.



## LITERATURE REVIEWS

There are many structures (e.g. Morum Sub-basin, Crayfish Platform) in the Otway Basin that can be individually discussed from the available literature; however, not all structural features can be covered in this review. Nevertheless, the evolution of sedimentary basins has long been recognised by researchers as being majorly influenced by the character and kinematic response of the underlying basement (Teasdale et al. 2003). Therefore the geometry of faulting in sedimentary basins is often attributed to the influence of pre-existing lithological heterogeneities or faults within the basement (Lee & Hwang 1993; Cooper & Hill 1997; Keep et al. 2000; Lyon et al. 2007). A number of studies have focussed on basement structures in the Otway Basin (Fig. 15) and is considered to be important for further evaluation in this review.

Teasdale et al. (2003) modelled basement terranes using aeromagnetic, gravity, seismic and well data to show their affect on basin architecture. Hill et al. (1995) aimed to show the implications of the eastern Otway Basin's structural framework across two major structural provinces using seismic data. Lyon et al. (2007) researched the basement controls on fault development in the Penola Trough. In addition, Teasdale et al (2003) provide a good series of figures that show major basement structures (i.e. faults) throughout different periods (as far back as the Palaeo-Mesoproterozoic to the Eocene), highlighting the changes in fault orientations associated with key periods of tectonic activity (Fig. 16). Miller et al. (2002) attributes different fault trends to rheological differences between basement terranes as they respond to extension. Hill et al. (1994) suggests that the near-orthogonal change in fault orientation observed from the eastern Port Campbell Embayment to the eastern Colac Trough-Torquay Sub-basin area is a function of their generation at different times rather than an abrupt transfer boundary. It is agreed by a number of workers (e.g. Miller et al. 2002; Hill et al. 1994; Krassay et al. 2004), however, that the lithospheric boundary between the rheologically-different basement terranes is the site of sinistral strike-slip movement. This accommodated adjacent differential extensional movement and was responsible for the formation of the Shipwreck Trough (Krassay et al. 2004). As previously mentioned this zone is known as the Sorell-Tasman Fault Zone and marks the boundary between the passive margin basin, with relatively little uplift to the west, and a failed rift basin with the uplifted SE Highlands to the east (Hill et al. 1994). Other authors have made similar observations (e.g. Teasdale et al. 2003; Lyon et al. 2007) and have concluded that preferential and episodic movement of basement faults from the Cretaceous through to Holocene times indicate basement faults are particularly prone to fault reactivation. These fault zones were shown by

McClay et al. (2004) to have strong similarities with oblique-rift analogue models (Cooper & Hill 1997).

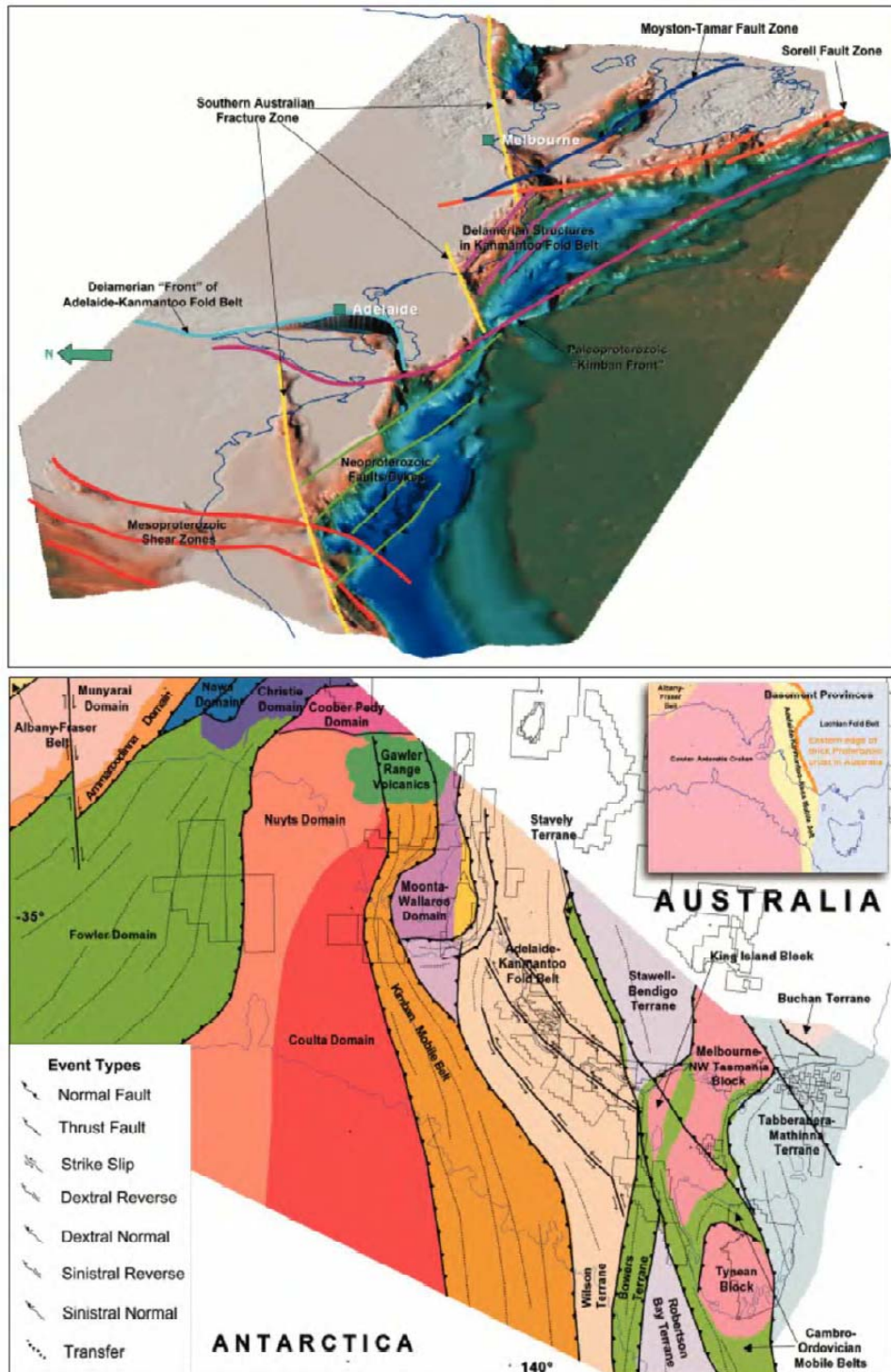
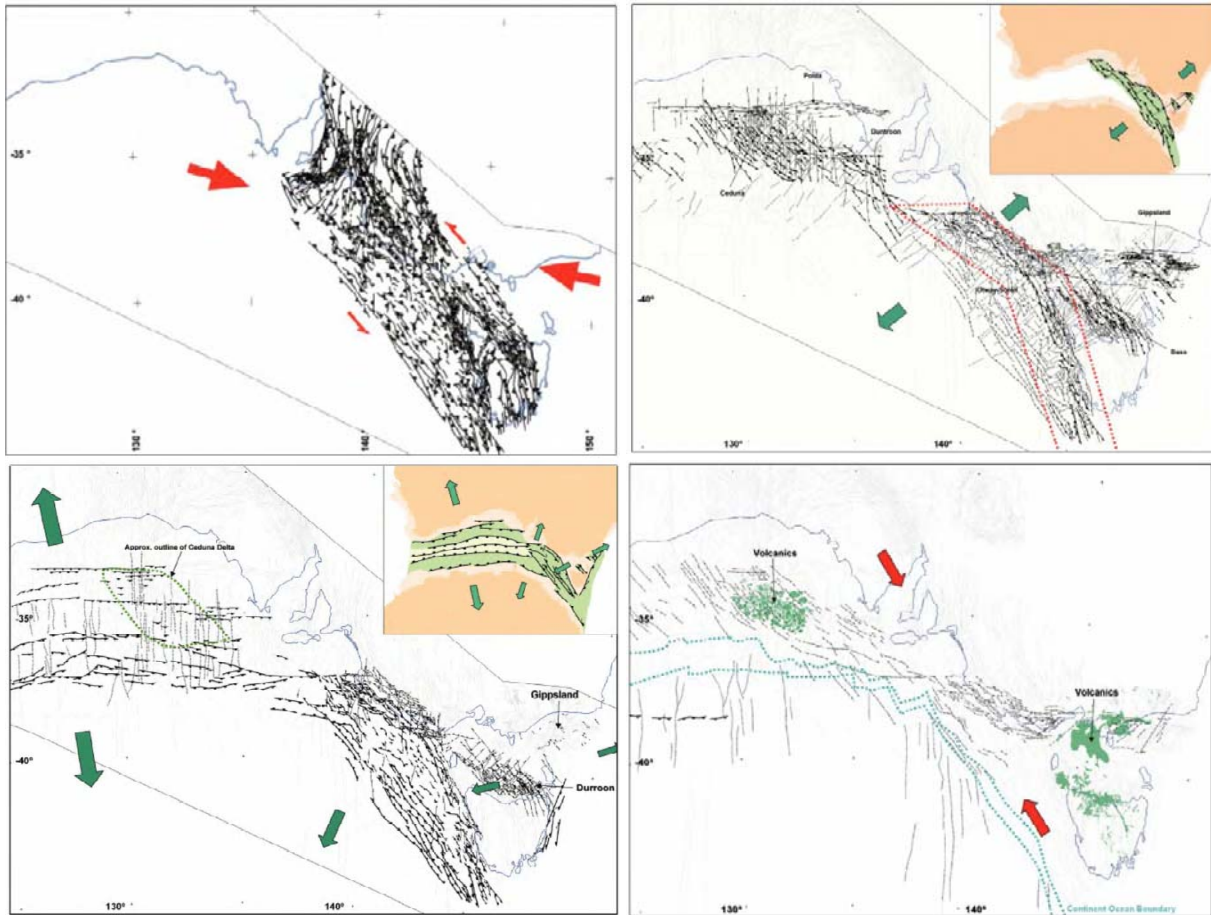


Figure 15: a) Perspective view of the southern margins SEEBASE model showing major basement structures that significantly influenced basin evolution and architecture b) Gondwana (i.e. pre-Mesozoic) configuration of basement provinces and terranes in SE Australia (Teasdale et al. 2003).



**Figure 16: Basement structures interpreted by Tresdale et al. (2003) to be active during: a) the Cambro-Ordovician Delamerian Orogeny; b) Early Cretaceous basin phase; c) Late Cretaceous basin phase; and d) Eocene inversion and sag phase.**

### *Vertical movements in the Otway Basin*

The Otway Basin has experienced two significant uplift events associated with basin inversion, uplift and erosion, with major differences in vertical motions east and west of the King Island High (see Fig. 11; Palmowski et al. 2001). The first and largest uplift and erosion event occurred in the mid-Cretaceous and the second occurred in the Miocene-Pliocene (Cooper & Hill 1997). A number of studies have been published on this matter with the majority looking at seismic profiles in order to identify and determine the faulting relations within stratigraphic units for associated inversion structures (Perincek & Cockshell 1995; Palmowski et al. 2001). Hill & Cooper (1996) presented a strategy for constructing 2D balanced cross sections across an inverted basin from previous studies (e.g. Hill et al. 1995). They incorporated thermochronological methods, namely vitrinite reflectance (VR) and apatite fission track analysis (AFTA), with seismic profile data and onshore mapping observations of unconformities and major structures to validate and constrain estimates of the

## LITERATURE REVIEWS

original thickness of syn-rift sections, subsequently eroded. This technique proved accurate, and further studies in the eastern Otway Basin were published (e.g. Cooper & Hill 1997). However, Duddy & Erout (2001), Duddy et al. (2003) and Green et al. (2004) recognised that thermochronological studies alone (based on AFTA and VR) were also useful in revealing and delineating episodes of basin inversion, regional uplift and erosion (i.e. exhumation) (Green et al. 2004). These thermochronological studies, however, only incorporate limited data from a small percentage (<20%) of wells drilled in the basin.

Figure 17 presents a series of thermal history reconstruction that show episodes of uplift in the Otway Basin. Excluding wells Trumpet-1, Minerva-1 and Morum-1, the thermal history reconstructions all show mid-Cretaceous uplift whereby cooling began around ~95 Ma. This correlated well with six AFTA samples analysed by Hill et al. (1995) from the core of the Otway Ranges which are interpreted to represent fairly rapid cooling from temperatures of approximately >150°C to temperatures of approximately <60°C at c. 90 Ma. Although these thermal history reconstructions show significant mid-Cretaceous uplift, estimates of the magnitude of erosion associated with this varies significantly. For example, Cooper & Hill (1997) and Hill et al. (1995) calculated around 3.5 km and 3 km, respectively (Fig. 18), whilst Duddy et al. (2003), Duddy & Erout (2001), and Green et al. (2004) calculated around 1.5 to 2 km of uplift and erosion near the Otway Ranges, respectively. This erosion was largely confined to and centred around the largest faults near the present coastline, indicating structural inversion (Hill et al. 1994, 1995). In contrast to these wells, thermal history data from Trumpet-1 and Minerva-1 show that the stratigraphic sections are presently close to or at maximum post-depositional temperatures/burial depths despite evidence of structural inversion (Duddy & Erout 2001; Duddy et al. 2003). Although the magnitude of uplift and erosion is similar to Mussel-1 and Anglesea-1 (~1.5 km), the thermal history reconstruction at Morum-1 shows uplift and erosion commencing in the Late Paleocene to Mid Eocene (~57-40 Ma; Duddy et al. 2003). Finally, the thermal history reconstructions that show Miocene uplift (Anglesea-1, Stoneyford-1 & Olangolah-1; Fig. 17) all indicate similar magnitudes of around 850-1000 m.

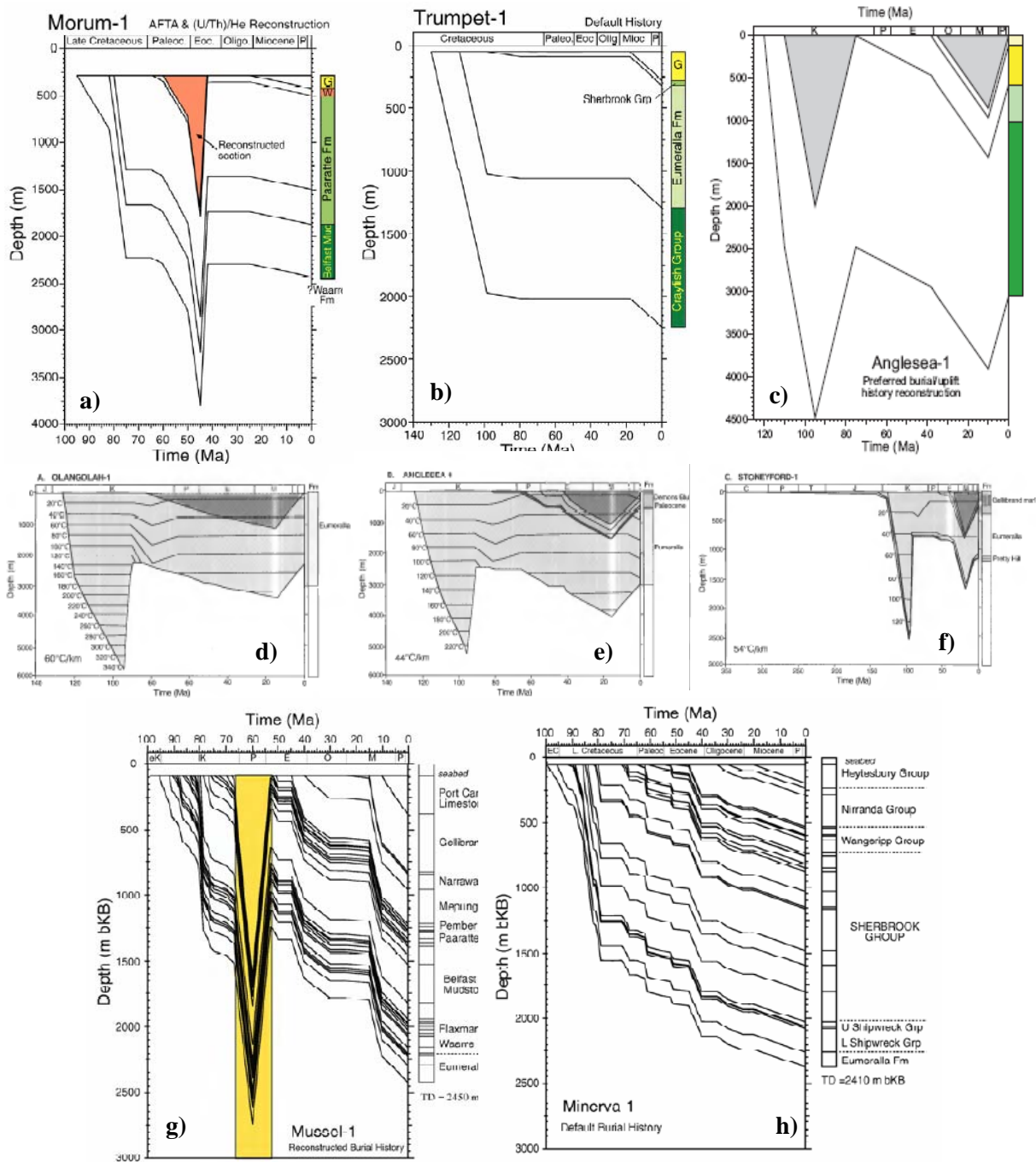
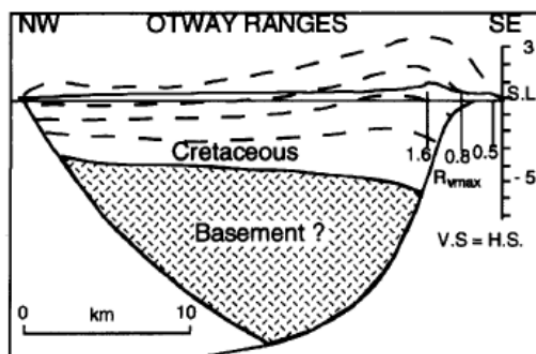


Figure 17: Collage of reconstructed burial histories derived from the thermal history constraints developed for the Otway Basin: *a*) Morum-1 (Duddy et al. 2003) showing 1.5 km of additional Paleocene to Mid-Miocene burial removed by uplift and erosion commencing at 45 Ma. *b*) Trumpet-1 (Duddy et al. 2003) showing no significant erosion and that it is at its maximum burial depth. *c*) Anglesea-1 (Green et al. 2004) showing 2 km of additional Mid-Cretaceous burial removed by uplift and erosion commencing at 95 Ma and 850 m deposited during the Oligocene-Mid Miocene and removed during exhumation between 10 – 0 Ma. *d*) Olangolah-1 (Cooper & Hill 1997) showing ~3 km of Mid-Cretaceous and ~1 km Miocene uplift respectively. *e*) Anglesea-1 (Cooper & Hill 1997) showing ~2.5 km of Mid-Cretaceous and ~1 km Miocene uplift respectively. *f*) Stoneyford-1 (Cooper & Hill 1997) showing ~1.5 km of Mid-Cretaceous and ~500 m Miocene uplift respectively. *g*) Mussel-1 (Duddy & Erout 2001) showing 1.5 km of addition Maastrichtian-Paleocene burial removed by uplift and erosion between 60-52 Ma. Conan-1 has similar results. *h*) Minerva-1 (Duddy & Erout 2001) showing no significant erosion and that it is at its maximum burial depth.



**Figure 5: VR and AFT data indicating Mid-Cretaceous uplift/denudation of ~3 km around the Otway Ranges with the structural style interpreted from field mapping and seismic data (Hill et al. 1995).**

In addition to using thermal history data from petroleum well, Cooper & Hill (1997) constructed denudation maps (Fig. 19) by incorporating modelled Early Cretaceous geothermal gradients with maximum palaeotemperature estimates, based on kinematic models of Burnham & Sweeney (1989) and Sweeney & Burnham (1990) that converted 90 surface VR sample data to temperatures. Cooper & Hill (1997) showed the Otway Ranges as a NE-SW trending inversion anticline during the mid-Cretaceous, with up to 3.5 Km of denudation along the crest and 1-2 km of denudation along the margins, which correlate well with uplift magnitudes proposed by Cooper & Hill (1997).

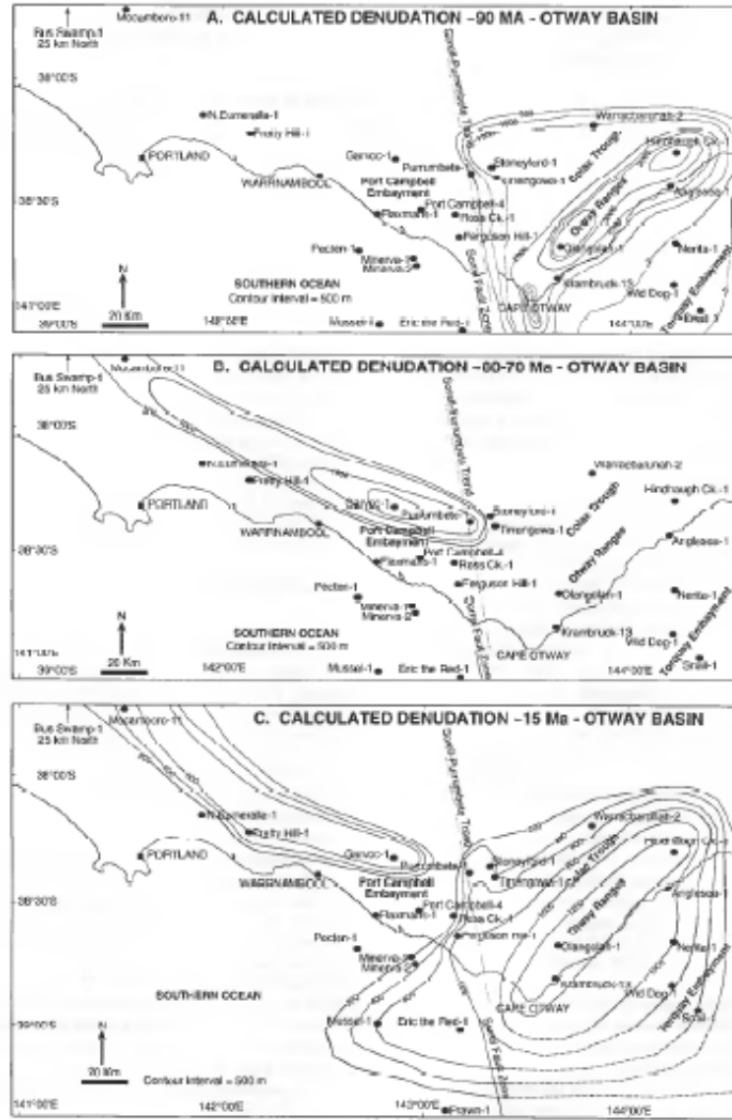
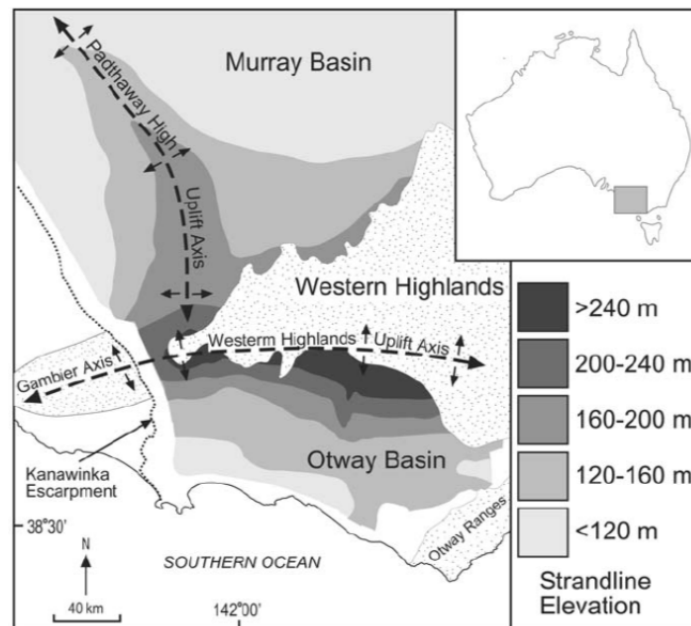


Figure 19: Denudation maps interpreted to represent major uplift and erosion events based on kinematic modelling of VR data from various wells in the Otway Basin for *a*) at ~ 90 Ma *b*) at ~80-70 Ma *c*) at ~15 Ma (after Cooper & Hill 1997).

Another approach which is gaining momentum for identifying and quantifying the magnitude and timing for Neogene uplift in SE Australia is a geomorphological approach whereby strandlines (palaeo-shorelines) can be used since the present elevation of strandlines give a good estimate of post-depositional uplift from the difference in elevation from when it was deposited at sea level (Wallace et al. 2005). A good example is provided on the northwest side of the Otway Ranges where Pliocene strandline systems equivalent to those of the Murray Basin onlap onto the ranges (Dickinson et al. 2001). This shows that individual strandlines can be traced from elevations of ~120 m near Cobden to ~245 m on the Ferguson Hill structure/anticline which implies between 175-240 m of Early Pliocene uplift when

considering eustatic effects (Sandiford 2003a). In addition, such strandlines are displaced across northeast-trending faults (e.g. the Colac Fault which has an estimated throw of ~50 m) and monoclines associated with the Simpson and Ferguson Hill structures indicating post-depositional movement (Sandiford 2003a) in which the earliest strandline sediments have been dated at around  $5.8 \pm 0.2$  Ma from Sr isotope ages (Wallace et al. 2005). Hence, uplift in this area has a maximum age constraint from the latest Miocene onwards, however, the unconformable nature of the Quaternary strandlines with those of the Pliocene in all of the basins may indicate a period of renewed Quaternary tectonism in south-eastern Australia (Wallace et al. 2005). For example, the intense Late Pliocene-Early Quaternary faulting at Hanson Plain and the Late Neogene tectonic relief generation in the Mt Lofty Range some 500 km further west (Sandiford 2003a). A similar strandline study by Wallace et al. (2005) shows good agreement with Sandiford (2003a) with uplift estimates along the broadly east-west Western Highlands – Dundas Tablelands and the northwest-trending Padthaway high of 250 m (Fig. 19). However, the Late Neogene uplift magnitudes concluded from geomorphological studies appear to be around 500 m less than estimates derived from thermochronological analyses.



**Figure 20:** After Wallace et al. (2005) showing the present elevation of Pliocene strandlines of south-western Victoria, indicating the amount of Pliocene-Quaternary uplift. It also shows two Pliocene or younger uplift axes are evident.

In addition to geomorphological approaches, other studies that have used offshore seismic and/or onshore stratigraphic data to identify Late Neogene uplift, as well as Mid-Cretaceous



uplift predominately around the Otway Ranges and adjacent Torquay Sub-basin and Colac Trough. Clear structural deformation, as well as regional uplift and denudation is apparent in the Mid Cretaceous from seismic reflection data with an unconformity truncating folded Aptian-Albian sequences and a minor angularity across this Mid Cretaceous unconformity suggests uplift over a large area (Hill et al. 1995).

The presence of Palaeocene-Eocene coals at 300-360 m in the 600 m high Otway Ranges resting unconformably on the Aptian-Albian Eumeralla Formation had long been recognised (Gloe et al. 1988) as evidence in which to provide a minimum amount of post-Eocene uplift (Hill et al. 1994). Dickinson et al. (2001) concluded significant deformation and exhumation of up to 400 m on the Nerita-1 structure and 600 m near the Otway Ranges coastline occurring during the Late Miocene and continuing into the Pliocene. This was indicated by seismic profiles in the Torquay Sub-basin, the regional angular unconformity at around the Mio-Pliocene boundary in the on and nearshore successions and the change from Oligocene-Miocene cool-water carbonates and brown-coal-dominated successions to more siliclastic-rich Pliocene sediments. Furthermore, they demonstrated folding of the Mio-Pliocene unconformity and showed that Pliocene structures affected Pleistocene sediments, which agrees well with Sandiford (2003b), and indicates Plio-Pleistocene deformation. In addition, Hill et al. (1995) observed that the 600 m high Otway Ranges are characterized by oversteepened creek profiles and mass movement which they suggest is the result of recent uplift.

## **HYDROCARBON SYSTEMS OF THE OTWAY BASIN**

The hydrocarbon systems of the southern Australian margin belong to the Austral Petroleum Supersystem, which is based on the age of their source rocks and common tectonic history (Bradshaw 1993). Within this supersystem, three subdivisions have been recognised for the Otway, Bass and Gippland Basins by Edwards et al. (1999) that are related primarily to different types of depositional environments for the source rocks and correlate geochemically to distinct oil families:

Austral 1 (A1) – Late Jurassic to earliest Cretaceous fluvio-lacustrine shales

Austral 2 (A2) – Early Cretaceous fluvial and coaly facies

Austral 3 (A3) – Late Cretaceous to earliest Tertiary fluvio-deltaic facies

## LITERATURE REVIEWS

Furthermore, Edwards et al. (1999) found that A1 comprised of at least six different oil families, four of which occur in the Otway Basin. Therefore, there are six identified Austral oil families (A1F1, A2F2, A1F3, A1F4, A2 and A3) in the Otway Basin. Table provides a summary of the six oil families including their corresponding: ages, defining geochemical features, environmental depositional source and corresponding rock units, location in the Otway Basin and wells where they have been encountered. However, further gas-oil-source correlations by Boreham et al. (2004) have shown that the originally interpreted A1F1 and A3 oil families are most likely drilling contaminants (e.g. gilsonite contamination) rather than true oil families. To add further complexity, Boulton et al. (2006) has suggested that a new, anoxic marine source facies may be active in the uppermost Eumeralla in the Morum sub-basin offshore South Australia, which could potentially introduce a new oil family (Hall & Keetley 2009). Wells that belong to A1 and A2 oil families can be seen in Fig. 20 (O'Brien et al. (2009).

A graphical summary of the Austral oil families can be seen in Fig. 21, which includes identified source, reservoir, seal rocks and traps. For more information on the Otway Basin Petroleum Systems, the reader is recommended to look at recent studies by Edwards et al. (1999), Boreham et al. (2004) and O'Brien et al. (2009) who present good research and overviews on this topic.



**Figure 21: Wells drilled in the Otway Basin which intersected strong A1 and/or A2 hydrocarbon shows or commercial quantities of hydrocarbons (O'Brien et al. 2009)**

LITERATURE REVIEWS

**Table 4: Summary of Otway Basin hydrocarbon system adapted from Boreham et al. (2004).**

Oil Families	Age	Defining Features	Sourced from....	Location	Found at....
A1F1 (?)		Light carbon isotopes, prominent C <sub>28</sub> sterane and high gammacerane	Saline lacustrine. Playa lake facies(?):		Crayfish-A1, Zema-1
A1F2	<i>Late Jurassic - Early Cretaceous</i>	Low Ph/Pr, no C <sub>30</sub> desmethyl steranes, high content of rearranged hopanes (diahopanes & neohopanes) and an abundance of land plant, bacterial and algal input.	Fresh water lacustrine organic facies: <b>Casterton Formation?</b> / <b>Crayfish Supersequence</b>	western Otway: Robe, Penola, St Clair and Tantanoola Troughs	Killanoola-1, Redman-1, Sawpit-1, Wynn-1
A1F3	<i>Late Jurassic - Early Cretaceous</i>	Higher land plant input (conifer derived diterpanes), low abundance of rearranged hopanes and high bicyclic drimanes	Fluvio-lacustrine to peat swamp: <b>Casterton Formation?</b> / <b>Crayfish Supersequence</b>		Nunga Mia-1 <sup>1</sup> and in the Katnook-Ladbroke Grove and Haselgrove / Haselgrove South fields
A1F4		Ubiquitous terrestrial markers together with marine markers C <sub>30</sub> steranes, dinosterane, high tricyclics and 30-norhopane	Calcareous lithology in a marginal marine setting:		Troas-1 <sup>2</sup>
A2	<i>Early Cretaceous (Aptian – Albian)</i>	Abundant C <sub>29</sub> steranes, moderate diasteranes, significant drimanes and presence of diterpanes, low rearranged hopanes (similar to A1F2 oils)	Dominant peat swamp organic facies exposed to oxic conditions. Terrestrial land-plant material Fluvial, coaly facies: <b>Eumeralla Supersequence</b>	eastern Otway: Shipwreck & Port Campbell Trough	Flaxman-1, La Bella-1, Lindon-1,-2, Minerva-1, Mylor-1, Port Campbell-4, Winderemere-1,-2, Thylacine-1, Geographe-1, Minerva-3, Casino-1,-2, Triton-1
			Mixed source from both <b>Crayfish</b> and <b>Eumeralla supersequences</b> (predominately Eumeralla) within local depocentres	central Otway	Caroline-1, Port Fairy 1;Troas-1(?), Breaksea Reef-1
A3 (?)	<i>Late Cretaceous – Early Tertiary</i>	Low Ph/Pr and high sulphur	Strong marine input with a significant terrestrial component. Fluvio-deltaic(?)	?	(Bass) Cormorant-1, Yolla-1

<sup>1</sup> Oil recovered from a drill stem test (O'Brien et al. 2009).

<sup>2</sup> Oil recovered from a repeat formation tester (O'Brien et al. 2009).

Although no commercial oil accumulations have been discovered, and commercial gas discoveries are currently limited to the Port Campbell Embayment/Trough in Victoria and the Penola Trough in South Australia (Duddy & Erout 2001), oil potential exists as there have been number of oil shows that demonstrate good, medium-gravity, waxy oil proneness (see Table 1). These have been concluded, however, as insufficiently mature to expel oil or have already leaked off (Mehin & Kamel 2002). These oil shows have been reported by Boreham et al. (2004) to have a strong geochemical association with their respective natural gases, suggesting that both are generated from the same source. In addition, Boreham et al. (2004)

## *LITERATURE REVIEWS*

also concluded that the gases and oils, and their respective source rocks have strong stratigraphic and geographic relationship, indicating mainly short- to medium-range migration distances from source to trap. This proximity to actively generating source kitchens is agreed by O'Brien et al. (2009) and also identifies this as being the principal control on the distribution of significant hydrocarbon accumulations in the Otway Basin.

The natural gas accumulations in the Otway Basin vary in composition and show clear geochemical differentiation between those from the western and eastern parts of the basin (Mehin & Kamel 2002), which supports different Petroleum system origins. For example, some gases are rich in methane (96.6%) and low in carbon dioxide (0.14%) whilst others have lower methane content (2.77%) and a higher proportion of carbon dioxide (95.4%) (Mehin & Kamel 2002). However, Mehin & Kamel (2002) suggests that the presence of wet-gas fractions, in addition to carbon dioxide in some petroleum accumulations, actually indicates that the carbon dioxide is not a product of thermal cracking of in-place natural gas. However, the wet-gas is possibly derived from a separate volcanic origin or from thermal decomposition of carbonates deep within the crust.

The different Austral Petroleum Systems are briefly discussed in the following sub sections.

## LITERATURE REVIEWS

### AUSTRAL 1 (A1) PETROLEUM SUPERSYSTEM

Traps:

- east–west striking, faulted anticlines, with closure at the producing Pretty Hill Formation level
- tilted fault blocks with footwall closure

Seal:

Vertical and cross-fault sealing by:

- Laira Formation (SA)
- Eumeralla Formation (Vic)

Reservoir:

- Pretty Hill Formation

Vertical migration

Source:

- Casterton Formation
- Crayfish Subgroup (Pretty Hill Formation & Laira Formation)

} approaching peak maturity for oil generation within the Robe and Penola troughs in South Australia

Maturity:

- Casterton is presently mature (VR = 0.7–1.0%). Ave TOC = 2.6% (in Victoria). Type II/III kerogen (Mehin & Constantine, 1999).
- Pretty Hill, top of the unit is presently early mature for oil generation (VR = 0.5–0.7%), reaching mid-level maturity (VR = 0.7–1.0%) towards the coast. Ave TOC = 1.7% (in Victoria). Principally type III kerogen (Mehin & Constantine, 1999).
- Laira, potentially generative for both oil and gas where it is thermally mature (Mehin & Constantine, 1999).

### AUSTRAL 2 (A2) PETROLEUM SUPERSYSTEM

Traps:

- faulted anticlines,
- tilted fault blocks with footwall closure

Seal:

In Port Campbell & Shipwreck Troughs

- Flaxman Formation
- Belfast Mudstone

Reservoir:

- Waarre Formation

Vertical migration along faults

Source:

- Eumeralla Formation

Maturity:

- Onshore, the top of the unit is presently immature for oil generation (VR < 0.50%) along the northern margin of the basin (Mehin and Link, 1996), but becomes increasingly mature (VR = 1.0–1.3%) offshore (Geary and Reid, 1998).
- The base of the unit, in comparison, is early mature for oil generation (VR = 0.5–0.7%) onshore along the northern margin of the basin and is within the gas generation window (VR = 1.3–2.6%) near the coast.

### AUSTRAL 3 (A3) PETROLEUM SUPERSYSTEM

Traps:

- Faulting (Morum)
- tilted fault blocks (Morum)
- anticlinal (Nelson)
- updip stratigraphic (Nelson)

Seal:

- Belfast
- Intra-formational mudstone within:
  - Paaratte Formation
  - Flaxman Sandstone
  - Paaratte Formation

Reservoir:

- Windermere Sandstone
- Timboon Sandstone
- Katnook Sandstone
- Pebble Point Formation

Source:

- Waarre Formation
- Flaxman Formation
- Belfast Mudstone

Maturity:

- Belfast Mudstone (Breaksea Reef 1 and Argonaut 1), TOC < 3.2% and HI ~ 100–180

**Figure 6: Summary of the Austral Oil Families**

### *A1 Petroleum System (Casterton Formation–Crayfish Sub-Group, Otway Group)*

In the western, South Australian region of the basin, more specifically within Robe and Penola Troughs, the oils have strong stratigraphic and geographic controls on A1 oil families

sourced from dominantly fluvio-lacustrine, syn-rift, organic facies of the Late Jurassic-Early Cretaceous Casterton Formation and Crayfish Supersequence (Hill et al. 1995; Boreham et al. 2004). From the Late Cretaceous onwards, the Casterton Formation has become over-mature for gas generation, however, the Pretty Hill Formation (within Crayfish Supersequence) has remained in the gas generation window in the axis of the Penola Trough since the latest Cretaceous (Hill & Boulton 2002). The A1 system is responsible for virtually all the hydrocarbons in onshore South Australia reservoirs within the Crayfish Subgroup. There have been no commercial A1 source discoveries in the Victorian part of the Otway Basin, however, perhaps due to equivalent source rocks now over-mature and therefore no longer hydrocarbon generative or due to expulsion occurring pre-trap formation (O'Brien et al. 2009).

The Crayfish Subgroup offshore South Australia and south of the Tartwaup Hinge Zone are presumed to underlie the 9 km thick Upper Cretaceous Sherbrook Group which are considered too deep to be considered as potential reservoirs (Boulton et al. 2002). Furthermore the widespread influx of over-mature, dry gas and a more recent influx of magmatic CO<sub>2</sub> to an initially in-place wet gas is evidence for cyclicity in the organic facies involving the Crayfish Group terrestrial land-plant sources (Krassay et al. 2004) and multiple charge histories within the western Otway Basin (Boreham et al. 2004).

### ***A2 Petroleum System (Eumeralla-Waarre Formations)***

In the eastern Otway Basin, there has been two phases of oil generation. Initial generation commenced in the Early Cretaceous at a time of early rifting and high heat flow but was destroyed by subsequent tectonic events, and a second major phase of generation and expulsion occurred in the Miocene and continuing to the present day (Duddy 1997; Duddy & Erout 2001). Greater than 99% of the gas and minor oil accumulations in the eastern (Victorian) Otway Basin (Port Campbell and Shipwreck Trough area; Foster & Hodgson 1995; Luxton et al. 1995) have been geochemically identified as belonging to the A2 oil family. These are primarily sourced from two coal-bearing sequences (one near the Aptian age basal section and the other of lower Albian age) within the Eumeralla Formation. These sections are about 200 m thick and consisting of multiple 2-3 m thick seams with intercalated mudstones rich in disseminated organic matter (Edwards et al. 1999; Boreham et al. 2004; O'Brien et al. 2009). Burial history modelling in the Shipwreck Trough by Ryan et al. (2005)

for generation and expulsion of A2 hydrocarbons has shown that Late Cretaceous deposition of the Sherbrook Group provided the necessary overburden to mature source intervals near the base of the Eumeralla Formation and that the Late Miocene inversion provided the necessary trapping structures. In contrast to the west, most natural gases are interpreted as the result of a single gas charge (Boreham et al. 2004) with excellent potential for the generation of gas and light oil across the basin (Geary & Reid 1998). Irrespective of the hydrocarbon accumulations' location (west, central or east), natural gases and their respective oils are generated immediately adjacent to the source horizons and mainly have short- to medium-range migration distances from source to trap and are not a result of the sandy intervals in the wells being on a pervasive oil migration fairway (Boreham et al. 2004).

The hydrocarbons in the central part of the basin in between Port Campbell and Penola Trough and have a mixed A1 and A2 source affinity within local depocentres, but are predominantly from Eumeralla Supersequence sources (A2) (Boreham et al. 2004).

### ***A3 Petroleum System (Belfast–Waarre–Paaratte–Pebble Point Formations)***

The A3 Petroleum System is responsible for the major oil and gas accumulations derived from the Upper Cretaceous-Lower Tertiary Latrobe Group in the Gippsland Basin, which have temporal equivalent stratigraphic intervals in the Otway Basin (i.e. the Sherbrook and basal Wangerrip Groups). Nevertheless, no significant discoveries have yielded in commercial quantities within these rock units in the Otway Basin (O'Brien et al. 2009). There are reports of oils found within Tertiary Sequences that were initially attributed to the A3 Petroleum System, such as in the Pebble Point Formation (e.g. Wilson-1, Lindon-1 & -2; Lavin 1998), but Boreham et al. (2004) concluded that the Otway Basin Tertiary Sequences are thermally immature for oil expulsion. Furthermore, their geochemical analyses on the Wilson-1 oil indicated it to be a drilling contaminant rather than naturally generated liquid hydrocarbons and the Lindon-1 & -2 oils are partially biodegraded and extensively altered (microbial activity and water washing; Tabassi & Davey, 1986) A2 oils which have migrated up from the older Eumeralla Formation (O'Brien et al. 2009).

Good quality source rocks have been reported in a number of wells occurring in the Turonian Waarre Formation and Belfast Mudstone and are regarded as potentially viable source rocks, especially in deeper, more distal marine parts, provided they are sufficiently buried (O'Brien et al. 2009). Basinward of the Tartwaup-Mussel Fault Zone, the Waarre

## *LITERATURE REVIEWS*

Formation has generated and expelled hydrocarbons in the Late Cretaceous due to rapid and significant loading by the Belfast Mudstone but remains thermally immature onshore and on the modern inner shelf (O'Brien et al. 2009). Although there is good potential source rocks, substantial commercial quantities of A3 hydrocarbons in the Otway Basin remains uncertain until further exploration in offshore deeper waters is undertaken. Moore et al. (2000) argues the maturity of these rocks to be a potential risk in this region of the basin and considered by Boulton et al. (2002) to be too deeply buried as potential reservoirs. As well as the studies already recommended to read on this topic, Moore et al. (2000) and Mehin & Link (1997) give a good assessment of the A3 Petroleum System in the Otway Basin including the source and maturity of the rocks, what are the good reservoirs and seals and, finally, the traps and play types encountered.



## REFERENCES

### *References*

- Aburas, A.N., Boulton, P.J. 2001. New insights into the structural development of the onshore Otway Basin. *In: Hill, K.C., Bernecker, T. (Eds), Eastern Australasian Basins Symposium*, Petroleum Exploration Society of Australia, Special Publication, 447–459.
- Allen, P.A., Allen, J.R., 2005. *Basin Analysis (2nd ed)*. Blackwell, Oxford.
- Allen, P.A., Corcoran, D.V., Clayton, G., 1998. Forward models of heat flow and inversion of vitrinite reflectance data in investigating Tertiary inversion events. *In: Simms, M. (Ed.), Ireland Since the Carboniferous: a 300 Million Year Enigma, Handbook*, Conference at Ulster Museum Belfast. Ulster Museum, Belfast.
- Archard, G., Stafford, J., Bardwell, K., Bagge, M., 1998. A review of techniques used to determine geological and thermal history in the Southern North Sea. *In: Düppenbecker, S.J. and Iliffe, J.E. (Eds), Basin Modelling: Practice and Progress*. Geological Society, London, Special Publication, **141**, 117–136.
- Athy, L.F., 1930. Density, porosity and compaction of sedimentary rocks. *AAPG Bulletin*, **14**, 1–24.
- Barbarand, J., Hurford, A.J., Carter, A., 2003a. Variation in apatite fission-track length measurement: implications for thermal history modelling. *Chemical Geology*, **198**, 77–106.
- Barbarand, J., Carter, A., Wood, I., Hurford, A.J., 2003b. Compositional and structural control of fission-track annealing in apatite. *Chemical Geology*, **198**, 107–137.
- Barker, C.E. and Pawliewicz, M.J., 1986. The correlation of vitrinite reflectance with maximum heating in humic organic matter. *In: Buntebarth, G., Stegena, L. (Eds), Palaeogeothermics*. Springer-Verlag, New York, 79–83.
- Beardmore, G.R., Cull, J.P., 2001. Crustal Heat Flow. *Cambridge University Press, Cambridge*.
- Blackmer, G.C., Omar, G.I., Gold, D.P., 1994. Post-Alleghanian unroofing history of the Appalachian Basin, Pennsylvania, from apatite fission-track analysis and thermal models. *Tectonics*, **13**, 1259–1276, doi:10.1029/94TC01507.
- Boreham, C.J., Hope, J.M., Jackson, P., Daveport, R., Earl, K.L., Edwards, D.S., Logan, G.A. Krassay, A.A., 2004. Gas–oil–source correlations in the Otway Basin, southern Australia. *In: Boulton, P.J., Johns, D.R., Lang, S.C. (Eds), Eastern Australasian Basins*

## REFERENCES

- Symposium II*, Petroleum Exploration Society of Australia, Special Publication, 603–627.
- Boult, P.J., Hibburt, J.E., (Eds), 2002. The petroleum geology of South Australia. Volume 1: Otway Basin, South Australia. Department of Primary Industries and Resources. Petroleum Geology of South Australia Series, 1, 2<sup>nd</sup> edition.
- Boult, P.J., White, M.R., Pollock, R., Morton, J.G.G., Alexander, E.M., Hill, A.J., 2002. Chapter 6: Lithostratigraphy and environments of deposition. *In*: Boult, P.J., Hibburt, J.E. (Eds), *The petroleum geology of South Australia. Volume 1: Otway Basin, South Australia*. Department of Primary Industries and Resources. Petroleum Geology of South Australia Series, 1, 2<sup>nd</sup> edition.
- Boult, P.J., McKirdy, D., Blevin, J., Heggeland, R., Lang, S., Vinall, D. 2005. The oil-prone Morum Sub-basin petroleum system, Otway Basin, South Australia. *MESA Journal*, **38**, 28–33.
- Bradshaw, M.T. 1993. Australian petroleum systems. *PESA Journal*, **21**, 43–53.
- Bray, R.J., Green, P.F., Duddy, I.R., 1992. Thermal history reconstruction using apatite fission track analysis and vitrinite reflectance: a case study from the UK East Midlands and Southern North Sea. *In*: Hardman, R.F.P. (Ed), *Exploration Britain: Geological insights for the next decade*. Geological Society, London, Special Publications, **67**, 3–25.
- Bulat, J., Stoker, M.S., 1987. Uplift determination from interval velocity studies, UK Southern North Sea. *In*: Brooks, J. and Glennie, K. (Eds), *Petroleum Geology of North West Europe*. Graham and Trotman, London, 293–305.
- Burnham, A.K., Sweeney, J.J., 1989. A chemical kinetic model of vitrinite maturation and reflectance. *Geochimica et Cosmochimica Acta*, **53**, 2649–2657.
- Carlson, W.D., Donelick, R.A., Ketcham, R.A., 1999. Variability of apatite fission track annealing kinetics: I. Experimental results. *American Mineralogist*, **84**, 1213–1223.
- C  l  rier, J., Sandiford, M., Lundbek Hansen, D., Quigley, M. 2005. Modes of active intraplate deformation, Flinders Ranges, Australia. *Tectonics*, **24**, TC6006, doi: 10.1029/2004TC001679.
- Cliff, D.C.B., Tye, S.C., Taylor, R., 2004. The Thylacine and Geographe gas discoveries, offshore eastern Otway Basin. *The APPEA Journal*, **44**, 441–461.

## REFERENCES

- Constantine, A., Liberman, N., 2001. Hydrocarbon prospectivity package for VIC/O-01(1), VIC/O-01(2) and VIC/O-01(3), eastern onshore Otway Basin, Victoria, Australia: 2001 Acreage Release: Victorian Initiative for Minerals and Petroleum 70.
- Cooper, G.T., 1995. Structural geology, thermochronology and tectonic evolution of the Torquay Embayment, Eastern Otway Basin. *PhD Thesis*, Monash University (unpublished).
- Cooper, M.A., Williams, G.A., 1989. Inversion Tectonics. *In*: Williams, G.A. (Ed). *Inversion Tectonics*, Geological Society, London, Special Publications, **44**.
- Cooper, G.T., Hill, C.K. 1997. Cross-section balancing and thermochronological analysis of the Mesozoic development of the eastern Otway Basin. *The APPEA Journal*, **37**, 390–413.
- Corcoran, D.V., Clayton, G., 2001. Interpretation of vitrinite reflectance profiles in sedimentary basins, onshore and offshore Ireland. *In*: Shannon, P.M., Haughton, P.D.W. and Corcoran, D.V. (Eds), *The Petroleum Exploration of Ireland's Offshore Basins*. Geological Society, London, Special Publications, **188**, 61–90.
- Corcoran, D.V., Doré, A.G., 2005. A review of techniques for the estimation of magnitude and timing of exhumation in offshore basins. *Earth-Science Reviews*, **72**, 129–168.
- Corcoran, D.V., Mecklenburgh, R., 2005. Exhumation of the Corrib Gas Field, Slyne Basin, Offshore Ireland. *Petroleum Geoscience*, **11**, 239–256.
- Crowhurst, P.V., Green, P.F., Kamp, P.J.J., 2002. Appraisal of (U-Th)/He apatite thermochronology as a thermal history tool for hydrocarbon exploration: An example from the Taranaki Basin, New Zealand. *AAPG Bulletin*, **86**, 1801–1819.
- Denham, D., Weekes, J., Krayshek, C., 1981. Earthquake evidence for compressive stress in the southeast Australian crust. *Journal of the Geological Society of Australia*, **28**, 323–332.
- Densley, M.R., Hillis, R.R., Redfearn, J.E.P., 2000. Quantification of uplift in the Carnarvon Basin based on interval velocities. *Australian Journal of Earth Sciences*, **47**, 111–122.
- Doré, A.G., Jensen, L.N., 1996. The impact of late Cenozoic uplift and erosion on hydrocarbon exploration: offshore Norway and some other uplifted basins. *Global and Planetary Change*, **12**, 415–436.

## REFERENCES

- Doré, A.G., Cartwright, J.A., Stoker, M.S., Turner, J.P., White, N.J., 2002a. Exhumation of the North Atlantic margin: introduction and background. *In: Doré, A.G., Cartwright, J.A., Stoker, M.S., Turner, J.P., White, N.J. (Eds), Exhumation of the North Atlantic Margin: Timing, Mechanisms and Implications for Petroleum Exploration*. Geological Society, London, Special Publications, **196**, 1–12.
- Doré, A.G., Corcoran, D.V., Scotchman, I.C., 2002b. Prediction of the hydrocarbon system in exhumed basins, and application to the NW European margin. *In: Doré, A.G., Cartwright, J.A., Stoker, M.S., Turner, J.P., White, N.J. (Eds), Exhumation of the North Atlantic Margin: Timing, Mechanisms and Implications for Petroleum Exploration*. Geological Society, London, Special Publications, **196**, 401–429.
- Dickinson, J.A., Wallace, M.W., Holdgate, G.R., Daniels, S. J., Gallagher, S.J., Thomas, L. 2001, Neogene tectonics in SE Australia: implications for petroleum systems. *The APPEA Journal*, **41**, 37–52.
- Dickinson, J.A., Wallace, M.W., Holdgate, G.R., Gallagher, S.J., Thomas, L. 2002. Origin and timing of the Miocene-Pliocene unconformity in Southeast Australia. *Journal of Sedimentary Research*, **72**(2), 288–303.
- Duddy, I.R., 1994. The Otway Basin: thermal, structural, tectonic and hydrocarbon generation histories. *NGMA/PESA Otway Basin Symposium Extended Abstracts*, **14**, 35–42.
- Duddy, I.R., 1997. Focussing exploration in the Otway Basin: understanding timing of source rock maturation. *The APPEA Journal*, **37**, 178–191.
- Duddy, I.R., Erout, B. 2001. AFTA-calibrated 2-D modelling of hydrocarbon generation and migration using Temispack: preliminary results from the Otway Basin. *In: Hill, K.C., Bernecker, T. (Eds), Eastern Australasian Basins Symposium*, Petroleum Exploration Society of Australia, Special Publication, 485–497.
- Duddy, I.R., Green, P.F., Bray, R.J., Hegarty, K.A., 1994. Recognition of the thermal effects of fluid flow in sedimentary basins. *In: Parnell, J. (Ed), Geofluids: Origin, Migration and Evolution of Fluids in Sedimentary Basins*. Geological Society, London, Special Publications, **78**, 325–345.
- Duddy, I.R., Green, P.F., Hegarty, K.A., Bray, R.J., O'Brien, G.W., 1998. Dating and duration of hot fluid events determined using AFTA and vitrinite reflectance-based thermal history reconstruction. *In: Parnell, J. (Ed), Dating and Duration of Fluid Flow and Fluid-Rock Interaction*. Geological Society, London, Special Publications, **144**, 41–51.

## REFERENCES

- Duddy, I.R., Erout, B., Green, P.F., Crowhurst, P.V., Boulton, P.J., 2003. Timing constraints on the structural history of the western Otway Basin and implications for hydrocarbon prospectivity around the Morum High, South Australia. *The APPEA Journal*, **43**, 59–83.
- Eaton, B.A., 1972. Graphical method predicts geopressures worldwide. *World Oil*, **183**, 51–56.
- Edwards, D.S., Struckmeyer, H.I.M., Bradshaw, M.T., Skinner, J.E. 1999. Geochemical characteristics of Australia's southern margin petroleum systems. *The APPEA Journal*, **39**, 297–321.
- England, P. and Molnar, P., 1990. Surface uplift, uplift of rocks, and exhumation of rocks. *Geology*, **18**, 1173–1177.
- Ewing, T.E., 2006. Mississippian Barnett Shale, Fort Worth Basin, north-central Texas: Gas shale play with multitrillion cubic foot potential—Discussion. *AAPG Bulletin*, **90**, 963–966, doi:10.1306/02090605132.
- Fall, A., Eichhubl, P., Cumella, S.P., Bodnar, R.J., Laubach, S.E., Becker, S.P., 2012. Testing the basin-centered gas accumulation model using fluid inclusion observations: Southern Piceance Basin, Colorado: *AAPG Bulletin*, **96**, 2297–2318, doi:10.1306/05171211149.
- Finlayson, D.M., Collins, C.D.N., Lukaszyk, I., Chudyyk, E.C. 1998. A transect across Australia's southern margin in the Otway Basin region: crustal architecture and the nature of rifting from wide-angle seismic profiling. *Tectonophysics*, **288**, 177–189.
- Fleischer, R.L., Price, P.B., Walker, R.M., 1965. Effects of temperature, pressure and ionization on the formation and stability of fission tracks in minerals and glasses. *Journal of Geophysical Research*, **70**, 1497–1502.
- Foster, J.D., Hodgeson, A.J. 1995. Port Campbell reviewed: methane and champagne. *The APPEA Journal*, **35**, 418–435.
- Galbraith, R.F., 1981. On statistical models for fission track counts. *Mathematical Geology*, **13**, 471–488.
- Galbraith, R.F., 1990. The radial plot: graphical assessment of spread in ages. *Nuclear Tracks*, **17**, 207–214.
- Gallagher, K., Brown, R., Johnson, C., 1998. Fission track analysis and its applications to geological problems. *Annual Reviews of Earth and Planetary Sciences*, **26**, 519–572.

## REFERENCES

- Gallagher, S.J., Holdgate, G.R. 2000. The palaeogeographic and palaeoenvironmental evolution of a Palaeogene mixed carbonate-siliciclastic cool-water succession in the Otway Basin, Southeast Australia. *Palaeogeography, Palaeoclimatology, Palaeoecology*, **156**, 19–50.
- Geoscience Australia website. [www.ga.gov/energy/province-sedimentary-basin-geology/petroleum/offshore-southern-Australia/otway.html](http://www.ga.gov/energy/province-sedimentary-basin-geology/petroleum/offshore-southern-Australia/otway.html); viewed 04/07/2009.
- GEOTRACK website. [www.geotrack.com.au/afta-why.html](http://www.geotrack.com.au/afta-why.html); viewed 17/06/2009.
- Geary, G.C., Reid, I.S.A., 1998. Hydrocarbon prospectivity of the offshore eastern Otway Basin, Victoria for the 1998 Acreage Release. Victorian Initiative for Minerals and Petroleum Report 55, Department of Natural Resources and Environment.
- Giles, M.R., Indrelid, S.L., James, D.M.D., 1998. Compaction - the great unknown in basin modelling. In: Duppenbecker, S.J., Iliffe, J.E. (Eds), *Basin Modelling: Practice and Progress*. Geological Society, London, Special Publications, **141**, 15–43.
- Gleadow, A.J.W., Duddy, I.R., 1981. A natural long-term annealing experiment for apatite. *Nuclear Tracks*, **5**, 169–174.
- Glenie, R.C. 1971. Upper Cretaceous and Tertiary rock-stratigraphic units in the Central Otway Basin. In: Wopfner, H., Douglas, J.G. (Eds), *The Otway Basin of southeastern Australia*. Special Bulletin of the Geological Surveys of South Australia and Victoria, 193–215.
- Gloe, C., Barton, C.M., Holdgate, G.R., Bolger, P.F., King, R.L., George, A.W. 1998. Brown Coal. In: Douglas, J.G., Ferguson, J.A. (Eds), *Geology of Victoria*, Melbourne: Victorian Division Geological Society of Australia Incorporated. 498–513.
- Green, P.F., 2002. Early Tertiary palaeo-thermal effects in North England: reconciling results from apatite fission track analysis with geological evidence. *Tectonophysics*, **349**, 131–144.
- Green, P.F., Duddy, I.R., 2013. Thermal history reconstructions in sedimentary basins using apatite fission-track analysis and related techniques. *SEPM Special Publication*, **103**, 65–104.
- Green, P.F., Duddy, I.R., Gleadow, A.J.W., Tingate, P.R., Laslett, G.M., 1985. Fission-track annealing in apatite: track length measurements and the form of the Arrhenius plot. *Nuclear Tracks*, **10**, 323–328.

## REFERENCES

- Green, P.F., Duddy, I.R., Gleadow, A.J.W., Tingate, P.R., Laslett, G.M., 1986. Thermal annealing of fission tracks in apatite: A qualitative description. *Chemical Geology*, **59**, 237–253.
- Green, P.F., Duddy, I.R., Laslett, G.M., Hegarty, K.A., Gleadow, A.J.W., Lovering, J.F., 1989. Thermal annealing of fission tracks in apatite: quantitative modelling techniques and extension to geological timescales. *Chemical Geology (Isotope Geoscience Section)*, **75**, 155–182.
- Green, P.F., Duddy, I.R., Bray, R.J., 1995. Applications of thermal history reconstruction in inverted basins. In: Buchanan, J.G., Buchanan, P.G. (Eds), *Basin Inversion*. Geological Society, London, Special Publications, **88**, 148–165.
- Green, P.F., Duddy, I.R., Bray, R.J., Duncan, W.I., Corcoran, D.V., 2001a. The influence of thermal history on hydrocarbon prospectivity in the Central Irish Sea Basin. In: Shannon, P.M., Haughton, P.D.W., Corcoran, D.V. (Eds), *The Petroleum Exploration of Ireland's Offshore Basins*. Geological Society, London, Special Publications, **188**, 171–188.
- Green, P.F., Thomson, K., Hudson, J.D., 2001b. Recognising tectonic events in undeformed regions: contrasting results from the midland Platform and East Midlands Shelf, Central England. *Journal of the Geological Society, London*, **158**, 59–73.
- Green, P.F., Duddy, I.R., Hegarty, K.A., 2002. Quantifying exhumation from apatite fission-track-analysis and vitrinite reflectance data: precision, accuracy and latest results from the Atlantic margin of NW Europe. In: Doré, A.G., Cartwright, J.A., Stoker, M.S., Turner, J.P., White, N. (Eds), *Exhumation of the North Atlantic Margin: Timing, Mechanisms and Implications for Petroleum Exploration*. Geological Society, London, Special Publications, **196**, 331–354.
- Green, P.F., Crowhurst, P.V., Duddy, I.R., 2004. Integration of AFTA and (U-Th)/He thermochronology to enhance the resolution and precision of thermal history reconstruction in the Anglesea-1 well, Otway Basin, SE Australia. In: Boulton, P.J., Johns, D.R., Lang, S.C. (Eds.), *Eastern Australasian Basins Symposium II*, Petroleum Exploration Society of Australia, Special Publication, 117–131.
- Hall, M., Keetley, J. 2009. Otway Basin: stratigraphic and tectonic framework. Geoscience Victoria 3D Victoria Report 2. *Department of Primary Industries*.

## REFERENCES

- Hao, F., Chen, J., 1992. The cause and mechanism of vitrinite reflectance anomalies. *Journal of Petroleum Geology*, **15**, 419–434.
- Hasebe, N., Barbarand, J., Jarvis, K., Carter, A., Hurford, A.J., 2004. Apatite fission track chronometry using laser ablation ICP-MS. *Chemical Geology*, **207**, 135–145.
- Hill, K.A., Cooper, G.T., Richardson, M.J. and Lavin, C.J., 1994. Structural framework of the eastern Otway Basin: inversion and interaction between two major structural provinces. *Exploration Geophysics*, **25**, 79–87.
- Hill, K.C., Hill, K.A., Cooper, G.T., O’Sullivan, A.J., O’Sullivan, P.B., Richardson, M.J., 1995. Inversion around the Bass Basin, SE Australia. *In: Buchanan, J.G. & Buchanan, P.G. (Eds), Basin Inversion*, Geological Society of London, Special Publication, **88**, 528–547.
- Hill, C.K., Cooper, G.T. 1996. A strategy for palinspastic restoration of inverted basins: thermal and structural analyses in SE Australia. *In: Buchanan, E G., Nieuwland, D. A. (Eds), Modern Developments in Structural Interpretation, Validation and Modelling*, Geological Society of London, Special Publication, **99**, 99–115.
- Hill, A.J., Boulton, P.J. 2002. Maturity modelling, hydrocarbon occurrences and shows. *In: Boulton, P.J., Hibbert, J.E. (Eds), The Petroleum Geology of South Australia. Volume 1: Otway Basin, South Australia*. Department of Primary Industries and Resources, Petroleum Geology of South Australia Series, 2nd ed., Chapter 9.
- Hillis, R.R., 1993. Tertiary erosion magnitudes in the East Midlands Shelf, onshore UK. *Journal of the Geological Society, London*, **150**, 1047–1050.
- Hillis, R.R., 1995a. Quantification of Tertiary exhumation in the United Kingdom Southern North Sea using sonic velocity data. *AAPG Bulletin*, **79**, 130–152.
- Hillis, R.R., 1995b. Regional Tertiary Exhumation in and around the United Kingdom. *Journal of the Geological Society, London*, **88**, 167–190.
- Hillis, R. R., Reynolds, S. D. 2000. The Australian Stress Map. *Journal of the Geological Society of London*, **157**, 915–921.
- Hillis, R.R., Sandiford, M., Reynolds, S.D., Quigley, M. C. 2008. Present-day stresses, seismicity and Neogene-to-Recent tectonics of Australia’s ‘passive’ margin: intraplate deformation controlled by plate boundary forces. *In: Johnson, H., Doré A.G., Gatliff, R.W., Holdsworth, R., Lundin, E.R., Ritchie, J.D. (Eds), The Nature and Origin of*



## REFERENCES

- Compression in Passive Margins*. Geological Society, London, Special Publications, **306**, 71–90.
- Holford, S.P., 2005. The Mesozoic-Cenozoic exhumation history of the Irish Sea Basin system, Western UK. *PhD Thesis*, University of Birmingham (unpublished).
- Holford, S.P., Green, P.F., Turner, J.P., 2005a. Palaeothermal and compaction studies in the Mochras borehole (NW Wales) reveal early Cretaceous and Neogene exhumation and argue against regional Palaeogene uplift in the southern Irish Sea. *Journal of the Geological Society, London*, **162**, 829–840.
- Holford, S.P., Turner, J.P., Green, P.F., 2005b. Reconstructing the Mesozoic-Cenozoic exhumation history of the Irish Sea basin system using apatite fission track analysis and vitrinite reflectance data. In: Doré, A.G., Vining, B.A. (Eds), *Petroleum Geology: North-West Europe and Global Perspectives - Proceedings of the 6th Petroleum Geology Conference*. Geological Society, London, 1095–1107.
- Holford, S.P., Turner, J.P., Green, P.F., Hillis, R.R., 2009a. Signature of cryptic basin inversion revealed by shale compaction data in the Irish Sea, western British Isles. *Tectonics*, **28**, TC4011, doi:10.1029/2008TC002359.
- Holford, S.P., Green, P.F., Hillis, R.R., Turner, J.P., Stevenson, C.T.E., 2009b. Mesozoic–Cenozoic exhumation and volcanism in Northern Ireland constrained by AFTA and compaction data from the Larne No. 2 borehole. *Petroleum Geoscience*, **15**, 239–257. DOI 10.1144/1354-079309-840
- Holford, S. P., Hillis, R.R., Duddy, I.R., Green, P.F., Tuitt, A.K., Stoker, M.S., 2010. Impacts of Neogene-Recent compressional deformation and uplift on hydrocarbon prospectivity of the passive southern Australian margin: *Journal of the Australian Petroleum Production and Exploration Association*, **50**, 267–286.
- Holford, S.P., Hillis, R.R., Duddy, I.R., Green, P.F., Tassone, D.R., Stoker, M.S., 2011. Paleothermal and seismic constraints on late Miocene-Pliocene uplift and deformation in the Torquay subbasin, southern Australian margin. *Australian Journal of Earth Sciences*, **58**, 453–562.
- Hubbert, M.K., Rubey, W.W., 1959. Role of pore fluid pressures in the mechanics of overthrusting faulting. *Geological Society of America Bulletin*, **70**, 115–205.

## REFERENCES

- Hurford, A.J., Green, P.F., 1983. The zeta age calibration of fission track dating. *Isotope Geoscience*, **1**, 285–317.
- Japsen, P., 1998. Regional velocity depth anomalies, North Sea Chalk: a record of overpressure and Neogene uplift and erosion. *AAPG Bulletin*, **82**, 2031–2074.
- Japsen, P., 2000. Investigation of multi-phase erosion using reconstructed shale trends based on sonic data. Sole Pit axis, North Sea. *Global and Planetary Change*, **24**, 189–210.
- Japsen, P., Chalmers, J.A., 2000. Neogene uplift and tectonics around the North Atlantic: overview. *Global and Planetary Change*, **24**, 165–173.
- Japsen, P., Bidstrup, T., Lidmar-Bergström, K., 2002. Neogene uplift and erosion of southern Scandinavia induced by the rise of the South Swedish Dome. In: Dore, A.G., Cartwright, J.A., Stoker, M.S., Turner, J.P., White, N. (Eds), *Exhumation of the North Atlantic Margin: Timing, Mechanisms and Implications for Petroleum Exploration*. Geological Society, London, Special Publications, **196**, 183–207.
- Japsen, P., Green, P.F., Nielsen, L.H., Rasmussen, E.S., Bidstrup, T., 2007. Mesozoic-Cenozoic exhumation events in the eastern North Sea Basin: a multi-disciplinary study based on palaeothermal, palaeoburial, stratigraphic and seismic data. *Basin Research*, **19**, 451–490.
- Japsen, P., Bonow, J.M., Green, P.F., Chalmers, J.A., Lidmar-Bergström, K., 2009. Formation, uplift and dissection of planation surfaces at passive continental margins - a new approach. *Earth Surface Processes and Landforms*, **34**, 683–699.
- Japsen, P., Bonow, J.M., Green, P.F., Cobbold, P.R., Chiossi, D., Lilletveit, R., Magnavita, L.P., Pedreira, A., 2012. Episodic burial and exhumation in NE Brazil after opening of the South Atlantic. *Geological Society of America Bulletin*, **124**(5), 800–816.
- Keep, M., Bishop, A. & Longley, I. 2000. Neogene wrench reactivation of the Barcoo Sub-basin, northwest Australia: implications for Neogene tectonics of the northern Australian margin. *Petroleum Geoscience*, **6**, 211–220.
- Kohn, B.P., Belton, D.X., Brown, R.W., Gladow, A.J.W., Green, P.F., Lovering, J.F. 2003. Comment on experimental evidence for the pressure dependence of fission track annealing in apatite. *Earth and Planetary Science Letters*, **215**, 299–306.
- Krassay, A.A., Cathro, D.L., Ryan, D.J. 2004. A regional tectonostratigraphic framework for the Otway Basin. In: Boulton, P.J., Johns, D.R., Lang, S.C. (Eds), *Eastern Australasian*

## REFERENCES

- Basins Symposium II*, Petroleum Exploration Society of Australia, Special Publication, 97–116.
- Laslett, G.M., Green, P.F., Duddy, I.R., Gleadow, A.J.W., 1987. Thermal annealing of fission tracks in apatite 2: A quantitative analysis. *Chemical Geology (Isotope Geoscience Section)*, **65**, 1–13.
- Lavin, C.J., 1998. Geology and prospectivity of the western Victorian Voluta Trough, Otway Basin. Acreage Release 1998, Victorian Institute for Minerals and Petroleum, Report 57.
- Leach, A.S., Wallace, M.W., 2001. Cenozoic canyons systems in cool water carbonates from the Otway Basin, Victoria, Australia. *Eastern Australasian Basins Symposium, A Refocused Energy Perspective for the Future*, Petroleum Exploration Society of Australia, Special Publication, 465–73.
- Lee, M. J., Hwang, Y. J. 1993. Tectonic evolution and structural styles of the East Shetland Basin. In: Parker J. R. (Ed), *Petroleum Geology of Northwest Europe: Proceedings of the 4th Conference*, Geological Society, London, 1137–1149.
- Leeder, M.R., 1999. Sedimentology and Sedimentary Basins. *Blackwell Science*, Oxford.
- Leslie, R.B. 1966. Petroleum exploration in the Otway Basin. Proceedings of the Eighth Commonwealth Minerals and Metallurgy Congress, Australia and New Zealand, **5**, 203–216.
- Lesti, C., Giordano, G., Salvini, F., Cas R., 2008. Volcano tectonic setting of the intraplate, Pliocene-Holocene, Newer Volcanic Province (southeast Australia): Role of crustal fracture zones. *Journal of Geophysical Research*, **113**, B07407, doi:10.1029/2007JB005110.
- Lister, G.S., Etheridge, M.A., Symonds, P.A. 1991. Detachment models for the formation of the passive continental margins. *Tectonics*, **10** (5), 1038–1068.
- Lovibond, R., Sutill, R.J., Skinner, J.E., Aburas, A.N. 1995. The hydrocarbon potential of the Penola Trough, Otway Basin. *The APEA Journal*, **35**, 358–371.
- Luo, X., Vasseur, G., 1995. Modelling of pore pressure evolution associated with sedimentation and uplift in sedimentary basins. *Basin Research*, **7**, 35–52.
- Luxton, C.W., Horan, S.T., Pickavance, D.L., Durham, M.S. 1995. The La Bella and Minerva gas discoveries, offshore Otway Basin. *The APPEA Journal*, **35**, 405–417.

## REFERENCES

- Lyon, P.J., Boulton, P.J., Hillis, R.R., Bierbrauer, K. 2007. Basement controls on fault development in the Penola Trough, Otway Basin, and implications for fault-bounded hydrocarbons. *Australian Journal of Earth Sciences*, **54**, 675–689.
- Magara, K., 1978. Thickness of removed sedimentary rocks, palaeo-pore pressure and palaeo-temperature, southeastern part of Western Canada basin. *AAPG Bulletin*, **60**, 554–566.
- Mavko, G., Mukerji, T., Dvorkin, J., 1998. The Rock Physics Handbook. *Cambridge University Press*, Cambridge.
- Mavromatidis, A., Hillis, R., 2005. Quantification of exhumation in the Eromanga Basin and its implications for hydrocarbon exploration. *Petroleum Geoscience*, **11**, 79–92.
- McClay, K.R., Whitehouse, P.S., Amilibia, A., De Vera, J., Djebbar, T. 2004. 4D Evolution of fault systems in sedimentary basins: a review. *In*: Boulton, P.J., Johns, D.R., Lang, S.C. (Eds), *Eastern Australasian Basins Symposium II*, Petroleum Exploration Society of Australia, Special Publication, 655-680.
- McQueen, A.F. 1962. The geology of the Otway Basin. *Australian Oil and Gas Journal*, **8**(2), 8–12.
- Mehin, K., Link, A.G. 1997. Late Cretaceous source rocks offshore Otway Basin, Victoria and South Australia. Victorian Initiative for Minerals and Petroleum Report 43, Department of Natural Resources and Environment.
- Mehin, K., Constantine, A.E. 1999. Hydrocarbon potential of the western onshore Otway Basin in Victoria: 1999 Acreage Release. Victorian Initiative for Minerals and Petroleum Report 62. Department of Natural Resources and Environment.
- Mehin, K. & Kamel, M., 2002. Gas resources of the Otway Basin in Victoria. Department of Natural Resources and Environment.
- Menpes, R.J., Hillis, R.R., 1995. Quantification of Tertiary exhumation from sonic velocity data, CelticSea/South-Western approaches. *In*: Buchanan, J.G., Buchanan, P.G. (Eds), *Basin Inversion*. Geological Society, London, Special Publications, **88**, 191–207.
- Miller, J. McL., Norvick, M.S., Wilson, C.J.L., 2002. Basement controls on rifting and the associated formation of ocean transform faults – Cretaceous continental extension of the southern margin of Australia. *Tectonophysics*, **359**, 131–155.
- Miranda, J.A., Wallace, M.W., McLaren, S., 2009. Tectonism and eustasy across a Late Miocene strandplain: The Loxton-Parilla Sands, Murray Basin, southeastern Australia. *Sedimentary Geology*, **219**, 24–43.

## REFERENCES

- Mitchum, R.M.JR., Van Wagoner, J.C. 1991. Highfrequency sequences and their stacking patterns: sequencestratigraphic evidence of high-frequency eustatic cycles. *Sedimentary Geology*, **70**, 131–160.
- Montgomery, S., Jarvie, D.M., Bowker, K.A., Pollastro, R.M., 2005. Mississippian Barnett Shale, FortWorth Basin, north-central Texas: Gas-shale play with multitrillion cubic foot potential. *AAPG Bulletin*, **89**, 155–175, doi:10.1306/09170404042.
- Moore, A.M.G., Stagg, H.M.J., Norvick, M.S. 2000. Deep-water Otway Basin: A new assessment of the tectonics and hydrocarbon prospectivity. *The APPEA Journal*, **5**, 66–85.
- Morton, J.G.G., Hill, A.J., Parker, G., Tabassi, A., 1994. Towards a unified stratigraphy for the Otway Basin (abs.). In: Finlayson, D.M. (Ed), *NGMA/PESA Otway Basin Symposium*, Melbourne, 1994. Extended abstracts. Australian Geological Survey Organisation, Record 1994/14, 7–12.
- Morton, J.G.G., Alexander, E.M., Hill, A.J., White, M.R. 1995. Lithostratigraphy and environments of deposition. In: Morton, J.G.G., Drexel, J.F. (Eds), *The petroleum geology of South Australia, Volume 1: Otway Basin*. Mines and Energy South Australia, Report 95/12, 127–139.
- Müller, R.D., Roest, W.R., Royer, J-Y., Gailagan, L.M., Sclater, J.G. 1997. Digital isochrons of the world's oceans. *Journal Geophysical Research*, **102** (B2), 3211–3214.
- Müller, R.D., Gaina, C., Clarke, S. 2000. Seafloor spreading around Australia. In: Veevers, J. (Ed), *Billion year earth history of Australia and neighbours in Gondwanaland*. GEMOC Press, Department of Earth and Planetary Sciences, Macquarie University, Sydney.
- Naeser, C.W., Faul, H., 1969. Fission track annealing in apatite and sphene. *Journal of Geophysical Research*, **74**, 705–710.
- Nelson, E., Hillis, R.R., Sandiford, M., Reynolds, S., Mildren, S. 2006. Present-day state-of-stress of southeast Australia. *The APPEA Journal*, **46**, 283–304.
- Noll, C.A. and Hall, M. 2003. Fluvial architecture and the tectonic control on deposition of onshore Eumeralla Formation, Otway Ranges, Victoria: implications for exploration in the Early Cretaceous Otway Basin. *The APPEA Journal*, **43**, 99–116.
- Norvick, M.S., Smith, M.A. 2001. Mapping the plate tectonic reconstruction of southern and southeastern Australia and implications for petroleum systems. *The APPEA Journal*, **41**, 15–35.

## REFERENCES

- Nuccio, V.F. & Roberts, L.N.R., 2003. Thermal maturity and oil and gas generation history of petroleum systems in the Uinta-Piceance Province, Utah and Colorado. *In* USGS Uinta-Piceance Assessment Team, comp., Petroleum systems and geologic assessment of oil and gas in the Uinta-Piceance Province, Utah and Colorado. *U.S. Geological Survey Digital Data Series*, **69-B**.
- Nyland, B., Jensen, L.N., Skagen, J., Skarpnes, O., Vorren, T., 1992. Tertiary uplift and erosion in the Barents Sea; magnitude, timing and consequences. *In*: Larsen, R.M., Brekke, H., Larsen, B.T., Talleraas, E. (Eds), *Structural and Tectonic Modelling and its Application to Petroleum Geology*. Norwegian Petroleum Society, Amsterdam, Special Publications, **1**, 153–162.
- O'Brien, G.W., Reeves, C.V., Milligan, P.R., Morse, M.P., Alexander, E. M., Willcox, J.B., Yunxuan, Z., Finlayson, D. M., Brodie, R.C. 1994. New ideas on the rifting history and structural architecture of the Western Otway Basin: evidence from the integration of aeromagnetic, gravity and seismic data. *The APEA Journal*, **34**, 529–554.
- O'Brien, G.W., Boreham, C.J., Thomas, H., Tingate, P. 2009. Understanding the Critical Success Factors Determining Prospectivity, Otway Basin, Victoria. *The APPEA Journal*, **49**, 129–70.
- Palmowski, D., Hill, K.C., Hoffmann, N., Bernecker, T., 2001. Otway Basin Rifting to Sea-Floor Spreading – Hydrocarbon implications. *In*: Hill, K.C., Bernecker, T. (Eds), *Eastern Australasian Basin Symposium*, Petroleum Exploration Society of Australia, Special Publication, 499–505.
- Palmowski, D., Hill, K.C., and Hoffman, N., 2004, Structural-stratigraphic styles and evolution of the offshore Otway Basin – a structural seismic analysis. *In*: Boulton, P.J., Johns, D.R., Lang S.C., (Eds), *Eastern Australasian Basins Symposium II*, Petroleum Exploration Society of Australia, Special Publication, 75–96.
- Partridge, A.D. 2001. Revised stratigraphy of the Sherbrook Group, Otway Basin. *In*: Hill, K.C., Bernecker, T. (Eds), *Eastern Australasian Basins Symposium*, Petroleum Exploration Society of Australia, Special Publication, 455–465.
- Perincek, D., Cockshell, C.D., 1995. The Otway Basin: Early Cretaceous rifting to Neogene inversion. *The APEA Journal*, **35**, 451–466.
- Petersen, H.I., Sherwood, N., Mathiesen, A., Fyhn, M.B.W., Dau, N.T., Russell, N., Bojesen-Koefoed, J.A., Nielsen, L.H., 2009. Application of integrated vitrinite reflectance and FAMM analyses for thermal maturity assessment of the northeastern Malay Basin,

## REFERENCES

- offshore Vietnam: Implications for petroleum prospectivity evaluation. *Marine and Petroleum Geology*, **26**, 319–332.
- Reed, J.S., Spotila, J.A., Eriksson, K.A., Bodnar, R.J., 2005. Burial and exhumation history of Pennsylvanian strata, central Appalachian Basin: An integrated study. *Basin Research*, **17**, 259–268, doi:10.1111/j.1365-2117.2005.00265.
- Reynolds, M.A., Evans, P.R., Bryan, R., Hawkins, P.J. 1966. The stratigraphic nomenclature of Cretaceous rocks in the Otway Basin. *Australian Oil and Gas Journal*, **13**(3), 2–33.
- Reynolds, S. D., Coblenz, D. & Hillis, R. R. 2003. Influences of plate-boundary forces on the regional intraplate stress field of continental Australia. *In*: Hillis, R. R. & Muller, R. D. (Eds), *Evolution and Dynamics of the Australian Plate*. Geological Society of Australia, Special Publication, **22**, 59–70.
- Rider, M.H., 1996. The Geological Interpretation of Well Logs. *Whittles Publishing*, Caithness.
- Riis, F., Jensen, L.N., 1992. Introduction: Measuring uplift and erosion - proposal for a terminology. *Norsk Geologisk Tidsskrift*, **72**, 223–228.
- Riis, F., 1996. Quantification of Cenozoic vertical movements of Scandinavia by correlation of morphological surfaces with offshore data. *Global and Planetary Change*, **12**, 331–357.
- Royer, J.Y., Rollet, N. 1997. Plate tectonic setting of the Tasmanian region. *Australian Journal of Earth Sciences*, **44**(5) 543–560.
- Ryan, D.J., Boreham, C.J., Deighton, I., Krassay, A.A., Cathro, D.L. 2005. Petroleum systems of the Otway Basin, Southern Australia: oil and gas in a complex multi-phase rift basin. 25th Annual GCSSEPM Foundation Bob F. Perkins Research Conference: Petroleum Systems of Divergent Continental Margin Basins, Dec 4-7, 2005, Houston, Texas.
- Sandiford, M. 2003a. Geomorphic constraints on the late Neogene tectonics of the Otway Ranges. *Australian Journal of Earth Sciences*, **50**, 69–80.
- Sandiford, M. 2003b. Neotectonics of southeastern Australia: linking the Quaternary faulting record with seismicity and in situ stress. *In*: Hillis, R. R. & Muller, D. R. (Eds), *Evolution and Dynamics of the Australian Plate*. Geological Society of Australia, Special Publication, **22**, 107–119.
- Sandiford, M., Wallace, M. & Coblenz, D. 2004. Origin of the in situ stress field in southeastern Australia. *Basin Research*, **16**, 325–338.

## REFERENCES

- Schlumberger, 1989. Log Interpretation Principles/Applications. *Schlumberger Educational Services*, London.
- Schneider, C.L., Hill, K.C., Hoffman, N. 2004. Compressional growth of the Minerva Anticline, Otway Basin, southeast Australia - Evidence of oblique rifting. *The APPEA Journal*, **44**, 463–480.
- Sclater, J.G., Christie, P.A.B., 1980. Continental stretching: an explanation of the post-mid-Cretaceous subsidence of the Central North Sea Basin. *Journal of Geophysical Research*, **85**, 3711–3739.
- Skagen, J.I., 1992. Methodology applied to uplift and erosion. *Norsk Geologisk Tidsskrift*, **72**, 307–311.
- Smith, G.C. 1988. Oil and Gas. In: Douglas, J.G., Ferguson, J.A. (Eds), *Geology of Victoria*. Melbourne: Victoria Division Geological Society of Australia Incorporated. 514–546.
- Summerfield, M.A., 1991. Global Geomorphology. *Longman*.
- Sweeney, J.J., Burnham, A.K., 1990. Evaluation of a simple model of vitrinite reflectance based on chemical kinetics. *AAPG Bulletin*, **74**, 1559–1570.
- Tabassi, A., Davey, L.K. 1986. Recovery of oil from the basal Tertiary Pebble Point Formation at Lindon No.1 – summary, results and implications. In: Glennie, R.C. (Ed), *Second SE Australian Oil Exploration Symposium*, Melbourne, 1985, 241–253.
- Teasdale, J.P., Pryer, L.L., Stuart-Smith, P.G., Rominr, K.K., Etheridge, M.A., Loutit, T.S., Kyan, D.M. 2003. Structural framework and basin evolution of Australia's southern margin. *The APPEA Journal*, **43**, 13–35.
- Thompson, B.R., Walker, G.M. 1985. Development of a stratigraphic data file for the Otway Basin. In: Otway 85 – Earth Resources of the Otway Basin Conference, Mount Gambier, 1985, Summary papers and excursion guides, Geological Society of Australia, 23–24.
- Tissot, B.P., (1969). Premieres donnees sur les mecanismes et la cinetique de la formation du petrole dans les sediments: simulation d'un schema reactionnel sur ordinateur *Rev. Inst. Fr. Petrol.* **24**, 470–501.
- Turner, J.P., Williams, G.A., 2004. Sedimentary basin inversion and intra-plate shortening. *Earth Science Reviews*, **65**, 277–304.



## REFERENCES

- Veevers, J.J., Powell, C.M., Roots. 1991. Review of seafloor spreading around Australia: I, Synthesis of the patterns of spreading. *Australian Journal of Earth Sciences*, **38**(4), 373–389.
- Vail, P.R., Audemard, F., Bowman, S.A., Eisner, P.N., Perez-Cruz, C. 1991. The stratigraphic signatures of tectonics, eustasy and sedimentology-an overview. *In: Einsele, G., Ricken, W., Seilacher, A. (Eds), Cycles and events in stratigraphy*, 617–659.
- Wallace, M.W., Dickinson, J.A., Moore, D.H., Sandiford, M. 2005. Late Neogene strandlines of southern Victoria: a unique record of eustasy and tectonics in southeast Australia. *Australian Journal of Earth Sciences*, **52**, 277–295.
- Wagner, G.A., 1979. Correction and interpretation of fission track ages. *In: Jager, E., Hunziker, J.C. (Eds), Lectures in Isotope Geology*. Springer-Verlag, Berlin, 170–205.
- Waples, D.W., (1980). Time and temperature in petroleum formation: application of Lopatin's method to petroleum exploration. *AAPG Bulletin*, **64**, 916–926.
- Ware, P.D., Turner, J.P., 2002. Sonic velocity of the Tertiary denudation of the Irish Sea basin. *In: Doré, A.G., Cartwright, J.A., Stoker, M.S., Turner, J.P., White, N. (Eds), Exhumation of the North Atlantic Margin: Timing, Mechanisms and Implications for Petroleum Exploration*. Geological Society, London, Special Publications, **196**, 355–370.
- Wendt, A.S., Vidal, O., Chadderton, L.T., 2002. Experimental evidence for the pressure dependence of fission track annealing in apatite. *Earth and Planetary Science Letters*, **201**, 593–607.
- White, A.H. 1968. Exploration in the Otway Basin. *APPEA Journal*, **8**, 78–87.
- White, M.R. 1995. Micropalaeontological analysis of 26 petroleum wells in the Gambier Basin, South Australia. Department of Mines and Energy, South Australian Report Book 95/6.
- Willcox, J.B., Stagg, H.M.J. 1990. Australia's southern margin: a product of oblique extension. *Tectonophysics*, **173**, 269–281.
- Wolf, R.A., Farley, K.A., Silver, L.T., 1996. Helium diffusion and low-temperature thermochronology of apatite. *Geochimica et Cosmochimica Acta*, **60**, 21, 4231–4140
- Wyllie, M.R.J., Gregory, J.A.R., Gardner, L.W., 1956. Elastic wave velocities in heterogeneous and porous media. *Geophysics*, **21**, 41–70.

## *REFERENCES*

### 3 Thesis Conclusions

The research, results and conclusions described within each individual paper in this thesis integrate multiple petroleum geology disciplines and concepts in order to provide a better understanding of ‘*Compressional deformation and exhumation in sedimentary basins at ‘passive’ continental margin, with implications for hydrocarbon exploration and development*’. This thesis has primarily focussed on the Otway Basin, located along Australia’s southern margin, with a secondary investigation focused on the Faroe-Shetland regional located along the northwestern European Atlantic margin. The complex tectonic histories in these regions make ideal natural laboratories to help understand syn-rift and post-rift passive margin exhumation, compressional deformation and neotectonics.

Exhumation magnitudes can be quantified and tightly constrained within “passive” continental margin sedimentary basins using an integrated approach that utilizes petrophysical, thermal history, palynological and seismic-stratigraphic data. For example, ~400-3600 m of post-Albian and ~300-1000 m of post-Danian net exhumation have been estimated for Otway Basin and Faroe-Shetland region, respectively. Whilst the cause and timing of exhumation along the Rona High, West Shetland and North Rona basins within the Faroe-Shetland region requires ongoing research, the distribution of exhumation in relation to mid-Cretaceous and Neogene neotectonic compressional structures within the Otway Basin indicates that exhumation was most likely controlled by short-wavelength basin inversion of syn-rift faults.

Formation pore pressures have generally assumed to be hydrostatic in the Otway Basin. Overpressures in the Upper Cretaceous Belfast and Flaxman formations in several wells in the Voluta Trough have been observed, however, with pore pressure magnitudes exceeding ~16 MPa/km at Bridgewater Bay-1, where ~700 m of Pliocene-Recent marine clastic sediments were deposited rapidly in submarine channels perhaps linked to a proto-Murray River.

Contemporary stress studies conducted along the southern Australian margin have shown that observed maximum horizontal stress orientations are consistent with the predictions of plate-scale finite-element stress modelling (i.e., approximately northwest-southeast in the Otway Basin). Whilst there is general consensus regarding the controls on contemporary stress *orientations* in most Australian margin basins, however, contemporary stress *magnitudes* constrained using petroleum exploration data appear to be inconsistent with geological observations. Using hydrocarbon exploration data alone indicates that

## THESIS CONCLUSIONS

contemporary stresses magnitudes in the central and eastern Otway Basin are reminiscent of a dominantly strike-slip faulting stress state; although it is shown that there is considerable variability across basin. When incorporating complementary geophysical datasets (e.g. seismic reflection, seismicity, magnetic, radiometric, gravity data) coupled with neotectonic geological faulting and folding observations that take into account lithology, underlying basement fabrics and structural style with depth, however, stress magnitude inconsistencies can be reconciled when these observations are taken into account.

It is demonstrated that estimated magnitudes of exhumation within the eastern Otway Basin could be accounted for solely by crustal shortening, despite bulk crustal strain rates declining since the late Miocene-early Pliocene to the present day based on calculated geological and seismogenic strain rates that also indicate ~30% of Quaternary deformation is aseismic. Furthermore, the orientation of shallower intra-basin stresses within the eastern Otway Basin, which are dominantly orthogonal to neotectonic structural features, is consistent with deeper basement stresses across southeastern Australia and plate-scale finite element modelling, validating the notion that plate-boundary forces are capable of generating mild but appreciable deformation and uplift within continental margin interiors. For this reason we postulate that fluctuations in intraplate stress magnitude and orientation governed by the dynamics of plate-boundary forces, in particular reorganisation of the northern North Atlantic spreading system, exert a major control on the spatial and temporal magnitudes of exhumation within the Faroe-Shetland region.

Within the Otway Basin, we address, at length, the implications of both mid-Cretaceous and Neogene exhumation and compression deformation on a number of important aspects with respect to hydrocarbon systems that can affect prospectivity in the Otway Basin. This includes impacts on hydrocarbon generation and charge with respect to the timing of trap formation, conventional trap and seal integrity, meteoric water flushing of conventional reservoirs. Whilst the impacts of exhumation have been documented and are better known with respect to *conventional* hydrocarbon plays, we also address the implications of exhumation and compressional deformation to globally emerging *unconventional* hydrocarbon plays. In particular, we discuss the impacts of burial and exhumation on the petrographical and geomechanical properties, and development of secondary porosity of the source-seal-reservoir rocks and suggest that these brittle, thermal matured rocks at shallower, economic depths is potentially favourable for unconventional plays, depending on the cause of exhumation.

## THESIS CONCLUSIONS

*Only if Charles Darwin understood that intraplate stresses generated from plate-boundary forces can cause significant amounts of compressional deformation, uplift and exhumation over time spans of one million to ten million years, he could have confidently explained to his fellow exploration party that a covering of strata has since been removed across the coast of Brazil – a “passive” continental margin.*

## **4 First Author Journal Publications**

***PAPER 1: Quantifying Cretaceous-Cenozoic exhumation in the Otway Basin using sonic transit time data: implications for conventional and unconventional hydrocarbon prospectivity***

**American Association of Petroleum Geologists Bulletin (2014), 98 (1), 67–117.**

***David R. Tassone, Simon P. Holford, Ian R. Duddy, Paul F. Green & Richard R. Hillis***

# Statement of Authorship

Title of Paper	Quantifying Cretaceous-Cenozoic exhumation in the Otway Basin, southeastern Australia, using sonic transit time data: Implications for conventional and unconventional prospectivity
Publication Status	<input checked="" type="radio"/> Published <input type="radio"/> Accepted for Publication <input type="radio"/> Submitted for Publication <input type="radio"/> Publication Style
Publication Details	Tassone, D.R., Holford, S.P., Duddy, I.R., Green., P.F., Hillis, R.R., (2014) Quantifying Cretaceous-Cenozoic exhumation in the Otway Basin using sonic transit time data: implications for conventional and unconventional hydrocarbon prospectivity. American Association of Petroleum Geologist Bulletin, 98 (1), 67–117.

## Author Contributions

By signing the Statement of Authorship, each author certifies that their stated contribution to the publication is accurate and that permission is granted for the publication to be included in the candidate's thesis.

Name of Principal Author (Candidate)	David R. Tassone		
Contribution to the Paper	Performed analysis on all petrophysical log data, interpreted data, wrote manuscript and acted as corresponding author		
Overall percentage (%)	70		
Signature		Date	02/04/2014

Name of Co-Author	Simon P. Holford		
Contribution to the Paper	Supervised development of work, helped in data interpretation, manuscript evaluation and editing of paper		
Overall percentage (%)	10		
Signature		Date	20/3/2014

Name of Co-Author	Ian R. Duddy		
Contribution to the Paper	Provided data and helped in data interpretation.		
Overall percentage (%)	10		
Signature		Date	20/3/2014

Please cut and paste additional co-author panels here.



# Statement of Authorship

Title of Paper	Quantifying Cretaceous-Cenozoic exhumation in the Otway Basin, southeastern Australia, using sonic transit time data: Implications for conventional and unconventional prospectivity
Publication Status	<input checked="" type="radio"/> Published <input type="radio"/> Accepted for Publication <input type="radio"/> Submitted for Publication <input type="radio"/> Publication Style
Publication Details	Tassone, D.R., Holford, S.P., Duddy, I.R., Green., P.F., Hillis, R.R., (2014) Quantifying Cretaceous-Cenozoic exhumation in the Otway Basin using sonic transit time data: implications for conventional and unconventional hydrocarbon prospectivity. American Association of Petroleum Geologist Bulletin, 98 (1), 67–117.

## Author Contributions

By signing the Statement of Authorship, each author certifies that their stated contribution to the publication is accurate and that permission is granted for the publication to be included in the candidate's thesis.

Name of Principal Author (Candidate)	Paul F. Green		
Contribution to the Paper	Minor input into technical concept and minor input into editing.		
Overall percentage (%)	5		
Signature	_____	Date	20/3/2014

Name of Co-Author	Richard R. Hillis		
Contribution to the Paper	Minor input into technical concept.		
Overall percentage (%)	5		
Signature	_____	Date	20/3/2014

Name of Co-Author	_____		
Contribution to the Paper	_____		
Overall percentage (%)	_____		
Signature	_____	Date	_____

Please cut and paste additional co-author panels here.

Tassone, D.R., Holford, S.P., Duddy, I.R., Green, P.F. & Hillis, R.R. (2014) Quantifying Cretaceous-Cenozoic exhumation in the Otway Basin, southeastern Australia, using sonic transit time data: implications for conventional and unconventional hydrocarbon prospectivity. *AAPG Bulletin*, v. 98(1), pp. 67-117

NOTE:

This publication is included on pages 102-152 in the print copy of the thesis held in the University of Adelaide Library.

It is also available online to authorised users at:

<http://dx.doi.org/10.1306/04011312111>

***4.1 PAPER 2: Overpressures in the central Otway Basin: the result of rapid Pliocene–Recent sedimentation?***

**Australian Petroleum Production & Exploration Association Journal (2011), 51, 439–458.**

***David R. Tassone, Simon P. Holford, Mark R. P. Tingay, Adrian .K. Tuitt, Martyn S. Stoker & Richard R. Hillis***

# Statement of Authorship

Title of Paper	Overpressures in the central Otway Basin: the result of rapid Pliocene-Recent sedimentation?
Publication Status	<input checked="" type="radio"/> Published <input type="radio"/> Accepted for Publication <input type="radio"/> Submitted for Publication <input type="radio"/> Publication Style
Publication Details	Tassone, D.R., Holford, S.P., Tingay, M.R.P., Tuitt, A.K., Stoker, M.S., Hillis R.R., (2011) Overpressures in the central Otway Basin: the result of rapid Pliocene-Recent sedimentation? Journal of the Australian Petroleum Production and Exploration Association, 51, 439-458.

## Author Contributions

By signing the Statement of Authorship, each author certifies that their stated contribution to the publication is accurate and that permission is granted for the publication to be included in the candidate's thesis.

Name of Principal Author (Candidate)	David R. Tassone		
Contribution to the Paper	Performed analysis on all petrophysical log data, interpreted and integrated data, wrote manuscript and acted as corresponding author		
Overall percentage (%)	65		
Signature		Date	

Name of Co-Author	Simon P. Holford		
Contribution to the Paper	Supervised development of work, helped in data interpretation, manuscript evaluation and editing		
Overall percentage (%)	10		
Signature		Date	20/3/2014

Name of Co-Author	Mark R.P. Tingay		
Contribution to the Paper	Major input into technical concept and editing.		
Overall percentage (%)	10		
Signature		Date	27/3/14

Please cut and paste additional co-author panels here.

# Statement of Authorship

Title of Paper	Overpressures in the central Otway Basin: the result of rapid Pliocene-Recent sedimentation?
Publication Status	<input checked="" type="radio"/> Published <input type="radio"/> Accepted for Publication <input type="radio"/> Submitted for Publication <input type="radio"/> Publication Style
Publication Details	Tassone, D.R., Holford, S.P., Tingay, M.R.P., Tuitt, A.K., Stoker, M.S., Hillis R.R., (2011) Overpressures in the central Otway Basin: the result of rapid Pliocene-Recent sedimentation? Journal of the Australian Petroleum Production and Exploration Association, 51, 439-458.

## Author Contributions

By signing the Statement of Authorship, each author certifies that their stated contribution to the publication is accurate and that permission is granted for the publication to be included in the candidate's thesis.

Name of Principal Author (Candidate)	Adrian K. Tuitt		
Contribution to the Paper	Minor input into data interpretation		
Overall percentage (%)	5		
Signature		Date	20/3/2014

Name of Co-Author	Martyn S. Stoker		
Contribution to the Paper	Minor input into technical concept		
Overall percentage (%)	5		
Signature		Date	21/03/14

Name of Co-Author	Richard R. Hillis		
Contribution to the Paper	Minor input into technical concept		
Overall percentage (%)	5		
Signature		Date	20/3/2014

Please cut and paste additional co-author panels here.

Tassone, D.R., Holford, S.P., Tingay, M.R.P., Tuitt, A.K., Stoker, M.S. & Hillis, R.R. (2011)  
Overpressures in the central Otway Basin: the result of rapid pliocene-recent sedimentation?  
*APPEA Journal*, v. 51, pp. 439-458

NOTE:

This publication is included on pages 156-175 in the print copy  
of the thesis held in the University of Adelaide Library.

4.2 **PAPER 3:** Contemporary stress and neotectonics in the Otway Basin, southeastern Australia

**Tectonophysics (*in-prep*), manuscript**

***David R. Tassone, Simon P. Holford, Rosalind King, Mark R.P. Tingay & Richard R. Hillis***

# Statement of Authorship

Title of Paper	Contemporary stress and neotectonics in the Otway Basin, southeastern Australia
Publication Status	<input type="radio"/> Published <input type="radio"/> Accepted for Publication <input type="radio"/> Submitted for Publication <input checked="" type="radio"/> Publication Style
Publication Details	Tassone, D.R., Holford, S.P., King, R., Tingay, M.R.P., Hillis R.R.. (in prep) Contemporary stress and neotectonics in the Otway Basin, southeastern Australia. Tectonophysics

## Author Contributions

By signing the Statement of Authorship, each author certifies that their stated contribution to the publication is accurate and that permission is granted for the publication to be included in the candidate's thesis.

Name of Principal Author (Candidate)	David R. Tassone		
Contribution to the Paper	Performed all stress analysis, interpreted and integrated data, wrote manuscript and acting as corresponding author		
Overall percentage (%)	70		
Signature		Date	02/04/2014

Name of Co-Author	Simon P. Holford		
Contribution to the Paper	Supervised development of work, helped in data interpretation, manuscript evaluation and editing of paper		
Overall percentage (%)	10		
Signature		Date	20/3/2014

Name of Co-Author	Rosalind King		
Contribution to the Paper	Major input into technical concept and editing		
Overall percentage (%)	10		
Signature		Date	04/04/2014

Please cut and paste additional co-author panels here.



# Statement of Authorship

Title of Paper	Contemporary stress and neotectonics in the Otway Basin, southeastern Australia
Publication Status	<input type="radio"/> Published <input type="radio"/> Accepted for Publication <input type="radio"/> Submitted for Publication <input checked="" type="radio"/> Publication Style
Publication Details	Tassone, D.R., Holford, S.P., King, R., Tingay, M.R.P., Hillis R.R., (in prep) Contemporary stress and neotectonics in the Otway Basin, southeastern Australia. Tectonophysics

## Author Contributions

By signing the Statement of Authorship, each author certifies that their stated contribution to the publication is accurate and that permission is granted for the publication to be included in the candidate's thesis.

Name of Principal Author (Candidate)	Mark R.P. Tingay		
Contribution to the Paper	Minor input into editing and technical concept		
Overall percentage (%)	5		
Signature		Date	27/3/14

Name of Co-Author	Richard R. Hillis		
Contribution to the Paper	Minor input into technical concept and editing		
Overall percentage (%)	5		
Signature		Date	20/3/2014

Name of Co-Author			
Contribution to the Paper			
Overall percentage (%)			
Signature		Date	

Please cut and paste additional co-author panels here.

1 Contemporary stress and neotectonics in the Otway Basin,  
2 southeastern Australia

3  
4 David R. Tassone<sup>1\*</sup>, Simon P. Holford<sup>1</sup>, Rosalind King<sup>2</sup>, Mark R.P. Tingay<sup>1</sup>, Richard  
5 R. Hillis<sup>3</sup>

6 <sup>1</sup>Australian School of Petroleum, Centre for Tectonics, Resources and Exploration (TRaX), The  
7 University of Adelaide, North Terrace, Adelaide, SA 5005, Australia

8 <sup>2</sup>Discipline of Geology and Geophysics, Centre for Tectonics, Resources and Exploration (TRaX),  
9 The University of Adelaide, North Terrace, Adelaide, SA 5005, Australia

10 <sup>3</sup>Deep Exploration Technologies CRC, 26 Butler Boulevard, Burbridge Business Park, Adelaide  
11 Airport, SA 5950, Australia

12 \*Corresponding author (e-mail: david.tassone@woodside.com.au)

13

14

15 **Abstract**

16 Southeastern Australia is characterised by relatively high levels of neotectonic activity for an  
17 intraplate region. This activity comprises compressional deformation and uplift, which is commonly  
18 ascribed to an intraplate stress regime controlled by far-field plate boundary forces. However, whilst  
19 the orientations of contemporary maximum horizontal stresses determined from petroleum  
20 exploration data are generally consistent with palaeostress trends inferred from neotectonic structural  
21 features and seismicity, there is less consistency between stress magnitudes. Whereas the neotectonic  
22 faulting record points to a reverse fault stress regime (i.e.,  $SH_{max} > Sh_{min} > S_V$ ), past studies of  
23 contemporary stress magnitudes using petroleum exploration data have mostly indicated normal or  
24 strike slip fault stress conditions (i.e.,  $SH_{max} > S_V > Sh_{min}$  or  $S_V > SH_{max} > Sh_{min}$ ). Here, we present a  
25 new analysis of contemporary stress orientations and magnitudes in southeastern Australia using  
26 petroleum exploration data from the Otway Basin, one of several basins that formed along  
27 Australia's southern margin during Cretaceous-Paleogene continental separation from Antarctica.  
28 Wellbore failure analysis of 11 wells indicates the maximum horizontal stress azimuth in this basin  
29 is  $\sim 135 \pm 15^\circ \text{N}$ , consistent with previous wellbore failure studies, results from stress modelling, and

30 palaeostress indicators in onshore pre-Permian basement rocks. Lithology, underlying structural  
31 fabrics and variations in structural style with depth exert important controls on horizontal stress  
32 magnitudes within the basin. Leak-off pressures are very high (often greater than lithostatic) in post-  
33 rift Oligocene-Miocene marl and carbonate-dominated formations, where neotectonic deformation is  
34 typically manifested by northeast-southwest trending, low amplitude and long wavelength folds. In  
35 Eocene and older syn-rift siliciclastic sections, leak-off pressures indicate that the least principle  
36 stress is horizontal, and sand-dominated formations typically display minimum horizontal stress  
37 gradients that are ~3-4 MPa/km lower than shale-dominated formations. Within the basin there is an  
38 overall increase in the minimum horizontal stress gradient of ~1-2 MPa/km from the west to east.  
39 This increase corresponds with a change in structural style across the basin. In the central Otway  
40 Basin, rift-related faults are near-parallel to the contemporary maximum horizontal stress azimuth  
41 and there are comparatively low levels of neotectonic activity, whilst in the eastern Otway Basin  
42 where rift-related faults strike near-orthogonal to the contemporary maximum horizontal stress  
43 azimuth, the level of neotectonic faulting and uplift is much higher. The observation of strike-slip  
44 fault stress regimes within syn-rift sections of the basin may be due to the underestimation of  
45 horizontal stress magnitudes interpreted from leak-off pressures. Alternatively, the observed  
46 partitioning of stress regimes and deformation styles with depth, whereby the shallow post-rift  
47 Oligocene to Miocene sequence potentially indicates a reverse fault stress state and the deeper syn-  
48 rift Cretaceous-Paleocene siliciclastic sequence indicates a strike-slip stress state, may reflect  
49 varying mechanical properties of the basin fill. Our results show how an integrated approach  
50 incorporating structural geology with geomechanical datasets can help reconcile contemporary *in-*  
51 *situ* stresses using petroleum exploration data with neotectonic geological observations.

52

### 53 **Keywords**

54 Otway Basin; southern Australian margin; *in-situ* stresses; inversion; compressional deformation;  
55 Neotectonics

## 56 **1 Introduction**

57 The Otway Basin in southeastern Australia formed as a result of the Late Jurassic to early Paleogene  
58 separation of Australia from Antarctica (Norvick and Smith, 2001; Krassay et al., 2004). A  
59 significant NW-SE compressional deformation event during the mid-Cretaceous interrupted this  
60 rifting (Fig. 1), causing regional exhumation and subsequent rifting to be focussed along the Tasman  
61 Fault Zone, effectively creating a failed rift system through Bass Strait (Fig. 2; Hill et al., 1995;  
62 Cayley, 2011). Following final continental separation at ~43 Ma, post-rift subsidence in the Otway  
63 Basin has been interrupted by several periods of uplift, exhumation and compressional deformation  
64 during the mid-Eocene and mid-Oligocene, with the most recent phase beginning during the late  
65 Miocene to early Pliocene and continuing to the present day (Fig. 1; Cooper and Hill, 1997; Krassay  
66 et al., 2004; Holford et al., 2014). This complex tectonic history makes the Otway Basin an ideal  
67 natural laboratory to help understand post-rift passive margin compressional deformation and  
68 neotectonics. Neogene, neotectonic compressional deformation is widespread over much of south-  
69 eastern Australia (Dickinson et al., 2002), consisting of two separate phases of deformation: an  
70 initial late Miocene-early Pliocene phase and a subsequent late Pliocene-Holocene phase (Fig. 1;  
71 Wallace et al., 2005). Within the on- and offshore Gippsland Basin (e.g., Strezleki Ranges) and in  
72 the vicinity of the Otway Ranges and adjacent offshore areas across the eastern Otway Basin, there  
73 is strong evidence for local Neogene basin inversion (Cooper and Hill, 1997; Holford et al., 2011a)  
74 and an abundance of neotectonic features, such as fault scarps, monoclines and anticlines. Assuming  
75 a vertical orientation is a principal stress orientation, these neotectonic features collectively point  
76 towards a reverse fault stress regime (Fig. 2; Sandiford, 2003a,b; Hillis et al., 2008; Clark et al.,  
77 2011). High levels of seismicity in the Otway Basin and over much of southeastern Australia  
78 (relative to other stable intraplate settings; e.g., Johnston, 1994) provide further evidence that  
79 neotectonic deformation continues to the present day (Fig. 2). Though geological observations from  
80 within the Otway Basin indicate that the intensity of this activity has declined since a peak during  
81 the late Miocene to early Pliocene (Sandiford, 2003b; Tassone et al., 2012).

82

83 A number of contemporary stress studies conducted in Australian basins (e.g., Hillis and Williams,  
84 1992, 1993; Hillis et al., 1995; Mildren and Hillis, 2000; Reynolds and Hillis, 2000; Reynolds et al.,  
85 2003b, 2004; Nelson et al., 2006a) have shown that observed maximum horizontal stress orientations  
86 are consistent with the predictions of plate-scale finite-element stress modelling. This implies that  
87 plate boundary forces exert a first-order control on the state of stress (Fig. 2; Hillis and Reynolds,

88 2000; Reynolds et al., 2003a; Dyksterhuis and Müller, 2008). Across both the Otway Basin and  
89 broader regions of southeastern Australia, stress modelling studies suggest that horizontal stress  
90 orientations primarily reflect the increased coupling of the Australian and Pacific plate boundaries  
91 associated with the formation of the southern Alps in New Zealand since the late Miocene to early  
92 Pliocene (Sandiford et al., 2004). However, whilst there is general consensus regarding the controls  
93 on contemporary stress *orientations* in most Australian margin basins, contemporary stress  
94 *magnitudes* constrained using petroleum exploration data appear to be inconsistent with geological  
95 observations (Hillis et al., 2008; King et al., 2012). For example, in the central and eastern Otway  
96 Basin, some recent studies (e.g., Bérard et al., 2008) have constrained a normal fault *in-situ* stress  
97 regime (i.e.,  $S_V > SH_{max} > Sh_{min}$ ) whilst others (e.g., Nelson et al., 2006a) indicate a strike-slip fault  
98 *in-situ* stress regime (i.e.,  $SH_{max} > S_V > Sh_{min}$ ). Indeed, these conflicting results may be due in part to  
99 the application of different techniques used to constrain horizontal stress magnitudes (Vidal-Gilbert  
100 et al., 2010). Establishing the causes of the incompatibility between petroleum data and neotectonic  
101 evidence, which clearly indicates a reverse fault stress regime (e.g., Cooper and Hill, 1997; Hillis et  
102 al., 2008; Holford et al., 2010, 2011a; Tassone et al., 2012, 2014), remains a challenging and  
103 outstanding issue (Couzens-Schultz and Chan, 2010; King et al., 2012).

104

105 In this study we use recently available petroleum exploration datasets, including petrophysical  
106 wireline and drilling data (Fig. 3), to constrain the *in-situ* stress states within the central and eastern  
107 Otway Basin. Recent offshore hydrocarbon discoveries and renewed exploration interest in the  
108 unconventional hydrocarbon potential of the onshore basin has provided a wealth of new data within  
109 the Victorian sector of the Otway Basin, that can be used to tackle the problem of the incompatible  
110 stress regimes indicated by petroleum datasets and geological evidence (c.f., Couzens-Schultz and  
111 Chan, 2010). In contrast to previous *in-situ* stress studies in the Otway Basin, which have mainly  
112 been concerned predominantly with constraining the state of stress (e.g., Hillis et al., 1995; Nelson et  
113 al., 2006a), we integrate a variety of complementary structural geology observations and geophysical  
114 datasets. These observations and datasets help define the roles of mechanical rock properties, pre-  
115 existing basement structures, and intra-basin structural heterogeneities imparted by rifting in  
116 influencing the nature of vertical and horizontal stress magnitudes throughout the basin.  
117 Furthermore, we apply new methods for constraining horizontal stress magnitude limits (c.f.,  
118 Couzens-Schultz and Chan, 2010). We show that petroleum exploration datasets when, integrated  
119 with other structural geology observation and geophysical datasets, can help understand and  
120 reconcile the state of *in-situ* stresses.

121

## 122 **2 Geological Background**

123 The Otway Basin is a large, broadly NW-SE trending extensional basin encompassing onshore and  
124 offshore parts of South Australia and Victoria, and Tasmanian waters (Fig. 2). Rifting in the Otway  
125 Basin commenced in the late Jurassic-early Cretaceous (Fig. 3) first in the western region (i.e., South  
126 Australian sector) then progressing to the central and eastern regions (i.e., Victorian sector),  
127 resulting in several distinct grabens and half-grabens with varying geometries and orientations (Fig.  
128 3: Perineck and Cockshell, 1995; Krassay et al., 2004). The early Cretaceous rift axis is located  
129 onshore and consists of ~W to NW trending depocentres in the western and central regions (e.g.,  
130 Penola Troughs) and ~NE trending depocentres in the eastern region (e.g., Colac Trough; Krassay et  
131 al., 2004). The near-orthogonal change in rift axis and fault strike occurs at ~143°E longitude and is  
132 primarily the result of episodic rifting at different times and in different directions (Hill et al.,  
133 1994,1995), probably related to substantial rheological differences in the basement across different  
134 Proterozoic/Palaeozoic boundaries (i.e., Delamerian and Lachlan; Miller et al., 2002; Cayley, 2011).  
135 This boundary broadly continues southwards through the Shipwreck Trough towards the Tasman  
136 Fracture Zone (i.e., Sorell Fault Zone) effectively separating the passive margin in the central parts  
137 and a failed rift zone in the eastern parts (Fig. 3; Hill et al., 1995; Miller et al., 2002; Cayley, 2011).  
138 Initial rift fills were dominated by carbonaceous lacustrine shales with minor interbedded sandstones  
139 and volcanics (Casterton Formation), and as the rate of extension increased into the Berriasian and  
140 Barremian syn-rift accommodation space was filled by amalgamated fluvial and lacustrine facies  
141 (Crayfish Subgroup; Krassay et al., 2004). A thick mudstone rich volcanoclastic succession  
142 (Eumeralla Formation) was deposited during a decrease in tectonic activity during the Aptian and  
143 Albian (Fig. 1; Krassay et al., 2004).

144

145 The basin experienced a pulse of ~NW-SE directed shortening, uplift and exhumation during the late  
146 Albian-Cenomanian (Duddy, 2003; Hill et al., 1995), resulting in a regional mid-Cretaceous  
147 unconformity (Fig. 1). Major uplift in the eastern Otway Basin effectively isolated the Torquay sub-  
148 basin (Krassay et al., 2004), whose late Cretaceous-Cenozoic stratigraphy shares a closer affinity  
149 with the Bass Basin to the east (Messent et al., 1999).

150

151 Western and central parts of the Otway Basin experienced renewed ~N-S to ~NE-SW directed  
152 rifting in the late Cretaceous (Perineck et al., 1994), with some workers arguing for a significant  
153 oblique (sinistral) component (Schneider et al., 2004). The locus of extension shifted to the south  
154 during the late Cretaceous, resulting in a series of ~NW-SE depocentres (e.g., the Voluta Trough)  
155 located to the south of the Tartwaup-Mussel fault zone (Fig. 3; Bernecker et al., 2003). The Upper  
156 Cretaceous Sherbrook Group generally comprises fluvial-deltaic and near shore to shallow marine  
157 siliciclastic deposits (Fig. 1).

158

159 The end of rifting in the Otway Basin is marked by a regional intra-Maastrichtian unconformity (Fig.  
160 1; Krassay et al., 2004), but evidence for seafloor spreading off the Otway Basin (i.e., first  
161 appearance of ocean crust) and thus continental separation between Australia and Antarctica is dated  
162 as middle Eocene (Norvick and Smith, 2001). Sedimentary successions in the Otway Basin become  
163 progressively more marine-influenced and calcareous throughout the Cenozoic, reflecting the  
164 progressive establishment of open marine circulation (McGowran et al., 2004; Blevin and Cathro,  
165 2008). Subsidence following intra-Maastrichtian breakup initiated a major transgression across the  
166 Otway Basin resulting in deposition of the siliclastic Wangerrip Group (Fig. 1; Bernecker et al.,  
167 2003). Small growth wedges bounded by basinward-dipping reactivated late Cretaceous normal  
168 faults in the Portland Trough (Fig. 3; Krassay et al., 2004), where the Wangerrip Group reaches a  
169 maximum thickness of >1200 m (Holdgate and Gallagher, 2003), imply that an extensional stress  
170 regime continued into the Palaeogene (Holford et al., 2014). It is separated by a major intra-Lutetian  
171 unconformity associated with significant localised erosion from the overlying prograding near shore  
172 to offshore marine clastics and carbonates of the late Eocene-early Oligocene Nirranda Group  
173 (Holdgate and Gallagher, 2003; Krassay et al., 2004). This unconformity also correlates with the  
174 onset of fast seafloor spreading in the southern Ocean at ~43 Ma (Veevers, 2000; McGowran et al.,  
175 2004). Since the mid-Eocene onset of fast spreading, the Australian continent has been subjected to a  
176 largely compressional stress field resulting from the configuration of the Indo-Australian Plate  
177 boundaries (Sandiford and Quigley, 2009).

178

179 The Nirranda Group reaches its maximum thickness of ~200 m in two major depocentres, in the Port  
180 Campbell Embayment and Portland Trough (Holdgate and Gallagher, 2003) and is separated from  
181 the overlying Heytesbury Group by a regional intra-Oligocene unconformity (Bernecker et al.,  
182 2003). The late Oligocene-late Miocene Heytesbury Group (maximum thickness >1600 m)

183 comprises marls and limestones deposited under fully marine conditions (Krassay et al., 2004). A  
184 regional, late Miocene-Pliocene unconformity (Dickinson et al., 2002; Holford et al., 2011b)  
185 separates the Heytesbury Group from the late Neogene succession of the Otway Basin, which is  
186 characterised by relatively thin and localised mixed siliclastic-carbonate sediments and basaltic  
187 volcanic rocks that usually unconformably or disconformably overlie Heytesbury Group strata  
188 (Dickinson et al., 2002; Tassone et al., 2011).

189

190 Finally with respect to hydrocarbon systems, the main source rocks in the Otway Basin are of early  
191 Cretaceous age, that is, the Casterton Formation and Crayfish Subgroup in onshore western and  
192 central parts and Eumeralla Formation in on- and offshore central and eastern parts (Fig. 1;  
193 Bernecker et al., 2003). The Pretty Hill Formation is the major reservoir unit in the onshore western  
194 and central parts and the basal Waarre Formation acting as the major regional reservoir interval in  
195 the on- and offshore eastern parts of the Otway Basin (Fig. 1; Bernecker et al., 2003). The Eumeralla  
196 Formation seals the Pretty Hill Formation reservoirs while Flaxman Formation and Belfast  
197 Mudstone (Fig. 1) seal the Waarre Formation reservoirs. Traps are structurally controlled and  
198 generally fault-bound, which have been affected by periods of deformation during the Eocene,  
199 Oligocene-early Miocene, and late Miocene-Pliocene (Brown, 1986; Dickinson et al., 2002). The  
200 most significant compressional and neotectonic structural features occur onshore in the eastern  
201 Otway Basin, in and around the Otway Ranges, and in the adjacent Torquay sub-basin (Fig. 3; Hill et  
202 al., 1994, 1995; Cooper and Hill, 1997; Geary and Reid, 1998; Messent et al., 1999; Miller et al.,  
203 2002; Dickinson et al., 2002; Sandiford, 2003b; Sandiford et al., 2004; Holford et al., 2010, 2011a,  
204 2014; Tassone et al., 2012, 2014; Holford et al., 2014). Similar to the Gippsland Basin, these  
205 structures comprise a combination of ~NE trending anticlines resulting from reactivation of syn-rift  
206 normal faults (Fig. 2). Boulton et al., (2008) has shown, nevertheless, that Neogene, neotectonic  
207 structures do extend into the central Otway Basin (Fig. 3).

208

### 209 **3 Determination of *In-Situ* Stresses within the Central and Eastern** 210 **Otway Basin**

211 Previous determinations of contemporary *in-situ* stress in the Otway Basin have utilized petroleum  
212 exploration data dominantly from the western Otway Basin within the South Australian sector (Hillis  
213 et al., 1995; Nelson et al., 2006a), although a few have focussed within the Port Campbell



214 Embayment (Bérard et al., 2008; Rogers et al., 2008) and offshore regions of Victoria (Nelson et al.,  
215 2006a). As there is often significant *in-situ* stress variation across basins (Bell, 1996; Tingay et al.,  
216 2006; Heidbach et al., 2007, 2010) and the observation that many of the neotectonic features lie in  
217 the eastern Otway Basin, unlike previous studies we have also considered the influence of  
218 underlying structural trends on the distribution of contemporary *in-situ* stresses. In order to do this,  
219 we have divided the Victorian sector of the Otway Basin, where less contemporary *in-situ* stress  
220 information is present, into two regions; the central and eastern regions at ~142.6°E longitude. In  
221 addition to onshore parts, the central region encompasses the Voluta Trough, Normanby Terrace,  
222 Mussel Platform and deeper water wells near the shelf break, whereas the eastern region  
223 encompasses Torquay sub-Basin, Prawn Platform and Shipwreck Trough wells northeast of the  
224 Tartwaup-Mussel hingeline (Fig. 3).

225

226 Assuming that one of the principal stress directions is vertical, and utilizing a large dataset from  
227 across the central and eastern regions, the five components that make up the simplified  
228 contemporary *in-situ* stress tensor in sedimentary rocks were determined. This includes the  
229 formation pore pressure ( $P_p$ ), vertical stress ( $S_v$ ) magnitude, minimum horizontal stress ( $SH_{min}$ )  
230 magnitude and maximum horizontal stress ( $SH_{max}$ ) magnitude and orientation. For each component  
231 of the stress tensor described below, the way in which the tensor component is constrained is firstly  
232 discussed, followed by the distribution of applicable available data and then results of the analyses.

233

### 234 3.1 Maximum Horizontal Stress ( $SH_{max}$ ) Orientations

#### 235 3.1.1 Constraining $SH_{max}$ orientations

236 The maximum horizontal stress ( $SH_{max}$ ) orientation is constrained in this study by identifying  
237 wellbore failure features such borehole breakouts (BO) and drilling-induced tensile fractures (DITF)  
238 (Zoback et al., 2003). Breakouts occur when the wellbore circumferential stress ( $\sigma_{\theta\theta}$ ) exceeds the  
239 compressive rock strengths of the wellbore wall, causing compressional shear failure surfaces to  
240 intersect and break-off in to the open wellbore (Fig. 4a; Gough and Bell, 1982). Drilling-induced  
241 tensile fractures occur when the pressure of the drilling mud exceeds the wellbore circumferential  
242 stress (Fig. 4a), typically resulting in vertical tensile fractures in the wellbore wall (Bell, 1990;  
243 Zoback, 2010). Breakouts form broad, flat enlargements of the borehole within the spalled wellbore  
244 aligned parallel with the minimal horizontal stress ( $SH_{min}$ ) orientation and orthogonal to the  $SH_{max}$

245 orientation (Fig. 4b), whereas DITFs form thin tensile cracks parallel to the  $SH_{max}$  orientation and  
246 are usually insensitive to caliper data (Fig. 4c; Hillis and Williams, 1992; Zoback, 2010).

247

248 Interpretation of resistivity or acoustic image log data is considered a more reliable approach to  
249 constrain  $SH_{max}$  orientations, rather than using four-arm or six-arm caliper data. This is because  
250 image logs not only clearly identify BOs, but also reveal DITFs, natural fractures, bedding planes  
251 and other sedimentary features (Heidbach et al., 2010). Analysis of wellbore failure features using  
252 either image log or caliper data require additional data in the form of dipmeter data. The dipmeter  
253 tool records the azimuth of wellbore drift relative to horizontal and magnetic north (HAZI), the  
254 inclination of the wellbore from vertical (DEVI), the azimuth of the reference pad in the wellbore  
255 plane relative to magnetic north (P1AZ) and the bearing of the first pad relative to the high side of  
256 the wellbore (RB; Reinecker et al., 2003). Whereas image log tools measure and image resistivity  
257 and acoustic variations, caliper data requires the width of the wellbore to be measured across two  
258 orthogonal pairs of caliper arms (four-arm caliper; Reinecker et al., 2003) or six independent arms  
259 positioned evenly around the wellbore circumference (six-arm; Wagner et al., 2004). As the four-  
260 arm or six-arm caliper tool is pulled up the wellbore, the tool rotates about a semi-vertical axis due  
261 to cable torque (Hillis and Williams, 1992). In zones of wellbore enlargement due to breakout, one  
262 caliper pair gets stuck in the enlargement direction and the tool stops rotating until another interval  
263 of round hole is encountered (Plumb and Hickman, 1985).

264

265 Successful discrimination of stress-induced wellbore BOs from other wellbore enlargement and  
266 elongation features that result from drilling, such as washout, mudcake and key seats (asymmetric  
267 abrasions due to wear by the drill string on the side of the wellbore that deviates from the vertical), is  
268 ensured by use of other wireline logging parameters (e.g., P1AZ and RB; Reinecker et al., 2003).  
269 Six-arm caliper data provides detailed information regarding the shape of the elongation wellbore, as  
270 the six arms move independently of one another allowing the tool to de-centralize and record radius  
271 lengths. For this reason, wellbore BO analysis of six-arm caliper tools is more complicated (c.f.,  
272 Wagner et al., 2004).

273

274 Drilling-induced tensile fractures are generally not associated with wellbore elongation; however, if  
275 orthogonal trends are observed using only caliper/dipmeter data, then it is impossible to differentiate  
276 the horizontal stress orientations (Hillis and Williams, 1992). Furthermore, BOs and DITFs from

277 deviated wells may not be reliable indicators of  $SH_{max}$  orientation because their orientations are  
278 controlled by the entire stress tensor (Mastin, 1988; Hillis and Reynolds, 2000). However, within a  
279 strike-slip fault stress regime, Mastin (1988) concludes that a wellbore deviated at least  $35^\circ$  from  
280 vertical is required before the horizontal projection of a BO differs by more than  $10^\circ$  from the  $Sh_{min}$   
281 direction.

282

### 283 **3.1.2 Data availability and distribution**

284 Image log data and caliper data from 12 petroleum wells in the central and eastern Otway Basin  
285 were available for this study to enable  $SH_{max}$  orientations to be determined (Fig. 3). Eight wells were  
286 from the Shipwreck Trough in the eastern Otway Basin, of which three wells used Schlumberger's  
287 Formation MicroImager (FMI) tool (Conan-1, Thylacine-1 and 2), three wells used Baker Atlas'  
288 SimulTaneous Acoustic and Resistivity Imager (STAR) tool (Henry-1ST1, Halladale-1DW1 and  
289 DW2) and two wells used Schlumberger's Formation MicroScanner (FMS) tool (Minerva-1 and 2A;  
290 Table 1). Wild Dog-1 in the Torquay sub-Basin, also in the eastern Otway Basin, ran a 6-arm caliper  
291 log (the tool was assumed to be centralised given that all the three caliper arms were measured as  
292 diameters), whilst the only well located in the central Otway Basin. Bridgewater Bay-1 in the Voluta  
293 Trough, ran 4-arm caliper logs (Table 1 and Fig. 3). In addition to the 10 offshore wells, two onshore  
294 wells from the eastern Otway Basin (Bellarine-1 and Wild Dog Road-1) ran FMI image tool data  
295 that were also available to constrain  $SH_{max}$  orientations. The maximum horizontal stress orientation  
296 at Bellarine-1 has recently been reported by Tassone et al., (2014), and is also included in this study  
297 for wellbore failure statistics.

298

299 The depth intervals in which these tools ran are listed in Table 1, along with other relevant  
300 parameters such as the maximum wellbore deviation (with respect to vertical), bit size used and  
301 imaged and logged intervals for specific formations. In addition to Dunbar-1 in the Port Campbell  
302 Embayment and Eric the Red-1 in the Prawn Platform, Minerva-1 and Minerva-2A have been  
303 previously interpreted by Nelson et al. (2006a), but are reinterpreted in this study to provide length-  
304 weighted statistics (not provided by Nelson et al., 2006a). Bérard et al., (2008) have published the  
305  $SH_{max}$  orientation in CRC-1 within the Port Campbell Embayment.

306

### 307 3.1.3 $SH_{max}$ orientations within the central and eastern Otway Basin

308 Our analysis has positively identified a number of drilling-induced wellbore failure features. In total,  
309 155 BOs and 69 DITFs were interpreted from image logs (i.e., FMI/ FMS/STAR) and 18 BOs were  
310 interpreted from caliper logs. Examples of BOs and DITFs from Henry-1ST1 and Minerva-1,  
311 respectively, can be seen in Fig. 4b and Fig. 4c. Cumulatively, the BOs identified total a combined  
312 length of 1981.5 m and DITFs total 138.0 m. Table 2 and Table 3 show the number of BOs and  
313 DITFs in each well, the total length, the mean orientation and standard deviation of the wellbore  
314 failure features, and the mean  $SH_{max}$  orientation for image logs and dipmeter data, respectively. In a  
315 number of wells, BOs had developed over 30% of the interpretable image log and ~70% of BOs  
316 interpreted by length, or ~1244 m in total, occur within the Upper Cretaceous Belfast Mudstone (Fig.  
317 5). The distribution of interpreted BOs and DITFs, represented as both number-weighted and length-  
318 weighted statistics, are shown in Fig. 6a and Fig. 6b. Figure 6c shows the resulting  $SH_{max}$   
319 orientations compared with those determined from previous published and unpublished studies,  
320 indicating consistent orientations in the central and eastern Otway Basin of  $\sim 135 \pm 15$  °N. Note, the  
321 determined  $SH_{max}$  orientations are predominantly of A-C quality according to the World Stress Map  
322 criteria (Heidbach et al., 2010), although lower D quality measurements also yield a consistent NW-  
323 SE trend. There is a regional clockwise rotation of  $\sim 10^\circ$  in  $SH_{max}$  orientation from the western to  
324 central Otway Basin, however (Nelson et al., 2006a). While regional  $SH_{max}$  orientations are  
325 remarkably consistent across the entire Otway Basin, it is worth mentioning the distribution of  
326 DITFs with depth interpreted within Bellarine-1 (see Fig. 23 from Tassone et al., (2014)). At ~450 m  
327 there is a local stress rotation from the regional orientation (i.e.,  $\sim 140^\circ$ N) to  $\sim 10^\circ$ N and then abruptly  
328 back to the regional orientation, possibly indicating proximal structural feature, such as a fault.

329

330 In the West Tuna Field in the neighbouring Gippsland Basin, however, Nelson et al., (2006b)  
331 observed from image log data coupled with tri-axial testing that strong cemented sandstones units  
332 acted as a stress-bearing framework in this highly horizontally stressed region, consequently  
333 partitioning stresses between ‘strong’ inter-bedded sandstones and ‘weaker’ shales such that BOs  
334 only occurred in the stronger sandstones. A similar observation was interpreted within siliciclastic  
335 rocks in the Perth Basin (King et al., 2008). This is in contrast to wellbore failure analyses in the  
336 Otway Basin wells that show the weaker finer-grained rocks preferentially resulted in BO, such as  
337 the Belfast Mudstone with compressive rock strength ( $C_0$ ) of  $\sim 9.77$  MPa and coefficient of internal  
338 friction ( $\mu_i$ ) of  $\sim 0.31$ , rather than the sandstones (Fig. 5a). This observation is more consistent with  
339 conventional wellbore failure analysis (Nelson et al., 2006b), however, this difference may largely

340 be due the strength of the sandstones in question. For example the quartz-rich Waarre C unit, the  
341 conventional reservoir in the eastern Otway Basin, has a relatively low  $C_0$  of ~21.21 MPa and  $\mu_i$  of  
342 ~0.76 (Fig. 5a), in comparison to the strong, cemented sandstone in the West Tuna Field  $C_0$  of (~60  
343 MPa and  $\mu_i$  of ~0.9; Nelson et al., 2006b). Thus it is unlikely to provide a similar stress-bearing  
344 framework.

345

## 346 3.2 Pore Pressure ( $P_p$ ) Magnitudes

### 347 3.2.1 Constraining $P_p$ magnitudes

348 Formation pore pressure ( $P_p$ ) magnitudes at depth have a significant impact on effective stress  
349 magnitudes and hence the complete *in-situ* stress tensor. Several wells located in the offshore eastern  
350 Otway Basin have  $P_p$  measurements from potential reservoir intervals determined using wireline  
351 formation tools (WFT), such as repeat formation tests, modular dynamic tests and reservoir  
352 characterization instruments. Wireline formation tools estimate  $P_p$  by isolating a section of wellbore  
353 with packers and measuring the rate at which the pressure stabilises in the isolated section as the  
354 wellbore pressure is reduced, drawing fluids from the formation (Nelson and Hillis, 2005). The  
355 success of these measurements rely on the permeability of the formation, and due to time and cost,  
356 such tests are mainly conducted in reservoir targets and are thus rarely done in low-permeability  
357 rocks, such as shales. If such data are unavailable, drilling mud-weight (MW or equivalent  
358 circulating densities, ECD) data can also be used as a proxy for  $P_p$  since the pressure of drilling mud  
359 is often kept just in excess of  $P_p$  in to avoid drilling problems such as fluid influxes (i.e., 'kicks') and  
360 to maximise drilling efficiency (van Ruth and Hillis, 2000). This approach can only be used as a  
361 proxy for  $P_p$  when increases in mud density are due to  $P_p$  changes, and not for other reasons, such as  
362 to improve wellbore stability or overcome tight (i.e., under-gauged) hole sections (van Ruth and  
363 Hillis, 2000; Reynolds et al, 2006). Finally, increases in background gas during drill pipe  
364 connections, that is connection gas (CG), can also be an indicator of increasing  $P_p$  if drilling mud  
365 weight remains unchanged (Mouchet and Mitchell, 1989; Sagala and Tingay, 2012).

366

### 367 3.2.2 Data availability and distribution

368 Wells that contain direct and indirect measurements of  $P_p$  are shown in (Fig. 3). In the central Otway  
369 Basin, two wells contained WFTs, four wells reported kicks and two well reported CGs. Mudweight  
370 and ECD data were also available 6 wells. In the eastern Otway Basin, 19 wells contained WFT data

371 and many of these wells also contained MW data, but only 3 wells were used to highlight there  
372 gradients as they were all similar.

373

### 374 3.2.3 $P_p$ gradients

375 Formation pore pressure data (i.e., WFT, kicks, CGs, MW) are plotted against true vertical depth  
376 below seabed or mudline (m TVDML) in Fig. 7. Previous contemporary stress studies have typically  
377 assumed that  $P_p$  gradients are hydrostatic (i.e., 10.0 MPa/km) across the Otway Basin (e.g., Nelson  
378 et al., 2006a). WFT data from Wild Dog-1 in the Torquay sub-Basin (Fig. 7b) indicate hydrostatic  
379 pressures (i.e., ~10.0 MPa/km) at depths shallower than ~1000 m TVDML, whilst WFT data from  
380 the deep water well Hill-1 similarly indicate hydrostatic pressures for depths shallower than ~2100  
381 m TVDML (Fig. 7a).

382

383 In contrast, in addition to hydrostatic  $P_p$ , permeable units from wells in both the Voluta and  
384 Shipwreck Troughs exhibit abnormal  $P_p$  indicative of overpressure. Wireline formation test data in  
385 the Voluta Trough from Fermat-1 indicate near hydrostatic pressures at depths shallower than ~3000  
386 m TVDML, though water ‘kicks’ with associated mud pit gains, together with WFT data at  
387 Normanby-1, located only ~5 km to the southeast, indicate a  $P_p$  gradient of >14 MPa/km at depths  
388 >3000 m TVDML (Fig. 7a). Drilling and mudlog data record several water and gas ‘kicks’ together  
389 with CGs at depths below ~3300 m TVDML at Callister-1 indicating high  $P_p$  gradients of ~14-17  
390 MPa/km (Fig. 7a). Petrophysical log-data in Bridgewater Bay-1 support significant  $P_p$  gradients >16  
391 MPa/km consistent with estimates from drilling mud-weight data, but also indicate that the top of  
392 overpressure within Upper Cretaceous fine-grained Belfast Mudstone strata begins at ~2900 m  
393 TVDML indicating that drilling was actually underbalanced for ~500 m (Fig. 7a; Tassone et al.,  
394 2011). Due to the lack of hydrocarbon shows in the Belfast Mudstone and rapid deposition of thick  
395 Upper Pliocene sediments within Miocene submarine canyons at Bridgewater Bay-1 well, Tassone  
396 et al. (2011) suggested a disequilibrium undercompaction mechanism for the generation of  
397 significant overpressures (Fig. 7a) in this area.

398

399 The discovery of the hydrocarbons within Upper Cretaceous strata (i.e., Waarre Formation and  
400 Thylacine Member; Fig. 1) and the subsequent development of numerous gas fields in the Shipwreck  
401 Trough has lead to the acquisition of many WFT data measurements in this part of the eastern Otway  
402 Basin. Changes in  $P_p$  gradient occur in a number of wells, indicating variations in formation fluid

403 density related to the occurrence of gas. Gas accumulations at Mineva-1 and Thylacine-1 occur at  
404 depths of ~1565 m TVDML and ~1920 m TVDML , respectively, and hydrocarbon buoyancy forces  
405 at these locations cause  $P_p$  gradients equivalent of up to ~12 MPa/km (Fig. 7b and Fig. 8a).  
406 Moderate overpressures observed in La Bella-1 do not appear to be associated with hydrocarbon  
407 buoyancy forces, however, because WFT data indicates two isolated overpressured intervals that are  
408 not in pressure communication with  $P_p$  gradients of ~10.5 MPa/km and ~11.7 MPa/km in the water-  
409 saturated zones of the Waarre C and Waarre A units, respectively (Fig. 8a). Although, the cause of  
410 these moderate overpressures is unclear, they may be associated with enhanced lateral transfer  
411 pressures at the crest of the tilted structure (Yardley and Swarbrick, 2000; Tassone et al., 2011),  
412 similar to some overpressures in the Cooper Basin (van Ruth and Hillis, 2000). A number of other  
413 gas fields show  $P_p$  discrepancies within vertical stratigraphic sequences or across faults. The Waarre  
414 B unit in the Casino Field separates two gas reservoirs (i.e., Waarre C and A units) with a pressure  
415 differential of approximately 200 psi (~1.379 MPa; Sharp and Wood, 2004). While WFT data from  
416 Minerva-1 and Minerva-2A show pressure communication across a southwest dipping fault (Fig.  
417 8b,d), other gas fields such as the Halladale/Blackwatch and Thylacine gas fields do not show  
418 pressure communication across faults at the Waarre Formation level (Fig. 8b,c,e,f). A fault seal  
419 analysis is required to determine if the differing fault geometries between Minerva and  
420 Halladale/Blackwatch Fields is the cause of the contrasting pressure compartmentalization (i.e.,  
421 structurally permeable and critically stressed) or if there is sand-on-sand juxtaposition across the  
422 fault (e.g., Lyon et al., 2005). Furthermore, it can be seen in Fig. 8c that Waarre C and Waarre A unit  
423 reservoirs display varying water  $P_p$  gradients, for example ~10.02 MPa/km at Thylacine-1 in  
424 comparison to ~9.91 MPa/km at Geographe-1, indicating that these reservoirs are not in pressure  
425 communication. Hence,  $P_p$  magnitudes may be compartmentalised by faults in which reservoirs are  
426 dissipating  $P_p$  gradients differentially or alternatively may have differing water densities.

427

428 Also noteworthy in the western-most Shipwreck Trough is a saltwater ‘kick’ encountered at  
429 Somerset-1 at ~2380 m TVDML and a recorded CG as well as gas “kick” at Triton-1ST1 in the  
430 Belfast Mudstone at ~3283 m TVDML, which indicated significantly high overpressures both with  
431  $P_p$  gradients of ~18.5 MPa/km (Fig. 7a). More work is required to understand the mechanism(s) of  
432 the significant overpressure experienced at these locations.

433

### 434 3.3 Vertical Stress ( $S_V$ ) Magnitudes

#### 435 3.3.1 Constraining $S_V$ magnitudes

436 For offshore wells, the total vertical stress ( $S_V$ ) magnitude is defined as the pressure exerted by the  
437 weight of the water column from the surface to the seabed, plus the pressure exerted by the weight of  
438 overlying rocks at a specified true vertical depth below mean sea level ( $Z$ ; *m TVDSS*) (Tingay et al.,  
439 2003a). It is expressed as:

$$440 S_V = (\rho_w \times g \times Z_w) + \int_{Z_w}^Z [\rho_b(Z) \times g] dZ \quad (1)$$

441 where  $\rho_b(Z)$  is the bulk density of the overlying rock column at depth  $Z$  (*m TVDSS*),  $g$  is the  
442 acceleration due to gravity,  $\rho_w$  is the density of seawater and  $Z_w$  is the water depth (Engelder, 1993).  
443 Petrophysical wireline well log data are typically acquired over large intervals of the well at high  
444 resolution (typically ~15 cm), and thus magnitudes of  $S_V$  at any depth can be constrained with a high  
445 degree of confidence because the vertical lithology variation of the sampled formations are taken  
446 into account in an unbiased way.

447

448 To calculate accurate  $S_V$  magnitudes, the bulk density log data was carefully filtered to remove  
449 spurious data that result from poor contact between the tool and the wellbore wall, caused by rugose  
450 wellbore conditions (Tingay et al., 2003a). The filtering process followed the procedure outlined by  
451 Tingay et al., (2003a), whereby bulk density data were assumed to be affected by rugosity if the  
452 density error log  $> \pm 0.1 \text{ g/cm}^3$  and the caliper log is  $\geq 5\%$  of the bit or hole size. Any wells that did  
453 not have all or some of these additional data were still analysed, but considered less reliable. Filtered  
454 (and non-filtered) logs were then also manually edited and 'de-spiked' to remove anomalous  
455 measurements, prior to calculating the vertical stress (Tingay et al., 2003a). Since the depth of water  
456 has a significant influence on  $S_V$  magnitudes with depth (Reynolds et al., 2003b) we have corrected  
457 for water pressure at seabed and referenced the depth to TVDML. Furthermore, since the principal  
458 stresses acting in the vicinity of a deviated wellbore wall are not aligned with the wellbore axis, a  
459 horizontal stress component may also be assumed, and so only density data from near-vertical ( $< 10^\circ$ )  
460 wellbore intervals were considered (Zoback et al., 2003).

461

462 Vertical stress magnitude calculations require that bulk rock densities be integrated from the seabed.  
463 As it is uncommon for bulk density wireline logs to be logged from the seabed, well check-shot  
464 velocity data (or from an offset well) was used to determine the average rock density from the



465 seabed to the top of the density log using the Nafe-Drake (Ludwig et al., 1970) velocity-density  
466 relationships.

467

### 468 **3.3.2 Data availability and distribution**

469 Twenty-four offshore wells that ran near-vertical density, sonic and caliper wireline well log data  
470 were available for this study to calculate  $S_V$  magnitudes. Of these twenty-four wells, twenty wells  
471 had check-shot velocity data acquired that were used to estimate average density values from seabed  
472 to the top of the bulk density log. Wells that did not have check-shot velocity data used closest offset  
473 wells with data. These wells are shown in Fig. 3.

474

### 475 **3.3.3 $S_V$ profiles**

476 The  $S_V$  magnitudes-depth profiles for all wells in this study are presented in Fig. 9. Overall, there is  
477 not a significant variation of  $S_V$  magnitudes with depth. Lower and upper bounds of  $S_V$  magnitudes  
478 with depth are well described by the power-law relationships:

$$479 \text{ Lower Bound: } S_{V\_Lower} \approx 21.58 \times Z^{1.0304} \quad (2)$$

$$480 \text{ Upper Bound: } S_{V\_Upper} \approx 21.58 \times Z^{1.0304} \quad (3)$$

481 where  $S_V$  is calculated in megapascals (MPa) and  $Z$  is true vertical depth in metres below seabed or  
482 mudline (TVDML). At a depth of ~2500 m TVDML, the difference in  $S_V$  magnitude within these  
483 bounds is ~4.66 MPa (Fig. 9). This variation is ~2.25 MPa and ~4.34 MPa less than that reported for  
484 the same depth in the Cooper Basin (c.f., Reynolds et al., 2006) and Carnarvon Basin (c.f., King et  
485 al., 2010), respectively. The larger variation in  $S_V$  magnitudes in the Cooper and Carnarvon basins  
486 are likely due to localised uplift and erosion in these basins (~900-1000 m; Densley et al., 2000;  
487 Mavromatidis and Hillis, 2005) that has brought denser sedimentary rocks to shallower depths (King  
488 et al., 2010). The Lower Cretaceous Eumeralla Formation is predominantly near maximum post-  
489 depositional burial depths in the offshore central and eastern Otway Basin (Tassone et al., 2014),  
490 which may explain the small amount of variation observed across this area. Where significant uplift  
491 and erosion has occurred in the Otway Basin, for example at Bellarine-1 in the eastern part of the  
492 study area (~1800 m; Tassone et al., 2014),  $S_V$  gradients are as high as ~26 MPa/km at 2000 m  
493 TVDML (Fig 9). This is ~3 MPa/km greater than the upper limit  $S_V$  magnitude-depth relationships  
494 defined in Eq. (3) (Fig. 9).

495

### 496 3.4 Minimum Horizontal Stress ( $Sh_{min}$ ) Magnitudes

#### 497 3.4.1 Constraining $Sh_{min}$ magnitudes

498 Minimal horizontal stress ( $Sh_{min}$ ) magnitudes were determined from leak-off tests (LOTs), which are  
499 commonly acquired during drilling operations after casing is cemented in place (Zoback, 2010).  
500 More reliable estimates of the  $Sh_{min}$  magnitudes are often attained from the instantaneous shut-in  
501 pressure (ISIP), or preferably the fracture closure pressure (FCP) during mini-frac or extended leak-  
502 off tests (XLOTs – Fig. 10; Addis, et al., 1998; Zoback, 2010). Unlike the Cooper Basin in central  
503 Australia, where exploration and development of low permeability hydrocarbon plays has resulted in  
504 a plethora of mini-frac data (c.f., Reynolds et al., 2006, Nelson et al., 2007), these tests are never  
505 routinely conducted in wells drilled in the Otway Basin. Leak-off pressures (LOPs) during LOTs  
506 represent the creation of a supposedly new hydraulic fracture in the surrounding host formation  
507 when increasing wellbore pressures suddenly drop causing a deviation from linearity in a pressure  
508 vs. time plot (Fig. 10). A fundamental assumption of LOTs is that hydraulic fractures will develop  
509 axial to vertical wellbores and are caused by tensile failure of the host formation (Brudy and Zoback,  
510 1999). Unfortunately, image logs are generally not run after LOTs (e.g., Evans et al., 1989) and,  
511 therefore, the orientation and nature of hydraulic fractures are often not verified.

512

513 While XLOTs, which are repeated cycles of LOTs, provide superior estimates of  $Sh_{min}$  magnitudes,  
514 lower bound LOPs from LOTs are generally considered to be good approximations of  $Sh_{min}$   
515 magnitude (Breckels and van Eekelen, 1982; Addis et al., 1998). This is especially true in near-  
516 vertical wellbore sections, because they are often similar to FPPs when flow rates and fluid  
517 viscosities are sufficiently low enough (Haimson and Fairhurst, 1967; Zoback, 2010). Furthermore,  
518 they do not impose an  $S_V$  component (and thus shear component), as would be the case in highly  
519 deviated sections (Brudy and Zoback, 1993). Observations of low LOPs (~30-60% less than  $S_V$ ) in  
520 active thrust belts, where a reverse-fault stress regime dominates has lead Couzens-Schultz and Chan  
521 (2010) to propose an alternate interpretation of LOT results. In this alternate interpretation, the  
522 magnitude of  $Sh_{min}$  is constrained by assuming that the LOP causes shear failure along pre-existing  
523 planes of weaknesses, rather than the traditional assumption of failure via new tensile fractures. This  
524 approach leads to slightly higher estimates of  $Sh_{min}$  magnitude (King et al., 2012) and can be  
525 estimated using Couzens-Schultz and Chan (2010):

$$Sh_{min\_lim} = S_v - \frac{2 \left( S_v - \left( LOP - \frac{C_0}{\mu_P} \right) \right) \sin \phi_P}{(1 + \sin \phi_P)} \quad (4)$$

where  $LOP$  is the leak-off pressure (MPa),  $C_P$  is the cohesion strength (MPa),  $\Phi_P$  is the angle of friction ( $^\circ$ ) and  $\mu_P$  is the coefficient of friction of the pre-existing discontinuity plane. Since it is assumed that leak-off occurs due to shear along a pre-existing plane of weakness, the  $C_0/\mu_P$  equates to zero as the pre-existing plane of weakness is assumed to be cohesionless.

Minimum horizontal stress magnitudes are arguably the least well constrained component of the *in-situ* stress tensor that can be directly measured in a single wellbore. This is because they are often reliant on one or maybe two LOTs at shallow depths below the surface and intermediate casing shoes, which are then often linearly extrapolated to depths of interest or used as calibration data points to extrapolate developed fracture gradient (i.e.,  $Sh_{min}$ ) prediction algorithms to reservoirs. A common factor in all these fracture gradient prediction algorithms (e.g., Matthews and Kelly, 1967; Eaton, 1969; Breckels and van Eekelen, 1981; Daines, 1982) is  $P_P$ ; moreover, an increase in  $P_P$  (i.e., overpressure) causes an increase in  $Sh_{min}$ , and vice versa (i.e., depletion). This coupling relationship between  $P_P/Sh_{min}$  has been characterised over both hydrocarbon field and basin-wide scales (e.g., Hillis, 2001; Tingay et al., 2003b), and it is worth noting that such a phenomenon cannot be discounted in overpressured rocks within the Otway Basin. A detailed investigation on this relationship, however, is beyond this scope of this study.

### 3.4.2 Data availability and distribution

The majority of LOT data used in this study were reported from basic data or completion reports and did not contain the actual pressure vs. time data (i.e., D quality c.f., King et al., 2008). Therefore, we assume LOPs were correctly interpreted and that reported LOPs are a good estimation of the  $Sh_{min}$  magnitudes (Haimson and Fairhurst, 1967). Comparing reported LOPs with actual pressure vs. time data was beyond the scope of this study, and we acknowledge that this may affect the veracity of our estimates of  $Sh_{min}$  magnitudes.

It has long been known that lithology exerts a strong influence on both ISIPs during mini-frac tests and LOPs during extended LOTS, which consequently influences the magnitude of  $Sh_{min}$  (Bush and Meyer, 1988; Warpinski 1989b; Warpinski and Tufel 1989, 1991; Evans et al., 1989; Addis et al.,

1998; Reynolds et al. 2006). Consequently, we have made use of the substantial amount of LOT data available from the Otway Basin. Eighty nine LOTs from 73 near-vertical ( $<10^\circ$  inclination) wellbores within the offshore and onshore central and eastern Otway Basin (Fig. 3) have been used to estimate  $Sh_{min}$  magnitudes. These tests have been acquired since early exploration and encompass differing formations (and lithologies) at various depths within sections believed to be close to maximum post-depositional burial depths (c.f., Corcoran and Doré, 2007; Tassone et al., 2014). In contrast to previous contemporary stress studies in the Otway Basin, we have grouped the LOT data by dominant lithology of the formation in which the test was run and by geographic location (i.e., central vs. eastern Otway Basin). Table 4 shows the formation-bulk lithology groupings used to differentiate the LOT data, as well as information regarding the deposition environments of the corresponding formations. The Heytesbury and Nirranda Groups, which mainly marl and carbonate dominated sections are the shallowest stratigraphic sequences in the Otway Basin (Fig. 1; approximately  $<1000-1500$  m TVDML) and are often favoured for cementing-in-place surface casing, thereby accounting for a large proportion ( $\sim 47\%$ ) of the available reported LOT data in this study.

571

### 3.4.3 $Sh_{min}$ gradients

Unlike petroleum exploration that requires conservative fracture gradient estimates for well design and safe drilling practice, we are interested in best-fit estimates of  $Sh_{min}$  to understand the regional contemporary *in-situ* stresses. Figure 11a and Fig. 11b shows the relationships between LOPs with depth, differentiated by lithology (i.e., marl/carbonate, sand, shale, sand/shale) and location within the Otway Basin (i.e., central and eastern). Although there is still considerable variation within each lithology, comparison of different lithologies shows that the highest best-fit  $Sh_{min}$  gradients occur within marl and carbonate-dominated formations, with best-fit  $Sh_{min}$  gradients of  $\sim 20.32$  MPa/km and  $\sim 21.19$  MPa/km for the central and eastern Otway Basin, respectively (Fig. 11a). The shale-dominated formations have best-fit  $Sh_{min}$  gradients of  $\sim 18.79$  MPa/km and  $\sim 20.89$  MPa/km, while sand-dominated formations have the lowest best-fit  $Sh_{min}$  gradients of  $\sim 15.93$  MPa/km and  $\sim 17.01$  MPa/km for the central and eastern Otway Basin, respectively (Fig. 11a). Undifferentiated sand/shale dominated formations have best-fit  $Sh_{min}$  gradients generally constrained between the shale (upper) and sand (lower) dominated formations (Table 4), although the central Otway Basin best-fit  $Sh_{min}$  gradient ( $\sim 15.37$  MPa/km) is slightly lower than sand-dominated best-fit  $Sh_{min}$  gradients in the same region (Fig. 11a). This may reflect the fact that LOT data for undifferentiated

588 sand/shale dominated formations in the eastern part of the study area were obtained in shalier units  
589 whereas LOT data in the central Otway Basin were obtained in sandier units.

590

591 Considering the difference between sandstone and shale dominated best-fit  $Sh_{min}$  gradients at typical  
592 reservoir-seal depths (e.g., ~2000 m TVDML in the Shipwreck Trough), the difference in  $Sh_{min}$   
593 magnitudes between these lithologies for the central and eastern regions is ~5.72 MPa and ~7.74  
594 MPa, respectively. These differences in LOPs, and thus estimates of  $Sh_{min}$  magnitudes, in siliciclastic  
595 rocks across both regions are consistent with the findings of Warpinski (1989a) who showed  
596 utilizing 60 mini-frac tests within a single well that reservoir (sand) units typically have  $Sh_{min}$   
597 magnitudes 5-12 MPa lower than non-reservoir (shale) units. A similar conclusion was proposed by  
598 Addis et al., (1998) who showed that XLOTs and LOTs in shale and mudstone dominated  
599 formations generally have higher stresses and fracture gradients in comparison to sand-dominated  
600 units. The observation of wide natural fractures in the sandstones abruptly terminating at shale-rich  
601 interfaces also led Warpinski and Tufel (1989) to reinforce that stress contrasts exist between shale  
602 and sand dominated units, with higher stresses in the shales. Thus, fracture gradients determined in  
603 shale and mudstone lithology rocks should not be directly extrapolated to reservoir sandstones,  
604 especially, if production has depleted  $P_P$  magnitudes (Addis et al., 1998; Hillis, 2001).

605

606 For all the lithology end-members (i.e., marl/carbonate, shale and sand dominated formations), best-  
607 fit  $Sh_{min}$  gradients in the eastern Otway Basin are ~1-2 MPa/km higher than in the central Otway  
608 Basin (Fig. 11a,b). Although there is a lot of overlap at shallower depths, especially within marl and  
609 carbonate dominated formation at depths deeper than ~800 m TVDML, there appears to be a more  
610 noticeable differentiation of LOPs within siliciclastic formations from across the basin (Fig. 11b).  
611 This clearly demonstrates that lithology has a major control on LOPs, and thus the magnitude of  
612  $Sh_{min}$  with depth, and indicates a relative increase in  $Sh_{min}$  gradients from west-to-east across the  
613 central to eastern parts of the basin.

614

### 615 3.5 Maximum Horizontal Stress ( $SH_{max}$ ) Magnitudes

#### 616 3.5.1 Constraining $SH_{max}$ magnitudes upper bounds

617 The magnitude of the maximum horizontal stress ( $SH_{max}$ ) is the most difficult component of the *in-*  
618 *situ* stress tensor to constrain because there is no way to measure it directly (White and Hillis, 2004).

619 It is well accepted that the Earth's crust is in a state of incipient, albeit slow, frictional failure  
620 equilibrium; seismicity in the brittle upper crust within stable continental regions provides strong  
621 evidence for this notion (e.g., Stein et al., 1992; Townend and Zoback, 2000). Assuming that one  
622 principal stress is vertical, the differences in magnitude between the maximum and minimum  
623 principal stresses at depth will be limited by the frictional strength of planar discontinuities such as  
624 faults (Jaeger and Cook, 1979). Frictional-limit theory states that stresses in the Earth's upper crust  
625 cannot be such that they exceed the frictional strength of pre-existing, optimally oriented faults  
626 (Sibson, 1974; Jaeger and Cook, 1979). Thus, a critically oriented fault is at frictional limits when:

$$627 \frac{S_1 - P_p}{S_3 - P_p} = \left[ (\mu^2 + 1)^{\frac{1}{2}} + \mu \right]^2 \quad (12)$$

628 where  $S_1$  and  $S_3$  are the maximum and minimum principal stress magnitudes, respectively,  $P_p$  is  
629 formation pore pressure and  $\mu$  is the coefficient of friction of a critically stressed, cohesionless pre-  
630 existing fault often assumed to be equal 0.6-0.85 (Byerlee, 1978). Frictional limit theory can be used  
631 to estimate the magnitude of  $S_1$  in seismically active regions (Zoback and Healy, 1984) and can  
632 provide an upper bound estimate of the magnitude of  $SH_{max}$  within strike-slip and reverse fault stress  
633 regimes (Jaeger and Cook, 1979) in seismically inactive regions (Reynolds et al., 2006). Since  $S_1$  in  
634 a normal fault regime is  $S_v$ , frictional limit theory cannot be used in a normal fault regime to  
635 constrain the upper magnitude limit of  $SH_{max}$  under such conditions. In strike-slip and reverse  
636 faulting regimes (c.f. Anderson, 1951), however,  $SH_{max}$  is the maximum principal stress magnitude,  
637 and so can be determined by:

$$638 \frac{SH_{max} - P_p}{S_v - P_p} \leq 3.119 \quad (13)$$

$$639 \frac{SH_{max} - P_p}{Sh_{min} - P_p} \leq 3.119 \quad (14)$$

640 as governed by reverse (i.e.,  $S_1 > S_2 > S_3 \equiv SH_{max} > Sh_{min} > S_v$ ) and strike-slip (i.e.,  $S_1 > S_2 > S_3 \equiv$   
641  $SH_{max} > S_v > Sh_{min}$ ) faulting regimes, respectively, when  $\mu = 0.6$  (Byerlee, 1978). Given that  $SH_{max} \geq$   
642  $Sh_{min}$ , the range of allowable values for horizontal principal stresses in the Earth's crust in ratio to  $S_v$   
643 at a given depth must plot within the black solid line constraints in Fig. 12 (Moos and Zoback,  
644 1990). If significant overpressure exist at depth, then effective stresses will decrease causing the  
645  $SH_{max}:S_v$  and  $Sh_{min}:S_v$  ratios to decrease (Fig. 12; Moos and Zoback, 1990; Zoback et al., 2003).

646

647 As previously discussed, LOPs are assumed to result from tensile rock failure in the form of  
 648 wellbore-axial hydraulic fractures. If LOPs occur because of shear failure along pre-existing planes  
 649 of weakness, however, Couzens-Schultz and Chan (2010) have proposed that the following  
 650 equations can be used to estimate the upper bound magnitude of  $SH_{max}$ :

$$651 \quad SH_{max\_lim} = S_V + \frac{2 \left( S_V - \left( LOP - \frac{C_p}{\mu_p} \right) \right) \sin \phi_p}{(1 - \sin \phi_p)} \quad (15)$$

652 where the parameters are identical to those noted in Eq. 4.

653

654 The presence of wellbore failure features, such as DITFs and/or BOs, can provide additional  
 655 constraints on  $SH_{max}$  magnitudes if mechanical rock properties such as compressive and tensile rock  
 656 strengths are known (Bell and Gough, 1979; Brundy and Zoback, 1999). However, since this study  
 657 is focused on establishing regional *in-situ* stress constraints rather than tightly constraining the state  
 658 of stress (i.e.,  $SH_{max}$  magnitude) for wellbore geomechanic applications (e.g., wellbore stability,  
 659 hydraulic fracturing, sand production), lower limits to  $SH_{max}$  magnitudes were not calculated using  
 660 the observation of wellbore failure features in this study.

661

### 662 3.6 Possible states of stress constrained from petroleum exploration data

663 Assuming that LOPs constrain  $Sh_{min}$  magnitudes, marl and carbonate-dominated formations exhibit  
 664 higher  $Sh_{min}$  gradients than  $S_{V\_Lower}$  over all depths for where these rocks are deposited (i.e., <1600 m  
 665 TVDM; Fig. 13). Furthermore, these  $Sh_{min}$  gradients are approximately equal to or higher than  
 666  $S_{V\_Upper}$  at depths less than ~380 m TVDML and ~710 m TVDML for the central and eastern  
 667 regions, respectively (Fig. 13). This implies that the shallow, post-rift Heytesbury and Nirranda  
 668 Groups are within a strike-slip to reverse faulting stress regime or potentially a pure reverse faulting  
 669 stress regime, if LOPs actually represent  $S_V$  (i.e.,  $S_3$ ) rather than  $Sh_{min}$  (i.e.,  $S_2$ ) (Evans and Engelder,  
 670 1989). In the latter instance, the amount by which  $Sh_{min}$  magnitudes exceeds  $S_V$  magnitudes is,  
 671 therefore, indeterminable using LOT data (Evens et al., 1989).

672

673 At this point, it is worth noting that during normal burial, mechanical and thermo-chemical  
 674 compaction (i.e., the reduction of porosity with depth) processes are generally non-linear (Athys,  
 675 1930). It is for this reason, Warpinski (1989a) emphasizes the perils of fitting linear stress-depth

676 regressions as it maintains the misconception that magnitudes of  $Sh_{min}$  always increases with depth  
677 regardless of parameters in addition to lithology, such as changes in stress states, pore pressures,  
678 temperatures and diagenesis throughout time (i.e., elastic/viscoelastic behaviour ; Warpinski 1989b).  
679 Unfortunately, however, there is insufficient data from within individual Otway Basin wells to  
680 constrain horizontal pressure-depth trends other than linear gradients at this stage, especially  
681 regional across the basin.

682

683 Throughout the central and eastern Otway Basin, LOPs obtained in sand-dominated formation are  
684 generally less than  $S_V$  magnitudes for all depths tested (Fig. 13), implying either a strike-slip or  
685 normal fault stress regime. In the central Otway Basin, LOPs from sandstones define a best-fit  $Sh_{min}$   
686 gradient of  $\sim 15.9$  MPa/km. Likewise, LOPs from shale-dominated formations in the central Otway  
687 Basin are also less than  $S_{V\_Lower}$  at all depths, providing further support for either a strike-slip or  
688 normal fault stress regime. However, LOPs from shale-dominated formations in the eastern Otway  
689 Basin indicate variably greater and lower  $Sh_{min}$  magnitudes in comparison to  $S_V$  magnitudes over  
690 various depths, implying that all faulting regimes may be possible (i.e., normal, strike-slip and  
691 reverse; Fig. 13b).

692

693 In addition to  $S_V$  and  $Sh_{min}$  stresses, Fig. 13 also shows maximum  $P_P$  gradients observed across the  
694 basin. Fig. 13a in particular shows the unlikely relationship between  $P_P$  and sand-dominated  $Sh_{min}$   
695 gradients when pore pressure/stress coupling is not taking into account if best-fit  $Sh_{min}$  gradients  
696 calibrated at shallow depths are linearly extrapolated to deeper depths and assuming permeable  
697 reservoirs retain  $P_P$ .

698

699 Maximum horizontal stress magnitudes are discussed in more detail and estimated in Section 6, after  
700 taking into consideration neotectonic geological observations and complementary geophysical  
701 datasets.

702

703 A best-fit  $Sh_{min}$  gradient for eastern Otway Basin shales is  $\sim 20.9$  MPa/km, which is less than  $S_{V\_Lower}$   
704 at depths  $>2010$  m TVDML. This indicates a potential partitioning of stress regimes with depth, with  
705 strike-slip faulting stress regime at deeper depths (e.g.,  $>2010$  m TVDML), and borderline strike-slip  
706 to reverse faulting stress conditions at shallower depths (e.g.,  $<2010$  m TVDML; Fig. 13b). In a



707 previous study, Nelson et al. (2006a) constrained a best-fit  $Sh_{min}$  gradient of  $\sim 18.5$  MPa/km in the  
708 eastern Otway Basin, which is generally less than our estimates of  $Sh_{min}$  gradient for marl, carbonate  
709 and shale-dominated formations throughout the basin (Table 4). Nelson et al. (2006a) suggested that  
710 the simplest explanation for the increase in  $Sh_{min}$  gradients from  $\sim 15.5$  MPa/km in the western  
711 Otway Basin (i., South Australian sector) to  $\sim 20$  MPa/km in the Gippsland Basin is largely due to  
712 the closer proximity to the New Zealand compressional boundary. However, the observation of  $Sh_{min}$   
713 gradients greater than  $\sim 20$  MPa/km in marl and carbonate dominated stratigraphic units throughout  
714 the basin and in shale-dominated stratigraphic units in the eastern Otway Basin implies that  
715 horizontal stress magnitudes are not purely related to plate boundary proximity.

716

#### 717 **4 Basement *In-Situ* Stresses**

718 Wellbore failure analysis of 12 petroleum wells has constrained the  $SH_{max}$  azimuth in the eastern  
719 Otway Basin to be broadly  $\sim 136.5 \pm 13.5^\circ$ N, which is consistent with previous *in-situ* stress studies in  
720 this region (Fig. 6c Nelson et al., 2006a, Bérard et al., 2008). However, such data only provide  
721 constraints on the orientation of stresses within the shallow upper crust (depths  $< 4$  km). In an  
722 attempt to obtain a more comprehensive understanding of the state of stress in the Otway Basin, here  
723 we combine our results with independent datasets that constrain the state of stress in the underlying  
724 basement, such as earthquake focal mechanism solutions (Denham et al., 1981, 1985; Bock and  
725 Denham, 1983; McCue et al., 1990; McCue and Paull, 1991; Leonard et al., 2002; Allen et al., 2005;  
726 Clark, 2009). We also consider the implications of Pliocene-Holocene volcanic eruption point  
727 alignments (Lesti et al., 2008).

728

729 Earthquake focal mechanisms represent the pattern of seismic radiation resulting from slip on a fault  
730 (Zoback, 2010). Table 5 and Fig. 14a show 19 published focal mechanisms for 17 earthquakes in the  
731 vicinity of the Otway Basin with magnitudes ranging from  $M_L = 3.2$  and 5.4 that occurred at depths  
732 between 5 and 21 km. These are superimposed over basement discontinuities identified from both  
733 field mapping and geophysical datasets (e.g., magnetic, radiometric, gravity and seismic;  
734 Vandenberg et al., 2000). All the focal mechanism solutions were determined from onshore  
735 earthquakes occurring within basement rocks.

736

737 No focal mechanisms solutions exist underlying the Otway Basin to directly compare with our  
738 estimates of  $SH_{max}$  orientation from wellbore failure analysis (Fig. 6). The two most proximal  
739 earthquakes to the central and eastern Otway Basin with focal mechanism solutions are both poorly  
740 constrained, allowing for alternative interpretations. McCue et al. (1990) suggested the 1987 Nhill  
741 earthquake in Western Victoria was consistent with a strike-slip focal mechanism solution (1a in Fig.  
742 14a). However, Leonard et al., (2002) shows an alternative focal mechanism solution is also possible  
743 with similar amounts of uncertainty; a thrust regime (1b in Fig. 14a) in which the P-axis ( $SH_{max}$   
744 orientation) is approximately aligned to nearby wellbore failure azimuths defined BOs and DITFs  
745 (Hillis et al., 1995; Nelson et al., 2006a). The only other focal mechanism solution in close  
746 proximity to the Victorian Otway Basin is the 1977 Balliang earthquake near Geelong just north of  
747 the northern Otway Basin boundary. This focal mechanism solution is also poorly constrained  
748 (Denham et al., 1981) and two alternative solutions have been presented: the original published  
749 solution by Denham et al. (1981) indicating a thrust fault regime and strike-slip faulting on a pre-  
750 existing normal fault (Leonard et al., 2002). Both solutions, nevertheless, yield a similar P-axis  
751 azimuth that is  $\sim 30^\circ$  rotated towards the north with respect to the  $SH_{max}$  orientation determined for  
752 the Lower Cretaceous rocks in Bellarine-1.

753

754 Four of the 17 focal mechanisms solutions, however, exist within basement rocks underlying  
755 Mesozoic-Cenozoic sedimentary rocks of the Gippsland Basin, where wellbore failure analysis  
756 defined by BOs and DITFs also indicate consistent  $SH_{max}$  orientations (Fig. 14a). Apart from the Mt  
757 Hotham earthquake in 1966 that indicates normal faulting focal mechanism solution (P-axis  $\approx 219^\circ$ ;  
758 Denham et al., 1985) and a possible focal mechanism solution for the Nhill earthquake in 1987 (P-  
759 axis  $\approx 264^\circ$ ; McCue et al., 1990; Leonard et al., 2002), all other focal mechanism solutions listed in  
760 Table 5 have a P-axis azimuth that trends broadly NW-SE. It is clear from the focal mechanism  
761 solutions, nevertheless, that earthquakes within pre-Permian basement rocks in south-eastern  
762 Australia are dominantly a combination of strike-slip and reverse faulting, and probably depends on  
763 which pre-Permian basement fault was being reactivated at the time. The broad consistency between  
764 stress orientations determined from both petroleum data and earthquake focal mechanisms suggests  
765 some degree of coupling between basement and the overlying sedimentary cover, consistent with  
766 observations from a number of seismogenic zones across Australia (Clark and Leonard, 2003).

767

768 The alignment of Pliocene-Holocene volcanoes in western Victoria, which overlaps the northern  
769 margin of the Otway Basin, provides additional evidence of the state of stress within the underlying  
770 basement (Fig. 14b; Lesti et al., 2008). Mapping the spatial density and alignment of deeply-sourced  
771 eruption points (Fig. 14b) led Lesti et al. (2008) to suggested that the dominant NW-SE trend reflects  
772 the opening (or reopening) of deep fractures favourably oriented parallel to the  $SH_{max}$  azimuth,  
773 whilst subsidiary N-S and E-W trends reflect reactivated basement discontinuities (Fig. 14). Hence,  
774 the alignments of eruption points highlight the influence of syn-volcanic tectonics and the *in-situ*  
775 stress field during Pliocene-Holocene times.

776

777 Regional  $SH_{max}$  orientations estimated from Pliocene-Holocene volcanic eruption point alignments,  
778 together with petroleum well data estimates and focal mechanism solutions across south-eastern  
779 Australia, agree well with plate-scale finite-element stress modelling (Walcott, 1998; Hillis and  
780 Reynolds, 2000; Reynolds et al., 2003a). Such modelling indicates the regional  $SH_{max}$  orientation in  
781 the Otway Basin, as well as south-eastern Australia, primarily reflects the increased coupling of the  
782 Australian and Pacific plate boundary along New Zealand's Alpine Fault (Sandiford, 2003b;  
783 Sandiford et al., 2004).

784

## 785 **5 Evidence of Neotectonic Compressional Deformation**

786 The onset of Neogene, neotectonic compressional deformation across southeastern Australia is  
787 marked by a regional late Miocene–early Pliocene angular unconformity that is well developed in  
788 the Otway Basin, particularly over localised neotectonic structures (Dickinson et al., 2002), and  
789 corresponds to a transition in the nature of basin-fill from carbonates to siliciclastics around 6–8 Myr  
790 ago (Sandiford, 2003b). Although this deformation occurs throughout the entire Otway Basin (Geary  
791 and Reid, 1998; Messent et al., 1999; Boulton et al., 2008), neotectonic compressional deformation in  
792 far more pronounced in eastern Otway Basin (Fig. 3). The key evidence for neotectonic deformation  
793 takes the form of folding and reverse faulting of upper Miocene and older strata in the Torquay Sub-  
794 Basin (e.g., Nerita Anticline; Fig. 15) and Otway Ranges region (Fig. 16; Cooper and Hill, 1997;  
795 Dickinson et al., 2002; Holford et al., 2011a). The ~40 m high cliff near Port Campbell in the eastern  
796 Otway Basin (Fig. 16) also reveals a low-angle fault within the middle to upper Miocene Port  
797 Campbell Limestone section (Fig. 17). This fault exhibits reverse motion with little observable

798 damage surrounding the fault and slightly offsets an unconformable surface at the top of the cliff  
799 (Fig. 17).

800

801 In addition to the Torquay Sub-basin and onshore regions, there is also clear evidence from seismic  
802 data for neotectonic compressional deformation in parts of the Shipwreck Trough and Mussel and  
803 Prawn platforms within the offshore eastern Otway Basin (Fig. 18). Within these regions, seismic  
804 mapping of the post-rift mid-Oligocene units (i.e., base-Heytesbury Group isochron; Fig. 1) shows  
805 that neotectonic compressional deformation is dominantly accommodated by low-amplitude (~100-  
806 500 m; Fig. 18b) folds with wavelengths of ~10-25 km that plunge towards the SW (Geary and Reid,  
807 1998; Tuitt et al., 2011) with less evidence of significant faulting (Fig. 18a). A number of these  
808 folds, such as the Miverva, Pecten and Crowes anticlines, strike parallel and are contiguous to  
809 onshore neotectonic structures (Fig. 18b). The onset of neotectonic deformation in the eastern Otway  
810 Basin also correlates well with apatite fission track data that show cooling of Cenozoic-Cretaceous  
811 rocks beginning between 5-10 Ma as result of up to 400-1500 m of uplift and erosion (Cooper and  
812 Hill, 1997; Dickinson et al., 2002; Green et al., 2004; Holford et al., 2011a; Tassone et al., 2012).

813

814 Pliocene and Quaternary strata overlying the regional late Miocene-early Pliocene angular  
815 unconformity in the onshore eastern Otway Basin also reveal evidence for neotectonic deformation  
816 (Clark et al., 2011). For this reason, we categorise the onset of regional Neogene compressional  
817 deformation that resulted in the late Miocene-early Pliocene angular unconformity as *early*  
818 neotectonic deformation, and subsequent deformation as *late* neotectonic deformation.

819

820 Based on displacement of Miocene strata, Pliocene strandlines, and Pliocene-Quaternary volcanic  
821 flows, Clark et al. (2011) have estimated late neotectonic deformation slip rates of between ~4-58  
822 m/Ma for ~1-2 Ma faults, monoclinial and anticlinal structural features in and adjacent to the Otway  
823 Ranges (Fig. 16 and Fig. 18a; Sandiford, 2003a,b). Similar analyses of neotectonic structures in the  
824 Gippsland Basin reveals slightly higher late neotectonic deformation slip rates (>63 m/Ma), which  
825 complements the observation of higher levels of present-day seismicity in this part of southeastern  
826 Australia (Fig. 2 and Fig. 14a). Excluding the Ferguson Hill Anticline (which is probably linked to  
827 an underlying basement fault), the basement-linked Selwyn and Rowsley faults that bound the  
828 northeastern and southeastern limits of the eastern Otway Basin (Fig. 19a), respectively, have been  
829 shown to have the highest late neotectonic deformation slip rates in the basin (Clark et al., 2011).

830 Determining longer-term (i.e., Era-scale) neotectonic deformation slip rates in the Otway Basin is  
831 more challenging, though the parallelism and conformable nature of most Pliocene strandlines across  
832 Victoria has been taken as evidence for very little deformation in the interval between 3-6 Ma. This  
833 demonstrates that most late neotectonic deformation occurred post 3 Ma (Fig. 1: Wallace et al.,  
834 2005; Clark et al., 2011), probably linked to an abrupt change in the Australian-Pacific plate  
835 interactions; from a steady strike-slip motion across the Alpine Fault exposed on New Zealand's  
836 South Island, to a steady transpressional regime (Walcott, 1998; Sandiford, 2003b).

837

838 Although no focal mechanism solutions have been determined in the eastern Otway Basin, recorded  
839 seismicity supports active brittle deformation at mid-crustal depths (Fig. 16). Furthermore, potential  
840 evidence of thermogenic hydrocarbon seeps above seabed pockmarks in the vicinity of neotectonic  
841 compressional deformation structures (e.g., Nerita Anticline; Fig. 16: Bishop et al., 1992; O'Brien et  
842 al., 1992) may also provide additional evidence of brittle deformation, but at shallow depths (<1  
843 km). Logan et al., (2010) debate, nevertheless, that some light hydrocarbon seeps are anthropogenic.  
844 It is important to highlight that whilst seismic profile data reveals less evidence of major brittle  
845 deformation, faulting comparable to the fault displacement observed in the cliffs near Port Campbell  
846 would be beyond that interpreted at the scale of seismic resolution.

847

848 Fig. 19a and Fig. 19b shows the distribution of late neotectonic features across the broader  
849 southeastern Australian region (Clark et al., 2011) encompassing the Mesozoic-Cenozoic-age Otway  
850 and Gippsland basins, the Cenozoic Murray-Darling Basin and basement regions, which mostly  
851 comprise the remnants of the early Palaeozoic Delamerian and Lachlan orogenies (Glen, 2005). This  
852 map also highlights the distribution of basement discontinuities identified from field mapping and  
853 geophysical datasets (e.g., magnetic, radiometric, gravity and seismic; Vandenberg et al., 2000),  
854 including the interpreted underlying extent of the Proterozoic Selwyn Block microcontinent (Fig.  
855 19a,b; Cayley, 2011). There appears to be a clear spatial and geometric relationship between late  
856 neotectonic deformation structures and underlying basement discontinuities, across both basement  
857 and basin regions. This demonstrates that basement structures may exert the first-order control on  
858 the locus of late neotectonic deformation in the Otway Basin. Most late neotectonic structures in the  
859 eastern Otway Basin also strike parallel to early neotectonic inversion structures (e.g., Torquay  
860 Anticline; Fig. 15, Fig. 16 and Fig. 18a), and are near-orthogonal to the contemporary  $SH_{max}$   
861 orientation identified from wellbore failure analysis of sedimentary rocks (Fig. 6c), as well as

862 basement stress orientation estimates (Fig. 14). This implies that both *late* and *early* neotectonic  
863 compressional deformation structures formed under similarly comparable stress fields (Sandiford,  
864 2003b).

865

## 866 **6 Linking Contemporary *In-Situ* Stresses Determined from** 867 **Petroleum Data with Geological and Geophysical Observations**

868 In the previous sections we presented contemporary *in-situ* stress magnitudes using petroleum  
869 exploration data and evidence of neotectonic compressional deformation from geological  
870 observations and focal mechanism solution data, emphasising key uncertainties associated on the  
871 former and identifying possible contemporary *in-situ* stress states. Whilst  $S_V$  magnitude-depth  
872 profiles vary relatively little across the central and eastern offshore Otway Basin, an important  
873 finding is that LOT data, which was used to estimate the magnitude of  $Sh_{min}$ , appears to be sensitive,  
874 with depth, to both lithology and structural province (Fig. 11). Yet despite the geological  
875 observations from seismic profile data and surface rock outcrops, the state of contemporary *in-situ*  
876 stress constrained from petroleum exploration data appears largely inconsistent with these  
877 observations.

878

### 879 **6.1 Influence of neotectonic compressional deformation on contemporary *in-situ*** 880 **stresses in shallower post-rift rocks**

881 Petroleum exploration data from the shallow, post-rift Heytesbury and Nirranda groups indicate a  
882 strike-slip to reverse faulting stress regime or potentially a pure reverse faulting stress regime, with  
883 less variation of LOPs across the central and eastern Otway basin in comparison to siliciclastic  
884 formations (Fig. 13). The observation of a low-angle reverse fault in the cliff near Port Campbell  
885 (Fig. 17) as well as neotectonic compressional structural features around the prominent 600 m high  
886 hills of the Otway Ranges (Fig. 16), that contain over-steepened creek profiles due to of recent uplift  
887 (Hill et al., 1995), all point towards a reverse faulting *in-situ* stress regime. Consequently, we infer  
888 that a pure reverse fault *in-situ* stress regime exists within the shallow, post-rift Heytesbury and  
889 Nirranda groups.

890

891 Frictional limit theory can be used to calculate the upper limit magnitudes of  $SH_{max}$  in these shallow  
892 post-rift marl and carbonate-dominated formations using Eq. (13), where  $S_3$  is either  $S_{V\_Lower}$  or  
893  $S_{V\_Upper}$ . Given that observed LOPs are generally higher than  $S_{V\_Upper}$ , we did not attempt to constrain  
894 horizontal stresses using the approach proposed by Couzens-Schultz and Chan (2010) (i.e., Eq. 15).  
895 From frictional limit theory we estimate  $SH_{max}$  gradients between ~40.6-46.5 MPa/km at a depth of  
896 1000 m TVDML (Fig. 20), for  $S_V$  magnitude bounds and hydrostatic conditions (i.e.,  $\rho_f = 1.02$   
897  $g/cm^3$ ). Seismic data generally reveals little evidence for faulting within the post-rift marls and  
898 carbonates of the Heytesbury Group, despite low-amplitude folding associated with late Miocene to  
899 Holocene inversion structures (Fig. 18). Therefore, as there are no significant pre-existing  
900 weaknesses in these rocks (i.e., faults generated from initial rifting), estimates of  $SH_{max}$  magnitudes  
901 using frictional limits should be considered minimum estimates. This also indicates that these  
902 shallow, post-rift marls and carbonate-dominated formations have predominantly accommodated  
903 compression through ductile deformation. Any faulting associated with these inversion structures are  
904 probably below the resolution of seismic data, similar to the small low-angle reverse faults seen in  
905 outcrop (Fig. 17).

906

907 We postulate that compressional deformation accommodated by folding in these post-rift Miocene  
908 marls and carbonate-dominated formations has been a less efficient means of releasing strain in  
909 comparison to fault slip (Fig. 21), potentially explaining the higher LOPs. It should be noted that  
910 other potential reasons for LOPs higher than  $S_V$  at these shallow depths is perhaps due to the  
911 wellbore wall lined with mud during the test (Evans et al., 1989) or perhaps gravimetric reduction  
912 due to regional erosion (Bush and Meyer, 1988; Warpinski and Tufel, 1989). Gravimetric reduction  
913 due to regional uplift and erosion can result in high horizontal to vertical stress ratios at shallow  
914 depths (Bush and Meyer, 1988); in particular if mudstones (or potentially ductile marls as is the case  
915 here) behave viscoelastically and effectively preserve a small amount of its higher stress state from  
916 its maximum palaeo-burial depth (Warpinski and Tufel, 1989).

917

## 918 **6.2 Reconciling horizontal stress inconsistencies constrained from petroleum** 919 **exploration data in deeper siliciclastic rocks with geological observations**

920 In contrast to the highly stressed, shallow post-rift marl and carbonate-dominated formations,  
921 petroleum exploration data indicates that deeper syn-rift siliciclastic formations have lower  $Sh_{min}$   
922 stresses. Furthermore, LOT data shows an overall increase in  $Sh_{min}$  gradients of ~1-2 MPa/km at

923 depths below ~800 m TVDML within the deeper syn-rift siliciclastic formations from east to west  
924 (Fig. 11a and Fig. 13). A major difference between the post-rift and syn-rift sequences in the Otway  
925 Basin is that the latter contains significant faulting. The siliciclastic units within the Paleocene  
926 Wangerrip Group, which witness the transition to post-rift conditions, generally record only minor  
927 faulting, but the underlying Cretaceous sequence contains a thick sequence of fault-controlled syn-  
928 rift sedimentation (Fig. 1, Fig. 14b,c,f, Fig. 15 and Fig. 18). Minimum horizontal stress magnitudes  
929 are lower in the deeper syn-rift, siliciclastic formations in the central Otway Basin, where faults  
930 generally strike near-parallel to the  $SH_{max}$  orientation and are higher in the eastern Otway Basin  
931 where faults generally strike near-orthogonal to the  $SH_{max}$  orientation (i.e., broadly NE-SW),  
932 reflecting a similar change in structural trends within the underlying basement (Fig. 19a). A normal  
933 to strike-slip fault stress regime is characterised in the central Otway Basin, where there is generally  
934 minor neotectonic (i.e., folding) compressional deformation (Fig. 3; Boulton et al., 2008), while a  
935 strike-slip to reverse fault stress regimes is observed in the eastern Otway Basin due to pronounced  
936 neotectonic compressional deformation (Fig. 16). It is reasonable to conclude that the existing  
937 structural fabrics (predominantly imposed during episodic Cretaceous rifting) exert a strong control  
938 on  $Sh_{min}$ , as well as  $SH_{max}$ . Given that there is less variation in LOPs within the shallower and folded  
939 post-rift marl and carbonate-dominated formations across both regions in comparison to the deeper  
940 and faulted syn-rift siliciclastic rocks, we suggest that sub-surface structural style or mode of  
941 compressional deformation exerts an important control on horizontal stress gradients in the central  
942 and eastern Otway Basin (Fig. 21).

943

### 944 **6.2.1 Eastern Otway Basin**

945 Changes in horizontal stress gradients (i.e., at a larger scale to slight lithological variation) resulting  
946 from sub-surface structural style (interpreted from seismic data) at some depth has been documented  
947 previously. For example, both Evans et al. (1989) and Couzens-Schultz and Chan, (2010) have  
948 shown that LOPs change from near-lithostatic pressures (i.e.,  $S_V$ ) at shallow depth intervals (<1000  
949 m), abruptly becoming much less than lithostatic pressures (~60-90%  $S_V$ ) in rocks at depths >1km in  
950 regions where independent geological evidence indicates reverse fault stress conditions. A possible  
951 explanation for the occurrence of lower LOPs in settings, where geological evidence indicate reverse  
952 fault stress conditions but petroleum exploration data indicate strike-slip fault stress conditions, is an  
953 instantaneous stress drop following brittle deformation (Couzens-Schultz and Chan, 2010). In the  
954 central and eastern Otway Basin, compressional strain in the deep, faulted syn-rift sections  
955 (particularly sandstones) may be efficiently released by slippage along faults during the late Miocene



956 to present-day. This probably occurs at both seismicity and sub-seismicity scales causing an  
957 associated effective stress increase at the faults and a total stress drop away from faults (i.e., regional  
958 *in-situ* stress field) following fault slippage and deformation (c.f., Sibson, 1995). Thus, LOTs tend to  
959 yield lower LOPs and indicate a strike-slip fault stress regime rather than a reverse slip fault stress  
960 regime despite clear geological evidence (Fig. 16: e.g., Mildren and Hillis, 2000; Reynolds et al.,  
961 2003b; Mildren et al., 2004; White and Hillis, 2004; Nelson et al., 2006a; King et al., 2008). If a  
962 LOP database is predominantly composed of LOTs performed within deeper, syn-rift and lower-  
963 horizontally stressed siliciclastic formations, then  $Sh_{min}$  gradients within shallower, post-rift  
964 formations may be underestimated in a compressional deformation regime, or vice versa.

965

966 Calculation of frictional limit theory assuming a strike-slip and reverse faulting stress regime would  
967 constrain  $SH_{max}$  magnitudes using  $S_3 = Sh_{min}$  and  $S_3 = S_V$ , respectively, in which case the latter would  
968 yield similar  $SH_{max}$  gradients bounds as for marl and carbonate-dominated formations when  $P_P$   
969 magnitudes are assumed to be hydrostatic and  $\mu = 0.6$ . Assuming such conditions, at 2500 m  
970 TVDML  $SH_{max}$  gradients are approximately <50.8 MPa/km for  $S_{V\_Upper}$ , respectively (since  $S_V$   
971 magnitudes has a power-law relationship with depth; Fig. 22b). The difficulty in assigning either  
972  $Sh_{min}$  or  $S_V$  as  $S_3$  from LOPs led Evans and Engelder (1989) to propose a conservative approach  
973 whereby it is assumed that  $Sh_{min} \approx S_V$  and LOPs only provide a lower bound estimate of  $Sh_{min}$   
974 magnitudes. Hence, for the sand and shale-dominated units in a strike-slip faulting stress regime,  
975 frictional limit theory calculates upper bounds for  $SH_{max}$  gradients of ~31.9 MPa/km and ~43.9  
976 MPa/km, respectively (Fig. 22b), which indicates significant variation in the upper gradient limit of  
977  $SH_{max}$  between ~13.1-18.9 MPa/km.

978

979 Estimating  $Sh_{min}$  magnitudes using the traditional frictional limit theory method for interpreting  
980 LOPs during LOTs does not allow for the possibility of a reverse faulting stress regime (King et al.,  
981 2012; Fig. 22c), despite geological evidence of neotectonic reverse faulting in the shallower  
982 stratigraphic sections. For this reason, we have further estimated horizontal stresses in the eastern  
983 Otway Basin using Eq. (4) and Eq. (15) of Couzens-Schultz and Chan (2010), which assume LOPs  
984 in LOTs are caused by shear failure of cohesionless pre-existing plane rather than tensile failure.  
985 This may provide further useful constraints in the sand-dominated formations, where observed LOPs  
986 are much lower than  $S_V$ , contrary to geological evidence. Not only does this new interpretation of  
987 LOT allow for normal and strike-slip faulting stress regimes, it does also provide new upper limits of

988  $SH_{max}$  magnitude for within a reverse faulting stress regime, which the traditional interpretations do  
989 not (Fig. 22c; King et al., 2012). Hence, the limits of horizontal stresses for sand and shale-  
990 dominated formations according to this method (Couzens-Schultz and Chan 2010) are bounded by  
991  $\sim 19.0\text{-}36.0$  MPa/km and  $\sim 21.6\text{-}27.8$  MPa/km, respectively, at 2500 m TVDML using  $S_V = S_{V\_Upper}$   
992 and assuming  $\mu_P = 0.6$  (Fig. 22b).

993

994 Using frictional limit theory and the method of Couzens-Schultz and Chan (2010), the difference in  
995 calculated  $SH_{max}$  gradient limits can be seen in Fig. 22b (i.e., compare (1) and (3) as well as (2) and  
996 (4)). This method demonstrates that the traditional assumption of a newly formed vertical tensile  
997 fracture during a LOT will typically underestimate the gradient of the  $Sh_{min}$  (King et al., 2012).

998 Furthermore, it can be seen in Fig. 22b that while  $SH_{max}$  gradient upper limits for sand-dominated  
999 formations increase in comparison to frictional limit constraints, it decreases  $SH_{max}$  gradient upper  
1000 limits for shale-dominated formations. Figure 22d shows that if the traditional LOT interpretation  
1001 yields a  $Sh_{min}$  gradient less than  $\sim 23.5\%$  of the  $S_V$  gradient (i.e., sand-dominated formation  $Sh_{min}$   
1002 gradient), it estimates a greater upper gradient limit of  $SH_{max}$  than would otherwise be calculated  
1003 from frictional limit theory, forcing higher horizontal stresses (Fig. 22b). Alternatively, if  $Sh_{min}$   
1004 gradients fall within this range (i.e., shale-dominated formation  $Sh_{min}$  gradient), then the alternative  
1005 method will calculate lesser upper gradient limits of  $SH_{max}$  with respect to frictional limit theory  
1006 (Fig. 22b), forcing a convergence of principle stresses towards isotropy ( $S_1 = S_2 = S_3$ ). Hence,  
1007 drastically reducing differential stresses ( $S_1 - S_3$ ) and mean stresses ( $(S_1 + S_2 + S_3)/3$ ) alike. Whilst  
1008 these alternate estimates of differential and mean stresses has important implications for  
1009 hydrocarbon exploration (i.e., fault reactivation propensity and wellbore stability; e.g., Lyon et al.,  
1010 2005; Nelson et al., 2006b), it may also help reconcile differences in differential stress magnitudes  
1011 between numerical modelling and those estimated from petroleum exploration data (c.f., Hillis and  
1012 Reynolds, 2000; Reynolds et al., 2003a; Dyksterhuis and Müller, 2008).

1013

### 1014 **6.2.2 Central Otway Basin**

1015 A normal to strike-slip *in-situ* stress regime has been deduced for the central Otway Basin based on  
1016 petroleum exploration data (Fig. 13a). If we consider the lower-stressed, sand-dominated formation  
1017 LOPs as the least principal stress (i.e.,  $S_3 = Sh_{min} \sim 15.9$  MPa/km), then frictional limit theory  
1018 calculates an  $S_1$  (i.e.,  $SH_{max}$ ) gradient of  $\sim 28.5$  MPa/km assuming hydrostatic  $P_P$  and  $\mu = 0.6$ . This is  
1019 greater than  $S_{V\_Upper}$  for depths within the Meso-Cenozoic sedimentary package (e.g., at 2500 m

1020 TVDML:  $Sh_{min} = 39.8 \text{ MPa} < S_{V\_Upper} = 57.7 \text{ MPa} < SH_{max} = 71.2 \text{ MPa}$ ). This reconfirms the  
1021 likelihood of a strike-slip fault stress regime as opposed to a normal fault stress regime (Fig. 22a).  
1022 Similarly, using the best-fit shale-dominated lithology  $Sh_{min}$  gradient in the central Otway Basin (i.e.,  
1023  $\sim 18.8 \text{ MPa/km}$ ), the  $SH_{max}$  gradient is  $\sim 37.4 \text{ MPa/km}$  using frictional limit theory at 2500 m  
1024 TVDML, indicating an  $\sim 9 \text{ MPa/km}$  difference in  $SH_{max}$  gradient between sand and shale-dominated  
1025 formations (Fig. 22a). Significant overpressure has been reported in the central Otway Basin,  
1026 however, which would result in  $SH_{max}$  gradients to decrease with increasing overpressure as  
1027 illustrated in Fig. 12.

1028

1029 Although there is evidence of small amplitude folding within Miocene marl and carbonates rocks  
1030 extended laterally westwards towards the South Australian Otway Basin with consistent NE-SW  
1031 trends (Fig. 3; c.f., Boulton et al., 2008), there is less evidence of major inversion compressional  
1032 deformation westwards away from the Otway Ranges. Hence, a strike-slip faulting stress state in  
1033 these deeper siliciclastic formations can adequately describe geological observations in the central  
1034 Otway Basin. This may also indicate a buckling style of compressional deformation within the  
1035 shallower highly-stressed ductile marl and carbonate-dominated formations in the central Otway  
1036 Basin where the inverted syn-rift faults are non-parallel to the shallower anticlinal trends. A potential  
1037 20 m ‘pop-up’ structure formed within the last 0.8 Myr in an otherwise very inter-dune coastal flat  
1038 near the South Australian-Victorian border (Boulton et al., 2008) may also be indicative of a strike-slip  
1039 faulting stress regime. Furthermore, evidence of recent hydrocarbon leakage about reactivated  
1040 basement faults, where minor neotectonic compressional deformation (Boulton et al., 2008) resulted in  
1041 palaeo-hydrocarbon columns (Lyon et al., 2007), supporting our constrained contemporary *in-situ*  
1042 stresses presented herein within this region.

1043

## 1044 **7 Conclusions**

1045 We have investigated the state of contemporary *in-situ* stresses in the Otway Basin using newly  
1046 available petroleum exploration data, with a key focus to link our results with complementary  
1047 geological observations and geophysical datasets. Unlike many previous *in-situ* stress studies in  
1048 basins around Australia (e.g., Reynolds et al., 2006; Nelson et al., 2006a), we have highlighted the  
1049 importance of factors such as underlying structural fabrics, and variations in mechanical properties  
1050 of syn- and post-rift basin-fill on stress magnitudes.

1051 Our main conclusions are as follows:

- 1052 • Wellbore failure analysis indicates the  $SH_{max}$  orientations in the central and eastern region of  
1053 the Otway Basin is  $\sim 135 \pm 15$  °N consistent with previous investigations using petroleum  
1054 exploration data (Hillis et al., 1995; Nelson et al., 2006a). Independent geological  $SH_{max}$   
1055 orientation constraints from focal mechanism solutions of basement earthquakes (Denham et  
1056 al., 1981, 1985; Bock and Denham, 1983; McCue et al., 1990; McCue and Paull, 1991;  
1057 Leonard et al., 2002; Allen et al., 2005; Clark, 2009) and Pliocene-Holocene volcanic vent  
1058 alignments (Lesti et al., 2008) are also broadly consistent with petroleum exploration data  
1059 estimates. This implies a coupling of stress conditions between the Meso-Cenozoic  
1060 sedimentary basin fill and the underlying basement.
- 1061 • Shallow, post-rift, upper Oligocene to upper Miocene-age marl and carbonate-dominant  
1062 formations generally report the highest LOPs in the basin, which are typically in excess of  $S_V$   
1063 magnitudes ( $>20$  MPa/km) above  $\sim 800$  m TVDML. Whilst other reasons may explain the  
1064 high LOPs across the entire basin (e.g., viscoelasticity due to recent uplift and erosion),  
1065 outcropping rocks show evidence of reverse neotectonic faulting and folding, in particular  
1066 in the eastern Otway Basin, indicating a reverse faulting *in-situ* stress regime.
- 1067 • Deeper siliciclastic rocks generally exhibit a strike-slip fault stress regime based petroleum  
1068 exploration data and frictional limit constraints (Jaeger and Cook, 1979). The observation  
1069 that  $Sh_{min}$  gradients in shales are typically  $\sim 3-4$  MPa/km greater than those in sandstones  
1070 confirms that lithology is a strong control on horizontal stress magnitudes in this basin.
- 1071 • There is a  $\sim 1-2$  MPa/km increase in  $Sh_{min}$  gradients within syn-rift rocks from west to east in  
1072 the basin. This coincides with both a change in structural trend and an increase in the  
1073 intensity of neotectonic compressional deformation, implying that horizontal stresses are  
1074 likely influenced by the orientation of underlying structural fabrics with respect to  
1075 contemporary horizontal stress field.
- 1076 • Whereas neotectonic compressional deformation in post-rift marl and carbonate-dominated  
1077 formations is accommodated primarily by folding and is rarely faulted, the deeper syn-rift  
1078 siliciclastic rocks are very faulted. We suggest, therefore, that compressional deformation  
1079 accommodated through folding is a less efficient means of releasing regional stress in  
1080 comparison with faulting (of optimally oriented planes of weakness). This could potentially  
1081 explain the stress partitioning with depth between the shallow post-rift Miocene rocks  
1082 indicative of a reverse stress state and deeper syn-rift Cretaceous-Paleocene siliciclastic rocks  
1083 indicative of a strike-slip stress state despite geological evidence.

- 1084
- 1085
- 1086
- 1087
- 1088
- 1089
- 1090
- In the eastern region where there is strong geological evidence of neotectonic compressional deformation, we constrained the magnitude of  $SH_{max}$  using an alternate method for interpreting LOPs (Couzens-Schultz and Chan 2010). This alternate method increases the  $SH_{max}$  gradient if LOPs are within ~23.5% of  $S_V$  gradient (and vice versa), which has important implications for hydrocarbon exploration and exploitation, such as borehole stability and fault sealing analyses as well as potentially reconciling differences in modelled and observed stress fields.

1091

## 1092 **8 Acknowledgements**

1093 This work forms part of ARC Discovery Project DP0879612, ASEG Research Foundation Project  
1094 RF09P04 and represents TRaX contribution ####. We thank Will Jones, Adam Smith, Ian Brown and  
1095 Huw Edwards of PGS for provision of SAMDA, and gratefully acknowledge Geoscience Australia,  
1096 DPI Victoria, Occam Technologies and Lakes Oil NL for access to seismic and well data. We would  
1097 also like to thanks Jerry Meyer and Scott Mildren of Ikon Technologies for technical assistance and  
1098 provision of their propriety software JRS Suite for wellbore analyses and IHS for provision of their  
1099 Kingdom Suite seismic interpretation software. Finally, we thank Ian Duddy and Paul Green of  
1100 Geotrack International for valuable discussions regarding the geology of the Otway Basin.

1101

## 1102 9 References

- 1103 Addis, M.A., Hanssen, TH., Yassir, N., Willoughby, D.R., Enever, J., 1998. A Comparison of leak-  
1104 off test and extended leak-off test data for stress estimation. Presented at the joint SPE/ISRM  
1105 Eurock '98 Conference. Trondheim, Norway, Minneapolis, July 1998, SPE/ISRM Paper  
1106 47235.
- 1107 Allen, I., Gibson, G., Cull, J.P., 2005. Stress-field constraints from recent intraplate seismicity in  
1108 southeastern Australia. *Australian Journal of Earth Sciences*, 52, 217–229.
- 1109 Anderson, E.M., 1951. The dynamics of faulting and dyke formation with applications to Britain.  
1110 Edinburgh, Oliver and Boyd.
- 1111 Athy, L.F., 1930. Density, porosity and compaction of sedimentary rocks. *American Association of*  
1112 *Petroleum Geologist Bulletin*, 14, 7675–7708.
- 1113 Bell, J.S., 1990. Investigating stress regimes in sedimentary basins using information from oil  
1114 industry wireline logs and drilling records. in: Hurst, A., Lovell, M., Morton, A. (Eds.),  
1115 Geological applications of wireline logs. Geological Society, London, Special Publication 48,  
1116 pp. 305–325.
- 1117 Bell, J.S., 1996. Petro Geoscience 1. In situ stresses in sedimentary rocks (part 2): applications of  
1118 stress measurements, *Geoscience Canada*, 23, 135–153.
- 1119 Bell, J.S., Gough, D.I., 1979. Northeast-southwest compressive stress in Alberta: evidence from oil  
1120 wells. *Earth Planetary Science Letters*, 45, 475–482.
- 1121 Bérard, T., Sinha, B.K., van Ruth, P., Dance, T., John, Z., Tan, C.P., 2008. Stress estimation at the  
1122 Otway CO<sub>2</sub> storage site, Australia. 2008 SPE Asia Pacific Oil & Gas Conference & Exhibition,  
1123 Perth, SPE 116422.
- 1124 Bernecker, T., Smith, M.A., Hill, K.A., Constantine, A.E., 2003. Oil and gas, fuelling Victoria's  
1125 economy. in: Birch, W.D. (Ed.), *Geology of Victoria*, Geological Society of Australia, Special  
1126 Publication, 23, 469–487.
- 1127 Bishop, J.H., Bickford, G.P., Heggie, D.T., 1992. South-eastern Australia surface geochemistry II:  
1128 light hydrocarbon geochemistry in bottom waters of the Gippsland Basin, eastern Otway  
1129 Basin, Torquay sub-Basin and the Durroon sub-Basin. Bureau of Mineral Resources Record  
1130 1992/54, Vols. 1 and 2.

- 1131 Blevin, J., Cathro, D., 2008, Australian Southern Margin Synthesis. Client report to Geoscience  
1132 Australia by FrOG Tech Pty Ltd. Project GA707,
- 1133 Bock, G., Denham, D., 1983. Recent earthquake activity in the Snowy Mountain region and its  
1134 relationship to major faults. *Journal of the Geological Society of Australia*, 30, 423–429.
- 1135 Boulton, P.J., Lyon, P., Camac, B., Hunt, S., Zwingmann, H., 2008. Unravelling the complex structural  
1136 history of the Penola Trough – revealing the St George Fault. in: Blevin, J.E., Bradshaw, B.E.,  
1137 Uruski, C. (Eds.), *Eastern Australasian Basins Symposium III*, Petroleum Exploration Society  
1138 of Australia Special Publication, pp. 81–93.
- 1139 Breckels, I.M., van Eekelen, H.A.M., 1982. Relationships between horizontal stress and depth in  
1140 sedimentary basins. *Journal of Petroleum Technology*, 34, 2191–2198.
- 1141 Brundy, M., Zoback, M.D., 1999. Drilling-induced tensile wall-fractures: implications for  
1142 determination of in situ stress orientations and magnitudes. *International Journal of Rock  
1143 Mechanics and Mining Sciences*, 36, 191–215.
- 1144 Bush, D.D., Meyer, B.S., 1988. In situ stress magnitude dependency on lithology. Presented at the  
1145 29<sup>th</sup> U.S. Symposium of Rock Mechanics. Minneapolis, June 1988, SPE Paper 88-0729
- 1146 Byerlee, J.D., 1978. Friction of Rocks. *Pure and Applied Geophysics*, 116, 615–626.
- 1147 Cayley, R.A., 2011. Exotic crustal block accretion to the eastern Gondwanaland margin in the Late  
1148 Cambrian-Tasmania, the Selwyn Block, and implications for the Cambrian-Silurian evolution  
1149 of the Ross, Delamerian, and Lachlan orogens. *Gondwana Research*, 19, 628–649.
- 1150 Clark, D. J., 2009. What is an “active” fault in the Australian intraplate context? A discussion with  
1151 examples from eastern Australia. *Australian Earthquake Engineering Society Newsletter*, June  
1152 2009, 3–6.
- 1153 Clark, D.J., Leonard, M., 2003. Principal stress orientations from multiple focal plane solutions: new  
1154 insight in to the Australian intraplate stress field, in: Hillis, R.R., Muller, D. (Eds.), *Evolution  
1155 and dynamics of the Australian Plate*, pp. 91–105. Geological Society of Australia Special  
1156 Publication 22 and Geological Society of America Special Paper 372.
- 1157 Clark, D.J., McPherson, A., Collins, C.D.N., 2011. Australia’s seismogenic neotectonic record: a  
1158 case for heterogeneous intraplate deformation. *Record* 2011/11. Geoscience Australia,  
1159 Canberra.

- 1160 Cooper, G.T., Hill, K.C., 1997. Cross-section balancing and thermochronological analysis of the  
1161 Mesozoic development of the eastern Otway Basin. *Journal of the Australian Petroleum*  
1162 *Production and Exploration Association*, 37, 390–414.
- 1163 Corcoran, D.V., Doré, A.G., 2007. Top seal assessment in exhumed basin settings – some insights  
1164 from Atlantic Margin and borderland basins, in: Koestler, A.G., Hunsdale, R. (Eds.),  
1165 *Hydrocarbon Seal Quantification: Norwegian Petroleum Society Special Publication 11*, pp.  
1166 89–107.
- 1167 Couzens-Schultz, B.A., Chan, A.W., 2010. Stress determination in active thrust belts: An alternative  
1168 leak-off pressure interpretation. *Journal of Structural Geology*, 22, 1061–1069.
- 1169 Daines, S.R., 1982, Aquathermal pressuring and geopressure evaluation. *American Association of*  
1170 *Petroleum Geologist Bulletin*, 66, 931–939.
- 1171 Denham, D., Weekes, J., Krayshek, C., 1981. Earthquake evidence for compressive stress in the  
1172 southeast Australian crust. *Journal of the Geological Society of Australia*, 28, 323–332.
- 1173 Denham, D., Gibson, G., Smith, R.S., Underwood, R., 1985. Source mechanisms and strong ground  
1174 motion from the 1982 Wonnangatta and the 1966 Mount Hotham earthquakes. *Australian*  
1175 *Journal of Earth Sciences*, 32, 37–46.
- 1176 Densley, M.R., Hillis, R.R., Redfearn, J.E.P., 2000. Quantification of Tertiary uplift in the  
1177 Carnarvon Basin based on interval velocities. *Australian Journal of Earth Sciences*, 47, 111–  
1178 122.
- 1179 Dickinson, J.A., Wallace, M.W., Holdgate, G.R., Gallagher, S.J., Thomas, L., 2002. Origin and  
1180 timing of the Miocene-Pliocene unconformity in Southeast Australia. *Journal of Sedimentary*  
1181 *Research*, 72 (2), 288–303.
- 1182 Duddy, I.R., 2003. Mesozoic, a time of change in tectonic regime, in: Birch W.D. (ed.), *Geology of*  
1183 *Victoria: Geological Society of Australia Special Publication 23*, pp. 239–286.
- 1184 Dyksterhuis, S., Müller, R.D., 2008. Cause and evolution of intraplate orogeny in Australia.  
1185 *Geology*, 36 (6), 495-498.
- 1186 Eaton, B.A., 1969. Fracture gradient prediction and its application in oil field operations. *Journal of*  
1187 *Petroleum Technology*, 21, 1353–1360.
- 1188 Edwards, J., Tickell, S.J., Wilcocks, A.J., Eaton, A. R., Cramer, M.L., King, R.L., Bourton, S.M.,  
1189 1996. Colac 1:250000 geological map: Geological Survey of Victoria.



- 1190 Engelder, T., 1993. *Stress Regimes in the Lithosphere*. Princeton, New Jersey, Princeton.
- 1191 Evans, K., Engelder, T., 1989. Some problems in estimating horizontal stress magnitudes in “thrust”  
1192 regimes. *International Journal of Rock Mechanics and Mining Sciences and Geomechanics*  
1193 *Abstracts*, 26 (6), 647–660.
- 1194 Evans, K., Engelder, T., Plumb, R.A., 1989, *Appalachian Stress Study 1: A detailed description of in*  
1195 *situ stress variation in Devonian Shales of the Appalachian Plateau: Journal of Geophysical*  
1196 *Research*, 94, 1729–1754.
- 1197 Geary, G.C., Ried, I.S.A., 1998. Hydrocarbon prospectivity of the offshore eastern Otway Basin,  
1198 Victoria, for the 1998 Acreage Release. Department of Natural Resources and Environment,  
1199 Victorian Initiative for Minerals and Petroleum Report 55.
- 1200 Glen, R.A., 2005. The Tasmanides of eastern Australia, in: Vaughan, A.P.M., Leat, P.Y., Pankhurst,  
1201 R.J. (Eds.), *Terrane Processes at the Margins of Gondwana*. Geological Society, London,  
1202 *Special Publications*, 246, pp. 23–96.
- 1203 Gough, D.I., Bell, J.S., 1982. Stress orientations from borehole wall fractures with examples from  
1204 Colorado, east Texas, and northern Canada. *Canadian Journal of Earth Sciences*, 19, 1358–  
1205 1370.
- 1206 Green, P.F., Crowhurst, P.V., Duddy, I.R., 2004. Integration of AFTA and (U-Th)/He  
1207 thermochronology to enhance the resolution and precision of thermal history reconstruction in  
1208 the Anglesea-1 well, Otway Basin, SE Australia, in: Boulton, P.J., Johns, D.R., Lang, S.C. (Eds.),  
1209 *Eastern Australasian Basins Symposium II*, Petroleum Exploration Society of Australia Special  
1210 *Publication*, pp. 117–131.
- 1211 Haimson, B.C., Fairhurst, C., 1967. Initiation and extension of hydraulic fractures in rocks. *Society*  
1212 *of Petroleum Engineers Journal* 7, 310–318.
- 1213 Heidbach, O., Reinecker, J., Tingay, M., Müller, B., Sperner, B., Fuchs, K., Wenzel, F., 2007. Plate  
1214 boundary forces are not enough: Second- and third-order stress patterns highlighted in the  
1215 *World Stress Map database*, *Tectonics*, 26, TC6014. doi:10.1029/2007TC002133.
- 1216 Heidbach, O., Tingay, M.R.P., Barth, A., Reinecker, J., Kurfeß, D., Müller, B., 2010, *Global crustal*  
1217 *stress patterns based on the 2008 World Stress Map database release: Tectonophysics*, v. 482,  
1218 p. 3–15.

- 1219 Hill, K.C., Hill, K.A., Cooper, G.T., Richardson, M.J., Lavin, C.J., 1994. Structural framework of  
1220 the eastern Otway Basin: inversion and interaction between two major structural provinces.  
1221 *Exploration Geophysics*, 25, 79–87.
- 1222 Hill, K.C., Hill, K.A., Cooper, G.T., O’Sullivan, A.J., O’Sullivan, P.B., Richardson, M.J., 1995.  
1223 Inversion around the Bass Basin, SE Australia, in: Buchanan, J.G., Buchanan, P.G. (Eds.),  
1224 Basin Inversion. Geological Society, London, Special Publication, 88, pp. 525–547.
- 1225 Hillis, R.R., 2001. Coupled changes in pore pressure and stress in oil fields and sedimentary basins.  
1226 *Petroleum Geoscience*, 7, 419–425.
- 1227 Hillis, R.R., William, A.F., 1992. Borehole breakouts and stress analysis in the Timor Sea, in: Hurst,  
1228 A., Griffiths, C.M., Worthington, P.F. (Eds.), *Geological Applications of Wireline Logs II*.  
1229 Geological Society, London, Special Publication, 65, pp. 157–168.
- 1230 Hillis, R. R., William, A.F., 1993. The contemporary stress field of the Barrow-Dampier Sub-basin  
1231 and its implications for horizontal drilling. *Exploration Geophysics*, 24, 567–576.
- 1232 Hillis, R.R., Reynolds, S.D., 2000. The Australian Stress Map. *Journal of the Geological Society*,  
1233 London, 157, 915–921.
- 1234 Hillis, R.R., Monte, S.A., Tan, C.P., Willoughby, D.R., 1995. The contemporary stress field of the  
1235 Otway Basin, South Australia: Implications for hydrocarbon exploration and production.  
1236 *Journal of the Australian Petroleum Production and Exploration Association*, 31, 1, 494–506.
- 1237 Hillis, R.R., Sandiford, M., Reynolds, S.D., Quigley, M.C., 2008. Present-day stresses, seismicity  
1238 and Neogene-to-Recent tectonics of Australia’s ‘passive’ margin: intraplate deformation  
1239 controlled by plate boundary forces, in: Johnson, H., Doré, A.G., Gatliff, R.W., Holdsworth,  
1240 R., Lundin, E.R., Ritchie, J.D. (Eds.), *The Nature and Origin of Compression in Passive*  
1241 *Margins*, Geological Society, London, Special Publications, 306, pp. 71–90.
- 1242 Holdgate, G.R., Gallagher, S.J., 2003. Tertiary, a period of transition to marine basin environments,  
1243 in: Birch, W.D. (Ed.), *Geology of Victoria*, Geol. Soc. Aust., Spec. Publ., 23, 289–335.
- 1244 Holford, S.P., Hillis, R.R., Duddy, I.R., Green, P.F., Tuitt, A.K., Stoker, M.S., 2010. Impacts of  
1245 Neogene-Recent compressional deformation and uplift on hydrocarbon prospectivity of the  
1246 passive southern Australian margin. *Journal of the Australian Petroleum Production and*  
1247 *Exploration Association*, 50, 267–286.

- 1248 Holford, S.P., Hillis, R.R., Duddy, I.R., Green, P.F., Tassone, D.R., Stoker, M.S., 2011a.  
1249 Palaeothermal and seismic constraints on late Miocene-Pliocene uplift and deformation in the  
1250 Torquay sub-basin, southern Australian margin. *Australian Journal of Earth Sciences*, 58, pp.
- 1251 Holford, S.P., Hillis, R.R., Hand, M., Sandiford, M., 2011b. Thermal weakening localizes intraplate  
1252 deformation along the southern Australian continental margin. *Earth and Planetary Science*  
1253 *Letters*, 305, 207–214.
- 1254 Holford, S.P., Tuitt, A.K., Hillis, R.R., Green, P.F., Stoker, M.S., Duddy, I.R., Sandiford, M., 2014.  
1255 Cenozoic deformation in the Otway Basin, southern Australian margin: implications for the  
1256 origin and nature of post-breakup compression at rifted margins. *Basin Research*, 26, 10–37,  
1257 doi: 10.1111/bre.12035
- 1258 Jaeger, J.C., Cook, N.G.W., 1979. *Fundamentals of Rock Mechanics*. Chapman and Hall, London.
- 1259 Johnston, A.C., 1994. Seismotectonic interpretations and conclusions from the stable continental  
1260 region seismicity database. in: Johnston, A.C., Coppersmith, K.J., Kanter, L.R., Cornell, C.A.  
1261 (Eds.), *The Earthquakes of Stable Continental Region – Volume 1: Assessment of Large*  
1262 *Earthquake Potential*. Electric Power Research Institute, Palo Alto, California, Report TR-  
1263 102261-V1.
- 1264 King, R.C., Hillis, R.R., Reynolds, S.D., 2008. In situ stresses and natural fractures in the Northern  
1265 Perth Basin, Australia. *Australian Journal of Earth Sciences*, 55 (5), 685–701.
- 1266 King, R.C, Neubauer, M., Hillis, R.R., Reynolds, S.D., 2010. Variation in vertical stress in the  
1267 Carnarvon Basin, NW Shelf, Australia. *Tectonophysics*, 482, 73–81.
- 1268 King, R.C, Holford, S.P., Hillis, R.R., Tuitt, A.K., Swierczek E., Backé, G., Tassone, D.R., Tingay,  
1269 M.R.P., 2012. Reassessing the in situ stress regimes of Australia’s petroleum basins. *Journal of*  
1270 *the Australian Petroleum Production and Exploration Association*, 52, 415–426.
- 1271 Krassay, A.A., Cathro, D.L., Ryan, D.J., 2004. A regional tectonostratigraphic framework for the  
1272 Otway Basin, in: Boulton, P.J., Johns, D.R., Lang, S.C. (Eds.), *Eastern Australasian Basins*  
1273 *Symposium II*. Petroleum Exploration Society of Australia, Special Publication, pp. 97-116.
- 1274 Leonard, M., Ripper, I.D., Yue, L., 2002. Australian fault plane solutions. *Geoscience Australia*  
1275 *Record* 2002/1.
- 1276 Lesti, C., Giordano, G., Salvini, F., Cas R., 2008. Volcano tectonic setting of the intraplate,  
1277 Pliocene-Holocene, Newer Volcanic Province (southeast Australia): Role of crustal fracture  
1278 zones. *Journal of Geophysical Research*, 113, B07407, doi:10.1029/2007JB005110.

- 1279 Logan, G.A., Jones, A.T., Kennaed, J.M., Ryan, G.J., Rollet, N., 2010. Australian offshore natural  
1280 hydrocarbon seepage studies, a review and re-evaluation. *Marine and Petroleum Geology*, 27,  
1281 26–45.
- 1282 Ludwig, W.J., Nafe, J.E., Drake, C.L., 1970. Seismic refraction, in: Maxwell, A.E., (Ed.), *The Sea*,  
1283 Vol 4, Wiley-Interscience, New York, pp. 53–84.
- 1284 Lyon, P.J., Boulton, P.J., Hillis, R.R., Mildren, S.D., 2005. Sealing by shale gouge and subsequent seal  
1285 breach by reactivation: a case study of the Zema Prospect, Otway Basin, in: Boulton P.J., Kaldi J.  
1286 (Eds.), *Evaluating Fault and Cap Rock Seals: American Association of Petroleum Geologist*  
1287 *Hedberg Series 2*, pp. 179–197.
- 1288 Lyon, P.J., Boulton, P.J., Hillis, R.R., Bierbrauer, K., 2007. Basement controls on fault development in  
1289 the Penola Trough, Otway Basin, and implications for fault-bounded hydrocarbon traps:  
1290 *Australian Journal of Earth Sciences*, 54, 675–689.
- 1291 Mardia, K., K.V., 1972. *Statistics of Directional Data*. Academic Press, London and New York.
- 1292 Mastin, L., 1988. Effect of borehole deviation on breakout orientations. *Journal of Geophysical*  
1293 *Research*, 93, 9187–9195.
- 1294 Matthews, W.R., Kelly, J., 1967. How to predict formation pressure and fracture gradient from  
1295 electric and sonic logs. *Oil and Gas Journal*, 92–106.
- 1296 Mavromatidis, A., Hillis, R.R., 2005. Quantification of exhumation in the Eromanga Basin and its  
1297 implications for hydrocarbon exploration. *Petroleum Geoscience*, 11, 79–92.
- 1298 McCue, K., Paull, E., 1991. Australian seismological report 1988. Australian Bureau of Mineral  
1299 Resources Report 304.
- 1300 McCue, K., Gibson, G., Wesson, V., 1990. The earthquake near Nhill, western Victoria, on 22  
1301 December 1987 and the seismicity of eastern Australia. *Journal of Australian Geology and*  
1302 *Geophysics*, 11, 415–420.
- 1303 McGowran, B., Holdgate, G.R., Li, Q., Gallagher, S.J., 2004. Cenozoic stratigraphic succession in  
1304 southeastern Australia. *Australian Journal of Earth Sciences*, 51, 459–496.
- 1305 Messent, B.E., Collins, G.I., West, B.G., 1999. Hydrocarbon Prospectivity of the Offshore Torquay  
1306 Sub-Basin, Victoria: Gazettal Area V99-1: Victorian Initiative for Minerals and Petroleum  
1307 Report 60.

- 1308 Mildren, S.D., Hillis, R.R., 2000. In situ stresses in the Bonaparte Basin, Australia: implications for  
1309 first- and second-order controls on stress orientations. *Geophysical Research Letters*, 27 (20),  
1310 3413–3416.
- 1311 Mildren, S.D., Hillis, R.R., Kivior, T., Kaldi, J.G., 2004. Integrated seal assessment and geologic  
1312 risk with application to the Skua Field, Timor Sea, Australia, in: Ellis, G.K., Baillie, P.W.,  
1313 Munson, T.J. (Eds.), *Timor Sea Petroleum Geoscience: Proceedings of the Timor Sea*  
1314 *Symposium*, Darwin, Northern Territory Geological Survey Special Publication, 1, pp. 275–  
1315 294.
- 1316 Miller, J.M., Norvick, M.S., Wilson, C.J.L., 2002. Basement controls on rifting and the associated  
1317 formation of ocean transform faults – Cretaceous continental extension of the southern margin  
1318 of Australia. *Tectonophysics*, 359, 131–155.
- 1319 Moos, D., Zoback, M.D., 1990. Utilization of observations of wellbore failure to constrain the  
1320 orientation and magnitude of crustal stresses: application to continental, deep sea drilling  
1321 project and ocean drilling program boreholes. *Journal of Geophysical Research*, 95, 9305–  
1322 9325.
- 1323 Mouchet, J. P., Mitchell, A., 1989. Abnormal pressures while drilling: Boussens, France, Elf  
1324 Aquitaine.
- 1325 Nelson, E.J., Hillis, R.R., 2005. In situ stresses of the West Tuna area, Gippsland Basin. *Australian*  
1326 *Journal of Earth Sciences*, 52, 299–313.
- 1327 Nelson, E.J., Hillis, R.R., Sandiford, M., Reynolds, S.D., Mildren, S.D., 2006a. Present-day state-of-  
1328 stress of southeast Australia. *Journal of the Australian Petroleum Production and Exploration*  
1329 *Association*, 46, 283–305.
- 1330 Nelson, E.J., Hillis, R.R., S.D., Mildren, S.D., 2006b. Stress partitioning and wellbore failure in the  
1331 West Tuna Area, Gippsland Basin. *Exploration Geophysics*, 37, 215–221.
- 1332 Nelson, E.J., Chipperfield, S.T., Hillis, R.R., Gilbert, J., McGowen, J., 2007. Using geological  
1333 information to optimize fracture stimulation practices in the Cooper Basin, Australia.  
1334 *Petroleum Geoscience*, 13, 3–16.
- 1335 Norvick, M.S., Smith, M.A., 2001. Mapping the plate tectonic reconstruction of southern and  
1336 southeastern Australia and implications for petroleum systems. *Journal of the Australian*  
1337 *Petroleum Production and Exploration Association*, 41, 15–35.

- 1338 O'Brien, G.W., Heggie, D.T., Hartman, B., Bickford, G., Bishop, J.H., 1992. Light hydrocarbon  
1339 geochemistry of the Gippsland, North Bass, Bass, Otway and Stansbury Basins and the  
1340 Torquay Sub-basin, South-Eastern Australia. Bureau of Mineral Resources Record 1992/52.
- 1341 Plumb, R.A., Hickman, S.H., 1985. Stress-induced borehole enlargement: a comparison between the  
1342 four-arm dipmeter and the borehole televiewer in the Auburn geothermal well. *Journal of*  
1343 *Geophysical Research*, 90, 5513–5521.
- 1344 Reinecker, J., Tingay, M., Müller, B., 2003. Borehole breakout analysis from four-arm caliper logs.  
1345 Guidelines for interpreting stress indicators: World Stress Map online publication:  
1346 <http://www.world-stress-map.org>.
- 1347 Reynolds, S., Hillis, R.R., 2000. The in situ stress field of the Perth Basin, Australia. *Geophysical*  
1348 *Research Letters*, 27 (20), 3421-3424.
- 1349 Reynolds, S., Coblenz, D.D., Hillis, R.R., 2003a. Influences on plate-boundary forces on the  
1350 regional intraplate stress field of continental Australia, in: Hillis, R.R., Müller, R.D. (Eds.),  
1351 *Evolution and Dynamics of the Australian Plate*, Geological Society of Australia Special  
1352 *Publication 22 and Geological Society of America Special Paper 372*, pp. 53-64.
- 1353 Reynolds, S., Hillis, R.R., Paraschivoiu, E., 2003b. In situ stress field, fault reactivation and seal  
1354 integrity in the Bight Basin, South Australia. *Exploration Geophysics*, 34, 174–181.
- 1355 Reynolds, S., Mildren, S.D., Hillis, R.R., Meyer, J.J., Flottmann, T., 2005. Maximum horizontal  
1356 stress orientations in the Cooper Basin, Australia: implications for plate-scale tectonics and  
1357 local stress sources. *Geophysical Journal International*, 160, 331-343.
- 1358 Reynolds, S., Mildren, S.D., Hillis, R.R., Meyer, J.J., 2006. Constraining stress magnitudes using  
1359 petroleum exploration data in the Cooper-Eromanga Basins, Australia. *Tectonophysics*, 415,  
1360 123–140.
- 1361 Rogers, C., van Ruth, P., Hillis, R.R., 2008. Fault reactivation in the Port Campbell Embayment  
1362 with respect to carbon dioxide sequestration, Otway Basin, Australia, in: Johnson, H., Doré,  
1363 A.G., Gatliff, R.W., Holdsworth, R., Lundin, E.R., Ritchie, J.D. (Eds.), *The Nature and Origin*  
1364 *of Compression in Passive Margins*. Geological Society, London, *Special Publications*, 306,  
1365 201–214.
- 1366 Sagala, A.J.I., Tingay, M.R.P., 2012. Analysis of overpressure and its generating mechanisms in the  
1367 Northern Carnarvon Basin from drilling data. *Journal of the Australian Petroleum Production*  
1368 *and Exploration Association*, 52, 375–390.

- 1369 Sandiford, M., 2003a. Geomorphic constraints on the late Neogene tectonics of the Otway Ranges.  
1370 Australian Journal of Earth Sciences, 50, 69–80.
- 1371 Sandiford, M., 2003b. Neotectonics of south-eastern Australia: linking the Quaternary faulting  
1372 record with seismicity and in situ stress, in: Hillis, R.R. Muller, R.D. (Eds.), Evolution and  
1373 Dynamics of the Australian Plate. Geological Society of Australia, Special Publication, 22, pp.  
1374 107–119.
- 1375 Sandiford, M., Quigley, M., 2009. TOPO-OZ: Insights into the various modes of intraplate  
1376 deformation in the Australian continent. Tectonophys., 474, 405–416.
- 1377 Sandiford, M., Wallace, M., Coblenz, D.D., 2004. Origin of the in situ stress field in south-eastern  
1378 Australia. Basin Research, 16, 325–338.
- 1379 Sayers, C.M., 2010. Geophysics Under Stress: Geomechanical Applications of Seismic and Borehole  
1380 Acoustic Waves. 2010 Distinguished Instructor Short Course: Distinguished Instructor Short  
1381 Course; Sponsored by the Society of Exploration Geophysicists and European Association of  
1382 Geoscientists and Engineers.
- 1383 Schneider, C.L., Hill, K.C., Hoffman, N., 2004. Compressional growth of the Minerva Anticline,  
1384 Otway Basin, Southeast Australia-evidence of oblique rifting. Journal of the Australian  
1385 Petroleum Production and Exploration Association, 44, 463–480.
- 1386 Sharp, N.C., Wood, G.R., 2004. Casino Gas Field, offshore Otway Basin, Victoria – the appraisal  
1387 story and some stratigraphic enlightenment. in: Boulton, P.J., Johns, D.R. Lang, S.C. (Eds.),  
1388 Eastern Australasian Basins Symposium II. Petroleum Exploration Society of Australia,  
1389 Special Publication, 97-116.
- 1390 Sibson, R.H., 1974. Frictional constraints on thrust, wrench and normal faults. Nature, 249, 542–  
1391 544.
- 1392 Sibson, R.H., 1995. Selective fault reactivation during basin inversion: potential for fluid  
1393 redistribution through fault-valve action. in: Buchanan, J.G., Buchanan, P.G. (Eds.), Basin  
1394 Inversion. Geological Society, London, Special Publication, 88, pp. 3–19.
- 1395 Stein, R.S., King, G.C., Lin, J., 1992. Change in failure stress on the southern San Andreas fault  
1396 system caused by the 1992 magnitude = 7.4 Landers earthquake. Science, 258, 1328–1332.
- 1397 Tassone, D.R., Holford, S.P., Tingay, M.R.P., Tuitt, A.K., Stoker, M.S., Hillis, R.R., 2011,  
1398 Overpressures in the central Otway Basin: the result of rapid Pliocene–Recent sedimentation?  
1399 Journal of the Australian Petroleum Production and Exploration Association, 51, 439–458.

- 1400 Tassone, D.R., Holford, S.P., Hillis, R.R., Tuit, A.K., 2012. Quantifying Neogene plate-boundary  
1401 controlled uplift and deformation of the southern Australian margin, in: Healy, D., Butler,  
1402 R.W.H., Shipton, Z.K., Sibson, R.H. (Eds.), *Faulting, Fracturing and Igneous Intrusion in the*  
1403 *Earth's Crust*. Geological Society, London, Special Publications, 367, 91–110.
- 1404 Tassone, D.R., Holford, S.P., Duddy, I.R., Green, P.F., Hillis, R.R., 2014. Quantifying Cretaceous-  
1405 Cenozoic exhumation in the Otway Basin using sonic transit time data: implications for  
1406 conventional and unconventional hydrocarbon prospectivity. *American Association of*  
1407 *Petroleum Geologist Bulletin*. 98 (1), 67–117.
- 1408 Tingay, M.R.P., Hillis, R.R., Swarbrick, R.E., Okpere, E.C., 2003a. Variation in vertical stress in the  
1409 Baram Basin, Brunei: tectonic and geomechanical implications. *Marine and Petroleum*  
1410 *Geology*, 20, 1201–1212.
- 1411 Tingay, M.R.P., Hillis, R.R., Morley, C.K., Swarbrick, R.E., Okpere, E.C., 2003b. Pore  
1412 pressure/stress coupling in Brunei Darussalam – implications for shale injection. in: Van  
1413 Rensbergen, P., Hillis, R.R., Maltman, A.J., Moreley, C.K., (Eds.), *Subsurface Sediment*  
1414 *Mobilization*, Geological Society, London, Special Publications, 216, 369–379.
- 1415 Tingay, M., Müller, B., Reinecker, J., Heidbach, O., 2006. State and origin of the present-day stress  
1416 field in sedimentary basins: new results from the World Stress Map Project, in: *Golden Rocks*,  
1417 *American Rock Mechanics Association 2006 Conference*, Paper 06–1049.
- 1418 Tingay, M.R.P., Heidbach O., Davies, R., Swarbrick, R., 2008. Triggering of the Lusi mud eruption:  
1419 Earthquake versus drilling initiation. *Geology*, 36 (8), 639–642.
- 1420 Tingay, M.R.P., Morley, C.K., Laird, A., Limpornpipat, O., Krisadasima, K., Pabchanda, S.,  
1421 Macintyre, H., 2013. Evidence for overpressure generation by kerogen-to-gas maturation in the  
1422 northern Malay Basin. *American Association of Petroleum Geologist Bulletin*, 94 (4), 639–  
1423 672.
- 1424 Totterdell, J., 2012. New exploration opportunities along Australia's southern margin. *Journal of the*  
1425 *Australian Petroleum Production and Exploration Association*, 52, 29–44.
- 1426 Townend, J., Zoback, M.D., 2000. How faulting keeps the crust strong. *Geology*, 28 (5), 399–402.
- 1427 Tuit, A.K., Holford, S.P., Hillis, R.R., Underhill, J.R., Ritchie, J.D., Johnson, H., Hitchen, K.,  
1428 Stoker, M.S., Tassone, D.R., 2011. Continental margin compression: A comparison between  
1429 compression in the Otway Basin of the southern Australian margin and the Rockall-Faroe area



- 1430 in the north east Atlantic margin. *Journal of the Australian Petroleum Production and*  
1431 *Exploration Association*, 51, 241–258.
- 1432 van Ruth, P., Hillis, R.R., 2000. Estimating pore pressure in the Cooper Basin, South Australia:  
1433 sonic log method in an uplifted basin. *Exploration Geophysics*, 31, 441–447.
- 1434 Vandenberg, A.H.M., Willman, C.E., Maher, S., Simons, B.A., Cayley, R.A., Taylor, D.H., Morand,  
1435 V.J., Moore, D.H., Radojkovic, A., 2000. The Tasman Fold Belt System in Victoria,  
1436 Geological Survey of Victoria Special Publication.
- 1437 Veevers, J.J., 2000, Change of tectono-stratigraphic regime in the Australian plate during the 99 Ma  
1438 (mid-Cretaceous) and 43 Ma (mid-Eocene) swerves of the Pacific. *Geology*, 28, 1274 47–50.
- 1439 Vidal-Gilbert, S., Tenthorey, E., Dewhurst, D., Ennis-King, J., van Ruth, P., Hillis, R.R., 2010.  
1440 Geomechanical analysis of the Naylor Field, Otway Basin, Australia: Implications for CO<sub>2</sub>  
1441 injection and storage. *International Journal of Greenhouse Gas Control*, 4, 827–839.
- 1442 Wagner, D., Muller, B., Tingay, M.R.P., 2004. Correcting for tool decentralization of oriented six-  
1443 arm caliper logs for determination of contemporary tectonic stress orientations. *Petrophysics*,  
1444 45 (6), 530–539.
- 1445 Walcott, R.I., 1998. Modes of oblique compression: late Cainozoic tectonics of the South Island of  
1446 New Zealand. *Reviews of Geophysics*, 36, 1–26.
- 1447 Wallace, M.W., Dickinson, J.A., Moore, D.H., Sandiford, M., 2005. Late Neogene strandlines of  
1448 southern Victoria: a unique record of eustasy and tectonics in southeast Australia. *Australian*  
1449 *Journal of Earth Sciences*, 52, 277–295.
- 1450 Warpinski, N.R., 1989a. Elastic and viscoelastic calculations of stresses in sedimentary basins.  
1451 Society of Petroleum Engineers paper SPE 15243
- 1452 Warpinski, N.R., 1989b. Determining the minimum in situ stress from hydraulic fracturing through  
1453 Perforations. *International Journal of Rock Mechanics and Mining Sciences and*  
1454 *Geomechanics Abstracts*, 26, 6, 523–531.
- 1455 Warpinski, N.R., Teufel, L.W., 1989. In-situ stresses in low-permeability, nonmarine rocks. *Journal*  
1456 *of Petroleum Technology*, 41, 405–414.
- 1457 Warpinski, N.R., Teufel, L.W., 1991. In situ stress measurements at Rainier Mesa, Nevada Test Site  
1458 – influence of topography and lithology on the stress state in tuff. *International Journal of*  
1459 *Rock Mechanics and Mining Sciences and Geomechanics Abstracts*, 28, 2/3, 143–161.

1460 White, A., Hillis, R.R., 2004. In-situ stress field and fault reactivation in the Mutineer and Exeter  
1461 Fields, Australian North West Shelf. *Exploration Geophysics*, 35, 217–223.

1462 Yardley, G.S., Swarbrick, R.E., 2000. Lateral transfer: A source of additional overpressures? *Marine*  
1463 *and Petroleum Geology*, 17, 523–538.

1464 Zoback, M.L., 1992. First- and second-order patterns of stress in the lithosphere: the world stress  
1465 map project. *Journal of Geophysical Research*, 97, 11,703–11,728.

1466 Zoback, M.D., 2010. *Reservoir Geomechanics*. Cambridge University Press, New York.

1467 Zoback, M.D., Healy, J.H., 1984. Friction, faulting, and “in situ” stresses. *Annales Geophysicae*, 2,  
1468 689–698.

1469 Zoback, M.D., Barton, C.A., Brudy, M., Castillo, D.A., Finkbeiner, T., Grollmund, B.R., Moos,  
1470 D.B., Peska, P., Ward, C.D., Wiprut, D.J., 2003. Determination of stress orientation and  
1471 magnitude in deep wells. *International Journal of Rock Mechanics & Mining Sciences*, 40,  
1472 1049–1076.

1473

1474

## 1475 **10 Figure Captions**

1476 Fig. 1: Stratigraphy of the Otway Basin showing the depositional regimes and major tectonic stages  
1477 that caused folding and faulting (modified after Duddy, 2003 and Geary and Reid, 1998). Inset is the  
1478 suggested tectonic activity across south-eastern Australia in the last 10 Myr interpreted from  
1479 strandlines (modified after Wallace et al., 2005).

1480 Fig. 2: Topographic map of the south-eastern Australia modified after Holford et al., (2011) showing  
1481 Meso-Cenozoic basin outlines, neo-tectonic faults and structural features (after Clark et al., 2011),  
1482 the distribution of earthquakes with magnitudes ( $M_L$ ) greater than 3.5 (after Sandiford et al., 2004;  
1483 Holford et al., 2011), and modelled stress trajectories (after Reynolds et al., 2003a; Nelsen et al.,  
1484 2006a). Also shown is the interpreted extent of underlying Proterozoic Selwyn Block in central  
1485 Victoria (after Cayley, 2011)

1486 Fig. 3: Structural elements map of the Victorian Otway Basin (modified after Totterdell, 2012)  
1487 showing the distribution of wells with available wire-line formation test (WFT) data to determine  
1488 formation pore fluid pressures ( $P_P$ ); wells with bulk density, sonic velocity and/or caliper data to  
1489 estimate vertical stress ( $S_V$ ) magnitudes; wells with reported leak-off tests (LOT) to estimate  
1490 minimum horizontal stress ( $Sh_{min}$ ) magnitudes; and wells with available image log and  
1491 calliper/dipmeter data to determine the orientation of maximum horizontal stress ( $SH_{max}$ ). The  
1492 Victorian Otway Basin has been divided into the central and eastern regions at  $\sim 142.6^\circ\text{E}$  (green  
1493 line) where pronounced Neogene compressional deformation occurs and the structural trend, due  
1494 predominantly to episodic Cretaceous rifting and crustal rheological differences, changes from  
1495  $\sim\text{NW/SE}$  (western region) to  $\sim\text{E-W}$  and  $\text{NE/SW}$  (eastern region). Neogene folds after Geary and  
1496 Reid (1998), Messent et al. (1999) and Boulton et al. (2008) with the latter shown in orange for parts in  
1497 western onshore Victoria.

1498 Fig. 4: a) Schematic diagram of stress-induced wellbore failure features development when the  
1499 circumferential stress around a vertical wellbore with exceeds the compressive rock strength or is  
1500 less than the tensile rock strength, in which breakouts (BO) and drilling-induced tensile fractures  
1501 (DITFs) form, respectively (modified after Reynolds et al., 2005). DITFs form parallel to the  
1502 orientation of  $SH_{max}$  whereas BOs form orthogonal to the orientation of  $SH_{max}$  (i.e., parallel to the  
1503 orientation of  $Sh_{min}$ ). b) Example of BO observed in Henry-1ST1. c) Example of DITF observed in  
1504 Minerva-1. Note the caliper response in b) due to BOs in comparison to the lack of caliper response  
1505 in c) where DITFs were observed.

1506 Fig. 5: Wellbore failure analysis statistics calculated for the 12 wells listed in Table 1. a) The  
1507 cumulative total length of interpreted BOs and DITFs for each stratigraphic formation logged. It can  
1508 be seen that significantly more BOs were confidently interpreted than DITFs and that BOs  
1509 predominantly occurred within finer-grained rocks. In particular, the Upper Cretaceous Belfast  
1510 Mudstone (seal) in which tri-axial testing shows (inset *i*) after Bérard et al., 2008) to be much  
1511 weaker than coarser-grained rocks such as the Waarre C reservoir unit of the Upper Cretaceous  
1512 Waarre Formation (inset *ii*). b) The percentage of BOs and DITFs, with respect to the total lengths,  
1513 developed within each stratigraphic formation logged showing that the BOs formed in the Belfast  
1514 Mudstone account for more than 70% of all BOs confidently interpreted.

1515 Fig. 6: Stress-induced wellbore failure features plotted as rose diagrams weighted by a) number and  
1516 b) length in metres. c) The corresponding orientations of  $SH_{max}$  calculated as the average between  
1517 the number- and length-weighted orientations. The size of the symbols relates to the quality of the  
1518 measurement as defined by the World Stress Map (i.e., Heidbach et al., 2010). It can be seen that the  
1519  $SH_{max}$  orientations determined in this study correlate very well with previously published and  
1520 unpublished estimates (e.g., Hillis et al., 1995; Nelson et al., 2006; Bérard et al., 2008).

1521 Fig. 7: Available wireline formation test (WFT), kick, connection gas (CG) and mud weight data  
1522 (MW, or equivalent circulation density; ECD), which measures and estimates  $P_p$  magnitudes,  
1523 respectively, plotted against true vertical depth (below mudline) for a) the central Otway Basin and;  
1524 b) the eastern Otway Basin. The distribution of  $P_p$  data can be seen in Fig. 3. Included in a) is the  
1525 predicted pore pressure (PPP) for Bridgewater Bay-1 based on petrophysical wire-line log data  
1526 indicating high overpressures matching increases in mud weight possibly in excess of ~16 MPa/km  
1527 (Tassone et al., 2011).

1528 Fig. 8: a) WFT data showing  $P_p$  magnitudes plotted against true vertical depth below mudline for  
1529 wells in the Shipwreck Trough differentiated by stratigraphic formations and units. The higher  
1530 (steeper) gradient with respect to the hydrostat indicates pores are gas saturated creating  
1531 hydrocarbon (i.e., gas) column buoyancy force overpressures. It can be seen that small columns of  
1532 gas are reservoired in the Nullawarre Greensand Member, nevertheless, larger gas columns are  
1533 typically reservoired in the Thylacine Sandstone Member, Flaxman and Waarre formations. In the  
1534 top right-hand corner shows WFT data from La Bella-1 indicating 2 zones of moderate  
1535 overpressures separated by an intra-formational sealing unit characterised by a high gamma ray  
1536 response. b) and c) show top-Waarre Formation isochron maps (in milliseconds) along with  
1537 interpreted faults for the Minerva (after O'Brien et al., 2006) and Halladale/Blackwatch (after  
1538 Constantine et al., 2007) gas fields, respectively. d) WFT data from within the Flaxman and Waarre

1539 formations across faults in the Minerva (b) and Halladale/Blackwatch (c) gas fields showing that  
1540 Minera-1 and Minerva-2A wells are in pressure communication (indicative of across fault  
1541 hydrocarbon migration) whereas Halladale-1DW1 and Halladale-1DW2 wells are not in pressure  
1542 communication with overpressures in Halladale-1DW1 suggesting a sealing fault. e) WFT data from  
1543 within the Thylacine Sandstone Member, Flaxman and Waarre formations from Geographe-1,  
1544 Thylacine-1 and Thylacine South-1. Similar to the Halladale/Blackwatch Gas Field, Thylacine  
1545 South-1 well has slight overpressures in comparison to Thylacine-1 well, which are separated by a  
1546 south-dipping fault. In comparison to Geographe-1 well, water-saturated pore fluid pressures are  
1547 slightly higher, which along with (a) suggests the  $P_{ps}$  are compartmentalized across the entire  
1548 Shipwreck Trough or have varying fluid densities as a result of salinity changes. f) Interpreted  
1549 regional composite seismic profile modified after O'Brien et al., (2006) showing rift-related faulting  
1550 between Geographe-1 and Thylacine-1 wells in which there is likely pressure compartmentalization.

1551 Fig. 9:  $S_V$  magnitude data plotted against true vertical depth (below mudline) for the central (9 wells)  
1552 and eastern (15 wells) Otway Basin showing similar amounts of variation across the entire offshore  
1553 Victorian Otway Basin, in which lower (Eq. 2) and upper (Eq. 3) bounds were estimated with a  
1554 power-law magnitude-depth relationship. At 2500 m below mudline, there is ~4.66 MPa difference  
1555 between the upper and lower bounds. Also shown is the  $S_V$  magnitude-depth profile of Bellarine-1  
1556 well (after Tassone et al., 2014) located in the eastern onshore Otway Basin (see Fig. 3). Here, the  
1557 Lower Cretaceous Eumeralla Formation rocks have been exhumed (net) by more than 1800 m  
1558 (Tassone et al., 2014) that has consequently resulted in denser rocks closer to surface and a  $S_V$   
1559 magnitude-depth profile at 2000 m below mudline ~3 MPa/km greater than the upper bound to the  
1560 offshore  $S_V$  magnitudes.

1561 Fig. 10: A schematic plot of an extended leak-off test (modified after Zoback, 2010).

1562 Fig. 11: a) Available LOT data (N=89) plotted against true vertical depth below mudline  
1563 differentiated by region (central or eastern; see Fig. 3) and lithology whereby LOPs are used as  
1564 estimates of  $Sh_{min}$  magnitudes. Lithology has been generalised based on the stratigraphy (Fig. 1) as  
1565 listed in Table 4 into either marl/carbonate, sand, shale or sand/shale dominated formations. The  
1566 distribution of LOT data can be seen in Fig. 3. The best-fit linear magnitude-depth gradients for each  
1567 lithology with respect to region, as well as their corresponding range, are shown in the top right-hand  
1568 corner of a). It can be seen that marl/carbonate dominated formations have the highest gradients  
1569 followed shale dominated formations and then sand dominated formations. b) The same LOT data  
1570 differentiated only by region showing higher gradients in the eastern Otway Basin than in the central

1571 Otway Basin. While there is smaller difference in magnitude within the shallower marl and  
1572 carbonate rocks across both regions, there is more appreciable difference in siliciclastic rocks (sand  
1573 and shale dominated formations) at depths deeper than ~800 m TVDML from the central (lower  
1574 gradients) to the eastern Otway Basin (higher gradients).

1575 Fig. 12: Allowable regions diagrams as a ratio to  $S_V$  magnitude whereby the upper limits to  $SH_{max}$   
1576 gradients are constrained by frictional limit theory (after Moos and Zoback, 1990). In overpressured  
1577 conditions, the upper to  $SH_{max}$  gradient would decrease that it would otherwise be for the same  
1578 depth. N-F: normal fault stress regime, SS-F: strike-slip fault stress regime, R-F: reverse fault stress  
1579 regime.

1580 Fig. 13: *In situ* stress summary of stress gradients estimated using petroleum exploration data in a)  
1581 the central and b) the eastern Otway Basin. It can be seen that LOT data in shallow marl/carbonate  
1582 dominated formations in both a) and b) have LOPs generally equal to or greater than  $S_V$  magnitudes  
1583 at the equivalent depth, suggesting a strike-slip to reverse *in-situ* faulting stress regime. Furthermore,  
1584 LOT data in the central Otway Basin (a) define lower  $Sh_{min}$  gradients within siliciclastic rocks (i.e.,  
1585 sand and shale dominated formations) in comparison the eastern Otway Basin (b) by ~1-2 MPa/km.  
1586 This may suggest a normal to strike-slip *in-situ* fault stress regime in the central Otway Basin and  
1587 possible either a normal, strike-slip or strike-slip to reverse *in-situ* fault stress regime in the eastern  
1588 Otway Basin within these deeper rocks.

1589 Fig. 14: a) Published focal mechanism solutions —for earthquakes occurring in southeastern  
1590 Australian with magnitudes ranging between  $M_L = 3.2$  and 5.4 at depths between 5-21 km (Denham  
1591 et al., 1981, 1985; Bock and Denham, 1983; McCue et al., 1990; McCue and Paull, 1991; Leonard et  
1592 al., 2002; Allen et al., 2005; Nelson et al., 2006a; Clark, 2009) superimposed over Palaeozoic  
1593 basement discontinuities identified from field mapping and geophysical datasets including magnetic,  
1594 radiometric, gravity and seismic (Messent et al., 1999; Vandenberg et al., 2000). Also shown are  
1595 estimates of  $SH_{max}$  orientations derived from wellbore failure analyses (this study; Nelson et al.,  
1596 2006a; Bérard et al., 2008; unpublished) and modelled stress trajectories (after Reynolds et al.,  
1597 2003a). The focal mechanism solution numbers correspond to those listed Table 5. It can be seen  
1598 that these focal mechanism solutions are located close to Palaeozoic basement discontinuities and  
1599 their P-axes are broadly NW/SE similar to wellbore failure features observed in petroleum  
1600 exploration data and modelled stress trajectories. Furthermore, they indicate either reverse and/or  
1601 strike-slip faulting regimes. b) Mapping of Pliocene-Holocene volcano alignments (i.e., Newer  
1602 Volcanics) in western Victoria (after Lesti et al., 2008) showing , that the dominant NW/SE trend  
1603 probably reflects the opening (or reopening) of deep fractures favourably oriented parallel to the

1604  $SH_{max}$  orientation (as determined from wellbore failure features and focal mechanisms) while the  
1605 N/S and E/W trends probably reflect reactivated Palaeozoic discontinuities (Lesti et al., 2008).

1606 Fig. 15: Interpreted seismic profile O40-21, perpendicular to the fold axes of the Nerita Anticline in  
1607 the Torquay sub-basin (modified after Messent et al., 1999; Holford et al., 2014). The Nerita  
1608 Anticline is interpreted as an inversion structure with erosional truncation (black arrows) at the late  
1609 Miocene-early Pliocene unconformity, which dips away from the anticlinal crest perhaps suggesting  
1610 neo-tectonic deformation.

1611 Fig. 16: Topographic map of the Colac Trough and Otway Ranges (after Constantine and Liberman,  
1612 2001) showing neotectonic features (e.g., faults, anticlines and monoclines), some with estimated  
1613 slip/deformation rates (Clark et al., 2011). Also illustrated are isochrons (two-way time in seconds)  
1614 of the intra-Oligocene unconformable surface mapped in the Shipwreck Trough and Prawn Platform  
1615 (i.e., base-Heytesbury Group; Geary and Reid, 1998) as well as in the Torquay sub-basin (i.e., base-  
1616 Torquay Group; after Holford et al., 2011) showing the similar trend in late Miocene-early Pliocene  
1617 structural features. Green line represents location of seismic profile O40-21 in Fig. 15. Also shown  
1618 are suspected light hydrocarbon seeps interpreted to be derived from a gas/condensate or dry  
1619 thermogenic gas 'source' (after Bishop et al., 1992; Messent et al., 1999) and earthquakes (after  
1620 Sandiford et al., 2004; Holford et al., 2011), with Seep 1 apparently associated with a sea-bed  
1621 pockmark (O'Brien et al., 1993).

1622 Fig. 17: Evidence of post-rift reverse faulting near the Otway Ranges. Small apparent low-angle  
1623 fault with reverse sense is observed in the mid to upper Miocene Port Campbell Limestone cliffs at  
1624 the Twelve Apostles site in the Port Campbell National Park (see Fig. 16 for location). The fault  
1625 slightly displaces the top of the cliff (i.e., late Miocene-early Pliocene unconformity) indicating fault  
1626 must have formed in the past ~5-10 Myr. Photographer is facing ~N-NE suggesting the fault dips  
1627 apparently broadly towards ~E-SE-S, near-parallel to the regional  $SH_{max}$  orientation. Cliff face is  
1628 approximately ~40 m high and people at the top of the cliff can be used for scale.

1629 Fig. 18: a) Surface geology map of the Port Campbell Embayment and northwestern margin of the  
1630 Otway Ranges (after Edwards et al. 1996) and isochrons (two-way time in seconds) of the intra-  
1631 Oligocene unconformable surface (i.e., base-Heytesbury Group) mapped in the Shipwreck Trough,  
1632 Mussel and Prawn platforms (Geary and Reid, 1998). Superimposed are the axes of offshore  
1633 Neogene folds (after Geary and Reid, 1998) that can be correlated to onshore neotectonic features  
1634 (Clark et al., 2011). Note that Ferguson Hill Anticline has Paleocene rocks outcropping surrounded  
1635 by upper Oligocene to upper Miocene rocks potentially suggesting appreciable amounts of Neogene

1636 erosion. b) Interpreted seismic profile OH91-113, perpendicular to the fold axis of low-amplitude  
1637 Neogene anticlines that plunge towards the SW within wavelengths of ~15-25 km (after Geary and  
1638 Reid, 1998; Holford et al., 2014). Black arrows indicate erosional truncation of strata beneath the  
1639 late Miocene-early Pliocene unconformity (MPU).

1640 Fig. 19 a) Neotectonic faults (after Clark et al., 2011) in Paleozoic basement rocks (red) and Meso-  
1641 Cenozoic basins (green) superimposed over Palaeozoic basement discontinuities identified from  
1642 field mapping and geophysical datasets (Messent et al., 1999; Vandenberg et al., 2000) showing a  
1643 clear relationship with the trends of neotectonic faults and underlying basement discontinuities. This  
1644 would suggest that the basement faults have a strong control with the locus of neotectonic  
1645 deformation in the Meso-Cenozoic passive margin sedimentary basins. Also shown is the interpreted  
1646 extent of underlying Proterozoic Selwyn Block in central Victoria (after Cayley, 2011). b)  
1647 Interpreted pre-Permian basement terranes (after Vandenberg et al., 2000) showing that neotectonic  
1648 deformation in the eastern onshore region occurs in the vicinity of the north-western boundary of the  
1649 Selwyn Block.

1650 Fig. 20: *In-situ* stress constraints for the shallow post-rift marl and carbonate dominated formations  
1651 of the Heytesbury and Nirranda groups. A reverse *in-situ* stress regime has been interpreted based on  
1652 petroleum exploration data and geological observations, thus, the minimum principle stress is  
1653 vertical (i.e.,  $S_3 = S_V$ ) and the amount by which  $S_{H_{min}}$  exceeds  $S_V$  is indeterminable. The upper limit  
1654 gradients of  $S_{H_{max}}$  are, therefore, calculated using Eq. (13) whereby  $S_3$  is either  $S_{V_{Lower}}$  or  $S_{V_{Upper}}$ .  
1655 Towards the shelf-break these constraints may be applicable to depths >1500 m TVDML (e.g., in  
1656 Triton-1ST1 well), nevertheless, it is generally for depths shallower than ~800-1000 m TVDML.  
1657  $S_{H_{max}}$  gradients are calculated to be ~40.6-46.5 MPa/km at 1000 m TVDML for  $S_{V_{Lower}}$  or  $S_{V_{Upper}}$ ,  
1658 respectively, for hydrostatic conditions.

1659 Fig. 21: A summary of regional *in-situ* stresses constrained from petroleum exploration data  
1660 integrated with geological observations that incorporate underlying structural trends across the basin,  
1661 mode of deformation with depth and lithology at larger-scale. Post-rift shallow Oligocene to  
1662 Miocene marl and carbonate dominated formations are folded (more ductile) with little evidence of  
1663 pre-existing planes of weakness and have high horizontal stresses indicative of a reverse *in-situ* fault  
1664 stress regime. In contrast, deeper syn-rift siliciclastic rocks are heavily faulted (many pre-existing  
1665 planes of weakness) and have lower horizontal stresses indicative of a strike-slip *in-situ* fault stress  
1666 regime. There is also an increase in horizontal stresses from the central Otway Basin where faults  
1667 typically strike ~NW/SE to the eastern Otway Basin where faults typically strike ~NE/SW.  
1668 Horizontal stress orientations are similar across both regions, are uniform over the entire basin



1669 sedimentary in-fill (excluding local stresses near faults) and agree well under focal mechanism  
1670 solutions that sample basement stresses, which also indicate reverse and strike-slip faulting  
1671 movements.

1672 Fig. 22: a) Generic *in-situ* stress magnitude constraints for deeper siliciclastic lithology rocks in the  
1673 central region with the upper limit gradients of  $SH_{max}$  calculated using frictional limit theory (Jaeger  
1674 and Cook, 1979) for  $S_3 = Sh_{min}$ , hydrostatic pressures and  $\mu=0.6$ . b) Generic *in-situ* stress gradient  
1675 constraints for deeper siliciclastic formations in the eastern Otway Basin with the upper limit  
1676 gradient of  $SH_{max}$  calculated using frictional limit theory (Jaeger and Cook, 1979) and the method of  
1677 Couzens-Schultz and Chan (2010) that assumes LOPs represent shear failure of a pre-existing plane  
1678 of weakness. Frictional limit theory uses  $S_3 = Sh_{min}$ ,  $S_3 = S_{V\_Upper}$ , hydrostatic pressures and  $\mu=0.6$ . c)  
1679 Allowable regions diagram (Moos and Zoback, 1990) illustrating how the method Couzens-Schultz  
1680 and Chan (2010) allows for the possibility of a reverse *in-situ* stress regime in comparison to the  
1681 traditional method of frictional limit theory when LOTs are interpreted to leak-off due to shear  
1682 failure along a plane of pre-existing weakness rather than tensile failure. d) Plot of  $Sh_{min}$  gradient  
1683 against the difference between the ratios of  $SH_{max}$  and  $S_V$  magnitudes calculated using frictional limit  
1684 theory and the method of Couzens-Schultz and Chan (2010). For  $Sh_{min}$  gradients within ~23.5 % of  
1685  $S_V$  magnitudes at the equivalent depth, then the method of Couzens-Schultz and Chan (2010) will  
1686 tend to decrease differential and mean stresses (within a strike-slip regime) in comparison to  
1687 frictional limit theory constraints (Jaeger and Cook, 1979), and vice versa.

1688

1689 **11 Tables**

1690 **Table 1: Victorian Otway Basin wells with image log and dipmeter data available for this study to constrain**  
 1691 **maximum horizontal stress ( $SH_{max}$ ) orientations. Listed are tool types, maximum well deviations encountered over**  
 1692 **corresponding depth ranges and stratigraphy in which was logged.**

Well	Tool Type*	Bit Size (In)	Max DEVI (°)	Data Depth Range <sup>#</sup>			Images
				Top (m bKB)	Bottom (m bKB)	Interval (m)	
Bellarine-1	FMI	8.5	1.00	278	978	700	Tertiary/ Eumeralla/Pretty Hill?
Bridgewater Bay-1	HDT	17.5	1.23	487	1607	1120	Heytesbury/Nirranda/Wangerrip/Timboon/Paaratte Timboon/Paaratte/Belfast Belfast/Flaxman/Waarre
		12.25	1.25	1586	3536	1950	
		8.5	1.25	3850	4183	333	
Conan-1	FMI	12.25	0.40	1675	1949	274	Belfast/Flaxman/Waarre/Eumeralla
Halladale-1DW1	STAR	8.5	20.54	775	1916	1141	Pember/Pebble Point/Massacre/Paaratte/Skull Creek/Nullawarre/Belfast/Flaxman/Waarre/Eumeralla
Halladale-1DW2	STAR	8.5	21.72	1668	1927	259	Belfast/Flaxman/Waarre/Eumeralla
Henry-1ST1	STAR	8.5	1.00	1725	2015	290	Skull Creek/Waarre/Eumeralla
Minerva-1	FMS	8.5	8.80	1189	2024	835	Belfast/Flaxman/Waarre Waarre/Eumeralla
		6.0	9.00	2110	2424	314	
Minerva-2A	FMS	12.25	3.90	1526	2170	644	Belfast/Flaxman/Waarre
Thylacine-1	FMI	8.5	2.97	2022	2503	481	Belfast/Flaxman/Waarre
Thylacine-2	FMI	8.5	3.51	2104	2530	426	?/Flaxman/Waarre ?/Flaxman/Waarre
			1.25	2245	2350	105	
Wild Dog-1	SED	8.5	1.07	724	1244	500	Torquay/Demons Bluff/Eastern View/Eumeralla
Wild Dog Road-1	FMI	8.5	34.5	1200	1676	476	Skull Creek/Nullawarre/Belfast/Waarre

1693 \* STAR – Baker Atlas SimulTaneous Acoustic and Resistivity Imager<sup>TM</sup>; FMI – Schlumberger Formation MicroImager; FMS – Formation  
 1694 MicroScanner; HDT – Schlumberger High Resolution Dipmeter tool (4-arm); SED<sup>TM</sup> – Halliburton Six-Arm Dipmeter tool.

1695

1696 **Table 2: Wellbore failure analysis of image log data showing the mean orientations of BO and DITF failure**  
 1697 **features and their corresponding standard deviations (i.e., circular statistics of Mardia, 1972) when weighted by**  
 1698 **number ( $N$ ) and length in metres. Also listed is the corresponding orientation of  $SH_{max}$  (average of number- and**  
 1699 **length-weighted estimates) and World Stress Map (WSM) quality rating after Heidnach et al. (2010).**

Well	Indicator	Number-Weighted			Length-Weighted			$SH_{max}$ Orientation ( $^{\circ}T$ )	WSM Quality Rating
		$N$	mean BO / DITF Orientation ( $^{\circ}T$ )	SD ( $^{\circ}$ )	Length (m)	mean BO / DITF Orientation ( $^{\circ}T$ )	SD ( $^{\circ}$ )		
Bellarine-1	BO	4	47.2	3.81	3.69	46.9	2.77	137.1	D
Bellarine-1	DITF	55	143.6	11.68	67.94	144.6	11.18	144.1	B
Bellarine-1	DITF_INC	40	237.5	17.55	-	-	-	147.5	-
Conan-1	BO	32	40.8	6.88	58.06	44.6	5.95	132.7	B
Halladale-1DW1	BO	20	34.3	3.91	194.41	35.3	2.98	124.5	A
Halladale-1DW1	DITF	2	123.3	2.06	2.43	122.6	2.03	123.0	D
Halladale-1DW2	BO	18	43.0	7.74	78.57	41.5	6.73	132.3	B
Henry-1ST1	BO	23	38.0	5.36	107.24	40.5	2.63	129.3	A
Minerva-1	BO	14	51.9	5.01	554.27	53.2	1.74	142.6	A
Minerva-1	DITF	7	131.3	7.45	36.52	131.5	7.80	131.4	C
Minerva-2A	BO	4	51.2	2.09	280.32	52.8	0.46	141.0	C
Minerva-2A	DITF	5	138.1	2.43	6.44	138.0	2.56	138.1	D
Thylacine-1	BO	3	42.2	4.49	3.67	40.8	4.64	131.5	D
Thylacine-2	BO	15	42.3	9.45	7.89	46.2	9.62	134.3	D
Wild Dog Road-1	BO	22	51.5	3.26	187.90	48.9	5.30	140.2	A
Wild Dog Road-1	DITF_INC	18	132.4	18.14	-	-	-	132.4	-

1700

1701

1702 **Table 3: Wellbore failure analysis of caliper/dipmeter data showing the mean orientations of BO failure features**  
 1703 **and their corresponding standard deviations (i.e., circular statistics of Mardia, 1972) when weighted by number**  
 1704 **( $N$ ) and length in metres. Also listed is the corresponding orientation of  $SH_{max}$  (average of number- and length-**  
 1705 **weighted estimates) and World Stress Map (WSM) quality rating after Heidbach et al. (2010).**

Well	Tool	Indicator	Number-Weighted			Length-Weighted			$SH_{max}$ Orientation ( $^{\circ}T$ )	WSM Quality Rating
			$N$	mean BO Orientation ( $^{\circ}T$ )	SD ( $^{\circ}$ )	Length	mean BO Orientation ( $^{\circ}T$ )	SD ( $^{\circ}$ )		
Bridgewater Bay-1	HDT	BO	15	49.0	10.51	486.00	52.2	8.04	140.6	A
Wild Dog-1	HMS	BO	3	57.7	16.60	19.46	60.6	15.30	149.1	D

1706

1707

1708  
1709  
1710  
1711  
1712

**Table 4: Best-fit  $Sh_{min}$  gradients differentiated by lithology and region derived from LOT data assuming LOPs were caused by tensile failure. Also listed is the number of data points ( $N$ ), range of values from the best-fit  $Sh_{min}$  gradient derived from the lower and upper limits, respectively, and coefficient of determination ( $R^2$ ).  $Sh_{min}$  gradients in MPa/km with depth referenced to the mudline. Lithology classifications are based on general characteristics of stratigraphic formations and groups.**

Lithology	Formation/Group	Region	Best-fit $Sh_{min}$ Magnitude Gradient (MPa/km)	$N$	- (MPa/km)	+ (MPa/km)	$R^2$	Eq.
Marl/ carbonate	Whales Bluff Formation/Port Campbell Limestone Gellibrand Marl/Jan Juc Formation/Puebla Formation/Narrawaturk Marl/undiff. Heytesbury Group/undiff. Nirranda Group	eastern	$Sh_{min\_Marl / carbonate\_East} \approx 21.19 \times Z$	36	5.40	7.09	0.7947	(5)
		central	$Sh_{min\_Marl / carbonate\_West} \approx 20.32 \times Z$	11	6.52	3.48	0.8059	(6)
Sand	Mepunga Formation/Dilwyn Formation/ Pebble Point Formation/Timboon Sandstone/Paaratte Formation	eastern	$Sh_{min\_Sand\_East} \approx 17.01 \times Z$	6	4.04	2.73	0.7441	(7)
		central	$Sh_{min\_Sand\_West} \approx 15.93 \times Z$	13	3.09	3.83	0.9094	(8)
Shale	Clifton Formation /Pember Mudstone/Belfast Mudstone/Laira Formation	eastern	$Sh_{min\_Shale\_East} \approx 20.89 \times Z$	9	7.88	0.48	0.9275	(9)
		central	$Sh_{min\_Shale\_West} \approx 18.79 \times Z$	6	2.54	1.64	0.9599	(10)
Sand/shale	Eumeralla Formation /Wangerrip Group/Sherbrook Group	eastern	$Sh_{min\_Sand / Shale\_East} \approx 19.30 \times Z$	5	1.45	1.15	0.9829	(11)
		central	$Sh_{min\_Sand / Shale\_West} \approx 15.37 \times Z$	5	2.25	0.81	0.9938	(11)

1713

1714

1715 **Table 5: Published focal mechanism solutions for earthquakes in southeastern Australia. Listed are their**  
 1716 **corresponding date, location, magnitude, depth, axis of compression (P-axis  $\equiv SH_{max}$  orientation), interpreted**  
 1717 **stress regime, World Stress Map (WSM) quality rating after Zoback (1992) and publication reference.**

Location	Date	Lat. ( $^{\circ}S$ )	Long ( $^{\circ}E$ )	$M_L$	Depth ( $km$ )	P-Axis ( $^{\circ}T$ )	Stress Regime	$N$ in Fig. 14a	WSM Quality	Reference
Berridale	18-May-59	-36.22	148.64	5.2	15	327	TF	15	D	Denham et al., 1981; Leonard et al., 2002
Mt Hotham	3-May-66	-37.042	147.158	5.5	15	219	NF	11	B	Denham et al., 1985; Leonard et al., 2002
Middlingbank	21-Jun-71	-36.22	148.78	4	5	136	SS	16	??	Bock and Denham, 1983; Leonard et al., 2002
Murrumbateman	6-May-74	-35.06	149.02	3.8	5	271	SS/TR	17	D	Denham et al., 1981; Leonard et al., 2002; Nelson et al., 2006a
The Pilot	8-Sep-76	-36.72	148.24	3.8	6	326	TF	13	D	Bock and Denham, 1983; Leonard et al., 2002
Balliang	2-Dec-77	-37.88	144.27	4.2	21	292	TF	2a	??	Denham et al., 1981; Leonard et al., 2002
						286	SS	2b	??	Denham et al., 1981; Leonard et al., 2002
Suggan Buggan	30-Nov-81	-36.09	148.33	3.7	7	95	SS	14	D	Bock and Denham, 1983; Leonard et al., 2002
Woonangatta	21-Nov-82	-37.205	146.956	5.4	17	113	TF	10	B	Denham et al., 1985; Leonard et al., 2002; Nelson et al., 2006a
Nhill	22-Dec-87	-36.107	141.539	4.9	6	264	SS/NF	1a	B	McCue et al., 1990; Leonard et al., 2002; Nelson et al., 2006a
						136	TF	1b	B	Denham et al., 1981; Leonard et al., 2002
Bunnaloo	3-Jul-88	-35.73	144.49	4	10	118	SS	3	C	McCue and Paull, 1991; Leonard et al., 2002
Thomson Reservoir	25-Sept-96	-37.863	146.422	5	11	141	TF	9	C	Allen et al., 2005
Tatong	27-Jun-97	-36.781	146.094	4.2	6	354.2	TF	6	C	Allen et al., 2005; Nelson et al., 2006a
Corryong	17-Jul-98	-36.441	148.005	4.7	20	332.2	SS	12	C	Allen et al., 2005; Nelson et al., 2006a
Boolarra South	29-Aug-00	-38.402	146.245	4.7	15	322	TF	7	D	Allen et al., 2005
Dumbalk	30-Oct-00	-38.56	146.05	3.2	16	161	SS	4	D	Leonard et al., 2002
Boolarra South	4-Jul-01	-38.74	146.34	3.4	7	286	SS	8	D	Leonard et al., 2002
Korumburra	24-Apr-09	??	??	4.6	8	??	SS	5	??	Clark, 2009

1718

Figure 1

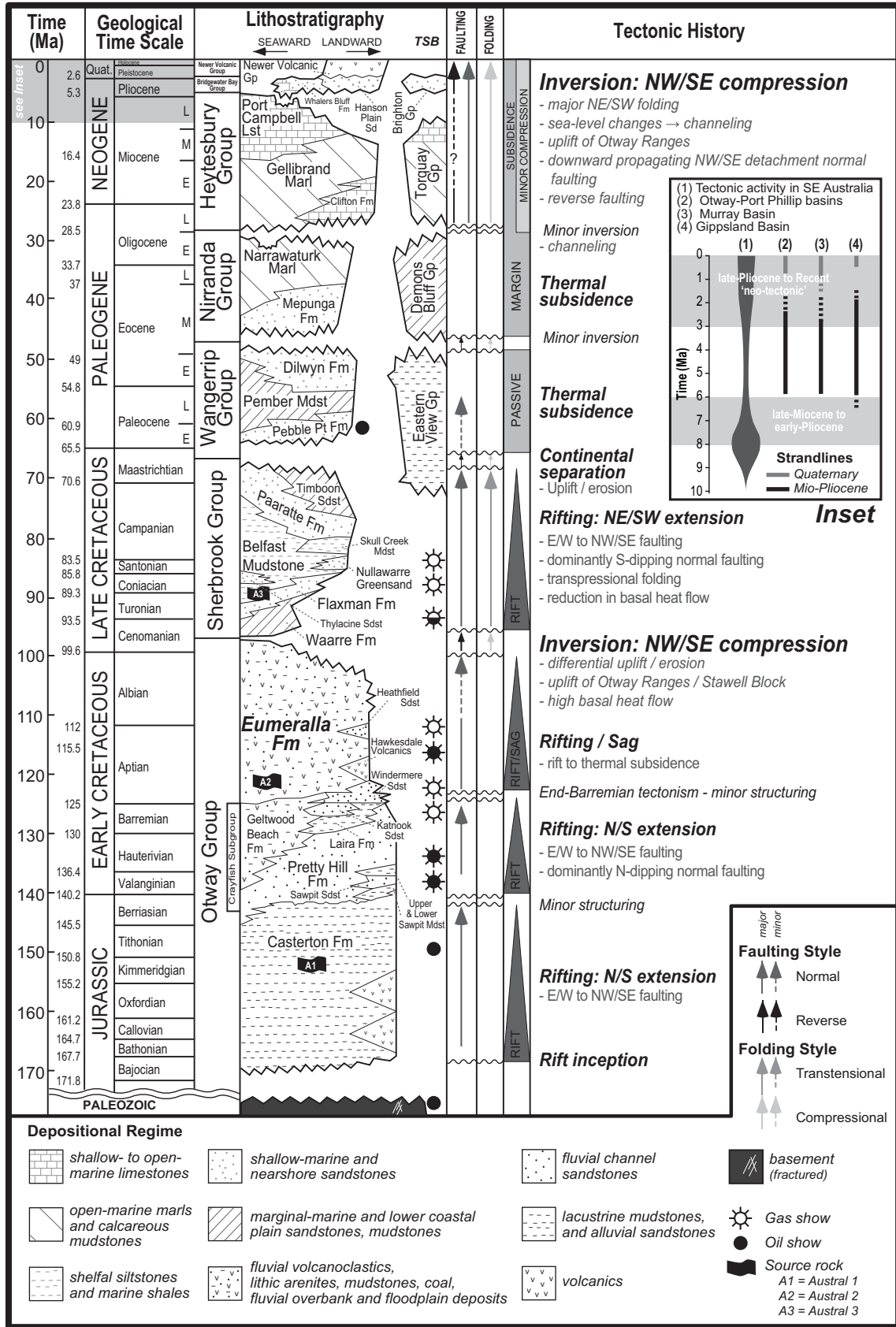


Figure 2

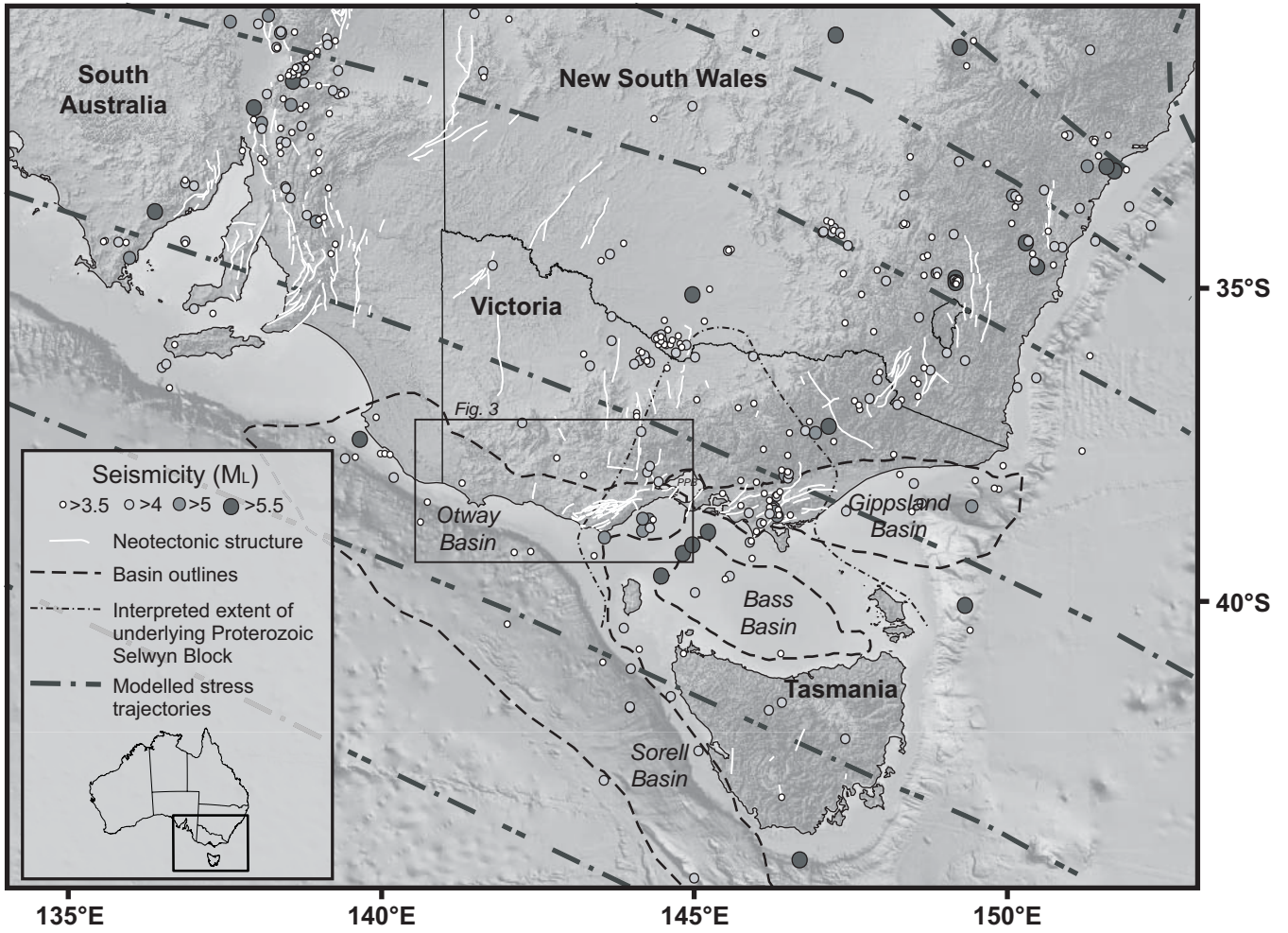
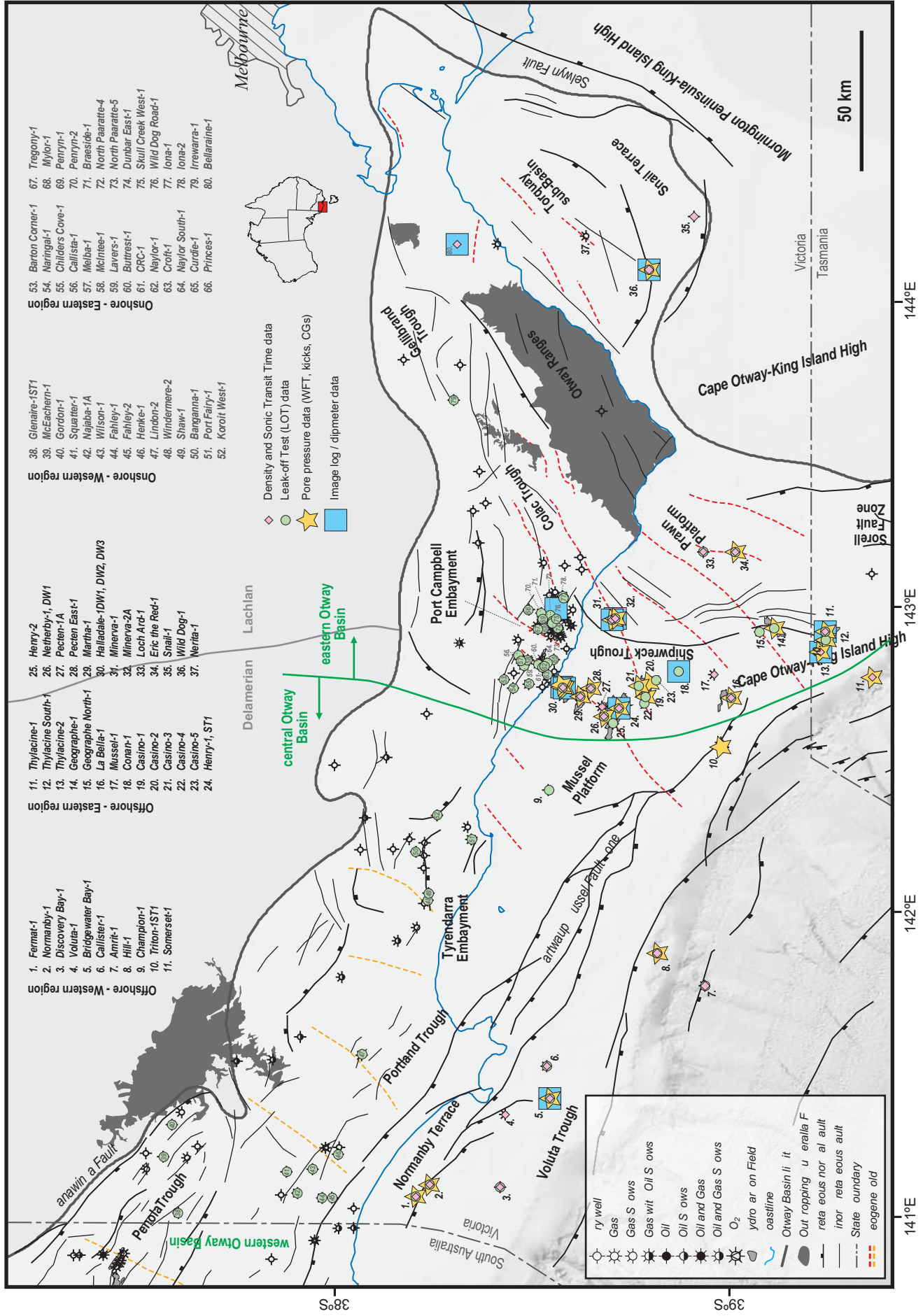
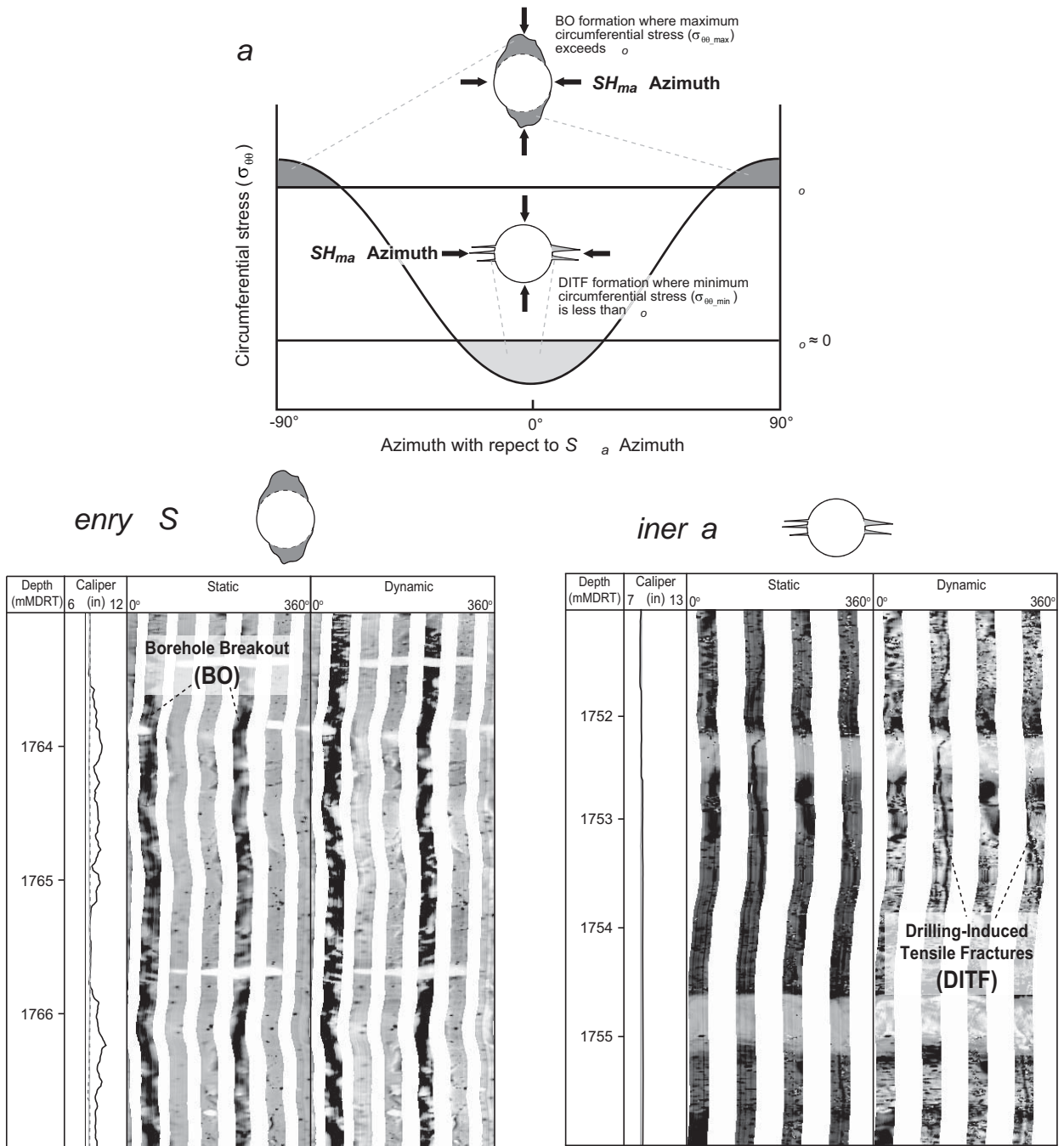


Figure 3

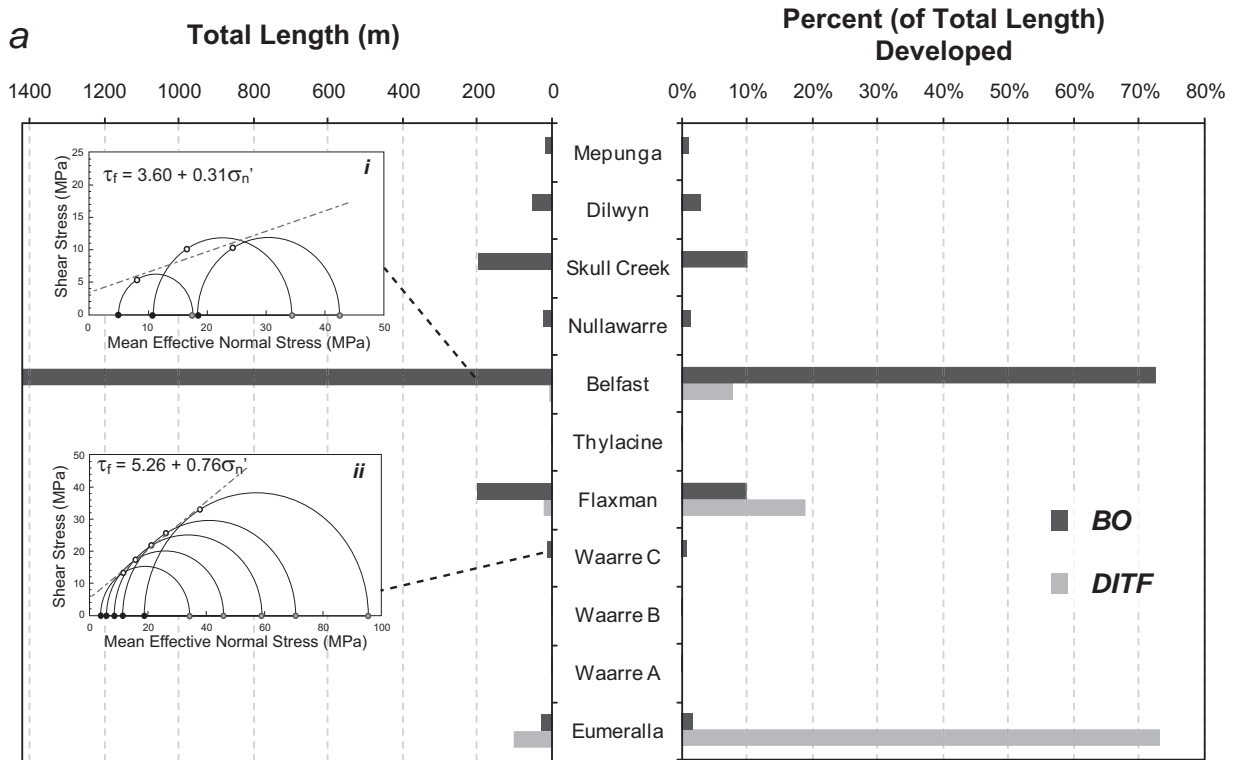




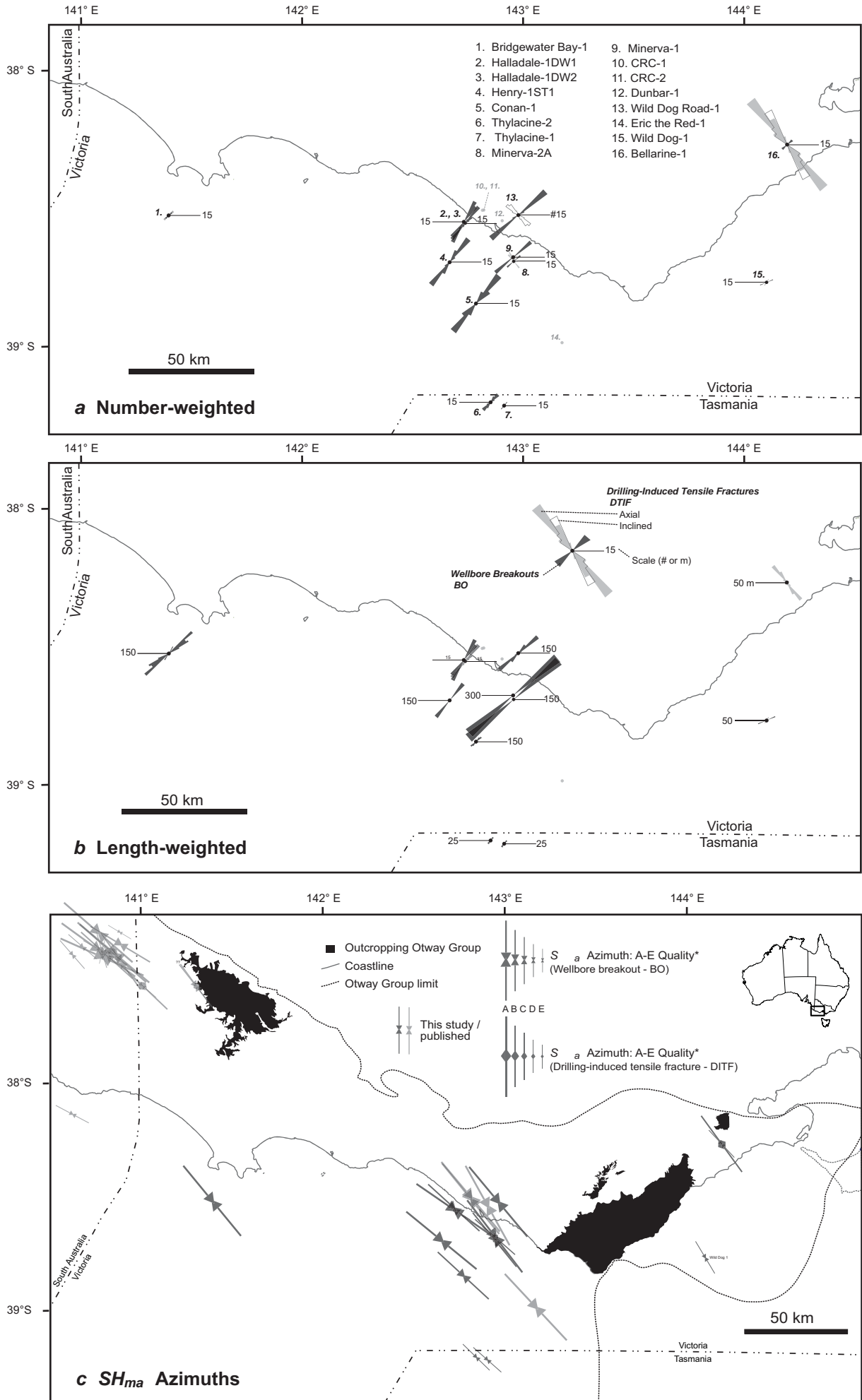
Figure



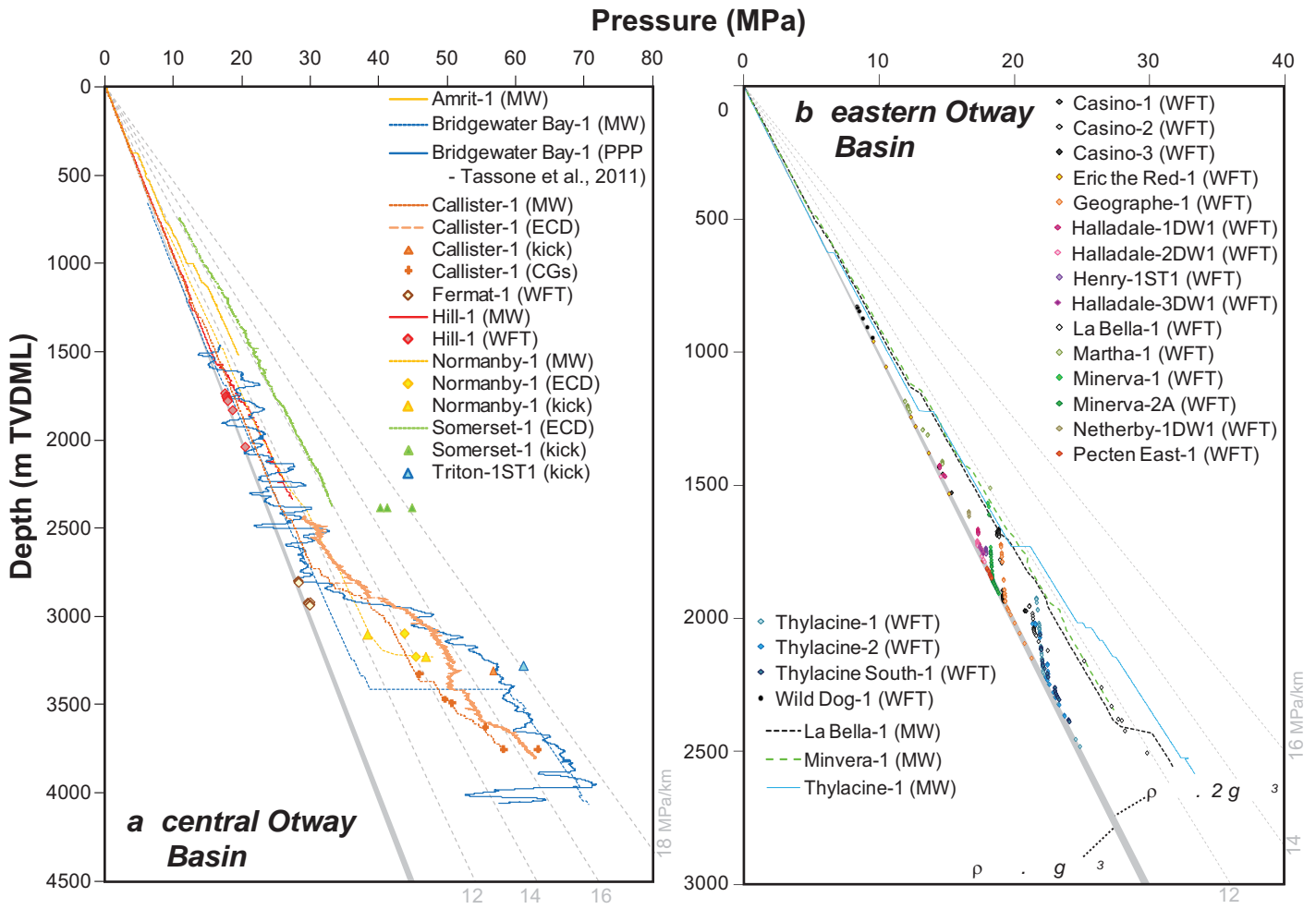
Figure



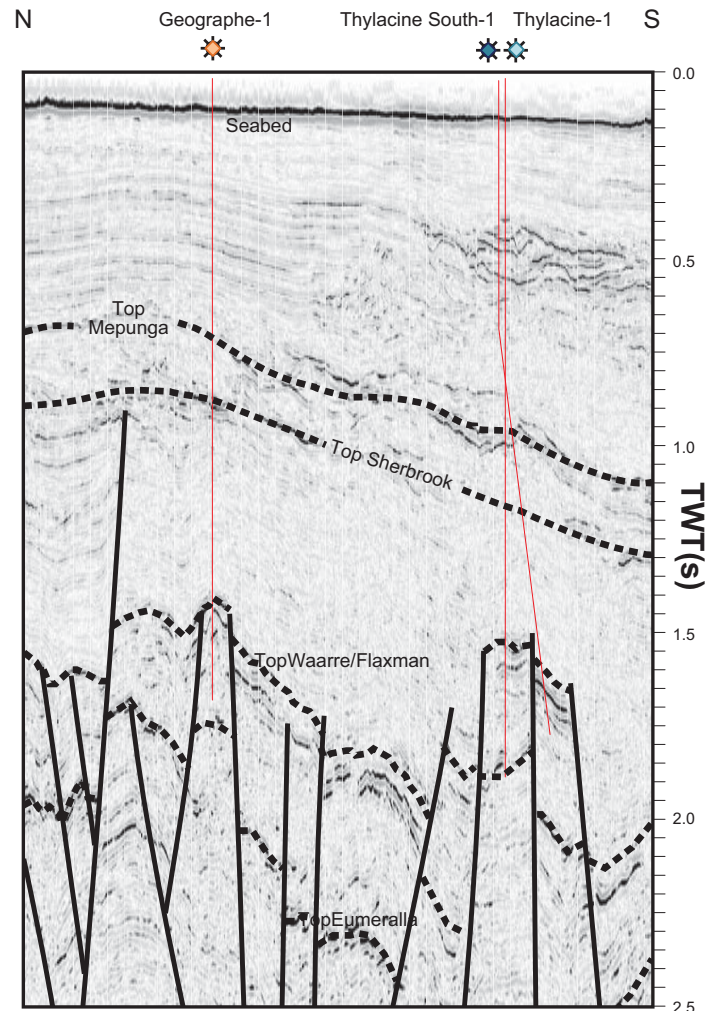
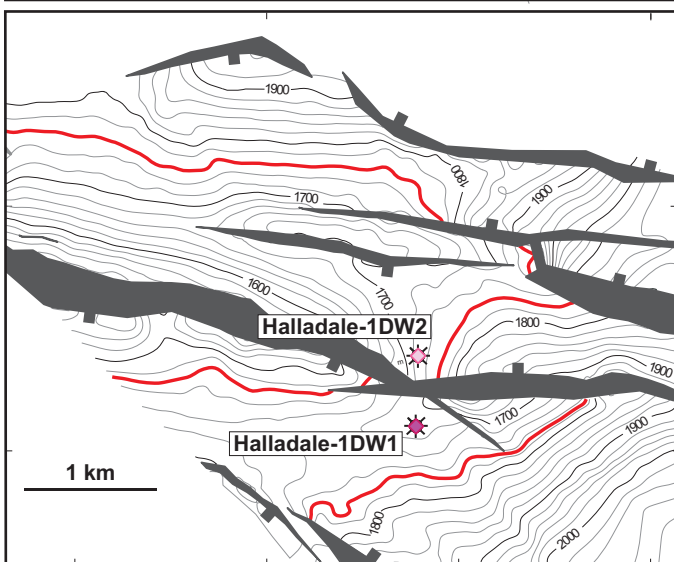
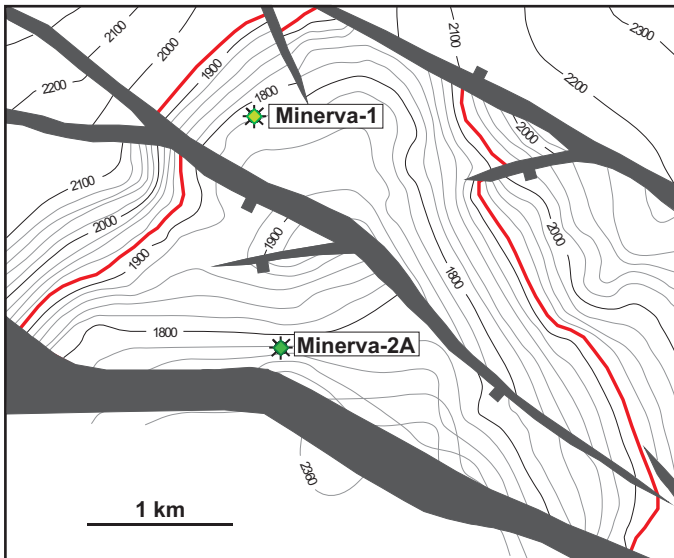
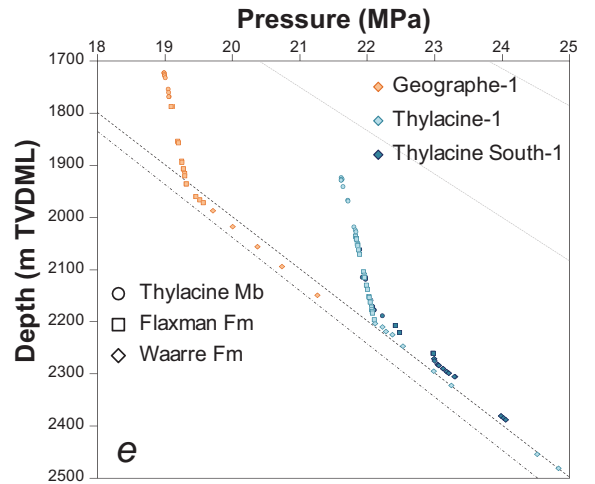
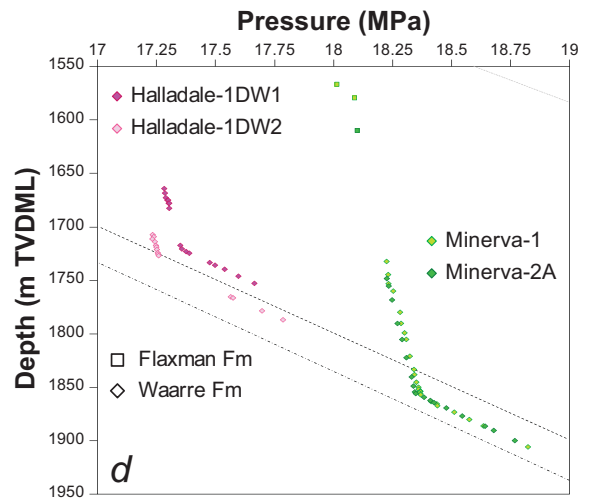
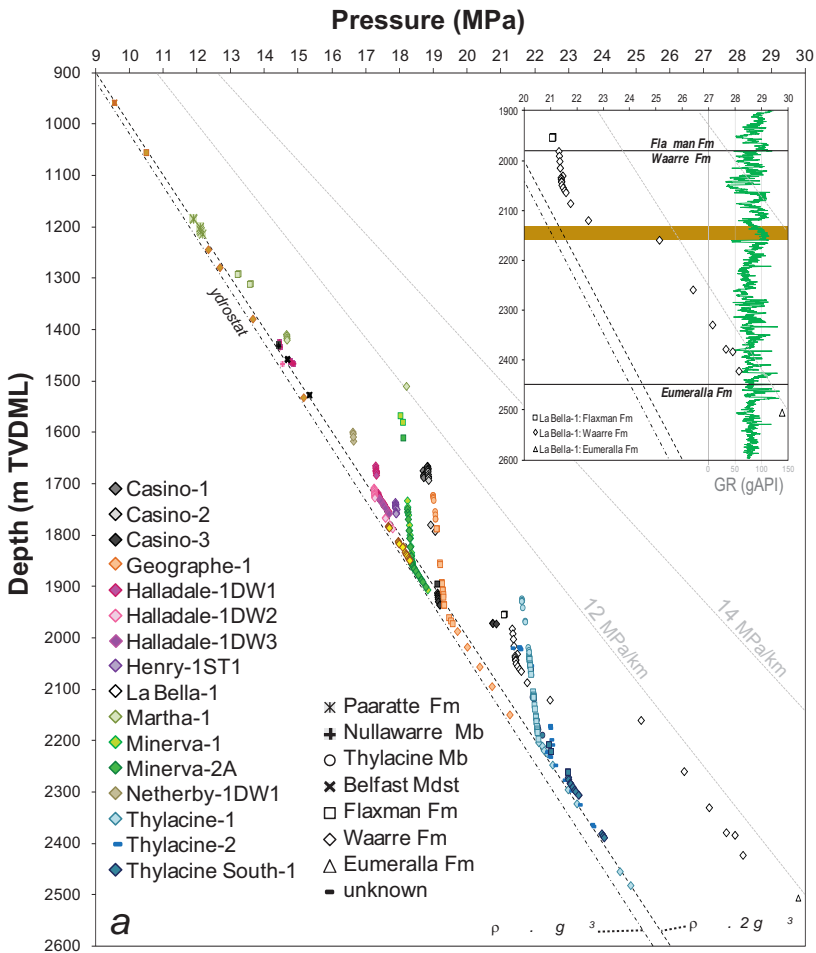
Figure



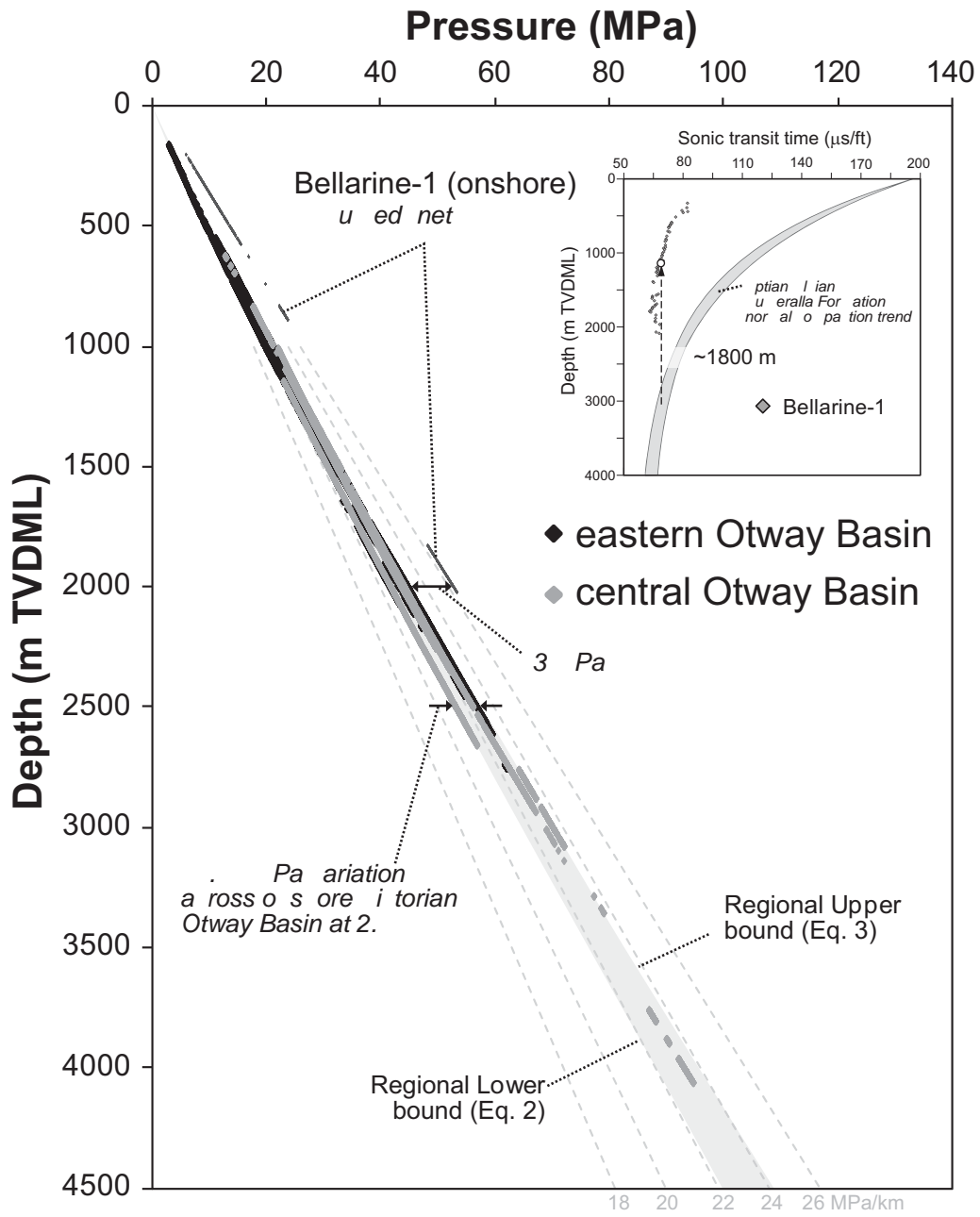
Figure



Figure



Figure



Figure

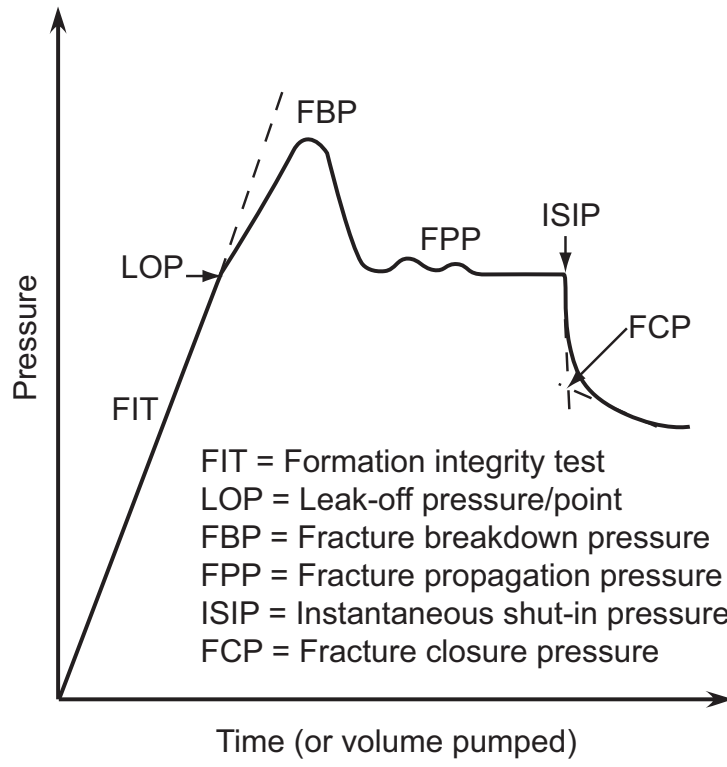






Figure 2

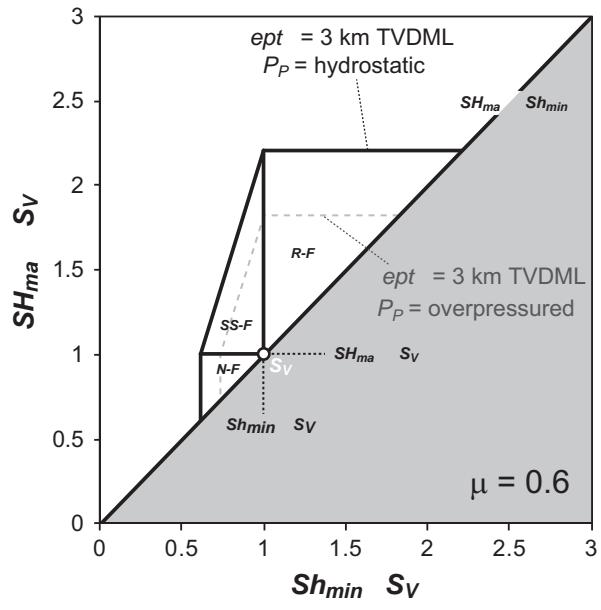
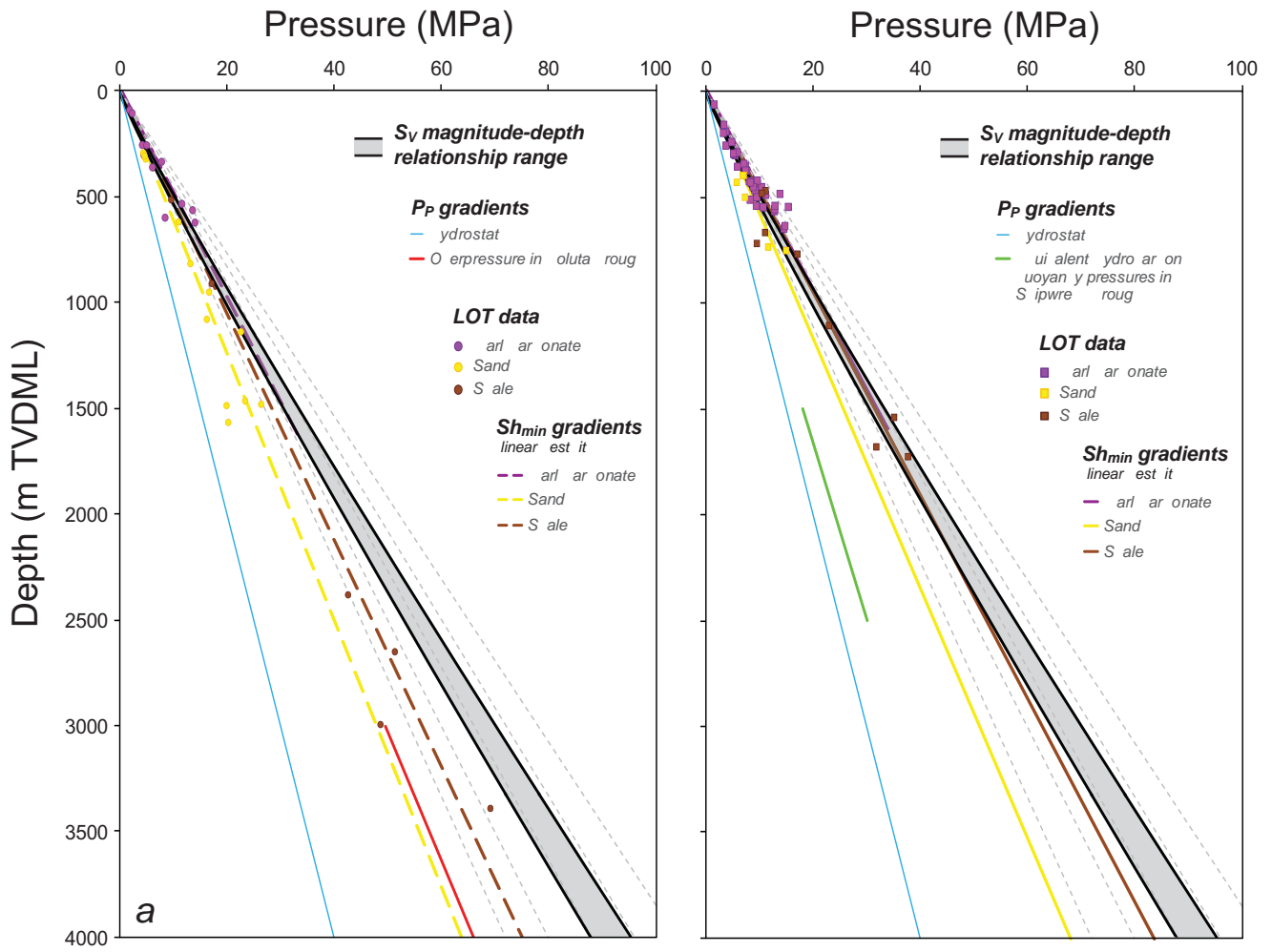
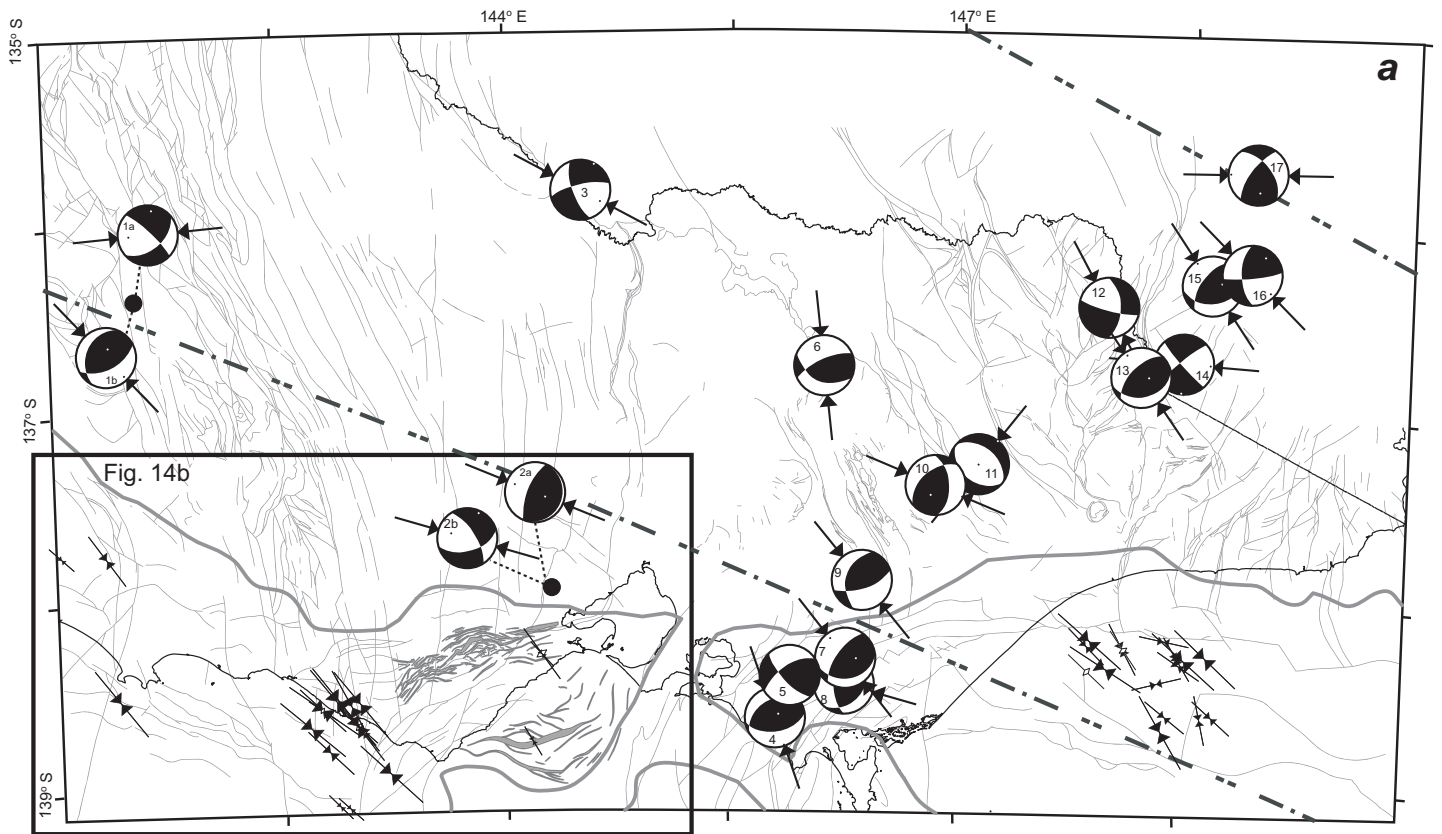










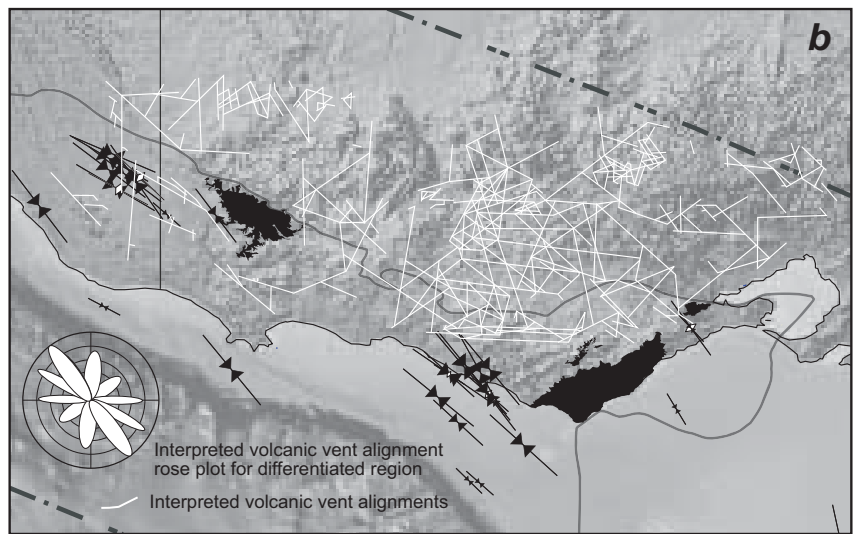
Figure 3



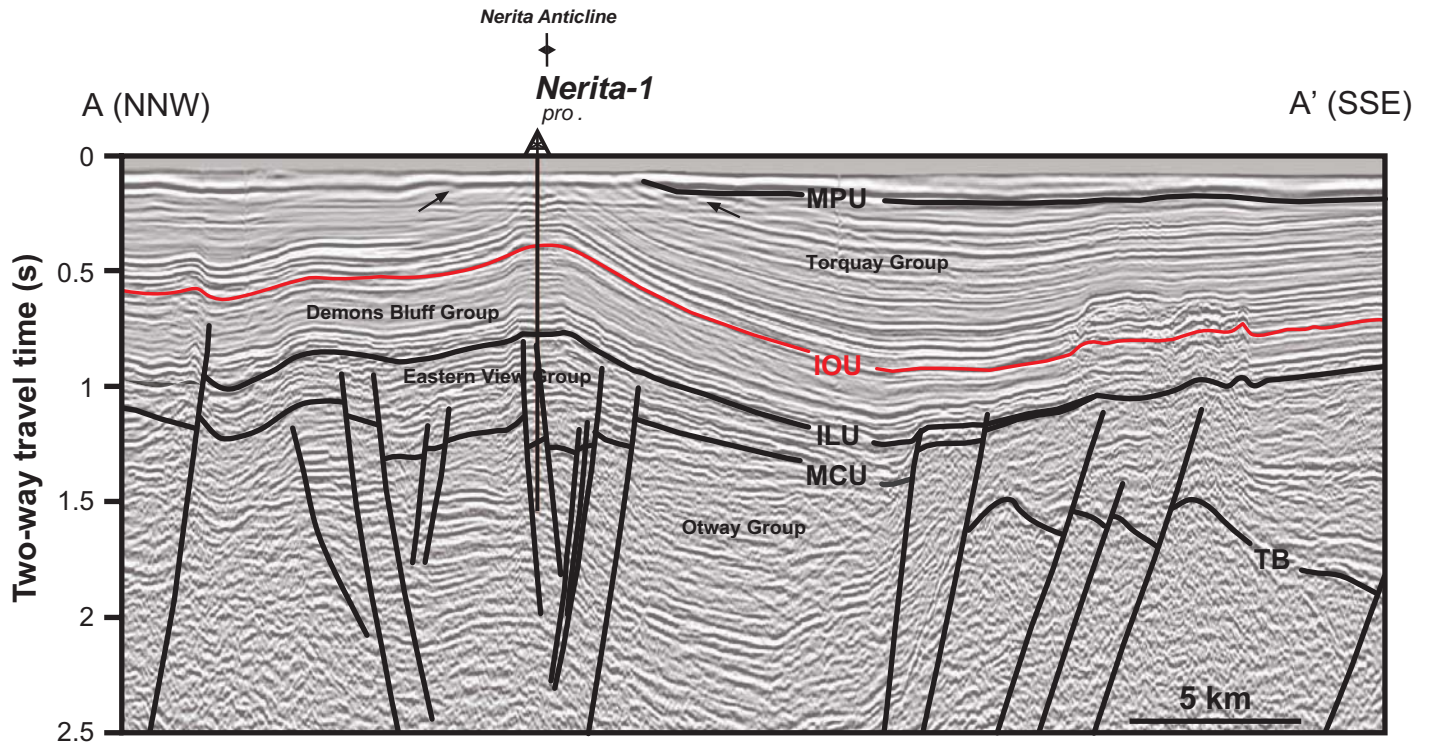
Figure



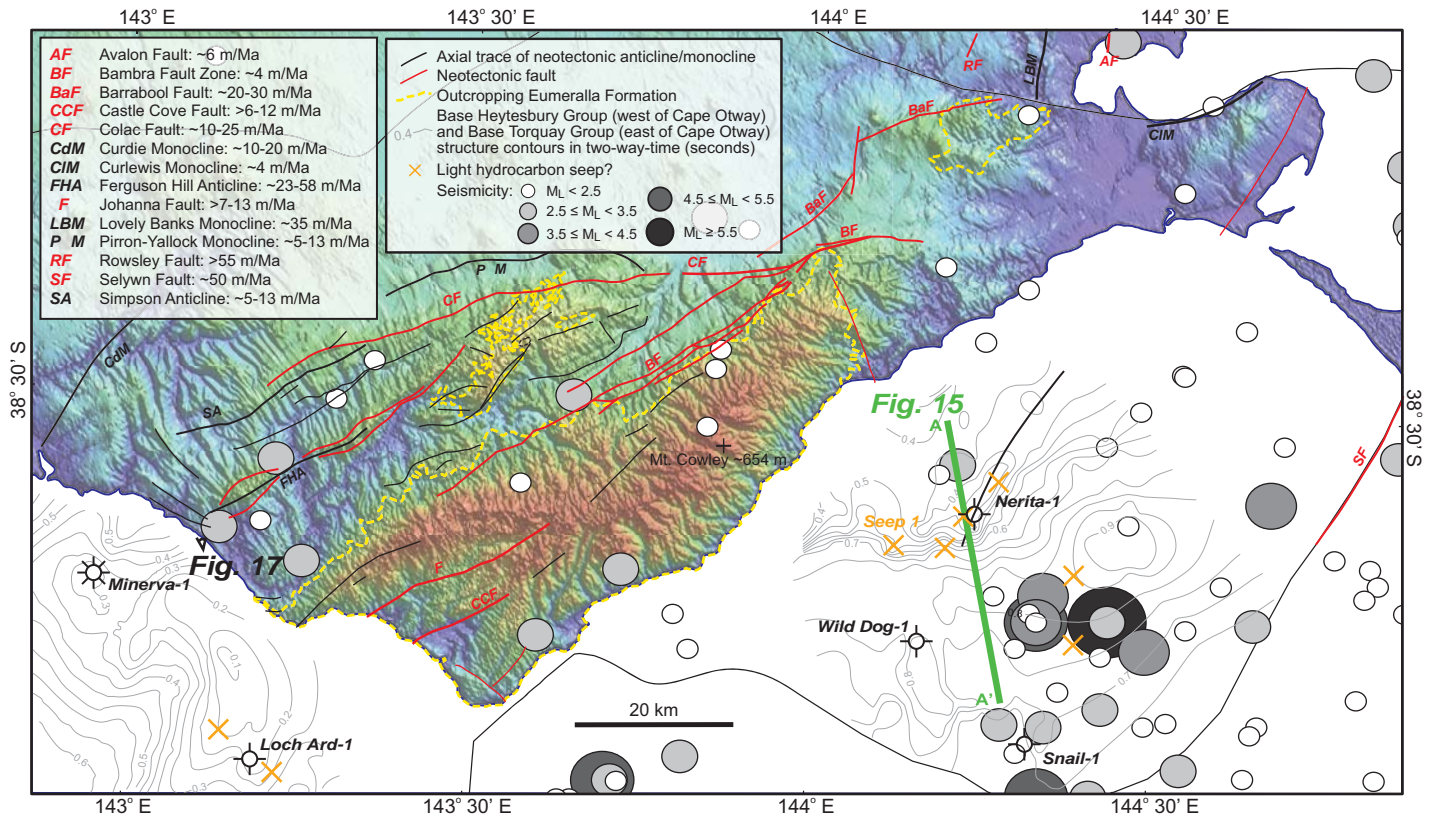
-  Focal mechanism solution (see Table 5)
-   $S_a$  azimuth from wellbore failure analysis
-  Modelled stress trajectories
-  Basement discontinuities
-  Interpreted basement fault from seismic data
-  Basin limits
-  Coastline / State boundary
-  Outcropping Eumeralla Formation



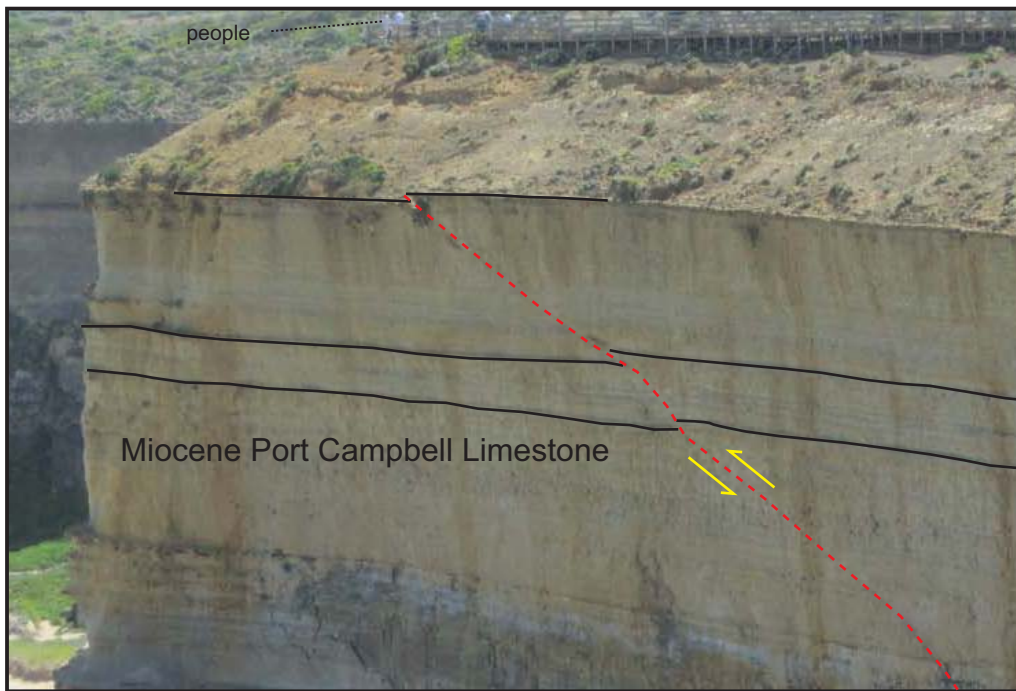
Figure



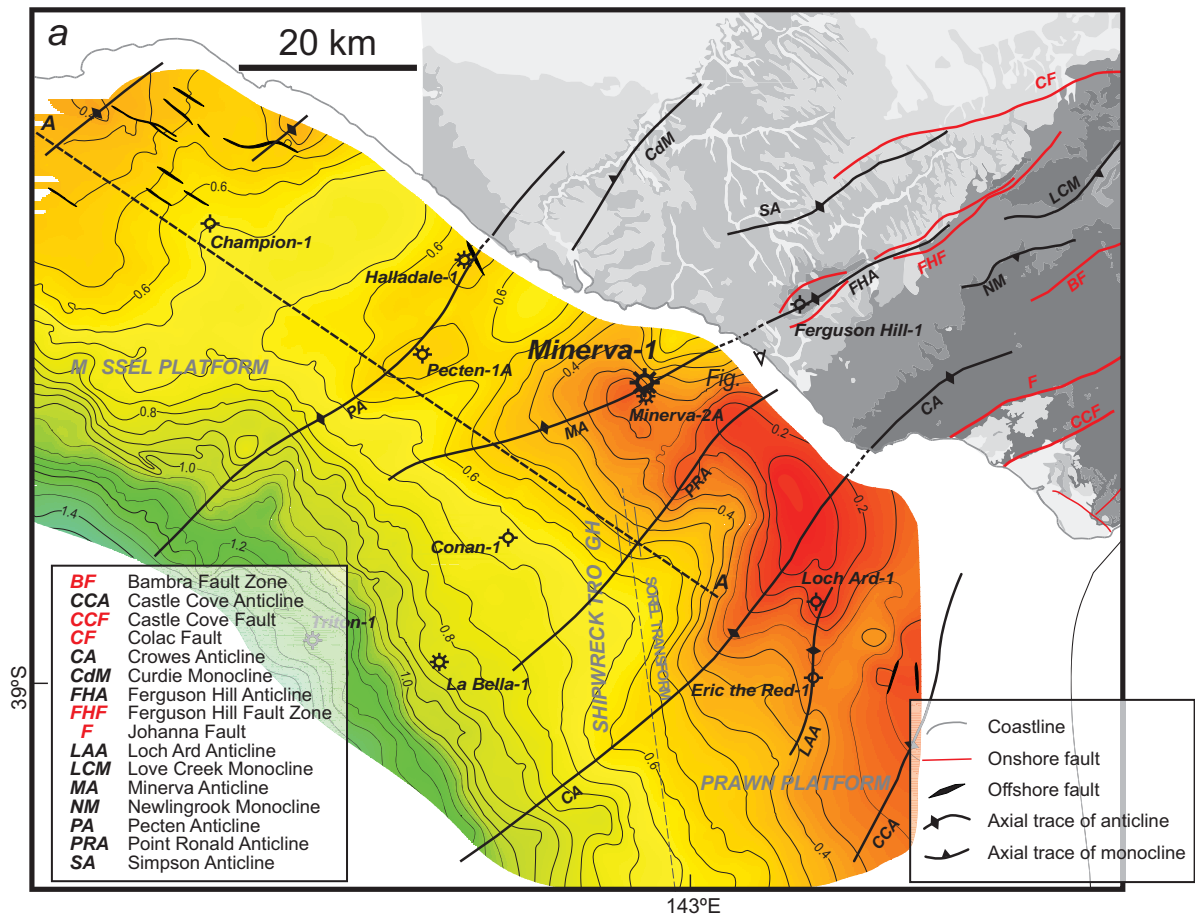
Figure



Figure

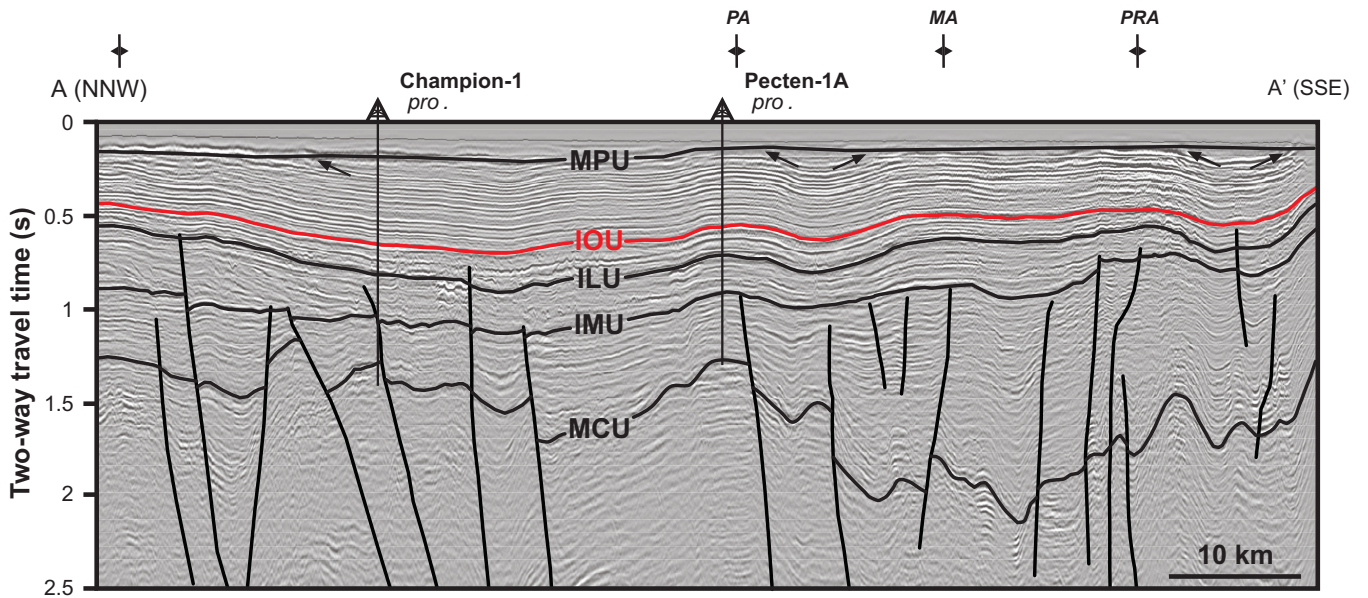


Figure



Onshore Surface Geology

- |  |  |
|--|--|
| Pleistocene to Holocene                              | Wangerrip Group                        |
| late Pliocene to early Pliocene unconsolidated — MPU | intra-aastrian unconsolidated — IMU    |
| Pliocene (Whalers Bluff Group)                       | Sherbrook Group <i>not outcropping</i> |
| intra-Oligocene unconsolidated — IOU                 | older Tertiary unconsolidated — MCU    |
| Heytesbury Group                                     | Otway Group                            |
| intra-Devonian unconsolidated — ILU                  |  |
| Nirranda Group                                       |  |



Figure

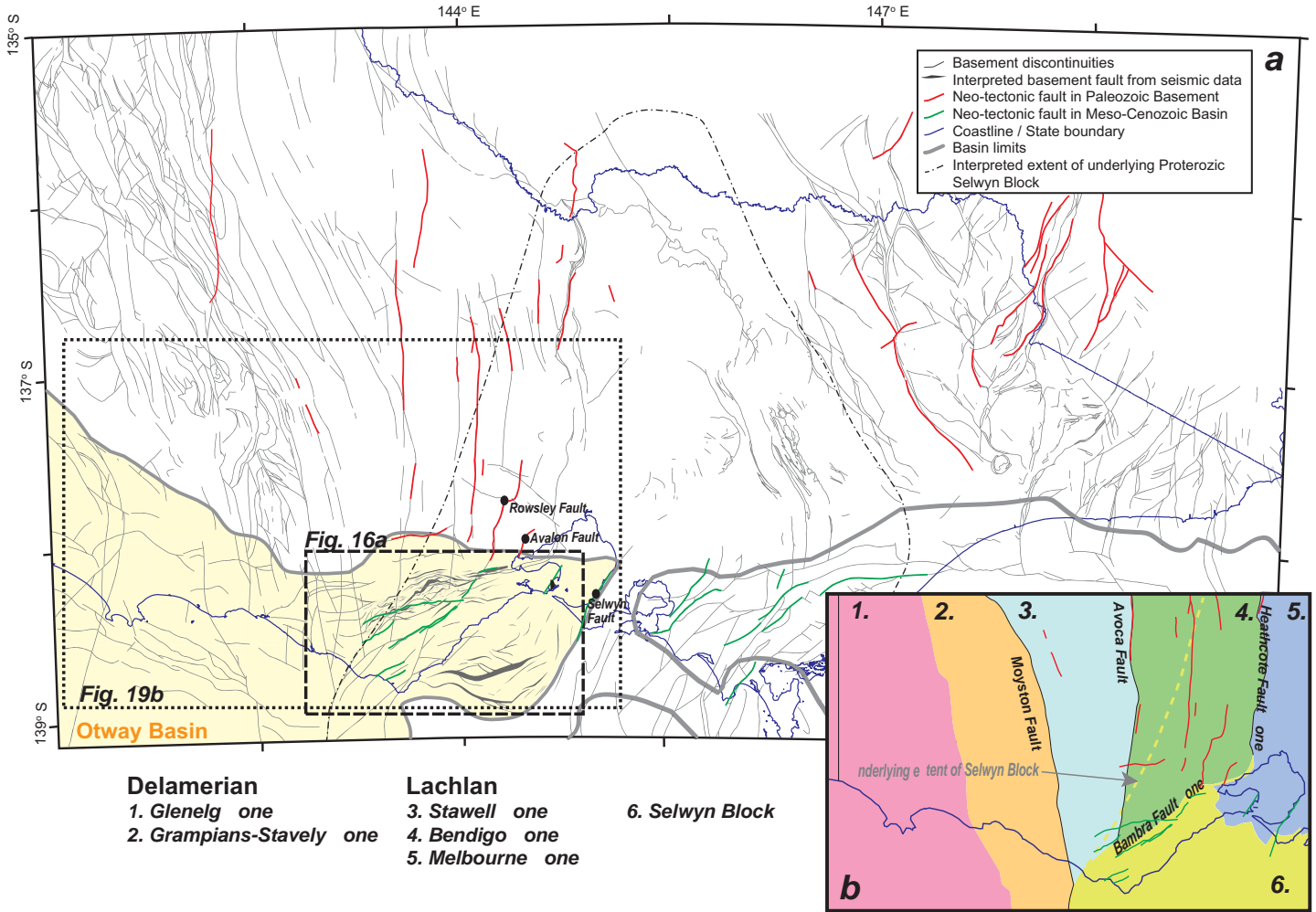




Figure 2

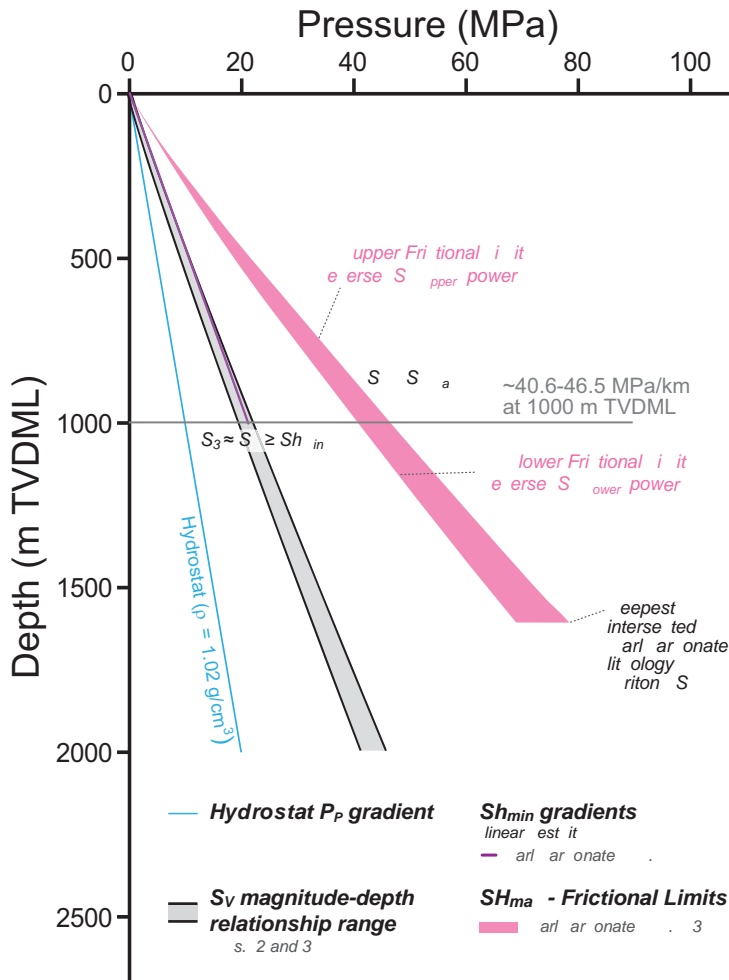
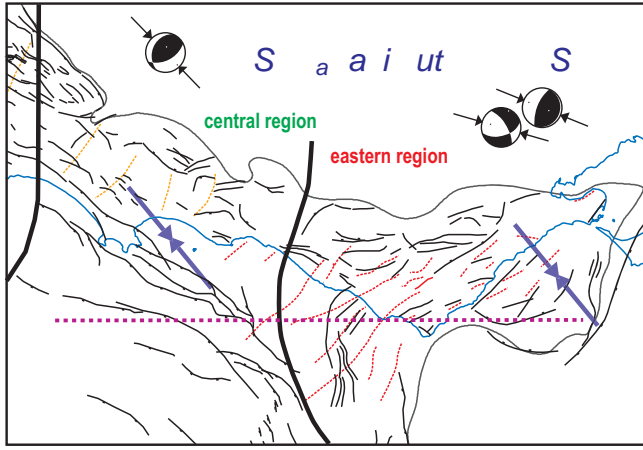


Figure 2

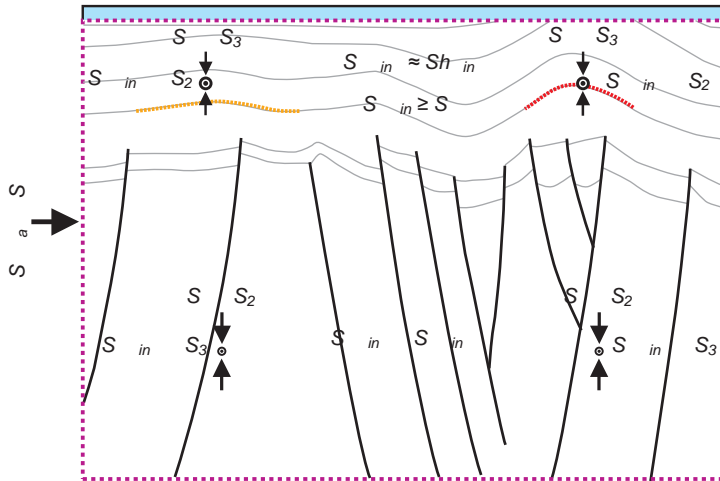


subtle compressional deformation, near-maximum burial, predominantly NW/SE Cretaceous Faults

pronounced compressional deformation, moderate Neogene exhumation, predominantly NE/SW Cretaceous Faults

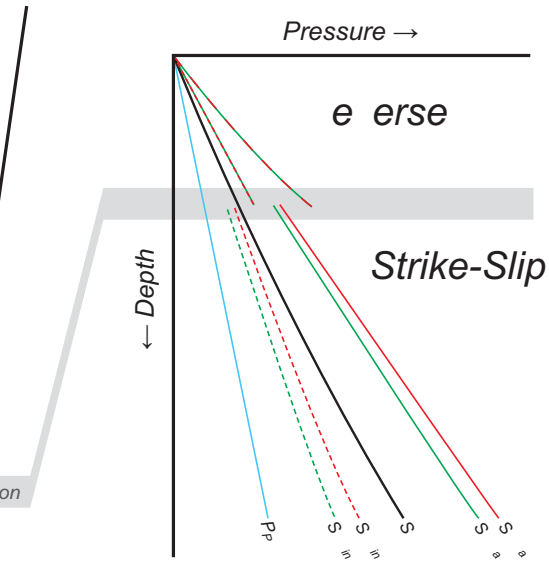
**Central region**

**Eastern region**



**Folding**

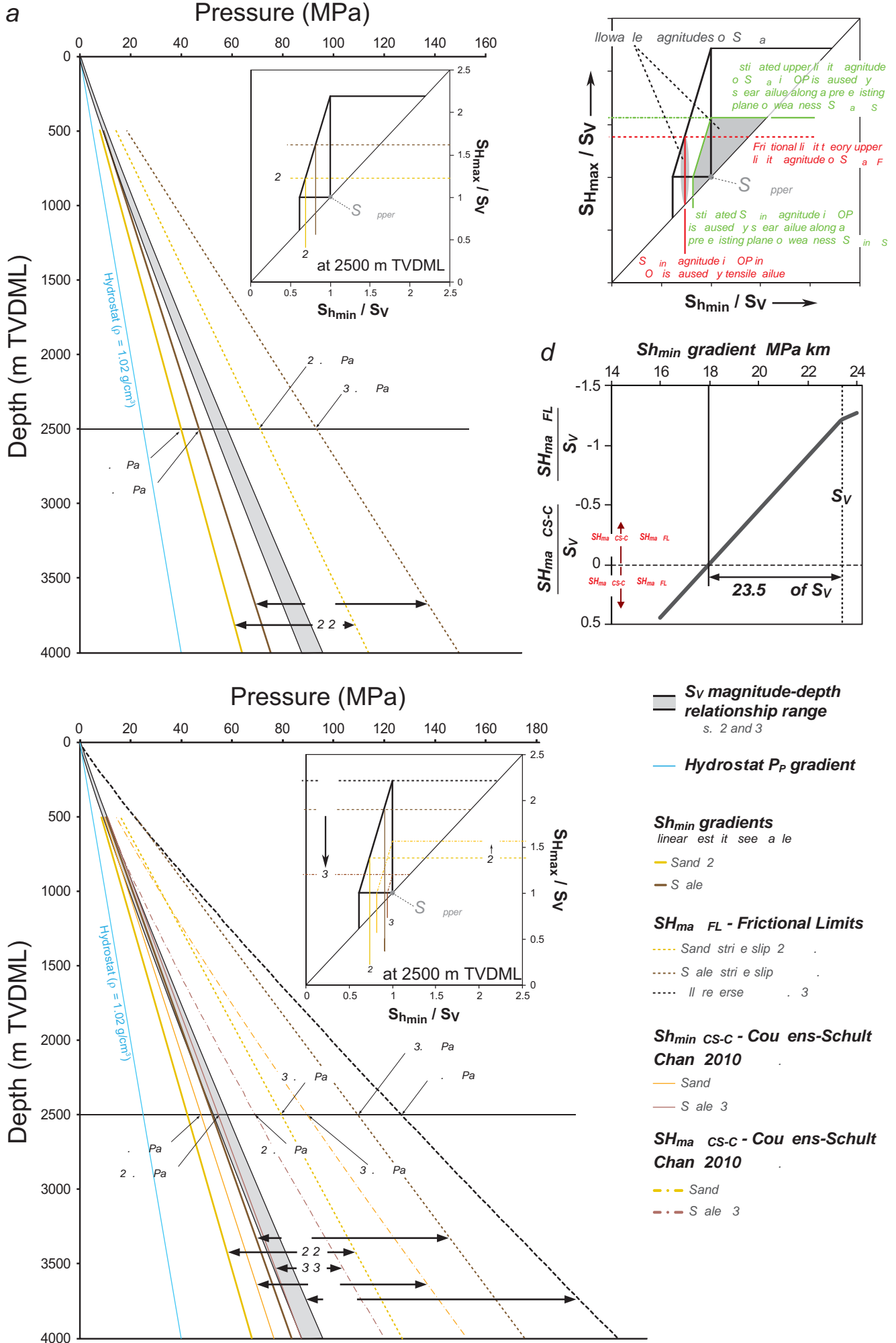
- post-rift
- no existing planes of weakness
- ore du tile
- shallow
- su seis i re erse aulting
- u ling
- less e i ient eans to a o odate
- release strain build-up?



**Faulting**

- syn ri t
- pre-existing planes of weakness
- ore rittle
- deeper
- complex tectonic history prior to post-rift sedimentation
- e i ient eans to a o odate
- release strain build-up?

Figure 22



**4.3 PAPER 4: *Quantifying Neogene plate-boundary controlled uplift and deformation of the southern Australian margin***

***IN Faulting, Fracturing and Igneous Intrusions in the Earth's Crust (Eds. D. Healy, R.W.H. Butler, Z.K. Shipton & R.H. Sibson), Geological Society of London, Special Publication (2012), 367, 91–110.***

***David R. Tassone, Simon, P. Holford, Richard R. Hillis & Adrian K. Tuitt***

# Statement of Authorship

Title of Paper	Quantifying Neogene plate-boundary controlled uplift and deformation of the southern Australian margin
Publication Status	<input checked="" type="radio"/> Published <input type="radio"/> Accepted for Publication <input type="radio"/> Submitted for Publication <input type="radio"/> Publication Style
Publication Details	Tassone, D.R., Holford, S.P., Hillis, R.R., Tuitt, A.K., (2012) Quantifying Neogene plate-boundary controlled uplift and deformation of the southern Australian margin. In: Healy, D., Butler, R. W. H., Shipton, Z. K. & Sibson, R. H. (eds) 2012. Faulting, Fracturing and Igneous Intrusion in the Earth's Crust. Geological Society, London, Special Publications, 367, 91–110. <a href="http://dx.doi.org/10.1144/SP367.7">http://dx.doi.org/10.1144/SP367.7</a>

## Author Contributions

By signing the Statement of Authorship, each author certifies that their stated contribution to the publication is accurate and that permission is granted for the publication to be included in the candidate's thesis.

Name of Principal Author (Candidate)	David R. Tassone		
Contribution to the Paper	Performed all earthquake analysis, interpreted data, wrote manuscript and acted as corresponding author		
Overall percentage (%)	80		
Signature		Date	02/04/2014

Name of Co-Author	Simon P. Holford		
Contribution to the Paper	Supervised development of work, helped in data interpretation, manuscript evaluation and editing		
Overall percentage (%)	10		
Signature		Date	20/3/2014

Name of Co-Author	Richard R. Hillis		
Contribution to the Paper	Minor input into technical concept and editing		
Overall percentage (%)	5		
Signature		Date	20/3/2014

Please cut and paste additional co-author panels here.

# Statement of Authorship

Title of Paper	Quantifying Neogene plate-boundary controlled uplift and deformation of the southern Australian margin
Publication Status	<input checked="" type="radio"/> Published <input type="radio"/> Accepted for Publication <input type="radio"/> Submitted for Publication <input type="radio"/> Publication Style
Publication Details	Tassone, D.R., Holford, S.P., Hillis, R.R., Tuitt, A.K., (2012) Quantifying Neogene plate-boundary controlled uplift and deformation of the southern Australian margin. In: Healy, D., Butler, R. W. H., Shipton, Z. K. & Sibson, R. H. (eds) 2012. Faulting, Fracturing and Igneous Intrusion in the Earth's Crust. Geological Society, London, Special Publications, 367, 91–110. <a href="http://dx.doi.org/10.1144/SP367.7">http://dx.doi.org/10.1144/SP367.7</a>

## Author Contributions

By signing the Statement of Authorship, each author certifies that their stated contribution to the publication is accurate and that permission is granted for the publication to be included in the candidate's thesis.

Name of Principal Author (Candidate)	Adrian K. Tuitt		
Contribution to the Paper	Minor input on data interpretation		
Overall percentage (%)	5		
Signature		Date	20/3/2014

Name of Co-Author			
Contribution to the Paper			
Overall percentage (%)			
Signature		Date	

Name of Co-Author			
Contribution to the Paper			
Overall percentage (%)			
Signature		Date	

Please cut and paste additional co-author panels here.

Tassone, D.R., Holford, S.P., Hillis, R.R. & Tuitt, A.K. (2012) Quantifying Neogene plate-boundary controlled uplift and deformation of the southern Australian margin. *In Faulting, Fracturing and Igneous Intrusion in the Earth's Crust, Special Publications*, v. 367, pp. 91-110

NOTE:

This publication is included on pages 264-283 in the print  
copy

of the thesis held in the University of Adelaide Library.

It is also available online to authorised users at:

<http://doi.org/10.1144/SP367.7>

***4.4 PAPER 5: Constraining Cenozoic exhumation in the Faroe-Shetland region using sonic transit time data***

**Basin Research, Special Publication (2014), 26, 38–72.**

***David R. Tassone, Simon P. Holford, Martyn S. Stoker, Paul F. Green, Howard Johnson, John R. Underhill & Richard R. Hillis***



# Statement of Authorship

Title of Paper	Constraining Cenozoic exhumation in the Faroe-Shetland region using sonic transit time data
Publication Status	<input checked="" type="radio"/> Published <input type="radio"/> Accepted for Publication <input type="radio"/> Submitted for Publication <input type="radio"/> Publication Style
Publication Details	Tassone, D.R., Holford, S.P., Stoker, M.S., Green, P.F., Johnson, H., Underhill, J.R., Hillis, R.R., (in press) Constraining Cenozoic exhumation in the Faroe-Shetland region using sonic transit time data. Basin Research 26, 38–72, doi: 10.1111/bre.12052

## Author Contributions

By signing the Statement of Authorship, each author certifies that their stated contribution to the publication is accurate and that permission is granted for the publication to be included in the candidate's thesis.

Name of Principal Author (Candidate)	David R. Tassone		
Contribution to the Paper	Performed analysis on all petrophysical log data, interpreted data, wrote manuscript and acted as corresponding author		
Overall percentage (%)	55		
Signature		Date	02/04/2014

Name of Co-Author	Simon P. Holford		
Contribution to the Paper	Supervised development of work, helped in data interpretation, manuscript evaluation and editing		
Overall percentage (%)	10		
Signature		Date	20/3/2014

Name of Co-Author	Martyn S. Stoker		
Contribution to the Paper	Major input into regional geology, data interpretation and editing		
Overall percentage (%)	10		
Signature		Date	21/03/14

Please cut and paste additional co-author panels here.

# Statement of Authorship

Title of Paper	Constraining Cenozoic exhumation in the Faroe-Shetland region using sonic transit time data
Publication Status	<input checked="" type="radio"/> Published <input type="radio"/> Accepted for Publication <input type="radio"/> Submitted for Publication <input type="radio"/> Publication Style
Publication Details	Tassone, D.R., Holford, S.P., Stoker, M.S., Green, P.F., Johnson, H., Underhill, J.R., Hillis, R.R., (2014) Constraining Cenozoic exhumation in the Faroe-Shetland region using sonic transit time data. Basin Research 26, 38–72, doi: 10.1111/bre.12052

## Author Contributions

By signing the Statement of Authorship, each author certifies that their stated contribution to the publication is accurate and that permission is granted for the publication to be included in the candidate's thesis.

Name of Principal Author (Candidate)	Paul F. Green		
Contribution to the Paper	Major input into technical concept, data interpretation and editing		
Overall percentage (%)	10		
Signature		Date	20/3/2014

Name of Co-Author	Howard Johnson		
Contribution to the Paper	Minor input into regional geology and editing		
Overall percentage (%)	5		
Signature		Date	21/03/14

Name of Co-Author	John R. Underhill		
Contribution to the Paper	Minor input into technical concept and editing		
Overall percentage (%)	5		
Signature		Date	7/4/14

Please cut and paste additional co-author panels here.

# Statement of Authorship

Title of Paper	Constraining Cenozoic exhumation in the Faroe-Shetland region using sonic transit time data
Publication Status	<input checked="" type="radio"/> Published <input type="radio"/> Accepted for Publication <input type="radio"/> Submitted for Publication <input type="radio"/> Publication Style
Publication Details	Tassone, D.R., Holford, S.P., Stoker, M.S., Green, P.F., Johnson, H., Underhill, J.R., Hillis, R.R., (2014) Constraining Cenozoic exhumation in the Faroe-Shetland region using sonic transit time data. Basin Research 26, 38–72, doi: 10.1111/br.12052

## Author Contributions

By signing the Statement of Authorship, each author certifies that their stated contribution to the publication is accurate and that permission is granted for the publication to be included in the candidate's thesis.

Name of Principal Author (Candidate)	Richard R. Hillis		
Contribution to the Paper	Minor input into technical concept		
Overall percentage (%)	5		
Signature		Date	20/3/2014

Name of Co-Author			
Contribution to the Paper			
Overall percentage (%)			
Signature		Date	

Name of Co-Author			
Contribution to the Paper			
Overall percentage (%)			
Signature		Date	

Please cut and paste additional co-author panels here.

Tassone, D.R., Holford, S.P., Stoker, M.S., Green, P., Johnson, H., Underhill, J.R. & Hillis, R.R.  
(2014) Constraining Cenozoic exhumation in the Faroe-Shetland region using sonic transit time data.  
*Basin Research*, v. 26(1), pp. 38-72

NOTE:

This publication is included on pages 288-322 in the print copy  
of the thesis held in the University of Adelaide Library.

It is also available online to authorised users at:

<http://doi.org/10.1111/bre.12052>

## **5 Contributions to Additional Journal Publications**

**5.1 PAPER A: Cenozoic Post-breakup Compressional Deformation and Exhumation of the Southern Australian Margin**

**Australian Petroleum Production & Exploration Association Journal (2011), 51, 613–638.**

*Simon P. Holford, Richard R. Hillis, Ian R. Duddy, Paul F. Green, Martyn S. Stoker, Adrian K. Tuitt, Guillaume Backé, David R. Tassone & Justin D. MacDonald*

Holford, S.P., Hillis, R.R., Duddy, I.R., Green, P.F., Stoker, M.S., Tuitt, A.K., Backe, G., Tassone, D.R. & MacDonald, J.D. (2011) Cenozoic post-breakup compressional deformation and exhumation of the southern Australian margin.  
*APPEA Journal*, v. 51, pp. 613-638

NOTE:

This publication is included on pages 325-350 in the print copy  
of the thesis held in the University of Adelaide Library.

**5.2 PAPER B: Continental margin compression: A comparison between compression in the Otway Basin of the southern Australian margin and the Rockall-Faroe area in the northeast Atlantic margin**

**Australian Petroleum Production & Exploration Association Journal (2011), 51, 241–258.**

***Adrian K. Tuitt, Simon P. Holford, Richard R. Hillis, John R. Underhill J. Derek Ritchie, Howard Johnson, Ken Hitchen, Martyn S. Stoker & David R. Tassone***



Tuitt, A., Holford, S.P., Hillis, R.R., Underhill, J.R., Ritchie, J.D., Hohnson, H., Hitchen, K., Stoker, M.S. & Tassone, D.R. (2011) Continental margin compression: a comparison between compression in the Otway Basin of the southern Australian margin and the Rockall-Faroe area in the northeast Atlantic margin.

*APPEA Journal*, v. 51, pp. 241-258

NOTE:

This publication is included on pages 352-369 in the print copy of the thesis held in the University of Adelaide Library.

**5.3 PAPER C: *Paleothermal and seismic constraints on late Miocene–Pliocene uplift and deformation in the Torquay sub-basin, southern Australian margin***

**[Australian Journal of Earth Sciences \(2011\), 58, 453–562](#)**

***Simon P. Holford, Richard R. Hillis, Ian R. Duddy, Paul F Green, David R. Tassone & Martyn S. Stoker***

Holford, S.P., Hillis, R.R., Duddy, I.R., Green, P.F., Tassone, D.R. & Stoker, M.S. (2011)  
Paleothermal and seismic constraints on late Miocene-Pliocene uplift and deformation in the Torquay  
sub-basin southern Australian margin.  
*Australian Journal of Earth Sciences*, v. 58(5), pp. 543-562

NOTE:

This publication is included on pages 371-391 in the print copy  
of the thesis held in the University of Adelaide Library.

It is also available online to authorised users at:

<http://doi.org/10.1080/08120099.2011.565074>

**5.4 PAPER D: *Reassessing the in-situ stress regimes of Australia's petroleum basins***

**Australian Petroleum Production & Exploration Association Journal (2012), 52, 415–425.**

***Rosalind King, Simon P. Holford, Richard R. Hillis Adrian K. Tuitt, Ernest Swierczek, Guillaume Backé, David R. Tassone & Mark R.P. Tingay***

King, R., Holford, S., Hillis, R., Tuitt, A., Swierczek, E., Backe, G., Tassone, D. & Tingay, M. (2012)  
Reassessing the in-situ stress regimes of Australia's petroleum basins.  
*APPEA Journal*, v. 52, pp. 415-425

NOTE:

This publication is included on pages 393-403 in the print copy  
of the thesis held in the University of Adelaide Library.

***5.5 PAPER E: Cenozoic deformation in the Otway Basin, southern Australian margin: implications for the origin and nature of post-breakup compression at rifted margins***

**Basin Research, Special Publication (2014),**

***Simon P. Holford, Adrian K. Tuitt, Richard R. Hillis, Paul F. Green, Martyn S. Stoker, Ian R. Duddy, Mike Sandiford & David R. Tassone***

Holford, S.P., Tuit, A.K., Hillis, R.R., Green, P.F., Stoker, M.S., Duddy, I.R., Sandiford, M. & Tassone, D.R. (2014) Cenozoic deformation in the Otway Basin, southern Australian margin: implications for the origin and nature of post-breakup compression at rifted margins. *Basin Research*, v. 26(1), pp. 10-37

NOTE:

This publication is included on pages 405-432 in the print copy of the thesis held in the University of Adelaide Library.

It is also available online to authorised users at:

<http://doi.org/10.1111/bre.12035>

## **6 Conference Attendances and Presentations**



**6.1 CONFERENCE 1: 21<sup>st</sup> International Geophysical Conference & Exhibition / Australian Society of Exploration Geophysicists and Petroleum Exploration Society of Australia – 22-26 August 2010, Sydney, Australia**

*CONFERENCE ATTENDENCES AND PRESENTATIONS*

*Quantification of Cretaceous-Cenozoic exhumation in the Otway Basin using sonic velocities and implications for hydrocarbon exploration*

*David R. Tassone, Simon P. Holford & Richard R. Hillis*

Tassone, D.R., Holford, S.P. & Hillis, R.R. (2010) Quantification of Cretaceous-Cenozoic exhumation in the Otway Basin using sonic velocities and implications for hydrocarbon exploration.

*Presented at 21st International Geophysical Conference & Exhibition / Australian Society of Exploration Geophysicists and Petroleum, 22-26 August, Sydney Australia*

NOTE:

This publication is included on pages 436-439 in the print copy of the thesis held in the University of Adelaide Library.

**6.2 CONFERENCE 2: *The E.M. Anderson Meeting – 6-8 September 2010, Glasgow, Scotland***

Tassone, D.R., Holford, S.P., Hillis, R.R. & Tuitt, A.K. (2010) Quantifying Neogene plate-boundary controlled uplift and deformation of the southern Australian margin.

*Presented at The E.M. Anderson Meeting, 6-8 September, Glasgow Scotland*

NOTE:

This publication is included on pages 441-443 in the print copy of the thesis held in the University of Adelaide Library.

**6.3 CONFERENCE 3: 51<sup>st</sup> Australian Petroleum Production and  
Exploration Association Conference & Exhibition – 10-13 April 2011,  
Perth, Australia**

Tassone, D.R., Holford, S.P., Tingay, M.R.P., Tuitt, A.K., Stoker, M.S. & Hillis, R.R. (2011)  
Overpressures in the central Otway Basin: the result of rapid Pliocene-recent sedimentation.  
*Presented at 51st Australian Petroleum Production and Exploration Association Conference &  
Exhibition, 10-13 April, Perth Australia*

NOTE:

This publication is included on pages 445-446 in the print copy  
of the thesis held in the University of Adelaide Library.

**6.4 CONFERENCE 4: 73<sup>rd</sup> European Association of Geoscientists and Engineers Conference & Exhibition – 23-26 May 2011, Vienna, Australia**



CONFERENCE ATTENDENCES AND PRESENTATIONS

*Late Cretaceous-Cenozoic Exhumation of the Faroe-Shetland Basins along the NW Atlantic Margin*

*David R. Tassone, Simon P. Holford, Martyn S. Stoker, Paul F. Green, Howard Johnson, John R. Underhill, Nick Schofield & Richard R. Hillis*

Tassone, D.R., Holford, S.P., Stoker, M.S., Underhill, J.R., Green, P.F. & Hillis, R.R. (2011) Late Cretaceous-Cenozoic exhumation of the Faroe-Shetland Basins along the NW Atlantic margin. *Presented at 73rd European Association of Geoscientists and Engineers Conference & Exhibition, 23-26 May, Vienna Austria*

NOTE:

This publication is included on pages 449-454 in the print copy of the thesis held in the University of Adelaide Library.

**6.5 CONFERENCE 5: American Association of Petroleum Geologists  
Annual Conference & Exhibition – 22-25 April 2012, Long Beach,  
United States of America**

Tassone, D.R., Holford, S.P., King, R.C., Tingay, M.R.P., Backe, G. & Hillis, R.R. (2012) New Constraints on the in situ stress tensor in the eastern offshore Otway Basin, south-eastern Australia: implications for the reactivation potential of sealing faults.  
*Presented at American Association of Petroleum Geologists Annual Conference & Exhibition, 22-25 April, Long Beach California*

NOTE:

This publication is included on pages 456-458 in the print copy of the thesis held in the University of Adelaide Library.